SOME STUDIES ON BREAKDOWN OF SOLID INSULATIONS AND IT'S MODELING USING SOFT COMPUTING TECHNIQUES

A thesis submitted to NIT Rourkela

in partial fulfillment of the requirement for the degree of

Doctor of Philosophy

In

Electrical Engineering

By

SANJEEB MOHANTY

Department of Electrical Engineering

National Institute of Technology

Rourkela-769008, India

December 2010

Dedicated to

The Mother (Sri Ma')

Acknowledgement

First of all, I would like to express my deep and sincere regard for my supervisor, **Prof. Saradindu Ghosh**, who was primarily responsible for bringing out the best in me in the area of this research work. This was made possible through endless rounds of discussions and translating those into something concrete. His painstaking patience in correcting all the articles, whether submitting to a Conference, Journal or the thesis work itself was simply superb.

Next, I would like to express my gratitude to **Prof. J.K. Satapathy, Prof. K.K. Mahapatra, Prof. B. Subuddhi, Dr. K.B. Mohanty.** All four of them in their capacity as **Members of Doctoral Scrutiny Committee** had extended their kind support and co-operation in my thesis work, despite their hectic schedules. I would also like to thank **faculty members** and **staff** of the Department of Electrical Engineering, for being a constant source of encouragement and co-operation during my thesis period. Special thanks are extended to Mr. S. Swain and Mr. B.K. Sahoo for preparing the samples from the insulation sheets.

I would also like to thank Prof. U.K. Mohanty, Prof. S. Bhattacharya, Prof. D.P. Tripathy, Dr. J. Bera, Dr. R. Majumdar, Mr. Rajesh Patnaik, Mr. Santosh Nanda for their pro-active co-operation and help in conducting different experiments.

Last, but not the least I would express my sincere gratitude to all family members, relatives and friends for their love, sacrifice and moral support at a critical juncture in my career and life.

Sanjeeb Mohanty
Roll No: 50702003

DECLARATION

I hereby declare that this submission is my own work and that, to the best of my knowledge and belief, it contains no material previously published or written by another person nor material which has been accepted for the award of any other degree or diploma of the university or other institute of higher learning, except where due acknowledgment has been made in the text.

Place: NIT, Rourkela. Signature :

Date: Name :

Roll No :

CERTIFICATE

This is to certify that Shri Sanjeeb Mohanty has worked on the thesis entitled **" Some Studies on Breakdown of Solid Insulations and it's Modeling using Soft Computing Techniques "** under my supervision and has fulfilled all the requirements for regulations of the institute relating to nature, period of research and presentation of seminar talk. It is also certified that the said thesis incorporates the results of original investigations made by Shri Sanjeeb Mohanty in the Department of Electrical Engineering, National Institute of Technology Rourkela under my guidance and supervision throughout. The thesis being submitted in partial fulfillment of his PhD degree in Engineering of the Institute, has not been submitted previously anywhere for any degree whatsoever either by him or by anyone else.

……

Dr. Saradindu Ghosh
Professor
Department of Electrical Engineering
National Institute of Technology
Durgapur-713209

ABSTRACT

Electrical power systems are experiencing significant changes at the worldwide scale both in size and in complexities. The generating capacities of power plants and application of high voltage has intensively increased due to their inherent advantages, such as, greater efficiency and cost effectiveness. It is, thus essential to know the property of the insulating materials for optimum solution in terms of cost and insulating capability. Out of so many properties of insulation materials, determination of the breakdown voltage continues to evoke a lot of interest to the Electrical Engineers in general and High Voltage Engineers in particular. Hence, it is possible to develop solid insulating materials with excellent breakdown strength and any attempt at modeling the phenomenon with the presence of void would go a long way in assessing the insulation quality. Some of the few important topics reviewed at the beginning of the thesis are the factors affecting the breakdown voltage in general, breakdown voltage study of different composite insulating materials and the factors affecting the breakdown voltage due to Partial Discharges (PD) in voids.

The merits of using a Soft Computing (SC) model over that of a Conventional model in order to predict the breakdown voltage of solid insulating materials due to PD in voids has been identified as one of the main objectives of the thesis. This is because the SC models are highly flexible and a model can be improved simply by providing additional training data. In addition, this kind of model can be developed more accurately in a shorter time. The SC approach consists of several computing paradigms, such as, Artificial Neural Network (ANN), Fuzzy Logic (FL), approximate reasoning, and derivative-free optimization methods, such as, Genetic Algorithms (GA) and Simulated Annealing (SA). The seamless integration of all these paradigms forms the core of SC, which is aimed at solving real-world decision-making, modeling problems. In addition to the prediction issue, the other main objective of the thesis is to visualize the state of the insulation with the application of voltage stress at different levels till breakdown. In order to carry out this objective, that is, to know the state of the insulation a Scanning Electron Microscope (SEM) is utilized here.

In order to predict the breakdown voltage using the SC models, the data is generated experimentally on the application of DC and AC power frequency voltages and the relative permittivity is measured for the solid insulating materials used. In addition, the generated data are statistically analyzed before being utilized for modeling. Also the breakdown voltage of

solid insulating materials under DC and AC has been studied as a function of the thickness of the material, the void depth, the void diameter. After the breakdown voltage data has been statistically analyzed, four SC techniques, such as, Multilayer Feedforward Neural Network (MFNN), Radial Basis Function Network (RBFN), Mamdani Fuzzy Logic (MFL) and Adaptive Sugeno Fuzzy Logic (ASFL) have been used to propose twenty four models for prediction based on their respective theories. The input and the output parameters are assumed to have triangular and trapezoidal shape in the two FL schemes. The evaluation criteria for the MFNN, RBFN and the ASFL are the Mean Square Error (MSE) for training patterns E_{tr} and the Mean Absolute Error (MAE) for testing patterns E_{ts}. Whereas for the MFL, the MAE for testing patterns is the main evaluation criteria.

Finally, the MAE for testing patterns has been compared with the experimental data for all the twenty four models based on the four SC techniques. A low value of MAE in each of the four cases indicates the effectiveness of such models. One of the important inferences that can be drawn is that for the four models (having four input parameters) corresponding to each of the four SC techniques, the two ANN structures perform better than the two FL inferencing schemes. The scope for future work is also outlined at the end of the thesis.

CONTENTS

Acknowledgement	i
Declaration	ii
Certificate	iii
Abstract	iv
Table of contents	vi
List of figures	x
List of tables	xiv
List of symbols	xxi

CHAPTER 1

INTRODUCTION AND LITERATURE SURVEY

1.1 Introduction	1
1.2 Breakdown of solid insulating materials	1
1.3 Factors affecting breakdown of solid insulating materials	3
1.4 Breakdown voltage study of composite solid insulating materials	9
1.5 Breakdown voltage behaviour of Nano-insulating material	14
1.6 Breakdown due to PD in cavities	15
1.7 Breakdown voltage prediction due to PD in cavities	21
1.8 Soft Computing applications to Insulations diagnosis	22
1.9 Motivation	24
1.10 Organization of the thesis	24

CHAPTER 2

EXPERIMENTAL PROCEDURE AND OBSERVATION

2.1 Introduction 26
2.2 Experimental procedure 26
2.2.1 Sample Preparation 26
2.2.2 Creation of void 27
2.2.3 Electrode Geometry 27
2.2.4 Measurement of DC Breakdown Voltage 30
2.2.5 Measurement of AC Breakdown Voltage 35
2.2.6 Measurement of relative permittivity of solid insulating materials 41
2.3 Statistical analysis of the experimental data 42
2.3.1 Sample Calculation under DC test condition 44
2.3.2 Sample Calculation under AC test condition 49
2.4 Monitoring of the state of solid insulating materials 65
2.5 Breakdown voltage variation under DC and AC conditions 79
2.6 Conclusion 84

CHAPTER 3

MODELING OF THE BREAKDOWN VOLTAGE USING MULTILAYER FEEDFORWARD NEURAL NETWORK

3.1 Introduction 85
3.2 Multilayer Feedforward Network 85
3.3 Modeling of Breakdown Voltage using MFNN 88
3.3.1 Prediction of the breakdown voltage due to PD in voids under DC conditions 90
3.3.2 Prediction of the breakdown voltage due to PD in voids under AC conditions 99
3.3.3 Extrapolation capability of the Model 6 113

3.3.4 Prediction of the breakdown voltage due to PD in voids under AC conditions (CIGRE Method II Electrode System) 115
3.4 Conclusion 118

CHAPTER 4

MODELING OF THE BREAKDOWN VOLTAGE USING RADIAL BASIS FUNCTION NETWORK

4.1 Introduction 119
4.2 Radial Basis Function Network 119
4.3 Modeling of Breakdown Voltage using RBFN 122
4.3.1 Prediction of the breakdown voltage due to PD in voids under DC conditions 122
4.3.2 Prediction of the breakdown voltage due to PD in voids under AC conditions 132
4.3.3 Extrapolation capability of RBFN 145
4.4 Conclusion 147

CHAPTER 5

MODELING OF THE BREAKDOWN VOLTAGE USING MAMDANI FUZZY LOGIC TECHNIQUE

5.1 Introduction 148
5.2 Mamdani Fuzzy Logic (MFL) 148
5.3 Modeling of Breakdown Voltage using MFL 154
5.3.1 Prediction of the breakdown voltage due to PD in voids under DC conditions 154
5.3.2 Prediction of the breakdown voltage due to PD in voids under AC conditions 166
5.3.3 Prediction of the breakdown voltage due to PD in voids using CIGRE Method II Electrode System under AC conditions 187
5.4 Conclusions 191

CHAPTER 6

MODELING OF THE BREAKDOWN VOLTAGE USING ADAPTIVE SUGENO FUZZY LOGIC TECHNIQUE

6.1 Introduction 192
6.2 Adaptive Sugeno Fuzzy Logic (ASFL) Inferencing 192
6.3 Modeling of Breakdown Voltage using ASFL 195
6.3.1 Prediction of the breakdown voltage due to PD in voids under DC conditions 197
6.3.2 Prediction of the breakdown voltage due to PD in voids under AC conditions 208
6.4 Conclusions 231

CHAPTER 7

MAJOR CONCLUSIONS AND FUTURE WORK

7.1 Introduction 233
7.2 Overview of the Thesis 233
7.3 Conclusions and future work 234

REFERENCES 238

DISSEMINATION OF THE WORK 248

BIOGRAPHY 249

LIST OF FIGURES

Figure No.	Figure Caption	Page Number
1.1	Variation of breakdown strength after the application of voltage	3
1.2	Geometrical Configuration of the cable	17
2.1	Cylinder-Plane Electrode System used for Breakdown Voltage Measurement	28
2.2	Arrangement of the complete experimental set up	28
2.3	Snapshot of a) High Voltage b) Ground Electrode	29
2.4	Experimental set up for recording relative permittivity values	41
2.5	Flowchart for obtaining maximum likelihood estimates	43
2.6	SEM (JEOL JSM -6480 LV)	66
2.7	SEM observations for White Minilex Paper samples; (a) Virgin, and stressed at (b) 14 kV, (c) 21 kV and (d) 28 kV (Breakdown) DC Voltages (t = 0.125mm, t_1 = 0.025mm and d =2 mm)	67
2.8	SEM observations for White Minilex Paper samples; (a) Virgin, and stressed at (b) 1.1 kV, (c) 1.6 kV and (d) 2.2 kV (Breakdown) AC Voltages (t = 0.18mm, t_1 = 0.125mm and d =4 mm)	69
2.9	SEM observations for Leatherite Paper samples; (a) Virgin, and stressed at (b) 1.0 kV, (c) 1.5 kV and (d) 2.0 kV (Breakdown) DC Voltages (t = 0.13mm, t_1 = 0.025mm and d =5 mm)	70
2.10	SEM observations for Leatherite Paper samples; (a) Virgin, and stressed at (b) 0.7 kV, (c) 1.0 kV and (d) 1.4 kV (Breakdown) AC Voltages (t = 0.13mm, t_1 = 0.125mm and d =1.5 mm)	72
2.11	SEM observations for Manila Paper samples; (a) Virgin, and stressed at (b) 0.75 kV, (c) 1.0 kV and (d) 1.5 kV (Breakdown) DC Voltages (t = 0.06mm, t_1 = 0.025mm and d =2 mm)	73
2.12	SEM observations for Manila Paper samples; (a) Virgin, and stressed at (b) 0.4 kV, (c) 0.6 kV and (d) 0.8 kV (Breakdown) AC Voltages (t = 0.06mm, t_1 = 0.025mm and d =3 mm)	75

Continued

Figure No.	Figure Caption	Page Number
2.13	SEM observations for Lather Minilex samples; (a) Virgin, and stressed at (b) 9 kV, (c) 13.5 kV and (d) 18 kV (Breakdown) DC Voltages (t = 0.245mm, t_1 = 0.125mm and d =2 mm)	76
2.14	SEM observations for Lather Minilex samples; (a) Virgin, and stressed at (b) 1.1 kV, (c) 1.6 kV and (d) 2.2 kV (Breakdown) AC Voltages (t = 0.245mm, t_1 = 0.025mm and d =3 mm)	78
2.15	Variation of Breakdown voltage of White Minilex, Leatherite Paper and Manila Paper with sample thickness t under DC test condition (t_1=0.125 mm, d=1.5 mm)	79
2.16	Variation of Breakdown voltage of White Minilex (t = 0.125mm), Leatherite Paper (t = 0.13mm), Manila Paper (t = 0.035mm) with the void diameter d under DC test condition (t_1=0.125 mm)	80
2.17	Variation of Breakdown voltage (kV) of White Minilex (t = 0.125mm), Leatherite Paper (t = 0.13mm), Manila Paper (t = 0.035mm) with the void depth t_1 under DC test condition (d=1.5 mm)	81
2.18	Variation of Breakdown voltage of White Minilex, Leatherite Paper and Manila Paper with sample thickness t under AC test condition (t_1=0.125 mm, d=1.5 mm)	82
2.19	Variation of Breakdown voltage (kV) of White Minilex (t = 0.125mm), Leatherite Paper (t = 0.13mm), Manila Paper (t = 0.035mm) with the void diameter d under AC test condition (t_1 = 0.125 mm)	83
2.20	Variation of Breakdown voltage (kV) of White Minilex(t=0.125mm), Leatherite Paper(t=0.13mm), Manila Paper(t=0.035mm) with the void depth t_1 under AC test conditions (d=1.5 mm)	84
3.1	Multilayer Feedforward Neural Network	86
3.2	Flowchart for the MFNN	89
3.3	MFNN (Model 1)	91
3.4	E_{tr} of the training data as a function of Number of iterations	92
3.5	MFNN (Model 2)	95
3.6	E_{tr} of the training data as a function of Number of iterations	96
3.7	E_{tr} of the training data as a function of Number of iterations	100

Continued

Figure No.	Figure Caption	Page Number
3.8	E_{tr} of the training data as a function of Number of iterations	103
3.9	E_{tr} of the training data as a function of Number of iterations	106
3.10	MFNN (Model 6)	110
3.11	E_{tr} of the training data as a function of Number of iterations	110
3.12	E_{tr} of the training data as a function of Number of iterations	116
4.1	A typical Radial Basis Functions Network (RBFN)	120
4.2	Flowchart for RBFN	123
4.3	RBF Network employed in Model 1	126
4.4	Variation of E_{tr} of the Training data as a function of Number of iterations	126
4.5	RBF Network used in Model 2	129
4.6	Variation of E_{tr} of the training data as a function of Number of iterations	130
4.7	Variation of E_{tr} of the training data as a function of Number of iterations	134
4.8	Variation of E_{tr} of the Training data as a function of Number of iterations	137
4.9	Variation of E_{tr} of the Training data as a function of Number of iterations	139
4.10	RBF Network used in Model 6	143
4.11	E_{tr} of the training data as a function of Number of iterations	143
5.1	Triangular MF	152
5.2	Trapezoidal MF	152
5.3	Flowchart for the MFL	153
5.4	Aggregated Fuzzy MFs for the Test inputs with Triangular MF	158
5.5	Aggregated Fuzzy MFs for the Test inputs with Trapezoidal MF	159
5.6	Aggregated Fuzzy MFs for the Test inputs with Triangular MF	164
5.7	Aggregated Fuzzy MFs for the Test inputs with Trapezoidal MF	165
5.8	Aggregated Fuzzy MFs for the Test inputs with Triangular MF	168
5.9	Aggregated Fuzzy MFs for the Test inputs with Trapezoidal MF	170

Continued

Figure No.	Figure Caption	Page Number
5.10	Aggregated Fuzzy MFs for the Test inputs with Triangular MF	173
5.11	Aggregated Fuzzy MFs for the Test inputs with Trapezoidal MF	174
5.12	Aggregated Fuzzy MFs for the Test inputs with Triangular MF	183
5.13	Aggregated Fuzzy MFs for the Test inputs with Trapezoidal MF	185
6.1	Flowchart for the ASFL	196
6.2	Variation of E_{tr} of the training data as a function of Number of iterations	199
6.3	Variation of E_{tr} of the training data as a function of Number of iterations	201
6.4	Variation of E_{tr} of the training data as a function of Number of iterations	203
6.5	Variation of E_{tr} of the training data as a function of Number of iterations	207
6.6	Variation of E_{tr} of the training data as a function of Number of iterations	210
6.7	Variation of E_{tr} of the training data as a function of Number of iterations	212
6.8	Variation of E_{tr} of the training data as a function of Number of iterations	215
6.9	Variation of E_{tr} of the training data as a function of Number of iterations	217
6.10	Variation of E_{tr} of the training data as a function of Number of iterations	227
6.11	Variation of E_{tr} of the training data as a function of Number of iterations	230

LIST OF TABLES

Table No.	Table Caption	Page Number
1.1	Differences between Degradation and Breakdown for a solid insulating material	2
1.2	Test results of PET Thermoplastics	4
1.3	Breakdown voltage of solid dielectrics at different frequencies	6
1.4	Variation of Breakdown voltage of polyethylene with thickness	7
1.5	Breakdown voltage of Leatherite paper as a function of insulation thickness	8
1.6	Breakdown voltage as a function of front duration of an impulse	9
1.7	Breakdown strength of PE and it's derivative	11
1.8	Values of the filler parts and diameter where peak of the breakdown voltage occurred	11
1.9	Breakdown voltage values for Polyethylene, EVA and the mixture of the two	12
1.10	Breakdown Voltage of Nano-Dielectrics	15
2.1	Experimental Breakdown Voltages for different Insulating samples under DC test conditions	31
2.2	Experimental Breakdown Voltages for different Insulating samples under AC test conditions	36
2.3	Relative Permittivity of the Insulating Materials used	42
2.4	Statistical analysis of the DC breakdown voltage	45
2.5	Statistical analysis of the AC breakdown voltage	50
2.6	Input and the Output parameters under DC test conditions	55
2.7	Input and the Output parameters under AC test conditions	60
2.8	Summary of the range of ß under DC and AC for all materials	65
3.1	Variation of E_{tr} with η_1 ($N_h = 2$, $\alpha_1 = 0.1$, Number of iterations = 400)	92
3.2	Variation of E_{tr} with α_1 ($N_h = 2$, $\eta_1 = 0.99$, Number of iterations = 400)	93
3.3	Variation of E_{tr} with N_h ($\eta_1 = 0.99$, $\alpha_1 = 0.86$, Number of iterations = 400)	93
3.4	Comparison of the experimental and modeled breakdown voltage	94

Continued

Table No.	Table Caption	Page Number
3.5	Variation of E_{tr} with η_1 (N_h = 2, α_1 = 0.1, Number of iterations = 400)	96
3.6	Variation of E_{tr} with α_1 (N_h=2 , η_1 =0.99, Number of iterations =400)	97
3.7	Variation of E_{tr} with N_h (η_1 = 0.99, α_1 = 0.6, Number of iterations = 400)	97
3.8	Comparison of the experimental and modeled breakdown voltage	98
3.9	Variation of E_{tr} with η_1 (N_h = 2, α_1 = 0.1, Number of iterations = 400)	100
3.10	Variation of E_{tr} with α_1 (N_h=2 , η_1 =0.99, Number of iterations=400)	101
3.11	Variation of E_{tr} with N_h (η_1 = 0.99, α_1= 0.85, iter = 400)	101
3.12	Comparison of the experimental and modeled breakdown voltage	102
3.13	Variation of E_{tr} with η_1 (N_h = 2, α_1 = 0.1, Number of iterations = 400)	103
3.14	Variation of E_{tr} with α_1 (N_h=2 , η_1 =0.99, Number of iterations=400)	104
3.15	Variation of E_{tr} with N_h (η_1 = 0.99, α_1 = 0.85, Number of iterations= 400)	104
3.16	Comparison of the experimental and modeled breakdown voltage	105
3.17	Variation of E_{tr} with η_1 (N_h = 2, α_1 = 0.6, Number of iterations = 400)	107
3.18	Variation of E_{tr} with α_1 (N_h=2 , η_1 =0.99, Number of iterations =400)	107
3.19	Variation of E_{tr} with N_h (η_1 = 0.99, α_1 = 0.65, Number of iterations = 400)	107
3.20	Comparison of the experimental and modeled breakdown voltage	108
3.21	Variation of E_{tr} with η_1 (N_h = 2, α_1 = 0.7, Number of iterations = 400)	111
3.22	Variation of E_{tr} with α_1 (N_h=2 , η_1 =0.99, Number of iterations=400)	111
3.23	Variation of E_{tr} with N_h (η_1 = 0.99, α_1 = 0.75, Number of iterations=400)	111
3.24	Comparison of the experimental and modeled breakdown voltage	112

Continued

Table No.	Table Caption	Page Number
3.25	Comparison of the experimental and modeled breakdown voltage (Extrapolation Capability)	114
3.26	Variation of E_{tr} with the N_h ($\eta_1 = 0.3$, $\alpha_1 = 0.9$, Number of iterations = 400)	116
3.27	Variation of E_{tr} with η_1 ($N_h = 3$, $\alpha_1 = 0.9$, Number of iterations = 400)	117
3.28	Variation of E_{tr} with α_1 ($N_h=3$, $\eta_1 =0.3$, Number of iterations=400)	117
3.29	Comparison of the experimental and modeled breakdown voltage	118
4.1	Variation of Training error E_{tr} with number of centers m_1 ($\eta_2 = 1.98$, Number of iterations = 400)	125
4.2	Variation of Training error E_{tr} with η_2 ($m_1 = 11$, Number of iterations = 400)	125
4.3	Comparison of the Experimental and the Modeled value of breakdown voltage	127
4.4	Variation of Training error E_{tr} with m_1 ($\eta_2 = 1.96$, Number of iterations = 400)	128
4.5	Variation of Training error E_{tr} with η_2 ($m_1 = 9$, Number of iterations = 400)	129
4.6	Comparison of the Experimental and the Modeled value of breakdown voltage	131
4.7	Variation of Training error E_{tr} with m_1 ($\eta_2 = 1.98$, Number of iterations = 400)	133
4.8	Variation of Training error E_{tr} with η_2 ($m_1 = 12$, Number of iterations = 400)	133
4.9	Comparison of the Experimental and the Modeled value of breakdown voltage	134
4.10	Variation of Training error E_{tr} with m_1 ($\eta_2 = 1.96$, Number of iterations = 400)	136
4.11	Variation of Training error E_{tr} with η_2 ($m_1 = 11$, Number of iterations = 400)	136
4.12	Comparison of the Experimental and the Modeled value of breakdown voltage	138
4.13	Variation of Training error E_{tr} with m_1 ($\eta_2 = 1.96$, Number of iterations = 400)	139
4.14	Variation of Training error E_{tr} with η_2 ($m_1 = 9$, Number of iterations = 400)	140
4.15	Comparison of the Experimental and the Modeled value of breakdown voltage	141

Continued

Table No.	Table Caption	Page Number
4.16	Variation of Training error with m_1 (η_2 = 1.96, Number of iterations = 400)	142
4.17	Variation of Training error E_{tr} with η_2 (m_1 = 9, Number of iterations = 400)	142
4.18	Comparison of the Experimental and the Modeled value of breakdown voltage	144
4.19	Comparison of the Experimental and modeled breakdown voltage (Extrapolation capability)	146
5.1	Relationship between the Linguistic and the Actual values from Input 1 to Input N_i	149
5.2	Relationship between the Linguistic and the Actual values for V	149
5.3	Typical Mamdani Rule Base	151
5.4	Relationship between the Linguistic and the Actual values for t and d	155
5.5	Relationship between the Linguistic and the Actual values for V_{dc}	156
5.6	Mamdani Rule Base	157
5.7	Comparison of the Experimental and Modeled values of the Breakdown voltage	158
5.8	Comparison of the Experimental and Modeled values of the breakdown Voltage	160
5.9	Relationship between the Linguistic and the Actual values for t, t_1 and d	161
5.10	Relationship between the Linguistic and the Actual values for V_{dc}	161
5.11	Mamdani Rule Base	163
5.12	Comparison of the Experimental and Modeled values of the breakdown Voltage	164
5.13	Comparison of the Experimental and Modeled values of the breakdown Voltage	166
5.14	Relationship between the Linguistic and the Actual values for V_{ac}	167
5.15	Mamdani Rule Base	168
5.16	Comparison of the Experimental and Modeled values of the breakdown Voltage	169

Continued

Table No.	Table Caption	Page Number
5.17	Comparison of the Experimental and Modeled values of the Breakdown voltage	170
5.18	Relationship between the Linguistic and the Actual values for V_{ac}	171
5.19	Mamdani Rule Base	172
5.20	Comparison of the Experimental and Modeled values of the Breakdown voltage	173
5.21	Comparison of the Experimental and Modeled values of the Breakdown voltage	175
5.22	Relationship between the Linguistic and the Actual values for t, t_1, d and ϵ_r	176
5.23	Relationship between the Linguistic and the Actual values for Identification numbers for the materials	176
5.24	Relationship between the Linguistic and the Actual values for V_{ac}	177
5.25	Mamdani Rule Base	178
5.26	Comparison of the Experimental and Modeled values of the Breakdown voltage	184
5.27	Comparison of the Experimental and Modeled values of the Breakdown voltage	186
5.28	Relationship between the Linguistic and the Actual values for t, t_1 and d	187
5.29	Relationship between the Linguistic and the Actual values for V_{ac}	188
5.30	Mamdani Rule Base	189
5.31	Comparison of the Experimental and Modeled values of the Breakdown voltage	190
5.32	Comparison of the Experimental and Modeled values of the Breakdown voltage	191
6.1	1^{st} Order Sugeno Rule Base	194
6.2	1^{st} Order Sugeno Rule Base	198
6.3	Variation of E_{tr} with η_3 (Number of iterations = 100)	199
6.4	Comparison of the experimental and modeled breakdown voltage	200

Continued

Table No.	Table Caption	Page Number
6.5	Variation of E_{tr} with η_3 (Number of iterations=100)	201
6.6	Comparison of the experimental and modeled breakdown voltage	202
6.7	1st Order Sugeno Rule Base	204
6.8	Variation of E_{tr} with η_3 (Number of iterations=100)	205
6.9	Comparison of the experimental and modeled breakdown voltage	205
6.10	Variation of E_{tr} with η_3 (Number of iterations=100)	206
6.11	Comparison of the experimental and modeled breakdown voltage	207
6.12	1st Order Sugeno Rule Base	209
6.13	Variation of E_{tr} vs. η_3 (Number of iterations=100)	210
6.14	Comparison of the experimental and modeled breakdown voltage	211
6.15	Variation of E_{tr} with η_3 (Number of iterations=100)	212
6.16	Comparison of the experimental and modeled breakdown voltage	213
6.17	1st Order Sugeno Rule Base	214
6.18	Variation of E_{tr} with η_3 (Number of iterations=100)	215
6.19	Comparison of the experimental and modeled breakdown voltage	216
6.20	Variation of E_{tr} with η_3 (Number of iterations=100)	217
6.21	Comparison of the experimental and modeled breakdown voltage	218
6.22	1st Order Sugeno Rule Base	220
6.23	Variation of E_{tr} with η_3 (Number of iterations=400)	228
6.24	Comparison of the experimental and modeled breakdown voltage	229

Continued

Table No.	Table Caption	Page Number
6.25	Variation of E_{tr} with η_3 (Number of iterations=400)	230
6.26	Comparison of the experimental and modeled breakdown voltage	231
7.1	Comparison of the MAE of the test data for the ANN techniques (in %)	235
7.2	Comparison of the MAE of the test data for the FL techniques (in %age)	235
7.3	Comparison of the Computational Overheads for the ANN techniques (in s)	236
7.4	Comparison of the Computational Overheads for the FL techniques (in s)	236

LIST OF SYMBOLS

Symbols Used	Meaning
Q	Quality factor
ϵ_r	Real permittivity
ϵ_i	Imaginary permittivity
ζ_f	Front duration of an impulse
V	Breakdown Voltage
E_g	Dielectric Strength of air
t	Thickness of the solid insulating material
g	Air gap length
A	Constant
n	Constant
k	Constant
B	Constant
ρ_v	Volume resistivity
tan(δ)	Loss tangent
d	Void diameter
t_1	Void depth
a_1	Void radius
p_1	Gas pressure
L	Time to failure

Continued

Symbols Used	Meaning
α	Scale Factor of the Weibull Distribution
β	Shape Factor of the Weibull Distribution
ά	Maximum Likelihood estimate (MLE) of α
ß	MLE of β
f(V)	The probality density function of the breakdown voltage
$ά_l$	90% lower confidence limits for ά
$ά_h$	90% upper confidence limits for ά
$ß_{DC}$	β under DC condition
$ß_{AC}$	β under AC condition
S(x)	Sigmoidal function
N_h	Number of hidden neurons in MFNN
N_i	Number of input neurons in MFNN

Continued

Symbols Used	Meaning
N_p	Number of training patterns
N_k	Number of neurons in output layer in MFNN
η_1	Learning rate in the MFNN
α_1	Momentum factor of the MFNN
w_b	Weights between hidden and the output layer in the MFNN
$\delta_k(m)$	Error for the k^{th} output at m^{th} iteration in the MFNN
S_b	Output from hidden layer in MFNN
w_a	Weights between hidden and input layer in the MFNN
$\delta_j(m)$	Error for the j^{th} output at m^{th} iteration in the MFNN
E_{tr}	Mean Square Error for training patterns in MFNN, RBFN and ASFL structures
V_1	Experimental value of breakdown voltage taken for training in MFNN, RBFN and ASFL structures
$V_2(m)$	Modeled value of the trained breakdown voltage after m^{th} iteration in MFNN, RBFN and ASFL structures
E_{ts}	Mean Absolute Error of the test data
N_s	Number of testing patterns
V_3	Experimental value of breakdown voltage taken for testing in MFNN, RBFN , ASFL and MFL structures

Continued

Symbols Used	Meaning
V_4	Modeled value of the tested breakdown voltage in MFNN, RBFN , ASFL and MFL structures
G	Fixed Radial Basis Functions
m_1	Number of chosen centers in the RBFN structure
d_{max}	Maximum distance between chosen centers in the RBFN structure
w_{aj}	Weights between the hidden layer and the output layer in the RBFN structure
$e_1(m)$	Error at the m^{th} iteration in the MFNN, RBFN and ASFL structure
η_2	Learning rate in the RBFN structure
R_1	Number of rules in MFL and ASFL structure
r_1	Variable ranging from 1 and R_1
w_{r1}	Firing strength of the r_1^{th} rule in the ASFL structure
w	Sum of the firing strengths in the ASFL structure
a_{r1m}, b_{r1m}, s_{r1m}	Coefficients of the thickness of the material, void depth and void diameter in the first order function for the r_1^{th} rule after m^{th} iteration in the ASFL structure
η_3	Learning rate in the ASFL structure
Ł	Set of linguistic values assigned to t and d in ASFL and MFL structure

Continued

Symbols Used	Meaning
$Ł_1$	Set of linguistic values assigned to t_1 in ASFL and MFL structure
$Ł_2$	Set of linguistic values assigned to $Є_r$ in ASFL and MFL structure
$Ł_3$	Set of linguistic values assigned to Identification number I in MFL and ASFL structure
μ_t, μ_{t1} and μ_d	Membership function assigned to t, t_1 and d in MFL and ASFL structure
μ_V	Membership function assigned to breakdown voltage in MFL structure
μ_{R1}	Clipped Fuzzified MF of the r_1^{th} rule in the MFL structure
$\mu_{A1}(V)$	Aggregated Fuzzy MFs for the MFL structure

Chapter 1

INTRODUCTION AND LITERATURE SURVEY

1.1 Introduction

With ever-increasing demand of electrical energy, the power system is growing both in size and in complexity. The generating capacities of power plants and application of high voltage has intensively increased due to it's inherent advantages, such as, greater efficiency and cost effectiveness. It is, thus essential to know the property of the insulating materials for optimum solution in terms of cost and insulating capability. Moreover, the reliability of power supply is ensured by having a reliable insulation system.

Under normal working conditions, insulation gradually loses its dielectric strength and overvoltage capacity because of general aging as well as due to local defects appearing in the form of voids in the insulation during manufacture, particularly in extruded and cast type insulation. The quality of a solid insulation is judged in several ways, such as, hydrophobicity, electroluminescence, crystallization kinetics, hygrothermal, chemiluminescence and breakdown voltage. Out of these, the breakdown voltage continues to evoke a lot of interest to the Electrical Engineers in general and High Voltage Engineers in particular. There are several potential applications of solid insulating materials such as, the underground cables, rotating machines, transformers and overhead transmission lines. Moreover, as the demand for electrical power is growing in the 21st century, better quality insulating materials starting from the generation to the distribution is a bare essential necessity. Hence, it is extremely important to develop solid insulating materials with excellent breakdown strength and any attempt at modeling the phenomenon with the presence of void would go a long way in assessing the insulation quality.

1.2 Breakdown of solid insulating materials

Fothergill [1] very clearly differentiates between the breakdown and degradation of a solid insulating material. According to him, the breakdown is an event that is sudden and

catastrophic and the insulation cannot withstand the service voltage following the breakdown. The degradation, on the other hand takes place over a period. It increases the probability of breakdown and decreases the breakdown voltage, erosion and pit formation are important in the degradation process and are followed by tree formation and/or final dielectric failure. The degradation process after a period of hours to weeks, leads to breakdown. Well-designed insulation systems, operated within the scope of design parameters, do not break or degrade. Both these processes are irreversible. Table 1.1 shows some of the differences between degradation and breakdown for a solid insulating material.

Table 1.1: Differences between Degradation and Breakdown for a solid insulating material [1]

Features	Breakdown	Degradation
Effect	Catastrophic insulation cannot be used afterwards	Leads to breakdown, reduces breakdown voltage
Speed	Fast occurs in << 1s	Hours, years
Evidence	Direct observation normally by eye	Observation would require microscope
Examples	Intrinsic, Thermal, Electromechanical, Electrochemical, Partial Discharge in cavities	Electrical Trees, Water trees

Figure 1.1 shows the variation of breakdown strength on application of voltage with time.

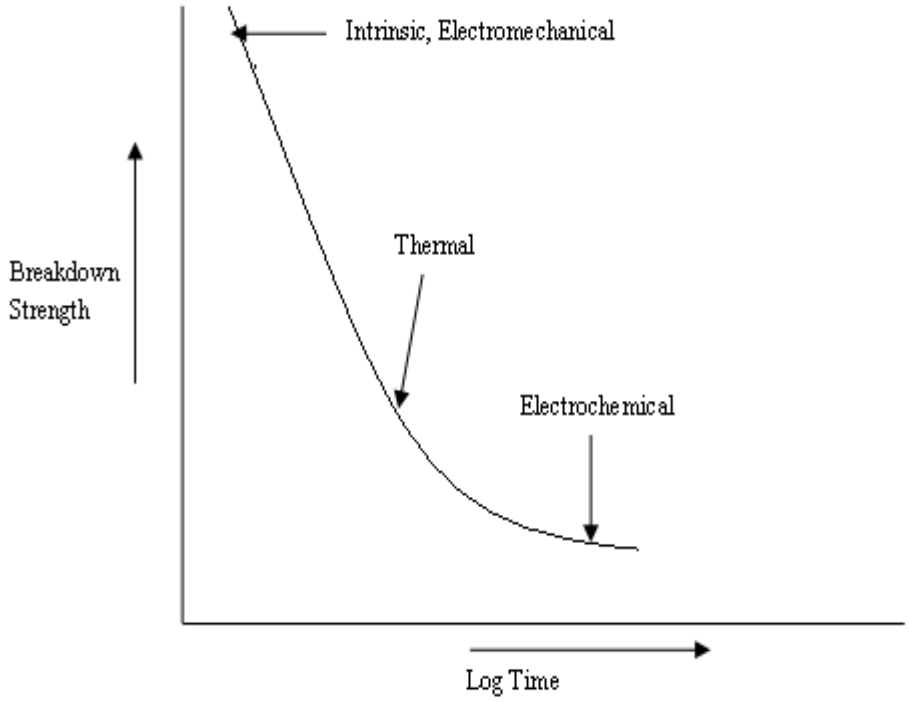

Fig.1.1: Variation of breakdown strength on application of voltage [2]

1.3 Factors affecting breakdown of solid insulating materials

The breakdown of solid insulating materials depends on the following factors:

- **Nature of Waveform**

The breakdown voltage of solid insulating material depends on the nature of the voltage waveform applied to , i.e., DC, AC & impulse [3-10]. Some important observations from the literatures are presented below:

i) The breakdown voltage of Cross-Linked Polyethylene (XLPE) [5] in the quasi-homogenous field strongly depends on the polarity and level of pre-applied DC voltage (impulse voltage superimposed on DC voltage). The insulation thickness in the range of 50 μm to 200 μm does not have a significant influence on breakdown behavior.

ii) The DC and AC breakdown voltage of Electro-active Paper [6] varies with the relative humidity levels. The shape parameter represents the slope of the Weibull plot. It is descriptive of spread of results of breakdown data. The smaller the value of shape parameter, the larger is the spread of results. The scale parameter represents the characteristic value, which

represents a cumulative probability of 63.2%. The larger value of scale parameter represents that average breakdown strength is higher.

iii) The breakdown voltage of Polyethylene Terephthalate Thermoplastics under DC and AC conditions has been studied by Grzybowski et. al [7]. It is found that the DC breakdown voltage of dry samples is much higher than that of AC voltage. This is due to increased dielectric losses occurring at high frequencies, which results in earlier failure of the insulation at low AC voltage. The DC breakdown voltage degraded significantly as a result of the water absorption. On the other hand, the reduction of AC breakdown voltage exposed to the water absorption was less significant in comparison to DC voltage. Table 1.2 shows the test results at different types of voltage and test conditions.

Table 1.2: Test results of PET Thermoplastics [7]

Breakdown Voltage Test	Maximum Breakdown Voltage (kV)	Average Breakdown Voltage (kV)
DC-Dry	97.2	80.7
DC-Wet	22.1	18.5
AC-Dry	37.9	34.7
AC-Wet	29.1	24.1

iv) The V-t Characteristics of polyurethane sample has been studied under AC conditions in [8]. The V-t characteristics of the polymer comprises of three zones. The first zone signifies the defects of the youth and is characterized by very fast discharges occurring in the cavities. The size of these defects of extrinsic type plays an important role in this zone. The size of the defects is big . A term known as voltage endurance constant is defined. This constant depends on the type of material and is an indication of the insulation quality. The value of the voltage endurance constant is closely related to the type of polymer decomposition. In the first zone, this value has been found out to be 15.96. The second zone represents the statistical dispersion of the intrinsic defects of the material. An intrinsic defect could be a microcavity due to lack of control during the polymerization. The discharge mechanism in the second zone changes with respect to the first zone. Thin layer of oxidation products is the main cause for changing the mechanism of discharges. These products are formed by the attack of the discharge at

dielectric surface. The discharge mechanism changes into a slower type of discharge and hence the voltage endurance constant revealed a relatively small value that is 1.66. The third zone is the real aging of the polymer, which is characterized by the formation of crystals. The discharges in the cavity now concentrate on some of these crystals. At the spots, where these discharges concentrate, a severe deterioration of dielectric takes place. The dielectric material is lost and this zone is the destructive zone. Hence, the voltage endurance constant value again picks up and becomes 7.34. The polyurethane is used as an insulating material in rotating machines.

v) The DC breakdown strength of Low Density Polyethylene (LDPE) is influenced by the microstructure of the polymer (crystallinity, crystal grain size) and the test conditions, such as, electrode material, temperature and humidity [9]. Due to the large surface rate and the surface energy of nano-SiO_x, there is a strong interaction between nano-SiO_x and Polyethylene resulting in physical cross-linking in the polyethylene matrix. Hence, the DC breakdown strength of the mixture increases.

vi) The impulse and the DC strength of Poly-p-xylene (PPX) film with 4 μm thicknesses are 5.9 & 4.1 MV/cm respectively [10]. The breakdown of the PPX film is due to electronic avalanche mechanism. The DC prestressing for a long time of 60 s has reduced the impulse breakdown strength for both the same and opposite polarity. Nevertheless, the DC prestressing for a short time less than 1 s increased the impulse breakdown strength for the same polarity. These results were explained by the positive space charge in the PPX film. The positive space charge from the anode plays an important role for the impulse breakdown strength.

vii) The high-density Polyethylene (HDPE) and Polypropylene random copolymers (PPR) exhibited the highest breakdown strength among Polyolefin [11]. The impulse breakdown strength of HDPE was 1.6 times larger than the conventional cross-linked polyethylene (XLPE). The impulse breakdown strength of HDPE improved due to improved crystallinity of the insulating material, brought about by heat annealing. The impulse breakdown strength is related with the annealing temperature of the cable. The breakdown characteristics are dependent on the thermal histories given under the higher temperature of their melting temperature. The reason of this remarkable improvement is thought to be the result of crystalline change of polyethylene caused by the annealing process in the melting state and cooling process.

- **Frequency**

The variation of frequency has an important role to play in affecting the breakdown voltage of solid dielectrics. Some observations made in this regard are:

i) The breakdown voltage at higher frequencies is much lower than the breakdown voltage at 50 Hz [12-13]. This is due to increased internal heating as well as intense partial discharges within the material.

ii) Elanseralathan et. al. have studied the breakdown voltage of solid insulating materials for airborne equipments at high frequencies [12]. The solid insulating materials are used for airborne equipments, such as, radar transmitters and power conditioning system for aircrafts. As the frequency increases, the weight of these airborne equipments reduces. Table 1.3 shows the variation of the breakdown voltage of some solid insulating materials at 50 Hz and higher frequencies.

Table 1.3: Breakdown voltage of solid dielectrics at different frequencies [12]

Material	PTFE	Polypropylene	Paper
Thickness(μm)	12.5	12.5	10
Breakdown Voltage at 83 KHz (V)	551	565	380
Breakdown Voltage at 50 Hz (KV)	1.1-2.18	2.46	1.58

- **Ageing**

The breakdown voltage of an insulating material, in general, decreases with the ageing of the dielectric. Three popular models have been discussed in the ageing process, such as, inverse power model, thermodynamic model and exponential model [13]. The ageing model constants for polypropylene film depend on the applied voltage and frequency. The deterioration process is due to the acceleration of the partial discharges and heat build up in the voids and micro-cavities of the insulating material when frequency is increased. With

increasing frequency, constant n of the power model remains constant. The inverse power model equation is given by

$$L = k^* V^{-n} \quad (1.1)$$

Where L= time to failure

V= Applied Voltage

k and n are constants determined from the experimental data.

- **Thickness of the Dielectric Material**

The thickness of the dielectric material affects the breakdown voltage [14-15]. The short time electric strength is more dependent on the thickness than the area of the samples [14]. Table 1.4 shows the effect of change in thickness on the breakdown voltage of the polyethylene.

Table 1.4: Variation of Breakdown voltage of polyethylene with thickness [14]

Thickness (mm)	Breakdown Voltage (air) (V/μm)
3.1	33
1.5	28
0.18	72
0.09	122

The breakdown voltage of the Leatherite paper varies with the insulation thickness in the presence of artificially created void [15]. Table 1.5 shows the variation of the breakdown voltage obtained by a step-stress test with the given insulation thickness for the time step of 15 s. The void depth and the void diameter are considered as 0.2 mm and 2 mm respectively. In addition, it is observed that the breakdown voltage decreases with the increase of the step duration of the accelerated Step-Stress test.

Table 1.5: Breakdown voltage of Leatherite paper as a function of insulation thickness [15]

Insulation thickness (mm)	Breakdown Voltage (kV)
0.175	3.8
0.225	4.1
0.3	4.1

- **Lamellar Growth**

The oriented lamellar growth at the interface and the local lamellar texture affects the breakdown voltage of XLPE cables insulation [16-17]. An interfacial diffusion method was devised to reduce the insulation thickness by improving the interfacial properties of XLPE cable [16]. This method is based on a proposed concept of the facilitation of the oriented lamellar growth at the interface by the addition of special ingredients to the semi-conducting layer. The oriented lamellar growth increases the breakdown strength of the XLPE insulation. It is confirmed that there is a strong correlation between average lamellar angle and the degree of the vertical orientation.

- **Electrode Gap Spacing**

The breakdown voltage of Silicon Rubber with different electrode gap spacing is reported in [18]. The gap spacing considered is 5, 10 and 20 mm. At each of this gap spacing, five values of breakdown voltage are noted and the average of these five readings is taken. It is found that at 5, 10, and 20 mm, the breakdown voltage strength is 30 kV/mm, 20 kV/mm and 15 kV/mm respectively. This clearly indicates that the breakdown voltage strength decreases with the increase in the gap spacing.

- **Complex Permittivity**

The complex permittivity and the loss factor, tanδ of a solid dielectric are directly proportional to each other and inversely proportional to the quality factor. The complex permittivity comprises of a real permittivity ϵ_r and an imaginary permittivity ϵ_i. The minimum of the breakdown voltage for Polyethylene Terephthalate (PET) film is conditioned by the decrease in the quality factor given as [19]

$$Q = 1/\tan\delta = \epsilon_r / \epsilon_i \qquad (1.2)$$

The decrease in the quality factor is related with the complex permittivity dispersion at different frequencies. Hence, at low frequencies where the complex permittivity dispersion is absent, the breakdown voltage variation is practically negligible. This is quiet evident from Table 1.6, where the values of the breakdown voltage are unchangeable for PET when the front duration of the voltage impulse ζ_f changes from 36 ms to 5000 ms. It may be noted that the range 36 ms to 5000 ms corresponds to 0.2 Hz to 28 Hz (low frequencies).

Table 1.6: Breakdown voltage as a function of front duration of an impulse [19]

ζ_f (ms)	5000	1630	528	287	177	76	36
Breakdown Voltage(KV)	16.6	16.8	16.3	16.7	16.2	16.7	16.4

- **Partial Discharge in cavities**

It has been well recognized in the past that one of the most common causes for insulation system failure occurs from void inclusions, which are usually introduced during the various manufacturing steps associated with the formation of insulating materials. The breakdown voltage of a solid insulating material depends on the Partial Discharge (PD) in cavities. This will be discussed in details in a different section of this Chapter.

1.4 Breakdown voltage study of composite solid insulating materials

In recent times, some interesting articles are published in the literature on the breakdown voltage of composite solid insulating materials, which are discussed briefly. In all

[20-35] cases, it is found that the breakdown strength increases, when a material is added to the base solid insulating material.

- **Solid - Solid Composite insulating material**

i) The Silane Cross-linked Polyethylene (SXLPE) has higher AC breakdown voltage than DCP XLPE [20]. The SXLPE has hard quality due to the introduction of Silicone and can be used for abrasion resistant cables.

ii) The AC electrical breakdown strength of five aromatic polymers at different film thicknesses was measured in Dibutyl Phthalate [21]. The breakdown field strength for thick samples showed a linear decrease with increasing sample thickness for all polymers except Poly Ether Ether Ketone (PEEK). The breakdown strength of thin samples is independent of the polymer structure. Under DC conditions, the breakdown field strength of polymers and the chemical structure had no correlation.

iii) The AC breakdown strength in PE is modified by grafting and blending techniques [22]. The grafted PE is of two types, such as, Acrylic Acid- grafted PE (LDPE-g- AA) and N-butyl-acrylate-grafted PE (LDPE-g-NBA). In LDPE-g- AA, heterocharge observed in PE decreases at low AA contents & homocharge is observed at high AA contents. In LDPE-g-NBA, heterocharge gets larger at all graft ratios of 0.12%. The AC breakdown voltage of grafted samples is higher than the controlled samples.

iv) The breakdown strength of the PE film is induced by the electron avalanche [23]. Additives can reduce the conduction current through the film, in high electric field region. The reduction of current is due to trapping effect or the excitation effect of the additive. Table 1.7 shows the breakdown strength of PE and it's additives at 10^{-6} mol/gm (concentration of additive).

Table 1.7: Breakdown strength of PE and it's derivative [23]

Polyethylene & it's derivatives	Breakdown voltage (MV/cm)
PE	4.5
PE/ab	5
PE/nb1	6
PE/nb2	7

v) The impulse breakdown strength of alumina filled epoxy resin has been studied as a function of the diameter of the filler and filler parts [24]. The peak of the treeing breakdown voltage of epoxy resin appeared with increasing the quantity of filler in spite of filler diameter. Table 1.8 shows the value of the diameter of the filler and filler parts where peak of the breakdown voltage occurred.

Table 1.8: Values of the filler parts and diameter where peak of the breakdown voltage occurred [24]

Filler parts	Diameter of filler (μm)
40	5
30	250
20	500

vi) Mineral oil, Synthetic oil or SF_6 gas are commonly used as an insulating material in many pieces of electric equipment in power substations. However, considering that demands of electricity are large in urban areas, use of oils would cause a concern for environmental protection. Furthermore, SF_6 is known to cause a severe greenhouse effect. However, the interfacial breakdown strength of a mixture of Silicon Rubber and Epoxy Resin has been studied using two types of model samples. This composite dielectric can be used for future power substation system as it is environment friendly [25].

vii) The biomaterials have attracted attention due to environmental problems [26]. One such example is the bamboo pulp-ice composite system, which is an alternative to glass fiber reinforced plastics (GFRP). The bamboo naturally decomposes and is characterized by

excellent elasticity and water absorption properties. The AC breakdown strength of the bamboo-ice composite system depends on the amount of water absorption of bamboo and increases with increasing water content.

viii) The breakdown strength of a three layer solid dielectric, in which the middle layer (barrier) has higher permittivity, is a function of the ratio of the permittivities of the barrier material to the insulating material and the ratio of the thickness of the barrier material to the insulating material [27]. The breakdown process in this composite solid dielectric material is due to the barrier effect which is lengthening the path of breakdown channel due to the increasing tangential component of the electric field vector at the interfaces.

ix) The breakdown voltage study of mixing a polar material, such as, Ethyl Vinyl Acetate (EVA) with polyethylene has been presented in [28]. EVA with polyethylene suppresses tree growth and enhances insulation lifetime. This type of dielectric material can be used for high voltage insulations. Table 1.9 shows the breakdown voltage values of Polyethylene, different varieties of EVA and the mixture of the two.

Table 1.9: Breakdown voltage values for Polyethylene, EVA and the mixture of two [28]

Materials	State of the material	Breakdown Voltage (kV/mm)
PE1	Quenched	145
EVA09	Quenched	135
EVA40	Quenched	77
Blend 1	Quenched	135
Blend 4	Quenched	93

- **Liquid - Solid Composite insulating material**

The breakdown voltage is improved by adding a liquid material to a solid insulating material and some literature review on this is presented below:

i) The dielectric breakdown strength of Polypropylene (PP) film increased from 640 V/μm to 810 V/μm, when the oil is diffused into the amorphous regions of the PP film [29]. This oil-impregnated propylene can be used for the high voltage capacitors. For further development of impregnated PP films the solubility of the oil in PP should be high enough to fill up the free volume of polymer completely.

ii) When solid cellulose fibers are mixed with insulating mineral oil medium, a composite insulating material known as transformer board results. This composite material gradually ages as compared to the solid cellulose fiber. It has been shown in [30] that after 29 years of service, the ageing has reduced the AC electric strength and AC withstand strength of transformer-board by 40 % and 25%. When the moisture content in the board is less than 4%, there is no change in the AC electric strength and AC withstand strength. This insulating material can be used for power transformer insulation.

iii) The comparison between the breakdown strength of ester impregnated cellulose with mineral oil impregnated cellulose has been carried out by D. Martin et. al [31]. When the ester oil is impregnated with cellulose, there is a matching of the dielectric constants of the ester oil and cellulose and the electric field is equally shared. Hence, the ester-impregnated cellulose has more breakdown voltage compared to the mineral oil impregnated cellulose.

- **Gas - Solid Composite insulating material**

Y. Kamiya et. al [32] presented an interesting article dealing with SF_6 impregnated SiR . The effect of the Secondary Cross-linking Treatment (SCLT) and vacuum treatment on the tree initiation voltage has been discussed. The main observations concerning the breakdown voltage are:

i) The SCLT volatizes low molecular weight components from SiR and improves the physical strength.

ii) Without vacuum evacuation, the breakdown strength of SF_6 impregnated SiR is greater than the untreated specimen. This is because SF_6 is an electronegative gas. SF_6 in free volume captures electrons by attaching and the number of electrons contributing to the electrical tree initiation is decreased. The number of electrons in air filled SiR Specimen reaching polymer chains is higher than that in SF_6 filled one. Hence, the electrical tree initiation voltage increase is expected in SF_6 impregnated SiR.

iii) This kind of solid insulating material can be used particularly for cable joints in power transmission lines.

1.5 Breakdown voltage behaviour of Nano-insulating material

The Nano materials in recent times have found lot of applications in all fields of Engineering and Electrical Engineering field is no exception to it. The researchers enlighten the breakdown voltage behaviour of Nano-insulating materials. Some of them are as follows:

i) The Nano-composites based on the clay systems have been widely investigated by T.M. Mathison et. al [33]**.** The breakdown voltage of organo-modified inorganic Nanofillers boehmite and montmorillonite in an epoxy matrix has been studied and it is found to decrease. This is because of the extent of the dispersion existing in the material on addition of the fillers. This material can be used in the high voltage industry.

ii) The effect of the layered Silicates on the breakdown voltage of Polyethylene has been investigated by Green and Vaughan [34]. The layered silicates offer improvement to partial discharge resistance in polyamide and hence the breakdown voltage of the layered silicates with Polyethylene increases. Also, it is found that isothermally crystallized material had more breakdown strength than it's quenched counterpart. This type of Nano-dielectric material can be used as insulation in the rotating machines. Table 1.10 shows the breakdown voltage of polyethylene and layered silicate mixed with polyethylene.

Table 1.10: Breakdown Voltage of Nano-Dielectrics [34]

SL No.	Materials	Breakdown Voltage (kV/mm)
1.	U (Quench)	171.4
2.	U(117 ºC)	190.6
3.	UC30PE(quench)	178.6
4.	UC30PE(117ºC)	180.6
5.	M (Quench)	174.1
6.	M2101(quench)	190.4

iii) The DC breakdown strength of Thermoplastic Polyetherimide (PEI) film and various Nanofilled PEI films has been compared in [35]. The semiconductive and partially oxidized Aluminum fillers lead to lower breakdown voltage compared to the virgin PEI film. However, the insulating fillers added to the PEI had a breakdown voltage almost the same as the breakdown voltage of PEI. In addition, it is found that the interfacial interaction of ceramic polymer plays an important role in the breakdown voltage of the Nanocomposite.

1.6 Breakdown due to PD in cavities

The Partial Discharge study has been an important topic in the field of solid insulations over the past few decades, which is very much evident from the large number of papers associated with it [36-46]. It is well known that voids within the solid insulating materials are the main sources of Partial Discharge (PD). These voids or cavities are essentially gas-filled and can result from many causes. In case of epoxy castings, gas-filled cavities can be caused by air leaking into the mould during curing. If the voltage between the electrodes is raised to the point that the field within the cavity goes above the breakdown strength for the gas within the cavity, a PD can take place. The time taken for breakdown to occur depends on the applied

voltage and the size of the cavity [47-48]. If an electron is present within the critical volume of the cavity, the electron is accelerated in the electric field and produces electron gain during collisions with other molecules. The electron grows exponentially resulting in the development of a streamer. A resistive channel is developed across the cavity in few ns. The conductivity of the streamer reduces the field across the cavity. The streamer dies, once the field across the cavity drops below that necessary to support the streamer, leaving large quantities of positive and negative charges. At the end of the PD process, the field in the cavity can be reduced to zero. If the field in the cavity is reduced to zero, electric field in the solid insulating sample is the same as if the cavity is filled with a conductor. Filling the cavity with a conductor would cause an increase in the capacitance between electrodes, which would cause a flow of charge into electrodes for a constant voltage across them. The charge, which flows into the electrodes, is the apparent PD magnitude.

It is found that the magnitude of the PD in insulating materials due to voids and thus breakdown due to PD in cavities, Partial Discharge Inception Voltage (PDIV) [49-72] and Partial Discharge Extinction Voltage (PDEV) is affected by several factors listed below:

- **Thickness and relative permittivity of the insulating Material**

The authors [14, 49-52] have developed mathematical relationships between the breakdown voltage due to PD in cavities, and with the thickness and relative permittivity of the material. In what follows is a brief description of those relationships:

i) Naidu et. al [50] have shown that the breakdown voltage due to PD decreases with the increase in thickness of the material. It depends on the dielectric strength of air, E_g, the relative permittivity, ϵ_r and the thickness, t of the material and the air gap length, g as

$$V = A*Eg*(g + t/\epsilon_r)^n \qquad (1.3)$$

Where A= 0.9508 and n=0.3496.

ii) Mason [51] and Dakin [52] have shown that the breakdown voltage due to PD depends on the thickness, t and the relative permittivity, ϵ_r of the material as

$$V = k*(t/\epsilon_r)^{0.46} \qquad (1.4)$$

where k = 0.2

The square-edged rod electrodes in air at 0.1 Mpa is taken for the purpose and the materials considered are Polyethylene (ϵ_r = 2.25), Mylar (ϵ_r = 3.2), Polymethyl Methacrylate (ϵ_r = 3.4), Zircon Ceramic (ϵ_r = 5.3), Alumina Ceramic (ϵ_r = 8.3) and Mica (ϵ_r = 3.4).

- **Void depth and size**

Nossier [53] has shown that the Partial Discharge Inception Voltage (PDIV) generally decreases with the increase in the void depth t_1. The analytical expression for the PDIV has been developed at atmospheric pressure for three different positions of void, that is, void at sheath, void at mid-dielectric and the void near the conductor surface. Figure 1.2 shows the geometrical configuration of the cable. The nearer the void was to the conductor, the smaller is

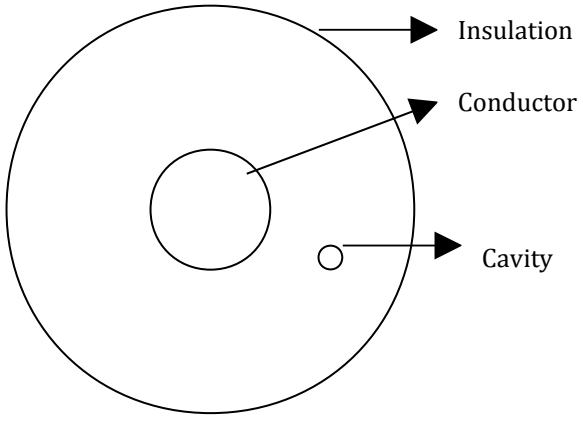

Fig. 1.2: Geometrical configuration of the cable

the PDIV. Since PDIV decreases with the increase in void depth t_1, it can be safely inferred that breakdown voltage due to PD in cavities would also decrease with increase in t_1.

- **Void shape**

The PDIV also depends on the void shape as can be seen from [54-57]. Crichton [55] has calculated this voltage for ellipsoidal and spheroidal voids. Reynolds [56] has calculated the PDIV of Polyethylene and Mylar with spheroidal voids of natural and artificial nature.

- **Nature of Voltage waveform**

The voltage waveform can also affect the PDIV [58-61].

i) F.S.Ahmed & A.S. Ahmed [59] have determined the PDIV using an IEC electrode geometry with sinusoidal voltages of 1 to 60 kHz and pulse repetition rate of 15.625 kHz.

ii) Densley [60] has analysed the PD phenomena in artificial air filled cavities of Polyethylene. During the initial test, 50% impulse inception stress was found to be much higher than discharge stress calculated from Paschen's curve. A main discharge occurs on or near the crest of the surge.

- **Immersion medium**

The breakdown voltage due to PD in cavities, PDIV and PDEV of insulating material is greatly influenced by an immersion medium such as Helium and Liquid Nitrogen [62-65] and some salient features of these literature are :

i) Schwenterley [62] have evaluated a thin polymer film insulation for use in superconducting underground transmission cables. The PDIV of three-layer disc samples of Polyethylene and 61 μm Polycarbonate with Helium impregnation ranging from 5.0 ^{o}k and 0.3 MPa to 11.5 ^{o}k and 1.5 MPa have been observed. The butt gaps are simulated by punching 1 mm diameter holes in some of the layers. The observed voltage varies strongly with the Helium conditions, increasing rapidly with the increase of the density.

ii) Densley [63] have determined the PDIV and PDEV of film-type and fibrous materials in Liquid Nitrogen. Generally, it is found that the PDIV and PDEV increases when these materials are dipped in Liquid Nitrogen. These materials can be used in electric power apparatus.

iii) A high temperature superconducting (HTS) cable has used a composite material involving Liquid Nitrogen / Polypropylene (PPLP) for which the PDIV is found [64]. The initial PD varies from 2 to 30 pC irrespective of the void condition. The PD Inception strength without the void was 5-10 % higher than that with the void.

iv) The breakdown voltage due to PD in cavities of some solid insulating materials has been predicted by Masood et. al. [65] in a medium of Liquid Nitrogen. The breakdown voltage for Crepe paper, Kraft Paper, Varnished Paper, pressboard, mica, bakelite, asbestos is found to be depending on the volume resistivity ρ_v, relative permittivity, ϵ_r and loss tangent tanδ.

The breakdown voltage is expressed by

$$V = A + B*\log (\rho_v / \epsilon_r * \tan\delta) \quad (1.5)$$

Where A and B are constants.

- **Void diameter**

The PDIV versus void size for a sphere-shaped void has been analyzed. It is seen that the PDIV decreases from 300 V/mm to 100 V/mm in a hyperbolic manner when void diameter increases from 1 to 10 mm[66] .

- **Temperature**

i) In [67] the PD investigations on epoxy-resin impregnated transformer coils have been carried out between -30^{o}c and 180^{o}c. The PD measurements show that the PDIV decreases with rising temperature. This is explained with the superposition of two temperature-dependent phenomena. First of all, the temperature dependent rising values of relative permittivity of epoxy resin strengthens electric field inside the cavity and secondly, the ignition condition in the void changes due to diffusion.

ii) Schifani et. al [68] has shown the effect of temperature on PD activity taking place inside spherical void in epoxy resin. It is also inferred that the PDIV decreases with the increase of temperature.

- **Void orientation**

In addition to the void shape, size, depth and diameter, the void orientation parallel & perpendicular to the axis of rotation plays an important role in the PDIV [69]. It is found that when the applied field is parallel to the void axis of rotation, the magnitude of the PDIV is higher than that when the applied field is perpendicular to the void axis of rotation.

- **Gas and the gas pressure within the void**

It has been shown by Boggs [47] that the PDIV in spherical voids in air is given by

$$V= (1+8.6/[\sqrt{(2*a*p_1)}])*(24.2*p_1) \quad (1.6)$$

Where p_1 is the gas pressure in Pascal and a is the cavity radius in meters.

Similarly, if air is replaced by SF_6, the PDIV is given by

$$V= 88.6*[p_1+ (2/a)] \quad (1.7)$$

Equation (1.6) indicates that the PDIV in SF_6 is greater than the PDIV in air obtained from equation (1.5).

From the aforesaid discussion, it is very clear that several factors can influence the breakdown due to PD in cavities, PDIV and PDEV. Prior to breakdown, the PD phenomena can subject to degradation of a solid insulating material. Due to degradation, two things can happen to a solid insulating material [70-72]. First of all, activated O_2 formed by the discharge is able to oxidize surface of the insulating material and yields H_2O and CO_2. Secondly, ozone with long life diffuses into the material to form an ozonide by reacting with a terminal double bond. The degradation and breakdown of a solid insulating material due to PD phenomenon can be observed very easily with the help of a Scanning Electron Microscope (SEM). It will be discussed in more details in the next Chapter.

1.7 Breakdown voltage prediction due to PD in cavities

The breakdown voltage due to PD in cavities is a nonlinear phenomenon. This is very evident from equations (1.2) to (1.6) and the magnitude of this voltage is critical for judging the quality of the insulation for industrial purpose. However, it is extremely difficult to predict this voltage. Hence, it is necessary to resort to the process of modeling in order to predict the magnitude of this breakdown as a function of different variables. Some literature can be found in which this voltage is predicted as a function of the thickness of the material [14-15, 21, 73] or as a function of position, size and shape of the void [47]. All these models described there are essentially conventional models, which are extremely rigid. However Kolev & Chalashkanov [74] have proposed an ANFIS structure for the prediction of the PDIV and PDEV using the experimental data from CIGRE Method II Electrode System provided in [75]. Similarly Ghosh & Kishore [76-77] have proposed ANN models for predicting the PDIV and PDEV of insulation samples. Hence, the rigidity in the conventional models have been appropriately taken care of by utilizing an ANFIS and ANN structure respectively.

The conventional models, which solve any application oriented problem, either involve the use of classical approximation theory or the development of quasi-empirical relationship. The classical approximation theory is the branch of mathematical analysis, studying methods for approximating some mathematical objects by others and studying questions related to the research and estimation of errors, which arise there. It deals with the approximation of real-valued functions on real intervals by certain basic functions, like ordinary or trigonometric polynomials and the Splines [78]. The Kernel based approximation [79], linear approximation method [80], Partial Least Square (PLS) regression [81] also belong to the classical approximation theory. The conventional method of solving any particular issue has it's limitations, as it is only valid for the range of input variable considered. Hence, these methods are inherently rigid in nature and there is hardly any scope of making it flexible.

The Soft Computing (SC) model on the other hand is highly flexible and a model can be improved simply by providing additional training data [82-83]. In addition, this kind of model can be developed more accurately in a shorter time. The SC is an emerging approach to computing which parallels the remarkable ability of the human mind to reason and learn in an environment of uncertainty and imprecision [84]. The SC approach consists of several computing, paradigms such as Artificial Neural Network (ANN), Fuzzy Logic (FL), approximate reasoning, derivative-free optimization methods, such as, Genetic Algorithms (GA) and Simulated Annealing (SA). The seamless integration of all these paradigms forms the core of

SC, which is aimed at solving real-world decision-making, modeling problems. These problems are usually imprecisely defined and require human intervention. Thus, the SC with their ability to incorporate human knowledge and adapt their knowledge base via optimization techniques play an important role in the design of intelligent systems.

1.8 Soft Computing applications to Insulation diagnosis

Apart from the breakdown voltage prediction due to PD in cavities, PDIV and PDEV the SC techniques can also be utilized for other types of insulation diagnosis issues. These issues are provided in details below:

- **Lifetime prediction of solid insulating materials**

Khachan & Laghari [85] have proposed an inverse power model in order to predict the lifetime of three capacitor dielectrics, namely polypropylene, polyimide and poly vinylidene fluoride. This model is essentially a conventional model which had the limitation mentioned in Section 1.7. On the other hand M. Hammer et.al. [86-87] have proposed two SC techniques one based on the ANN structure and the other based on the FL structure in order to predict the lifetime of Relanex. This insulating material can be used for the Electrical Machine windings. The ANN structure could provide an adaptive system and the FL structure could deal with imprecision and uncertain data [88] by fuzzifying the input output patterns.

- **Detection of Electrical Trees**

The detection of electrical trees can be considered to be the most important way of monitoring the degradation occurring in a solid insulating material. In order to detect the electrical trees, A. Samee et. al [89] have described an aging model which is based on the concept of generation of micro-voids due to thermally activated, electrically-enhanced breakage of bond structure of polymeric insulation. Also Noskov et. al [90] and K. Wu et. al [91] have proposed a model of PD development for the detection of electrical trees. This model is based on the concepts of electric field redistribution, charge transport and channel conductivity during the propagation of PD along channels. Both the above mentioned models had an inherent drawback, as the detection of electrical trees was by trending of PD data and

are hence they are essentially data driven models [88]. In addition, noise and other PD sources (corona from nearby high voltage conductors, PD in test equipment), contribute frequently to PD measurements, the PD generated due to trees is obscured. But A. Cavallini et. al.[92] have suggested that instead of trending the PD data, it is better to study the behaviour of the times between PDs. The inter-times have been analyzed by a fuzzy engine as a basis to infer the presence of electrical trees.

- **PD pattern classification**

The PD pattern classification issue in solid insulating materials has also some interesting literature recently [93-102]. A model suggested by Kranz & Krump [93] has performed a statistical analysis of charge, energy and phase angle on measured PD signals. A PC aided PD evaluation high speed electronic device for on-line measurement and digital conversion of PD signals has been used for implementing this model. The demerit of this approach is that it is highly expensive. Also it could not handle a situation in high voltage cables, where there are few cavities present in the insulation very close to each other and the resultant PD pattern of individual cavities exhibit only small differences in their respective discharge pulse amplitudes. Hence, the need arose to identify PD pulse patterns in more vague, or at least less specific terms. This is only possible by using SC techniques for the purpose of classification. N. C. Sahoo et. al. [94] have extensively reviewed the literatures on FL for classifying PD patterns for insulating materials in HV power apparatus. T.K. Abdel-Galil et. al [95] have proposed a fuzzy decision tree approach in order to classify the PD patterns. S. Gopal et. al[96] have described the cavity size in terms of large, small and medium linguistic values and in the process have also proposed a Fuzzified approach to PD pattern recognition. D. Dey et. al.[97] have suggested a novel cross-wavelet transform which is used for feature extraction from a raw noisy PD signal. Lalitha & Satish[98] have proposed fractal image compression techniques which can classify PD patterns in a single step involving the compression and feature extraction. Satish & Zaengl[99] have recognized 3-d PD patterns by using ANN structures for insulation in power apparatus. M. G. Danikas et. al.[100-101] have recognized PD patterns in gas insulated switchgear and transformers by using the ANN structures. Similarly ANN structures have also been used by T. Okamoto et. al.[102] for recognizing PD patterns for three different kinds of electrodes.

- **Time to flashover characteristics**

P.S. Ghosh et. al.[103] have used an ANN structure in order to estimate the time to flashover characteristics of a transmission line insulator used in the power sector. It has been shown that the time to flashover is a function of the length of the insulator, applied voltage and the resistance per unit length.

1.9 Motivation

From the previous sections (especially Sections 1.6 and 1.7), it is quite evident that SC model is an important and a flexible model in predicting the breakdown voltage due to PD in voids. The use of this model in order to tackle this PD issue needs further exploration as the prediction of this breakdown voltage is so important industrially. Moreover, it is also an interesting exercise to know the state of the solid insulating materials at different stages of the applied voltage ultimately leading to breakdown. This curiosity was satisfied by observing the samples of the solid insulating materials under a Scanning Electron Microscope (SEM).

1.10 Organization of the thesis

This thesis primarily attempts at modeling of PD initiated breakdown voltage of solid insulating materials by different SC techniques. The requisite experimental breakdown voltage data under both DC and AC conditions are generated in the laboratory with artificially created void and insulation dimensions using Cylinder-Plane Electrode System. Further, attempt is made to predict the breakdown voltage using experimental data taken from literature generated using CIGRE Method – II Electrode System. This thesis contains seven chapters; out of which Chapter 2 to Chapter 6 are the contributory Chapters.

Chapter 1 has reviewed the existing literatures on the breakdown voltage of the solid insulating materials in general while giving more emphasis on the breakdown due to PD in cavities. The advantage of using SC models over the Conventional models in solving the prediction of breakdown due to PD in cavities and other insulation diagnosis issues have been discussed thoroughly in this Chapter.

Chapter 2 discusses the experimental set up for the Cylinder-Plane Electrode System used for obtaining the breakdown voltage data under DC and AC conditions. Also the statistical

analysis of the breakdown voltage is carried out. In addition, the SEM results for some solid insulating materials under these conditions are presented. Also, the breakdown voltage of some solid insulating materials are studied as a function of the thickness of the material, void depth, void diameter and relative permittivity of the material.

Chapter 3 deals with a brief theory of the Multilayer Feedforward Neural Network (MFNN) based on the Backpropagation Algorithm (BPA), which is subsequently used for the formulation of models for predicting the breakdown voltage of solid insulating materials due to PD in cavities under both DC and AC conditions. Seven models are proposed by using the experimental data obtained from the Cylinder-Plane and the CIGRE Method II Electrode Systems.

Chapter 4 discusses the theory of Radial Basis Function Network (RBFN), in brief. Subsequently, this network structure is utilized for prediction of breakdown voltage. Six models proposed using this structure have used the experimental data generated from Cylinder- Plane Electrode System.

Chapter 5 describes a brief theory of the Fuzzy Logic technique with Mamdani inferencing. This technique is then used to propose six breakdown voltage models. These models have used the experimental data generated from both the Cylinder-Plane and the CIGRE Method II Electrode Systems.

Chapter 6 describes the theory of another FL tehnique, namely, Adaptive Sugeno Fuzzy Logic (ASFL) inferencing. The five models explored with this inferencing have used the experimental data generated from the Cylinder Plane Electrode System.

Finally, **Chapter 7** summarises the main findings, draws certain conclusions arising out of the thesis work and compares of the MAE of the test data E_{ts} obtained from the various models of Chapter 3 to 6 using similar data to show the effectiveness of the SC techniques used here. At the end, it outlines the scope for the future research.

A complete list of references has been given towards the end of the thesis. Finally, a concise list of publications in-peer reviewed international journals and conferences related to present research work has been presented at the end.

Chapter 2

EXPERIMENTAL PROCEDURE AND OBSERVATION

2.1 Introduction

As mentioned in Chapter 1, the primary objective of this thesis work is to visualize the state of the insulation with the application of voltage stress at different levels till breakdown and to develop different soft computing models, which will be able to predict the breakdown voltage of solid insulating materials due to PD in cavities. In order to carry out the first objective, that is, to know the state of the insulating material a Scanning Electron Microscope (SEM) is utilized here. For modeling purpose, breakdown voltage data are generated experimentally on application of DC and AC power frequency voltages and relative permittivity are measured for the solid insulating materials used. In addition, the generated data are statistically analyzed before being utilized for modeling.

2.2 Experimental Procedure

The procedure adopted for the generation of experimental value of the breakdown voltage is as follows:

2.2.1. Sample Preparation

The samples are prepared from five commercially available insulating sheets, namely White Minilex Paper, Leatherite Paper, Glass Cloth, Manila Paper and Lather Minilex of different thicknesses. The variation of thicknesses is as follows:

White Minilex Paper: 0.26 mm, 0.18 mm and 0.125 mm.
Leatherite Paper: 0.235 mm, 0.175 mm and 0.13 mm.
Glass Cloth: 0.195 mm and 0.155 mm.
Manila Paper: 0.06 mm and 0.035 mm.
Lather Minilex: 0.245 mm, 0.185 mm and 0.12 mm.

Thus, the thickness range is varying from 0.035 mm to 0.26 mm. Before testing, the conditioning procedure was adopted to the test specimen in accordance with that laid in ASTM Handbook [104]. This ensures that the surfaces of the insulating sample are clean and dry,

since the contamination on the insulating specimen or absorption of moisture may affect the breakdown voltage.

2.2.2 Creation of void

The voids of different sizes are artificially created by means of a spacer made up of Kapton film, with a circular punched hole at the centre. The diameters of the voids are 1.5 mm, 2 mm, 3 mm, 4 mm and 5 mm. The thicknesses of the Kapton spacer used are of 0.025 mm and 0.125 mm. Thus, the sizes of the void, that is, the volume of air space, depends on a typical diameter of the punched hole and thickness of the spacer. Utmost care has been taken to maintain the surface smoothness of the punched holes.

2.2.3 Electrode Geometry

The electrode system used in this work for breakdown voltage measurements is shown in Figure 2.1. Figure 2.2 shows the arrangement of the complete experimental set and Figure 2.3 shows the snapshots of the High Voltage electrode and the ground electrode. To get a high reproducibility of the tests and low data scatter, the cell sample was built following a standard assembling methodology. It consists of a cylinder-plane electrode configuration, including a cavity in the middle. The depth of the void was fixed by the Kapton film as explained before. The electrodes, both high voltage and low voltage, are made of brass. They are polished, buffed and cleaned with ethanol before the start of the experiment. Further, the electrodes contact surfaces are cleaned by ethanol between two consecutive applications of voltage to avoid contaminations that may arise due to application of voltage. Sufficient care is taken to keep the electrode surfaces untouched and free from scratches, dust and other impurities. The insulation sample is sandwiched between the electrodes with the help of insulating supports as shown. The main characteristic of the employed electrode system is that discharges occur in a concentrated area and continue corroding the insulation until breakdown takes place. The breakdown was considered to be due to a real puncture of the sample.

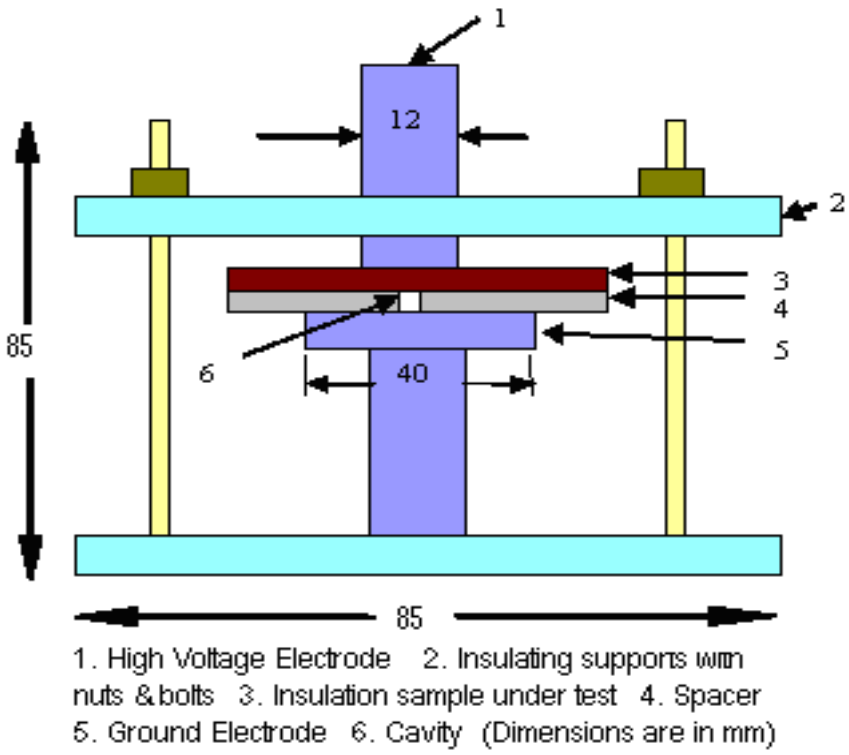

Figure 2.1 Cylinder-Plane Electrode System used for Breakdown Voltage Measurement

Figure 2.2: Arrangement of the complete experimental set up

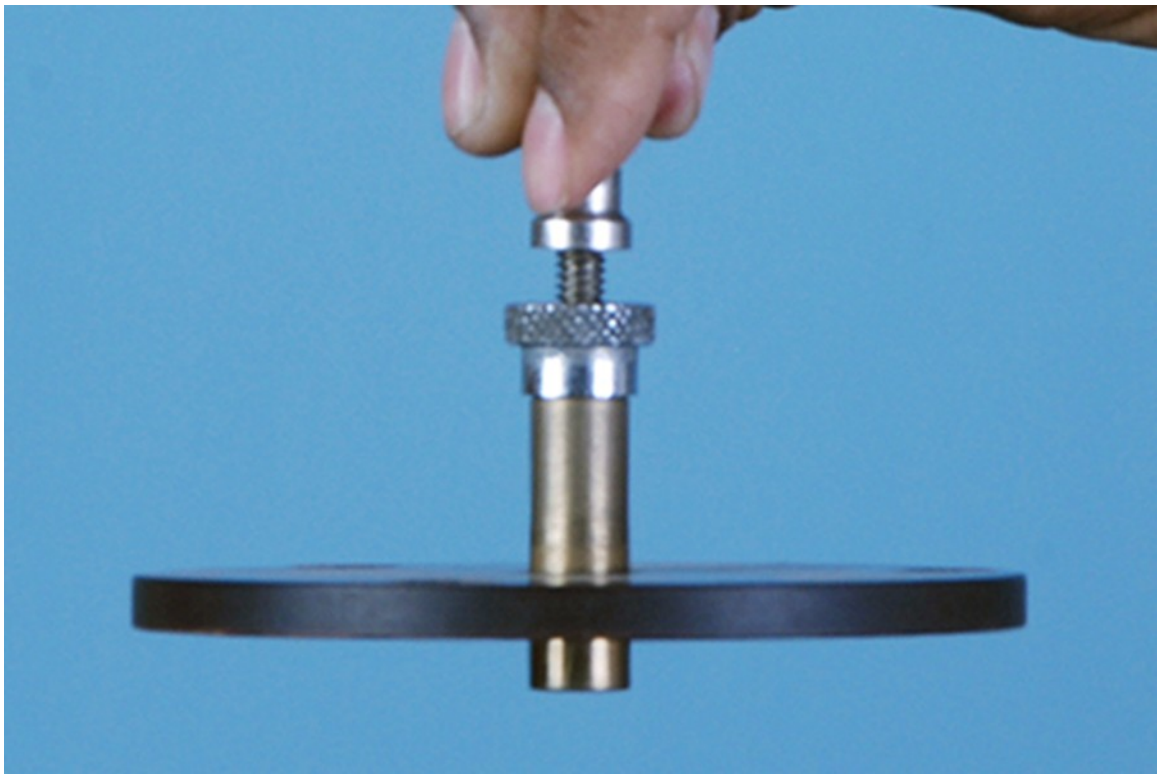

a)

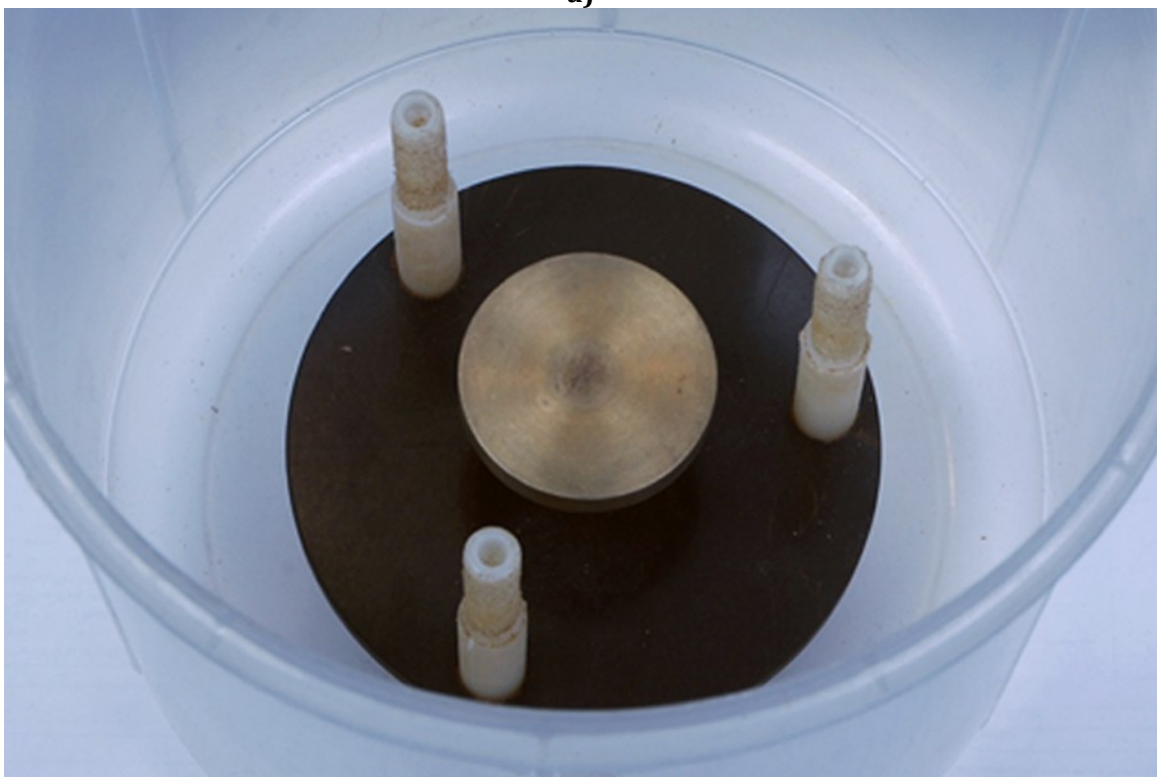

b)

Figure 2.3: Snapshot of the a) High Voltage b) Ground Electrode

2.2.4 Measurement of DC Breakdown Voltage

The DC voltage applied to the set-up was obtained from a 40 kV AC/DC Series Hipot Tester (MODEL: HD 100, Accuracy = ± 2 %, Resolution: 500 V) manufactured by Hipotronics, USA. The voltage is raised in steps of 500 V and held constant for a period of 30 s at each level until the breakdown occurs for materials, such as Leatherite Paper and Manila Paper. However, for materials, such as White Minilex, Glass Cloth and Lather Minilex the voltage is raised in steps of 1kV and the rest of the procedure is the same. For high reproducibility, nine breakdown voltage values are obtained for a particular thickness of the material and a particular void condition. All the tests are carried out in air at room temperature and atmospheric pressure. The breakdown voltage data obtained are then corrected for atmospheric condition before being used for the statistical analysis. The experimental data generated under DC conditions are presented in Table 2.1 and the values in the last column indicate the arithmetic mean of nine breakdown voltage values.

Table 2.1: Experimental Breakdown Voltages for different Insulating samples under DC test conditions

SL No.	Material Used	Thickness of the material (mm)	Void Depth (mm)	Void Diameter (mm)	Mean value of Breakdown Voltage (Experimental) (kV)
1.	White Minilex	0.125	0.025	1.5	23.44
2.		0.125	0.025	2.0	22.88
3.		0.125	0.025	3.0	23.22
4.		0.125	0.025	4.0	24.44
5.		0.125	0.025	5.0	22.55
6.		0.18	0.025	1.5	23.55
7.		0.18	0.025	2.0	23.22
8.		0.18	0.025	3.0	24.44
9.		0.18	0.025	4.0	23.77
10.		0.18	0.025	5.0	22.88
11.		0.26	0.025	1.5	23.33
12.		0.26	0.025	2.0	23.00
13.		0.26	0.025	3.0	24.44
14.		0.26	0.025	4.0	23.77
15.		0.26	0.025	5.0	23.22
16.		0.125	0.125	1.5	24.44
17.		0.125	0.125	2.0	23.55
18.		0.125	0.125	3.0	22.55
19.		0.125	0.125	4.0	23.22
20.		0.125	0.125	5.0	23.77
21.		0.18	0.125	1.5	23.00
22.		0.18	0.125	2.0	24.33
23.		0.18	0.125	3.0	23.77
24.		0.18	0.125	4.0	22.88
25.		0.18	0.125	5.0	24.33
26.		0.26	0.125	1.5	23.22
27.		0.26	0.125	2.0	23.55
28.		0.26	0.125	3.0	23.44
29.		0.26	0.125	4.0	23.77
30.		0.26	0.125	5.0	22.88

Continued

SL No.	Material Used	Thickness of the material (mm)	Void Depth (mm)	Void Diameter (mm)	Mean value of Breakdown Voltage (Experimental) (kV)
31.	Leatherite Paper	0.13	0.025	1.5	1.94
32.		0.13	0.025	2.0	1.97
33.		0.13	0.025	3.0	1.91
34.		0.13	0.025	4.0	2.02
35.		0.13	0.025	5.0	1.88
36.		0.175	0.025	1.5	2.44
37.		0.175	0.025	2.0	2.36
38.		0.175	0.025	3.0	2.30
39.		0.175	0.025	4.0	2.36
40.		0.175	0.025	5.0	2.39
41.		0.235	0.025	1.5	3.19
42.		0.235	0.025	2.0	3.22
43.		0.235	0.025	3.0	3.16
44.		0.235	0.025	4.0	3.27
45.		0.235	0.025	5.0	3.13
46.		0.13	0.125	1.5	1.94
47.		0.13	0.125	2.0	1.86
48.		0.13	0.125	3.0	1.91
49.		0.13	0.125	4.0	1.97
50.		0.13	0.125	5.0	1.91
51.		0.175	0.125	1.5	2.44
52.		0.175	0.125	2.0	2.36
53.		0.175	0.125	3.0	2.41
54.		0.175	0.125	4.0	2.30
55.		0.175	0.125	5.0	2.36
56.		0.235	0.125	1.5	3.19
57.		0.235	0.125	2.0	3.11
58.		0.235	0.125	3.0	3.16
59.		0.235	0.125	4.0	3.16
60.		0.235	0.125	5.0	3.27

Continued

SL No.	Material Used	Thickness of the material (mm)	Void Depth (mm)	Void Diameter (mm)	Mean value of Breakdown Voltage (Experimental) (kV)
61.	Glass Cloth	0.155	0.025	1.5	13.00
62.		0.155	0.025	2.0	13.33
63.		0.155	0.025	3.0	13.33
64.		0.155	0.025	4.0	13.44
65.		0.155	0.025	5.0	13.33
66.		0.195	0.025	1.5	17.66
67.		0.195	0.025	2.0	17.33
68.		0.195	0.025	3.0	17.11
69.		0.195	0.025	4.0	17.44
70.		0.195	0.025	5.0	17.77
71.		0.155	0.125	1.5	13.33
72.		0.155	0.125	2.0	13.55
73.		0.155	0.125	3.0	13.55
74.		0.155	0.125	4.0	13.11
75.		0.155	0.125	5.0	13.33
76.		0.195	0.125	1.5	17.33
77.		0.195	0.125	2.0	17.22
78.		0.195	0.125	3.0	17.88
79.		0.195	0.125	4.0	17.66
80.		0.195	0.125	5.0	17.11

Continued

SL No.	Material Used	Thickness of the material (mm)	Void Depth (mm)	Void Diameter (mm)	Mean value of Breakdown Voltage (Experimental) (kV)
81.	Manila Paper	0.035	0.025	1.5	1.44
82.		0.035	0.025	2.0	1.47
83.		0.035	0.025	3.0	1.42
84.		0.035	0.025	4.0	1.53
85.		0.035	0.025	5.0	1.39
86.		0.06	0.025	1.5	1.44
87.		0.06	0.025	2.0	1.36
88.		0.06	0.025	3.0	1.42
89.		0.06	0.025	4.0	1.53
90.		0.06	0.025	5.0	1.38
91.		0.035	0.125	1.5	1.47
92.		0.035	0.125	2.0	1.42
93.		0.035	0.125	3.0	1.44
94.		0.035	0.125	4.0	1.53
95.		0.035	0.125	5.0	1.36
96.		0.06	0.125	1.5	1.42
97.		0.06	0.125	2.0	1.39
98.		0.06	0.125	3.0	1.47
99.		0.06	0.125	4.0	1.42
100.		0.06	0.125	5.0	1.44

Continued

SL No.	Material Used	Thickness of the material (mm)	Void Depth (mm)	Void Diameter (mm)	Mean value of Breakdown Voltage (Experimental) (kV)
101.	Lather Minilex	0.12	0.025	1.5	10.00
102.		0.12	0.025	2.0	10.11
103.		0.12	0.025	3.0	10.33
104.		0.12	0.025	4.0	10.67
105.		0.12	0.025	5.0	10.33
106.		0.185	0.025	1.5	15.78
107.		0.185	0.025	2.0	16.22
108.		0.185	0.025	3.0	16.11
109.		0.185	0.025	4.0	16.00
110.		0.185	0.025	5.0	15.88
111.		0.245	0.025	1.5	15.88
112.		0.245	0.025	2.0	16.00
113.		0.245	0.025	3.0	15.77
114.		0.245	0.025	4.0	16.44
115.		0.245	0.025	5.0	16.00
116.		0.12	0.125	1.5	10.44
117.		0.12	0.125	2.0	10.33
118.		0.12	0.125	3.0	10.55
119.		0.12	0.125	4.0	10.55
120.		0.12	0.125	5.0	10.67
121.		0.185	0.125	1.5	15.89
122.		0.185	0.125	2.0	16.00
123.		0.185	0.125	3.0	15.77
124.		0.185	0.125	4.0	16.44
125.		0.185	0.125	5.0	15.89
126.		0.245	0.125	1.5	16.00
127.		0.245	0.125	2.0	15.88
128.		0.245	0.125	3.0	15.77
129.		0.245	0.125	4.0	16.11
130.		0.245	0.125	5.0	15.77

2.2.5 Measurement of AC Breakdown Voltage

In this case an AC voltage of 50 Hz is applied from the same Hipot Tester (Resolution: 200 V rms) to the insulating sample. The voltage is raised in steps of 200V (rms). Rest of the procedure is identical to that presented in Section 2.2.4 . The experimental data generated

under AC conditions are depicted in Table 2.2 and the values in the last column indicate the arithmetic mean of nine breakdown voltage values.

Table 2.2: Experimental Breakdown Voltages for different Insulating samples under AC test conditions

SL No.	Material Used	Thickness of the material (mm)	Void Depth (mm)	Void Diameter (mm)	Mean value of Breakdown Voltage (Experimental) (kV)
1.	White Minilex	0.125	0.025	1.5	2.24
2.		0.125	0.025	2.0	2.25
3.		0.125	0.025	3.0	2.21
4.		0.125	0.025	4.0	2.27
5.		0.125	0.025	5.0	2.23
6.		0.18	0.025	1.5	2.23
7.		0.18	0.025	2.0	2.25
8.		0.18	0.025	3.0	2.21
9.		0.18	0.025	4.0	2.27
10.		0.18	0.025	5.0	2.25
11.		0.26	0.025	1.5	2.21
12.		0.26	0.025	2.0	2.27
13.		0.26	0.025	3.0	2.21
14.		0.26	0.025	4.0	2.24
15.		0.26	0.025	5.0	2.27
16.		0.125	0.125	1.5	2.24
17.		0.125	0.125	2.0	2.23
18.		0.125	0.125	3.0	2.23
19.		0.125	0.125	4.0	2.25
20.		0.125	0.125	5.0	2.27
21.		0.18	0.125	1.5	2.21
22.		0.18	0.125	2.0	2.23
23.		0.18	0.125	3.0	2.24
24.		0.18	0.125	4.0	2.25
25.		0.18	0.125	5.0	2.23
26.		0.26	0.125	1.5	2.24
27.		0.26	0.125	2.0	2.23
28.		0.26	0.125	3.0	2.24
29.		0.26	0.125	4.0	2.25
30.		0.26	0.125	5.0	2.25

Continued

SL No.	Material Used	Thickness of the material (mm)	Void Depth (mm)	Void Diameter (mm)	Mean value of Breakdown Voltage (Experimental) (kV)
31.	Leatherite Paper	0.13	0.025	1.5	1.31
32.		0.13	0.025	2.0	1.28
33.		0.13	0.025	3.0	1.25
34.		0.13	0.025	4.0	1.27
35.		0.13	0.025	5.0	1.31
36.		0.175	0.025	1.5	1.81
37.		0.175	0.025	2.0	1.78
38.		0.175	0.025	3.0	1.75
39.		0.175	0.025	4.0	1.77
40.		0.175	0.025	5.0	1.81
41.		0.235	0.025	1.5	2.24
42.		0.235	0.025	2.0	2.23
43.		0.235	0.025	3.0	2.27
44.		0.235	0.025	4.0	2.25
45.		0.235	0.025	5.0	2.27
46.		0.13	0.125	1.5	1.28
47.		0.13	0.125	2.0	1.31
48.		0.13	0.125	3.0	1.27
49.		0.13	0.125	4.0	1.33
50.		0.13	0.125	5.0	1.25
51.		0.175	0.125	1.5	1.78
52.		0.175	0.125	2.0	1.83
53.		0.175	0.125	3.0	1.75
54.		0.175	0.125	4.0	1.81
55.		0.175	0.125	5.0	1.75
56.		0.235	0.125	1.5	2.21
57.		0.235	0.125	2.0	2.27
58.		0.235	0.125	3.0	2.24
59.		0.235	0.125	4.0	2.27
60.		0.235	0.125	5.0	2.23

Continued

SL No.	Material Used	Thickness of the material (mm)	Void Depth (mm)	Void Diameter (mm)	Mean value of Breakdown Voltage (Experimental) (kV)
61.	Glass Cloth	0.155	0.025	1.5	2.21
62.		0.155	0.025	2.0	2.21
63.		0.155	0.025	3.0	2.27
64.		0.155	0.025	4.0	2.23
65.		0.155	0.025	5.0	2.27
66.		0.195	0.025	1.5	2.24
67.		0.195	0.025	2.0	2.21
68.		0.195	0.025	3.0	2.25
69.		0.195	0.025	4.0	2.21
70.		0.195	0.025	5.0	2.27
71.		0.155	0.125	1.5	2.21
72.		0.155	0.125	2.0	2.27
73.		0.155	0.125	3.0	2.24
74.		0.155	0.125	4.0	2.21
75.		0.155	0.125	5.0	2.23
76.		0.195	0.125	1.5	2.24
77.		0.195	0.125	2.0	2.27
78.		0.195	0.125	3.0	2.24
79.		0.195	0.125	4.0	2.21
80.		0.195	0.125	5.0	2.25

Continued

SL No.	Material Used	Thickness of the material (mm)	Void Depth (mm)	Void Diameter (mm)	Mean value of Breakdown Voltage (Experimental) (kV)
81.	Manila Paper	0.035	0.025	1.5	0.83
82.		0.035	0.025	2.0	0.80
83.		0.035	0.025	3.0	0.76
84.		0.035	0.025	4.0	0.86
85.		0.035	0.025	5.0	0.82
86.		0.06	0.025	1.5	0.80
87.		0.06	0.025	2.0	0.76
88.		0.06	0.025	3.0	0.83
89.		0.06	0.025	4.0	0.86
90.		0.06	0.025	5.0	0.78
91.		0.035	0.125	1.5	0.76
92.		0.035	0.125	2.0	0.83
93.		0.035	0.125	3.0	0.78
94.		0.035	0.125	4.0	0.80
95.		0.035	0.125	5.0	0.86
96.		0.06	0.125	1.5	0.83
97.		0.06	0.125	2.0	0.78
98.		0.06	0.125	3.0	0.76
99.		0.06	0.125	4.0	0.80
100.		0.06	0.125	5.0	0.78

Continued

SL No.	Material Used	Thickness of the material (mm)	Void Depth (mm)	Void Diameter (mm)	Mean value of Breakdown Voltage (Experimental) (kV)
101.	Lather Minilex	0.12	0.025	1.5	2.21
102.		0.12	0.025	2.0	2.25
103.		0.12	0.025	3.0	2.24
104.		0.12	0.025	4.0	2.23
105.		0.12	0.025	5.0	2.23
106.		0.185	0.025	1.5	2.24
107.		0.185	0.025	2.0	2.23
108.		0.185	0.025	3.0	2.25
109.		0.185	0.025	4.0	2.24
110.		0.185	0.025	5.0	2.25
111.		0.245	0.025	1.5	2.24
112.		0.245	0.025	2.0	2.23
113.		0.245	0.025	3.0	2.24
114.		0.245	0.025	4.0	2.23
115.		0.245	0.025	5.0	2.23
116.		0.12	0.125	1.5	2.23
117.		0.12	0.125	2.0	2.27
118.		0.12	0.125	3.0	2.24
119.		0.12	0.125	4.0	2.27
120.		0.12	0.125	5.0	2.25
121.		0.185	0.125	1.5	2.21
122.		0.185	0.125	2.0	2.27
123.		0.185	0.125	3.0	2.24
124.		0.185	0.125	4.0	2.23
125.		0.185	0.125	5.0	2.27
126.		0.245	0.125	1.5	2.24
127.		0.245	0.125	2.0	2.27
128.		0.245	0.125	3.0	2.23
129.		0.245	0.125	4.0	2.23
130.		0.245	0.125	5.0	2.27

2.2.6 Measurement of relative permittivity of solid insulating materials

In order to measure the relative permittivity, insulating samples are silver coated with 12mm in diameter at the identical zone, on both the sides. The silver-coated samples were then pressed between the two brass sample holder electrodes of an Impedance Gain / Phase Analyzer (Model No: 1260, Accuracy = 0.1%, Frequency Resolution = 1 in 65 million) manufactured by Solartron, U.K. An AC voltage of 0.1 V (rms) at 50 Hz was applied to the samples from the Impedance Gain / Phase Analyzer and relative permittivity values of the insulating materials are recorded. Figure 2.4 shows the experimental set up for recording the relative permittivity values. Table 2.3 shows the measured values of the relative permittivity of materials at 50 Hz frequency.

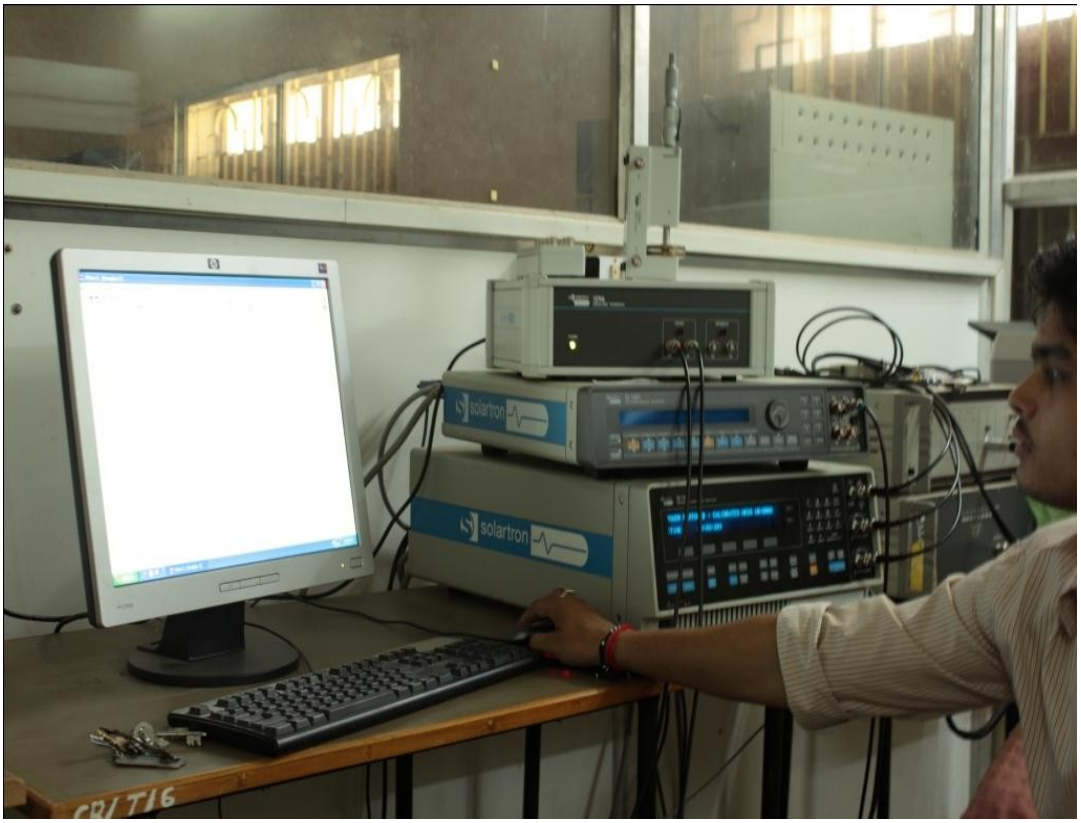

Figure 2.4 Experimental set up used for recording relative permittivity values

Table 2.3: Relative Permittivity of the Insulating Materials used

Materials	ϵ_r
White Minilex	4.40
Leatherite Paper	4.21
Glass Cloth	4.97
Manila Paper	4.68
Lather Minilex	5.74

2.3 Statistical Analysis of the experimental data

The breakdown voltage of any solid insulating material for any particular thickness and void condition is a random process, implying that this voltage might be widely scattered for certain combinations of thickness and void condition. Hence, it is necessary to evolve a mechanism for quantifying the degree of scattering. Moreover, from the point of view of prediction using soft computing techniques, we need a single effective value. Both of the above-mentioned objectives are appropriately taken care of by carrying out the statistical analysis of the experimental values of the breakdown voltage.

The statistical analysis has been carried out on all the 130 sets of breakdown voltage data presented in the last column of Tables 2.1 and 2.2. For each set, the 9 voltage values were assumed to be a part of the random process obeying Weibull [105-107] Distribution. The probability density function of this distribution is given by

$$f(V) = (\beta/\alpha^{\beta}) * V^{\beta-1} * \exp(-(V/\alpha)^{\beta}) \quad (2.1)$$

Where β = Shape Factor of the Weibull Distribution which gives a measure of the dispersion of the data. The less the value of β, the more is the scattering of the data.

α = Scale Factor of the Weibull Distribution or 63.2% probability of breakdown

V = Breakdown Voltage

The maximum Likelihood estimates (MLE) of α and β are denoted by ά and ß. These are obtained by finding the partial derivatives of Logarithm of Likelihood function with respect to α and β and equating the partial derivatives to zero. As a result of this exercise, we arrive at two equations as follows:

$$\sum_{i=1}^{N} \ln(V_i) = (N*\ln(\acute{\alpha})) + \left(\sum_{i=1}^{N} (V_i/\acute{\alpha})^{ß} * \ln (V_i/\acute{\alpha}) \right) - (N/ ß) \quad (2.2)$$

$$\acute{\alpha}^{ß} = (1/N) * \sum_{i=1}^{N} V_i^{ß} \quad (2.3)$$

Here, N = 9.

The 90% confidence limits for ά are denoted by $\acute{\alpha}_l$ and $\acute{\alpha}_u$ and are defined as

$$\acute{\alpha}_l = \acute{\alpha} * \exp(-0.76/ ß) \quad (2.4)$$

$$\acute{\alpha}_u = \acute{\alpha} * \exp(0.76/ ß) \quad (2.5)$$

Figure 2.5 shows the flow chart for calculating maximum likelihood estimates ά and ß.

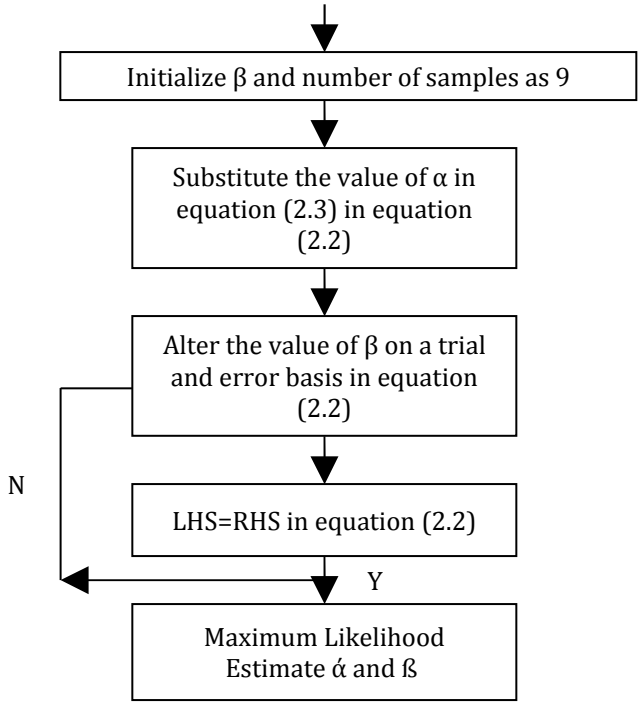

Figure 2.5 : Flow Chart for obtaining the Maximum Likelihood Estimate of α and β

2.3.1 Sample Calculation under DC test condition

The calculation details are given for Serial No. 61 in Table 2.1, which corresponds, to Glass Cloth having thickness of 0.155 mm. The nine values of the breakdown voltage are 12, 12, 12, 12, 13, 13, 14, 14 and 15 kV respectively and their arithmetic mean is 13 kV. Since equations (2.2) and (2.3) are transcendental in nature, trial and error approach is adopted to calculate the MLE for these nine values. They are estimated as ά = 13.5088 and ß = 12.5. The lower value $ά_l$ and the upper value $ά_u$ of the 90% confidence limits of ά are calculated using equations (2.4) and (2.5) as 12.7091 and 14.3524. The same procedure is adopted in calculating ά, ß, $ά_l$ and $ά_u$ for the rest 129 sets, with each set consisting of nine breakdown voltage values. Table 2.4 shows the values of ά, ß, $ά_l$ and $ά_u$ corresponding to all the 130 sets.

Table 2.4: Statistical analysis of the DC breakdown voltage

SL No.	Materials Used	ά	ß	$ά_l$	$ά_u$
1.	White Minilex	24.7700	8.91	22.75	26.98
2.		24.0900	9.71	22.28	26.05
3.		24.5602	8.51	22.46	26.86
4.		25.4903	12.27	23.96	27.12
5.		23.8500	8.13	21.72	26.19
6.		24.7000	11.20	23.08	26.43
7.		24.5602	8.51	22.46	26.86
8.		25.4903	12.27	23.96	27.12
9.		24.9200	11.10	23.27	26.69
10.		24.0900	9.71	22.28	26.05
11.		24.7000	8.53	22.60	27.00
12.		24.3201	8.34	22.21	26.64
13.		25.4903	12.27	23.96	27.12
14.		24.9200	11.10	23.27	26.69
15.		24.5602	8.51	22.46	26.86
16.		25.4903	12.27	23.96	27.12
17.		24.7000	11.20	23.08	26.43
18.		23.8500	8.13	21.72	26.19
19.		24.5602	8.51	22.46	26.86
20.		24.9200	11.10	23.27	26.69
21.		24.3201	8.34	22.21	26.64
22.		25.6608	9.75	23.74	27.74
23.		24.9200	11.10	23.27	26.69
24.		24.0900	9.71	22.28	26.05
25.		25.6608	9.75	23.74	27.74
26.		24.5602	8.51	22.46	26.86
27.		24.7000	11.20	23.08	26.43
28.		24.7700	8.91	22.75	26.98
29.		24.9200	11.10	23.27	26.69
30.		24.0900	9.71	22.28	26.05

Continued

SL No.	Materials Used	ά	ß	$ά_l$	$ά_u$
31.	Leatherite Paper	2.0361	10.47	1.89	2.18
32.		2.0575	11.65	1.93	2.20
33.		2.0127	9.56	1.85	2.18
34.		2.1127	12.93	1.99	2.24
35.		1.9713	10.66	1.83	2.11
36.		2.5382	13.10	2.39	2.68
37.		2.5591	14.53	2.43	2.70
38.		2.5152	11.97	2.36	2.68
39.		2.6125	16.10	2.49	2.74
40.		2.4731	13.30	2.33	2.62
41.		3.2899	17.00	3.14	3.44
42.		3.3105	18.83	3.18	3.45
43.		3.2673	15.56	3.11	3.43
44.		3.3637	20.84	3.24	3.48
45.		3.2248	17.34	3.09	3.36
46.		2.0500	9.14	1.88	2.22
47.		1.9449	9.95	1.80	2.10
48.		1.9957	11.62	1.87	2.13
49.		2.0575	11.65	1.93	2.20
50.		2.0127	9.56	1.85	2.18
51.		2.5527	11.44	2.39	2.73
52.		2.4470	12.45	2.30	2.60
53.		2.4972	14.52	2.37	2.63
54.		2.5152	11.97	2.36	2.68
55.		2.6125	16.10	2.49	2.74
56.		3.3051	14.88	3.14	3.48
57.		3.1989	16.20	3.05	3.35
58.		3.2487	18.86	3.12	3.38
59.		3.2673	15.56	3.11	3.43
60.		3.3637	20.84	3.24	3.48

Continued

SL No.	Materials Used	ά	ß	$ά_l$	$ά_u$
61.	Glass Cloth	13.5058	12.50	12.71	14.35
62.		13.8725	12.72	13.06	14.73
63.		13.9502	11.21	13.03	14.93
64.		13.8818	16.30	13.25	14.54
65.		13.7763	15.33	13.11	14.48
66.		17.8760	55.71	17.64	18.12
67.		17.5761	37.05	17.22	17.94
68.		17.2933	40.00	16.97	17.62
69.		17.6896	39.70	17.35	18.03
70.		17.9443	80.20	17.78	18.12
71.		13.8725	12.72	13.06	14.73
72.		14.0961	13.21	13.31	14.93
73.		14.0100	15.19	13.33	14.73
74.		13.5873	13.47	12.76	14.29
75.		13.9502	11.21	13.03	14.93
76.		17.5761	37.05	17.22	17.94
77.		17.4463	36.70	17.09	17.81
78.		17.9865	57.00	17.75	18.23
79.		17.8760	55.71	17.63	18.12
80.		17.2933	40.00	16.97	17.63

Continued

SL No.	Materials Used	ά	ß	$ά_l$	$ά_u$
81.	Manila Paper	1.5328	7.85	1.39	1.69
82.		1.5548	8.76	1.43	1.70
83.		1.5088	7.16	1.35	1.68
84.		1.6090	9.76	1.48	1.74
85.		1.4682	7.97	1.33	1.61
86.		1.5456	6.84	1.38	1.72
87.		1.4413	7.43	1.30	1.60
88.		1.4913	8.71	1.37	1.63
89.		1.6090	9.76	1.48	1.74
90.		1.4682	7.97	1.33	1.61
91.		1.5548	8.76	1.43	1.70
92.		1.5088	7.16	1.35	1.68
93.		1.5456	6.84	1.38	1.72
94.		1.6090	9.76	1.48	1.74
95.		1.4413	7.43	1.30	1.60
96.		1.4913	8.71	1.37	1.63
97.		1.4682	7.97	1.33	1.61
98.		1.5548	8.76	1.43	1.70
99.		1.5088	7.16	1.35	1.68
100.		1.5456	6.84	1.38	1.72

Continued

SL No.	Materials Used	ά	ß	$ά_l$	$ά_u$
101.	Lather	10.4930	9.72	9.71	11.35
102.	Minilex	10.5760	10.48	9.84	11.37
103.		10.7673	11.95	10.10	11.47
104.		11.0973	12.86	10.05	11.72
105.		10.8598	9.91	9.84	11.37
106.		16.3897	13.16	15.47	17.37
107.		16.8256	14.30	15.96	17.75
108.		16.7663	13.20	15.82	17.76
109.		16.6824	12.34	15.68	17.74
110.		16.5625	12.02	15.54	17.64
111.		16.4542	14.17	15.60	17.36
112.		16.5388	15.18	15.73	17.38
113.		16.3228	13.99	15.46	17.23
114.		17.0022	16.21	16.23	17.80
115.		16.6824	12.34	15.69	17.74
116.		10.8742	12.72	10.24	11.54
117.		10.9330	8.71	10.01	11.93
118.		11.0012	11.90	10.32	11.72
119.		11.0839	10.31	10.32	11.72
120.		11.0973	12.86	10.30	11.93
121.		16.5625	12.02	15.55	17.65
122.		16.5388	15.18	15.74	17.39
123.		16.3228	13.99	15.46	17.24
124.		17.0022	16.21	16.23	17.80
125.		16.4542	14.17	15.60	17.36
126.		16.5388	15.18	15.74	17.39
127.		16.5625	12.02	15.55	17.65
128.		16.3228	13.99	15.46	17.23
129.		16.7663	13.20	15.82	17.76
130.		16.3897	13.16	15.47	17.37

2.3.2 Sample Calculation under AC test condition

The calculation details are given for Serial No. 35 in Table 2.2 which corresponds to Leatherite Paper having thickness of 0.13 mm. The nine values of the breakdown voltages are

1.2, 1.2, 1.2, 1.3, 1.3, 1.4, 1.4, 1.4, 1.4 kV respectively and their arithmetic mean is 1.31 kV. On using equations (2.2) and (2.3), the value of ά = 1.3513 and ß = 18.45 for these nine values. $ά_l$ and $ά_u$, the 90% confidence limits of ά, are calculated from equation (2.4) and (2.5) as 1.2968 and 1.4081 respectively. Similar procedure has been adopted in calculating ά, ß, $ά_l$ and $ά_u$ for the rest 129 sets with each set consisting of nine breakdown voltage values. Table 2.5 shows the values of ά, ß, $ά_l$ and $ά_u$ corresponding to all the 130 sets.

Table 2.5: Statistical analysis of the AC breakdown voltage

SL No.	Materials Used	ά	ß	$ά_l$	$ά_u$
1.	White Minilex	2.2807	28.70	2.22	2.34
2.		2.2909	30.70	2.23	2.35
3.		2.2294	51.30	2.20	2.26
4.		2.3170	30.00	2.26	2.38
5.		2.2447	47.10	2.21	2.28
6.		2.2697	27.30	2.21	2.34
7.		2.2909	30.70	2.23	2.35
8.		2.2294	51.30	2.20	2.26
9.		2.3170	30.00	2.26	2.38
10.		2.2909	30.70	2.23	2.35
11.		2.2294	51.30	2.20	2.26
12.		2.3088	36.80	2.26	2.36
13.		2.2294	51.30	2.20	2.26
14.		2.2885	24.10	2.22	2.36
15.		2.3170	30.00	2.26	2.38
16.		2.2885	24.10	2.22	2.36
17.		2.2447	47.10	2.21	2.28
18.		2.2697	27.30	2.21	2.34
19.		2.2909	30.70	2.23	2.35
20.		2.3088	36.80	2.26	2.36
21.		2.2294	51.30	2.20	2.26
22.		2.2697	27.30	2.21	2.34
23.		2.2885	24.10	2.22	2.36
24.		2.2909	30.70	2.23	2.35
25.		2.2697	27.30	2.21	2.34
26.		2.2885	24.10	2.22	2.36
27.		2.2697	27.30	2.21	2.34
28.		2.2885	24.10	2.22	2.36
29.		2.2909	30.70	2.23	2.35
30.		2.2909	30.70	2.23	2.35

Continued

SL No.	Materials Used	ά	ß	$ά_l$	$ά_u$
31.	Leatherite Paper	1.3452	20.65	1.30	1.40
32.		1.3306	16.36	1.27	1.39
33.		1.2972	14.46	1.23	1.37
34.		1.3221	14.90	1.26	1.39
35.		1.3513	18.45	1.30	1.41
36.		1.8459	28.70	1.80	1.90
37.		1.8313	22.65	1.77	1.90
38.		1.7981	20.60	1.76	1.89
39.		1.8229	22.65	1.77	1.90
40.		1.8520	25.57	1.80	1.91
41.		2.2885	24.10	2.22	2.36
42.		2.2697	27.30	2.21	2.34
43.		2.2885	24.10	2.22	2.36
44.		2.2909	30.70	2.23	2.35
45.		2.3088	36.80	2.26	2.36
46.		1.3306	16.36	1.27	1.40
47.		1.3452	20.65	1.30	1.40
48.		1.3221	14.90	1.26	1.39
49.		1.3637	25.30	1.32	1.40
50.		1.2972	14.47	1.23	1.37
51.		1.8313	22.65	1.77	1.90
52.		1.8640	34.75	1.82	1.90
53.		1.7981	20.00	1.73	1.86
54.		1.8520	25.57	1.80	1.90
55.		1.7981	20.00	1.73	1.87
56.		2.2294	51.30	2.20	2.26
57.		2.3170	30.00	2.26	2.38
58.		2.2885	24.10	2.22	2.36
59.		2.3088	36.80	2.26	2.36
60.		2.2697	27.30	2.21	2.34

Continued

SL No.	Materials Used	ά	ß	$ά_l$	$ά_u$
61.	Glass Cloth	2.2294	51.30	2.20	2.26
62.		2.2294	51.30	2.20	2.26
63.		2.3088	36.80	2.26	2.36
64.		2.2697	27.30	2.21	2.34
65.		2.3170	30.00	2.26	2.38
66.		2.2885	24.10	2.22	2.36
67.		2.2294	51.30	2.20	2.26
68.		2.2909	30.70	2.23	2.35
69.		2.2294	51.30	2.20	2.26
70.		2.3088	36.80	2.26	2.36
71.		2.2294	51.30	2.20	2.26
72.		2.3170	30.00	2.26	2.38
73.		2.2885	24.10	2.22	2.36
74.		2.2294	51.30	2.20	2.26
75.		2.2697	27.30	2.21	2.34
76.		2.2885	24.10	2.22	2.36
77.		2.3170	30.00	2.26	2.38
78.		2.2885	24.10	2.22	2.36
79.		2.2294	51.30	2.20	2.26
80.		2.2909	30.70	2.23	2.35

Continued

SL No.	Materials Used	ά	ß	$ά_l$	$ά_u$
81.	Manila Paper	0.8758	9.70	0.81	0.95
82.		0.8479	7.85	0.77	0.93
83.		0.8154	6.85	0.73	0.91
84.		0.9089	10.48	0.85	0.98
85.		0.8683	8.80	0.80	0.95
86.		0.8479	7.85	0.77	0.93
87.		0.8154	6.85	0.73	0.91
88.		0.8758	9.70	0.81	0.95
89.		0.9089	10.48	0.85	0.98
90.		0.8388	7.31	0.76	0.93
91.		0.8154	6.85	0.73	0.91
92.		0.8758	9.70	0.81	0.95
93.		0.8388	7.31	0.76	0.93
94.		0.8479	7.85	0.77	0.93
95.		0.9089	10.48	0.85	0.98
96.		0.8758	9.70	0.81	0.95
97.		0.8388	7.31	0.76	0.93
98.		0.8154	6.85	0.73	0.91
99.		0.8479	7.85	0.77	0.93
100.		0.8388	7.31	0.76	0.93

Continued

SL No.	Materials Used	ά	ß	$ά_l$	$ά_u$
101.	Lather Minilex	2.2294	51.30	2.20	2.26
102.		2.2909	30.70	2.23	2.35
103.		2.2807	28.70	2.22	2.34
104.		2.2447	47.10	2.21	2.28
105.		2.2697	27.30	2.21	2.34
106.		2.2885	24.10	2.22	2.36
107.		2.2697	27.30	2.21	2.34
108.		2.2909	30.70	2.23	2.35
109.		2.2807	28.70	2.22	2.34
110.		2.2909	30.70	2.23	2.35
111.		2.2807	28.70	2.22	2.34
112.		2.2697	27.30	2.21	2.34
113.		2.2885	24.10	2.22	2.36
114.		2.2697	27.30	2.21	2.34
115.		2.2447	47.10	2.21	2.28
116.		2.2697	27.30	2.21	2.34
117.		2.3170	30.00	2.26	2.38
118.		2.2885	24.10	2.22	2.36
119.		2.3088	36.80	2.26	2.36
120.		2.2909	30.70	2.23	2.35
121.		2.2294	51.30	2.20	2.26
122.		2.3170	30.00	2.26	2.38
123.		2.2885	24.10	2.22	2.36
124.		2.2447	47.10	2.21	2.28
125.		2.3170	30.00	2.26	2.38
126.		2.2885	24.10	2.22	2.36
127.		2.3170	30.00	2.26	2.38
128.		2.2447	47.10	2.21	2.28
129.		2.2697	27.30	2.21	2.34
130.		2.3088	36.80	2.26	2.36

The Table 2.6 shows the input and the output parameters for all the five insulating materials under DC conditions. The thickness of the material, void depth, void diameter constitute of the input parameters and these have been taken directly from Table 2.1. The breakdown voltage is the output parameter and these values are obtained from the values of ά in Table 2.4. Similarly , under AC conditions the input and the output parameters have been taken from Table 2.2 and from the values of ά in Table 2.5 respectively to form Table 2.7.

Table 2.6: Input and the Output parameters under DC test conditions

SL No.	Material Used	Thickness of the material (mm)	Void Depth (mm)	Void Diameter (mm)	Breakdown Voltage (kV)
1.	White Minilex	0.125	0.025	1.5	24.7700
2.		0.125	0.025	2.0	24.0900
3.		0.125	0.025	3.0	24.5602
4.		0.125	0.025	4.0	25.4903
5.		0.125	0.025	5.0	23.8500
6.		0.18	0.025	1.5	24.7000
7.		0.18	0.025	2.0	24.5602
8.		0.18	0.025	3.0	25.4903
9.		0.18	0.025	4.0	24.9200
10.		0.18	0.025	5.0	24.0900
11.		0.26	0.025	1.5	24.7000
12.		0.26	0.025	2.0	24.3201
13.		0.26	0.025	3.0	25.4903
14.		0.26	0.025	4.0	24.9200
15.		0.26	0.025	5.0	24.5602
16.		0.125	0.125	1.5	25.4903
17.		0.125	0.125	2.0	24.7000
18.		0.125	0.125	3.0	23.8500
19.		0.125	0.125	4.0	24.5602
20.		0.125	0.125	5.0	24.9200
21.		0.18	0.125	1.5	24.3201
22.		0.18	0.125	2.0	25.6608
23.		0.18	0.125	3.0	24.9200
24.		0.18	0.125	4.0	24.0900
25.		0.18	0.125	5.0	25.6608
26.		0.26	0.125	1.5	24.5602
27.		0.26	0.125	2.0	24.7000
28.		0.26	0.125	3.0	24.7700
29.		0.26	0.125	4.0	24.9200
30.		0.26	0.125	5.0	24.0900

Continued

SL No.	Material Used	Thickness of the material (mm)	Void Depth (mm)	Void Diameter (mm)	Breakdown Voltage (kV)
31.	Leatherite Paper	0.13	0.025	1.5	2.0361
32.		0.13	0.025	2.0	2.0575
33.		0.13	0.025	3.0	2.0127
34.		0.13	0.025	4.0	2.1127
35.		0.13	0.025	5.0	1.9713
36.		0.175	0.025	1.5	2.5382
37.		0.175	0.025	2.0	2.5591
38.		0.175	0.025	3.0	2.5152
39.		0.175	0.025	4.0	2.6125
40.		0.175	0.025	5.0	2.4731
41.		0.235	0.025	1.5	3.2899
42.		0.235	0.025	2.0	3.3105
43.		0.235	0.025	3.0	3.2673
44.		0.235	0.025	4.0	3.3637
45.		0.235	0.025	5.0	3.2248
46.		0.13	0.125	1.5	2.0500
47.		0.13	0.125	2.0	1.9449
48.		0.13	0.125	3.0	1.9957
49.		0.13	0.125	4.0	2.0575
50.		0.13	0.125	5.0	2.0127
51.		0.175	0.125	1.5	2.5527
52.		0.175	0.125	2.0	2.4470
53.		0.175	0.125	3.0	2.4972
54.		0.175	0.125	4.0	2.5152
55.		0.175	0.125	5.0	2.6125
56.		0.235	0.125	1.5	3.3051
57.		0.235	0.125	2.0	3.1989
58.		0.235	0.125	3.0	3.2487
59.		0.235	0.125	4.0	3.2673
60.		0.235	0.125	5.0	3.3637

Continued

SL No.	Material Used	Thickness of the material (mm)	Void Depth (mm)	Void Diameter (mm)	Breakdown Voltage (kV)
61.	Glass Cloth	0.155	0.025	1.5	13.5058
62.		0.155	0.025	2.0	13.8725
63.		0.155	0.025	3.0	13.9502
64.		0.155	0.025	4.0	13.8818
65.		0.155	0.025	5.0	13.7763
66.		0.195	0.025	1.5	17.8760
67.		0.195	0.025	2.0	17.5761
68.		0.195	0.025	3.0	17.2933
69.		0.195	0.025	4.0	17.6896
70.		0.195	0.025	5.0	17.9443
71.		0.155	0.125	1.5	13.8725
72.		0.155	0.125	2.0	14.0961
73.		0.155	0.125	3.0	14.0100
74.		0.155	0.125	4.0	13.5873
75.		0.155	0.125	5.0	13.9502
76.		0.195	0.125	1.5	17.5761
77.		0.195	0.125	2.0	17.4463
78.		0.195	0.125	3.0	17.9865
79.		0.195	0.125	4.0	17.8760
80.		0.195	0.125	5.0	17.2933

Continued

SL No.	Material Used	Thickness of the material (mm)	Void Depth (mm)	Void Diameter (mm)	Breakdown Voltage (kV)
81.	Manila Paper	0.035	0.025	1.5	1.5328
82.		0.035	0.025	2.0	1.5548
83.		0.035	0.025	3.0	1.5088
84.		0.035	0.025	4.0	1.6090
85.		0.035	0.025	5.0	1.4682
86.		0.06	0.025	1.5	1.5456
87.		0.06	0.025	2.0	1.4413
88.		0.06	0.025	3.0	1.4913
89.		0.06	0.025	4.0	1.6090
90.		0.06	0.025	5.0	1.4682
91.		0.035	0.125	1.5	1.5548
92.		0.035	0.125	2.0	1.5088
93.		0.035	0.125	3.0	1.5456
94.		0.035	0.125	4.0	1.6090
95.		0.035	0.125	5.0	1.4413
96.		0.06	0.125	1.5	1.4913
97.		0.06	0.125	2.0	1.4682
98.		0.06	0.125	3.0	1.5548
99.		0.06	0.125	4.0	1.5088
100.		0.06	0.125	5.0	1.5456

Continued

SL No.	Material Used	Thickness of the material (mm)	Void Depth (mm)	Void Diameter (mm)	Breakdown Voltage (kV)
101.	Lather Minilex	0.12	0.025	1.5	10.4930
102.		0.12	0.025	2.0	10.5760
103.		0.12	0.025	3.0	10.7673
104.		0.12	0.025	4.0	11.0973
105.		0.12	0.025	5.0	10.8598
106.		0.185	0.025	1.5	16.3897
107.		0.185	0.025	2.0	16.8256
108.		0.185	0.025	3.0	16.7663
109.		0.185	0.025	4.0	16.6824
110.		0.185	0.025	5.0	16.5625
111.		0.245	0.025	1.5	16.4542
112.		0.245	0.025	2.0	16.5388
113.		0.245	0.025	3.0	16.3228
114.		0.245	0.025	4.0	17.0022
115.		0.245	0.025	5.0	16.6824
116.		0.12	0.125	1.5	10.8742
117.		0.12	0.125	2.0	10.9330
118.		0.12	0.125	3.0	11.0012
119.		0.12	0.125	4.0	11.0839
120.		0.12	0.125	5.0	11.0973
121.		0.185	0.125	1.5	16.5625
122.		0.185	0.125	2.0	16.5388
123.		0.185	0.125	3.0	16.3228
124.		0.185	0.125	4.0	17.0022
125.		0.185	0.125	5.0	16.4542
126.		0.245	0.125	1.5	16.5388
127.		0.245	0.125	2.0	16.5625
128.		0.245	0.125	3.0	16.3228
129.		0.245	0.125	4.0	16.7663
130.		0.245	0.125	5.0	16.3897

Table 2.7: Input and the Output parameters under AC test conditions

SL No.	Material Used	Thickness of the material (mm)	Void Depth (mm)	Void Diameter (mm)	Breakdown Voltage (kV)
1.	White Minilex	0.125	0.025	1.5	2.2807
2.		0.125	0.025	2.0	2.2909
3.		0.125	0.025	3.0	2.2294
4.		0.125	0.025	4.0	2.3170
5.		0.125	0.025	5.0	2.2447
6.		0.18	0.025	1.5	2.2697
7.		0.18	0.025	2.0	2.2909
8.		0.18	0.025	3.0	2.2294
9.		0.18	0.025	4.0	2.3170
10.		0.18	0.025	5.0	2.2909
11.		0.26	0.025	1.5	2.2294
12.		0.26	0.025	2.0	2.3088
13.		0.26	0.025	3.0	2.2294
14.		0.26	0.025	4.0	2.2885
15.		0.26	0.025	5.0	2.3170
16.		0.125	0.125	1.5	2.2885
17.		0.125	0.125	2.0	2.2447
18.		0.125	0.125	3.0	2.2697
19.		0.125	0.125	4.0	2.2909
20.		0.125	0.125	5.0	2.3088
21.		0.18	0.125	1.5	2.2294
22.		0.18	0.125	2.0	2.2697
23.		0.18	0.125	3.0	2.2885
24.		0.18	0.125	4.0	2.2909
25.		0.18	0.125	5.0	2.2697
26.		0.26	0.125	1.5	2.2885
27.		0.26	0.125	2.0	2.2697
28.		0.26	0.125	3.0	2.2885
29.		0.26	0.125	4.0	2.2909
30.		0.26	0.125	5.0	2.2909

Continued

SL No.	Material Used	Thickness of the material (mm)	Void Depth (mm)	Void Diameter (mm)	Breakdown Voltage (kV)
31.	Leatherite Paper	0.13	0.025	1.5	1.3452
32.		0.13	0.025	2.0	1.3306
33.		0.13	0.025	3.0	1.2972
34.		0.13	0.025	4.0	1.3221
35.		0.13	0.025	5.0	1.3513
36.		0.175	0.025	1.5	1.8459
37.		0.175	0.025	2.0	1.8313
38.		0.175	0.025	3.0	1.7981
39.		0.175	0.025	4.0	1.8229
40.		0.175	0.025	5.0	1.8520
41.		0.235	0.025	1.5	2.2885
42.		0.235	0.025	2.0	2.2697
43.		0.235	0.025	3.0	2.2885
44.		0.235	0.025	4.0	2.2909
45.		0.235	0.025	5.0	2.3088
46.		0.13	0.125	1.5	1.3306
47.		0.13	0.125	2.0	1.3452
48.		0.13	0.125	3.0	1.3221
49.		0.13	0.125	4.0	1.3637
50.		0.13	0.125	5.0	1.2972
51.		0.175	0.125	1.5	1.8313
52.		0.175	0.125	2.0	1.8640
53.		0.175	0.125	3.0	1.7981
54.		0.175	0.125	4.0	1.8520
55.		0.175	0.125	5.0	1.7981
56.		0.235	0.125	1.5	2.2294
57.		0.235	0.125	2.0	2.3170
58.		0.235	0.125	3.0	2.2885
59.		0.235	0.125	4.0	2.3088
60.		0.235	0.125	5.0	2.2697

Continued

SL No.	Material Used	Thickness of the material (mm)	Void Depth (mm)	Void Diameter (mm)	Breakdown Voltage (kV)
61.	Glass Cloth	0.155	0.025	1.5	2.2294
62.		0.155	0.025	2.0	2.2294
63.		0.155	0.025	3.0	2.3088
64.		0.155	0.025	4.0	2.2697
65.		0.155	0.025	5.0	2.3170
66.		0.195	0.025	1.5	2.2885
67.		0.195	0.025	2.0	2.2294
68.		0.195	0.025	3.0	2.2909
69.		0.195	0.025	4.0	2.2294
70.		0.195	0.025	5.0	2.3088
71.		0.155	0.125	1.5	2.2294
72.		0.155	0.125	2.0	2.3170
73.		0.155	0.125	3.0	2.2885
74.		0.155	0.125	4.0	2.2294
75.		0.155	0.125	5.0	2.2697
76.		0.195	0.125	1.5	2.2885
77.		0.195	0.125	2.0	2.3170
78.		0.195	0.125	3.0	2.2885
79.		0.195	0.125	4.0	2.2294
80.		0.195	0.125	5.0	2.2909

Continued

SL No.	Material Used	Thickness of the material (mm)	Void Depth (mm)	Void Diameter (mm)	Breakdown Voltage (kV)
81.	Manila Paper	0.035	0.025	1.5	0.8758
82.		0.035	0.025	2.0	0.8479
83.		0.035	0.025	3.0	0.8154
84.		0.035	0.025	4.0	0.9089
85.		0.035	0.025	5.0	0.8683
86.		0.06	0.025	1.5	0.8479
87.		0.06	0.025	2.0	0.8154
88.		0.06	0.025	3.0	0.8758
89.		0.06	0.025	4.0	0.9089
90.		0.06	0.025	5.0	0.8388
91.		0.035	0.125	1.5	0.8154
92.		0.035	0.125	2.0	0.8758
93.		0.035	0.125	3.0	0.8388
94.		0.035	0.125	4.0	0.8479
95.		0.035	0.125	5.0	0.9089
96.		0.06	0.125	1.5	0.8758
97.		0.06	0.125	2.0	0.8388
98.		0.06	0.125	3.0	0.8154
99.		0.06	0.125	4.0	0.8479
100.		0.06	0.125	5.0	0.8388

Continued

SL No.	Material Used	Thickness of the material (mm)	Void Depth (mm)	Void Diameter (mm)	Breakdown Voltage (kV)
101.	Lather Minilex	0.12	0.025	1.5	2.2294
102.		0.12	0.025	2.0	2.2909
103.		0.12	0.025	3.0	2.2807
104.		0.12	0.025	4.0	2.2447
105.		0.12	0.025	5.0	2.2697
106.		0.185	0.025	1.5	2.2885
107.		0.185	0.025	2.0	2.2697
108.		0.185	0.025	3.0	2.2909
109.		0.185	0.025	4.0	2.2807
110.		0.185	0.025	5.0	2.2909
111.		0.245	0.025	1.5	2.2807
112.		0.245	0.025	2.0	2.2697
113.		0.245	0.025	3.0	2.2885
114.		0.245	0.025	4.0	2.2697
115.		0.245	0.025	5.0	2.2447
116.		0.12	0.125	1.5	2.2697
117.		0.12	0.125	2.0	2.3170
118.		0.12	0.125	3.0	2.2885
119.		0.12	0.125	4.0	2.3088
120.		0.12	0.125	5.0	2.2909
121.		0.185	0.125	1.5	2.2294
122.		0.185	0.125	2.0	2.3170
123.		0.185	0.125	3.0	2.2885
124.		0.185	0.125	4.0	2.2447
125.		0.185	0.125	5.0	2.3170
126.		0.245	0.125	1.5	2.2885
127.		0.245	0.125	2.0	2.3170
128.		0.245	0.125	3.0	2.2447
129.		0.245	0.125	4.0	2.2697
130.		0.245	0.125	5.0	2.3088

For the purpose of prediction by soft computing techniques, 130 values of the input and the output parameters each from Tables 2.6 and Table 2.7, under DC and AC test conditions are used separately for the proposed models, presented in the subsequent Chapters.

It has been already mentioned after equation (2.1) that ß give a measure of the dispersion of the breakdown voltage data. The more the value of ß, the less is the dispersion of the data. Hence, by merely examining the values of ß obtained in Table 2.4 and 2.5, the insulating materials fall under three main categories.

A) The degree of dispersion is greater in DC than AC, i.e., $ß_{DC} < ß_{AC}$

B) The degree of dispersion is nearly the same for both DC and AC, i.e., $ß_{DC} \approx ß_{AC}$

C) The degree of dispersion is less in DC than AC, i.e., $ß_{DC} > ß_{AC}$

Table 2.8 summarizes the range of ß under DC and AC for all materials with all thickness.

Table 2.8: Summary of the range of ß under DC and AC for all materials

SL No.	Insulating Materials	Category	$ß_{DC}$	$ß_{AC}$
1.	White Minilex of all thickness	A	8.51 - 12.27	24.10 - 51.30
2.	Glass Cloth (thickness 0.155 mm)	A	11.21 - 16.42	24.10 to 51.30
3.	Lather Minilex of all thickness	A	8.71 - 16.71	24.10 - 51.30
4.	Leatherite Paper of all thickness	A	9.56 – 20..85	14.90 - 51.30
5.	Glass Cloth (thickness 0.195 mm)	C	36.70 - 80.20	24.10 - 51.30
6.	Manila Paper of all thickness	B	6.84 – 9.76	6.85 - 10.49

2.4 Monitoring of the state of solid insulating materials

Apart from the breakdown voltage prediction due to PD in cavities, the monitoring of the state of the insulation and it's interpretation is also another important and challenging task. In order to monitor the state of the insulation after application of various voltages, the samples of the solid insulating materials mentioned in Section 2.2.1 were observed under Scanning Electron Microscope (SEM). Figure 2.6 shows the SEM (JEOL JSM-6480LV). The SEM was operated in low vacuum mode in order to observe the samples, which are difficult to view due to excessive surface charging.

Figure 2.6 : SEM (JEOL JSM-6480LV)

Interpretation of SEM images

The SEM images for the samples of some of the solid insulating materials are discussed below.

- **White Minilex (DC)**

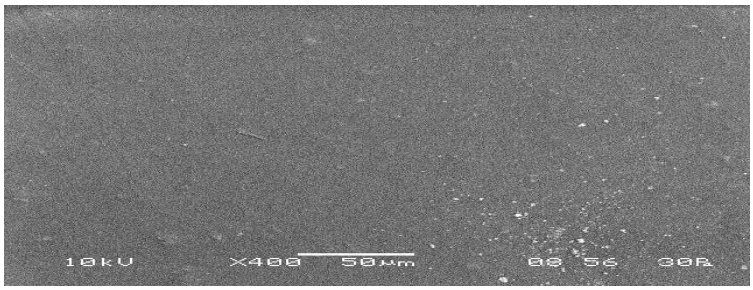

a)

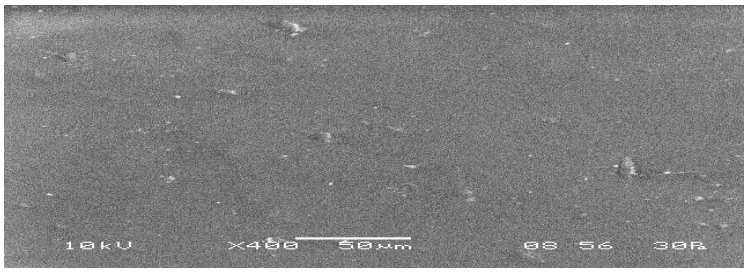

b)

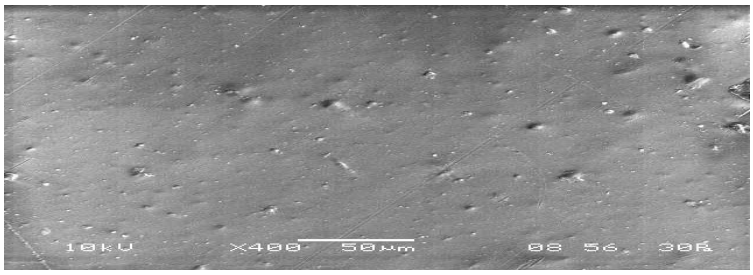

c)

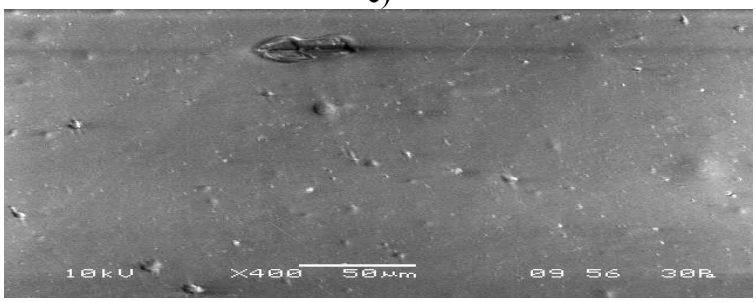

d)

Figure 2.7: SEM observations for White Minilex Paper samples; (a) Virgin, and stressed at (b) 14 kV, (c) 21 kV and (d) 28 kV (Breakdown) DC Voltages (t = 0.125mm, t_1 = 0.025mm and d =2 mm).

Figure 2.7 shows the SEM observations for the (a) virgin samples of White Minilex Paper (thickness of 0.125 mm) and the samples stressed with a voltage of (b) 14 kV, (c) 21 kV and (d) 28 kV (DC conditions) respectively, while the void depth was 0.025mm and void diameter was 2 mm. The breakdown of the sample took place at a voltage level of 28 kV. The accelerated voltage for the SEM was kept at 10 kV and the vacuum level was 30 Pa. The center of the samples in Figure (a) to (d) was magnified 400 times. Figure (a) is clearly a very healthy sample as expected. In Figures (b) and (c) some spots may be seen on the surface of the sample with Figure (c) turning more whitish compared to (b). Figure (d) clearly indicates the increased roughness of the sample with some spots and shallow cracks. The roughness of the sample shows the increased SE emission.

Similarly, in Figure 2.8, the SEM observations for the (a) virgin samples of White Minilex Paper (thickness of 0.18 mm) and the samples stressed with a voltage of (b) 1.1 kV, (c) 1.6 kV and (d) 2.2 kV (AC conditions) respectively , while the void depth was 0.125mm and void diameter was 4 mm. The breakdown of the sample took place at a voltage level of 2.2 kV. The accelerated voltage for the SEM was kept at 15 kV and the vacuum level was 30 Pascals. In the virgin sample (i.e. in Figure (a)) and the sample stressed at 50 % of the breakdown voltage (i.e. in Figure (b)) it is noted that the samples are reasonably healthy. But Figure (b) appears to be more whitish compared to Figure (a) and the deterioration of the samples at 75% of the breakdown voltage is quiet conspicuous with spots becoming very prominent. Figure 2.3 (d) is quiet similar to Figure 2.2 (d) indicating the increased roughness of the sample with spots and some shallow cracks on the onset of breakdown and the reason for this being the same.

- **White Minilex (AC)**

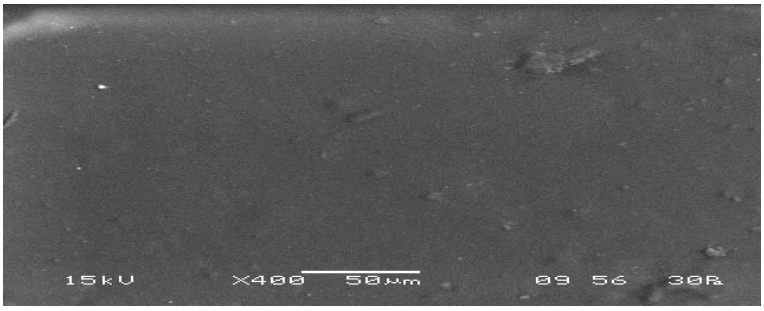

a)

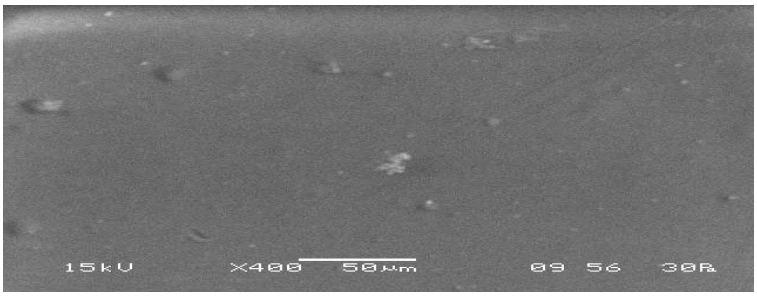

b)

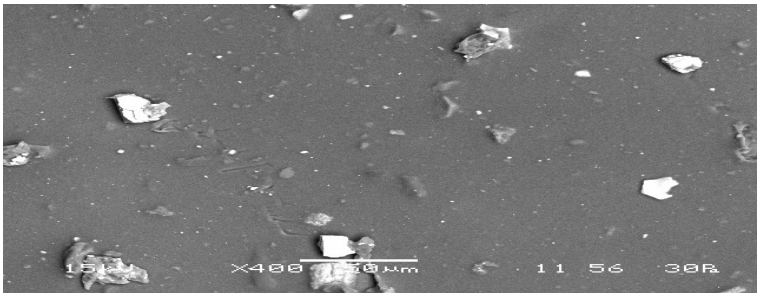

c)

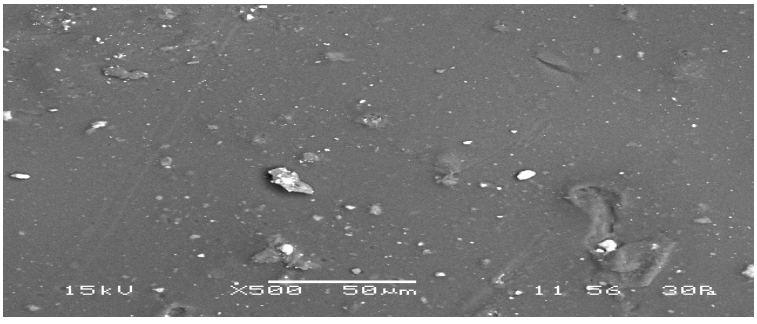

d)

Figure 2.8: SEM observations for White Minilex Paper samples; (a) Virgin, and stressed at (b) 1.1 kV, (c) 1.6 kV and (d) 2.2 kV (Breakdown) AC Voltages (t = 0.18mm, t_1 = 0.125mm and d =4 mm).

- **Leatherite Paper (DC)**

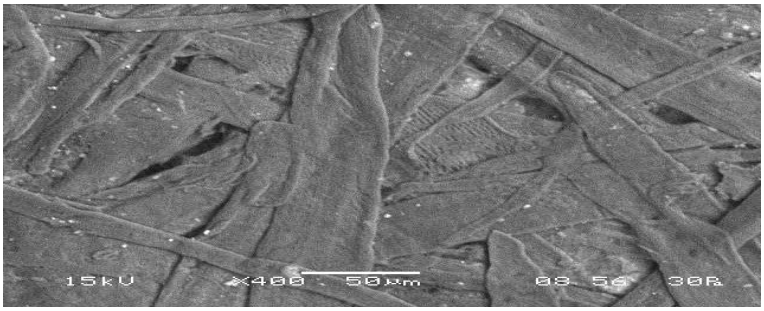

a)

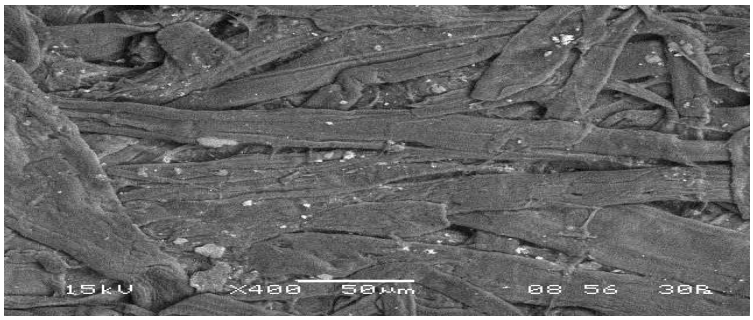

b)

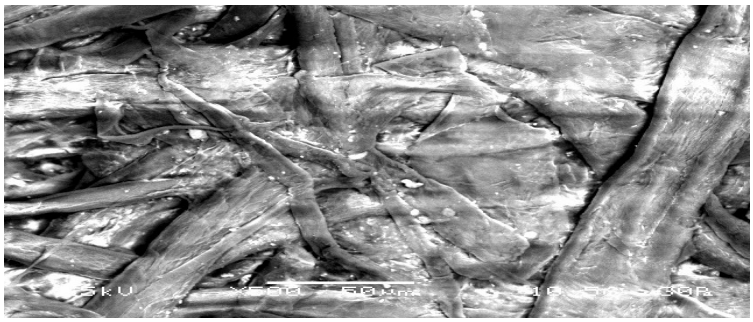

c)

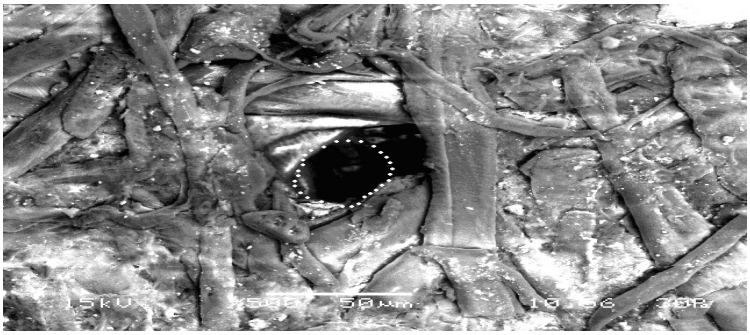

d)

Figure 2.9: SEM observations for Leatherite Paper samples; (a) Virgin, and stressed at (b) 1.0 kV, (c) 1.5 kV and (d) 2.0 kV (Breakdown) DC Voltages (t = 0.13mm, t_1 = 0.025mm and d =5 mm).

Figure 2.9 shows the SEM observations for the (a) virgin samples of Leatherite Paper (thickness of 0.13 mm) and the samples stressed with a voltage of (b) 1.0 kV, (c) 1.5 kV and (d) 2.0 kV (DC conditions) respectively, while the void depth was 0.025mm and void diameter was 5 mm. The breakdown of the sample took place at a voltage level of 2.0 kV. The center of the samples are healthy in Figure (a) and (b) as expected. But at 75% of the breakdown voltage (i.e. in Figure (c)) the center of the sample appears to be more whitish, indicating excessive charging of the sample. It also means that the sample has started deteriorating. The Figure (d) clearly shows a puncture taking place right at the center along with the whitish colour of the sample. The puncture is having an area of approximately 50 μm by 35 μm (1750 μm^2). The puncture also implies that the center of the sample is highly stressed and the breakdown is due to PD in cavities of the sample.

Similarly, in Figure 2.10 shows the SEM observations for the (a) virgin samples of Leatherite Paper (thickness of 0.13 mm) and the samples stressed with a voltage of (b) 0.7 kV, (c) 1.0 kV and (d) 1.4 kV (AC conditions) respectively, while the void depth was 0.125mm and void diameter was 1.5 mm. The breakdown of the sample took place at a voltage level of 1.4 kV. In this case also the scenario is very similar to the Leatherite Paper under DC. Figure (a) and b) are healthy samples. The samples starts to become whitish at 75% of the breakdown voltage (i.e. in Figure (c)), indicating the general roughness and deterioration of the sample. From Figure (d) it can be safely inferred that the PD activity is more prominent under AC rather than DC as the puncture area is 180 μm by 100 μm.

- **Leatherite Paper (AC)**

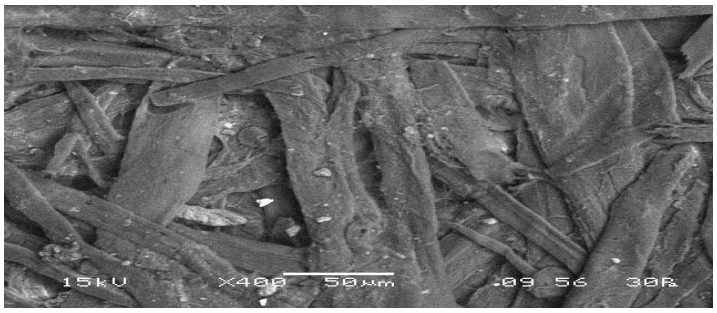

a)

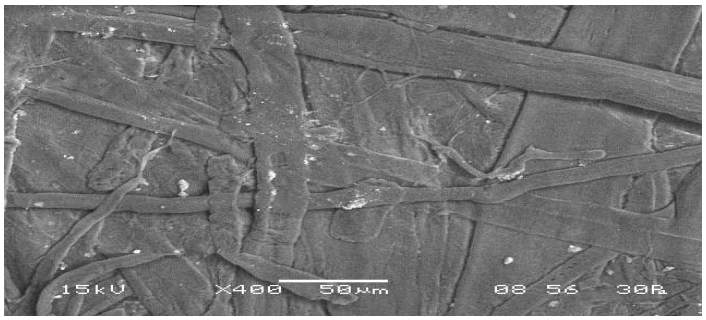

b)

c)

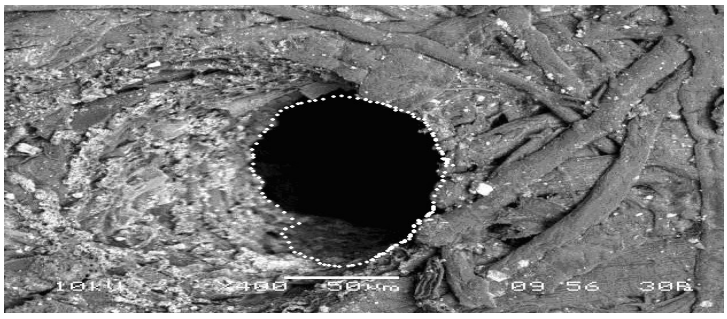

d)

Figure 2.10: SEM observations for Leatherite Paper samples; (a) Virgin, and stressed at (b) 0.7 kV, (c) 1.0 kV and (d) 1.4 kV (Breakdown) AC Voltages (t = 0.13mm, t_1 = 0.125mm and d =1.5 mm).

- **Manila Paper (DC)**

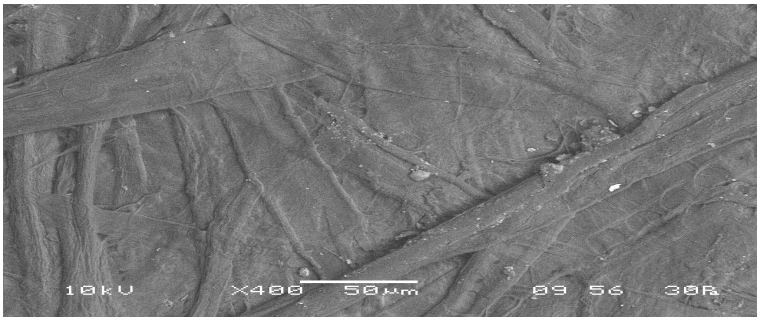

a)

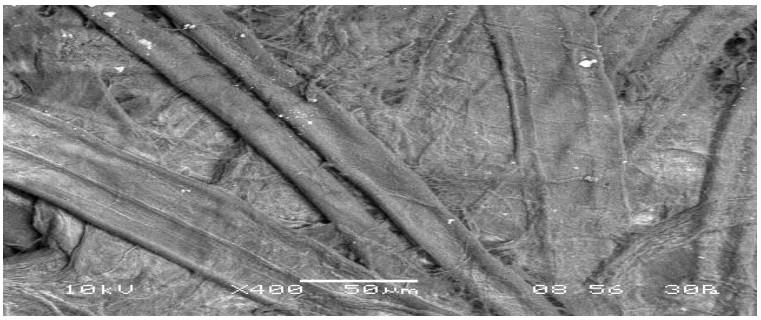

b)

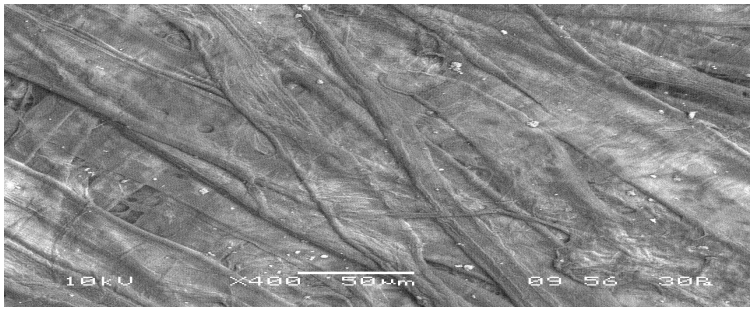

c)

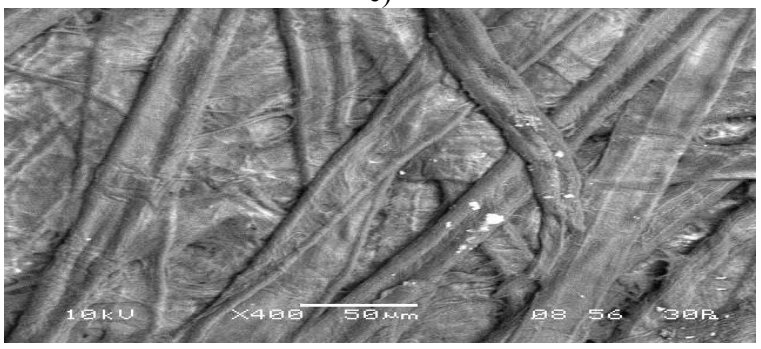

d)

Figure 2.11: SEM observations for Manila Paper samples; (a) Virgin, and stressed at (b) 0.75 kV, (c) 1.0 kV and (d) 1.5 kV (Breakdown) DC Voltages (t = 0.06mm, t_1 = 0.025mm and d =2 mm).

Figure 2.11 shows the SEM observations for the (a) virgin samples of Manila Paper (thickness of 0.06 mm) and the samples stressed with a voltage of (b) 0.75 kV, (c) 1.0 kV and (d) 1.5 kV (DC conditions) respectively, while the void depth was 0.025mm and void diameter was 2 mm. The breakdown of the sample took place at a voltage level of 1.5 kV. In Figure (a) the sample is in it's healthy virgin state. But at 50%, 75 % and 100% of the breakdown voltage the center of the sample appears whitish, implying that the weathering process deteriorates the samples. The whitish colour signifies the appearance of chemical pollutants such as SO_2 and ozone which may degrade the material. Since there is no complete puncture taking place at the center of the sample, the sample of Manila Paper under DC is not that much overstressed compared to Leatherite Paper under DC (Figure 2.9 d).

Similarly, in Figure 2.12 shows the SEM observations for the (a) virgin samples of Manila Paper (thickness of 0.06 mm) and the samples stressed with a voltage of (b) 0.4 kV, (c) 0.6 kV and (d) 0.8 kV (AC conditions) respectively, while the void depth was 0.025mm and void diameter was 3 mm. The breakdown of the sample took place at a voltage level of 0.8 kV. The virginity of the sample is quiet obvious in Figure (a). The state of the insulation hardly changes in Figure (b). But in Figure (c) the center of the sample appears whitish implying it's roughness. On the onset of breakdown in Figure (d) the sample is not only whitish but a conspicuous rupture appears at it's center. The puncture may be due to bond breaking and chain scission. This also confirms that in paper type insulating materials such as Leatherite Paper and Manila Paper the PD activity is more prominent in AC than DC. The area of the puncture is around 3000 μm^2.

- **Manila Paper (AC)**

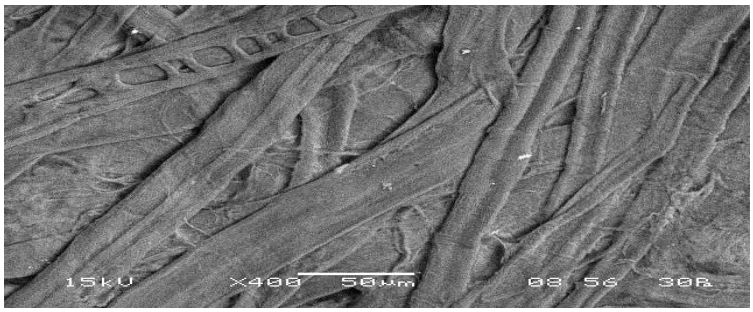

a)

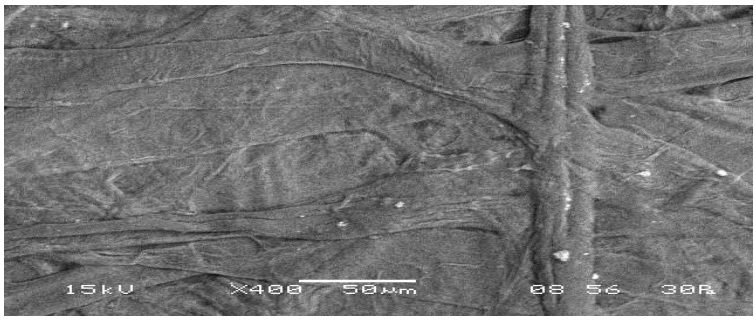

b)

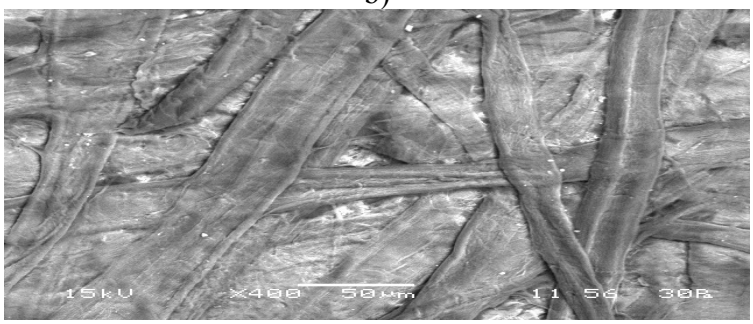

c)

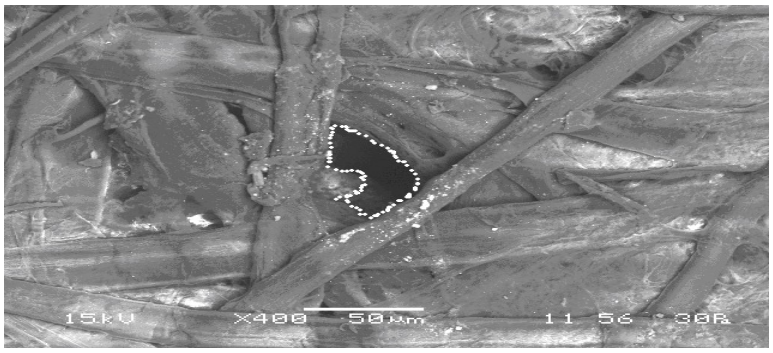

d)

Figure 2.12: SEM observations for Manila Paper samples; (a) Virgin, and stressed at (b) 0.4 kV, (c) 0.6 kV and (d) 0.8 kV (Breakdown) AC Voltages (t = 0.06mm, t_1 = 0.025mm and d =3 mm).

- **Lather Minilex (DC)**

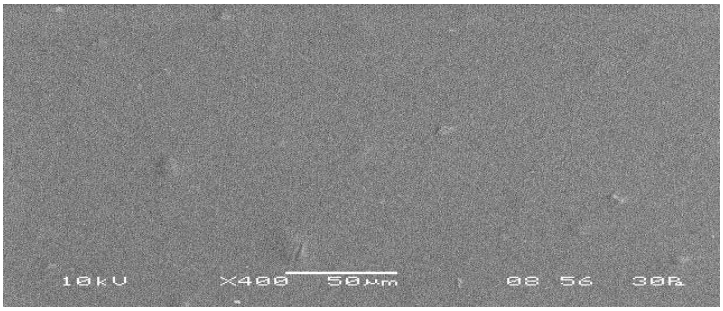

a)

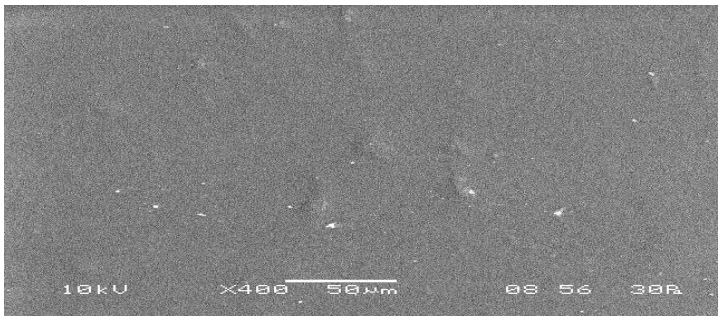

b)

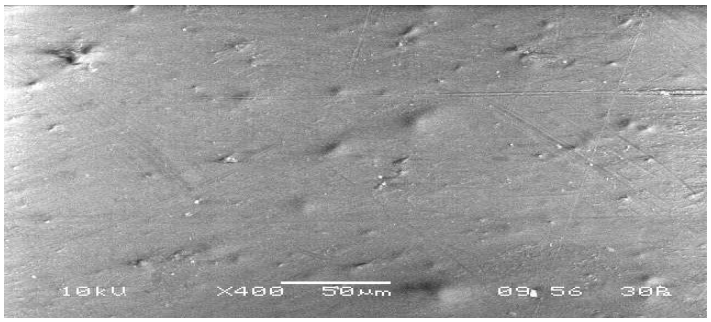

c)

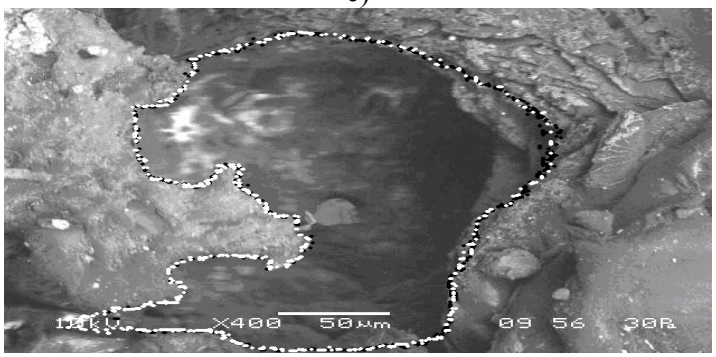

d)

Figure 2.13: SEM observations for Lather Minilex samples; (a) Virgin, and stressed at (b) 9 kV, (c) 13.5 kV and (d) 18 kV (Breakdown) DC Voltages (t = 0.245mm, t_1 = 0.125mm and d =2 mm).

Figure 2.13 shows the SEM observations for the (a) virgin samples of Lather Minilex (thickness of 0.245 mm) and the samples stressed with a voltage of (b) 9 kV, (c) 13.5 kV and (d) 18 kV (DC conditions) respectively, while the void depth was 0.125mm and void diameter was 2 mm. The breakdown of the sample took place at a voltage level of 18 kV. Figure (a) is the virgin state of the sample. In Figure (b) some white spots may be seen on the center of the sample indicating that the deterioration has started taking place. The Figure (c) is possibly the best example of chalking as the center of the sample appears whitish with some spots. In Figure (d) the complete rupture has taken place at the center of the sample. The puncture area is approximately 350 μm by 200 μm and it may be due to breaking of chemical bonds in the insulating material.

Similarly, in Figure 2.14 shows the SEM observations for the (a) virgin samples of Lather Minilex (thickness of 0.245 mm) and the samples stressed with a voltage of (b) 1.1 kV, (c) 1.6 kV and (d) 2.2 kV (AC conditions) respectively, while the void depth was 0.025mm and void diameter was 3 mm. The breakdown of the sample took place at a voltage level of 2.2 kV. Figure (a) shows the healthiest sample. In Figure (b) some white spots are visible. The sample further deteriorates with increase in voltage as may be seen from Figure (c) and (d). The appearance of whitish colour may indicate excessive charge accumulation on the surface of the sample. Since no puncture takes place on the onset of breakdown, it would mean that PD activity for Lather Minilex is less under AC than DC. This scenario is precisely opposite of the PD activity taking place in paper based samples, such as Leatherite Paper and Manila Paper.

- **Lather Minilex (AC)**

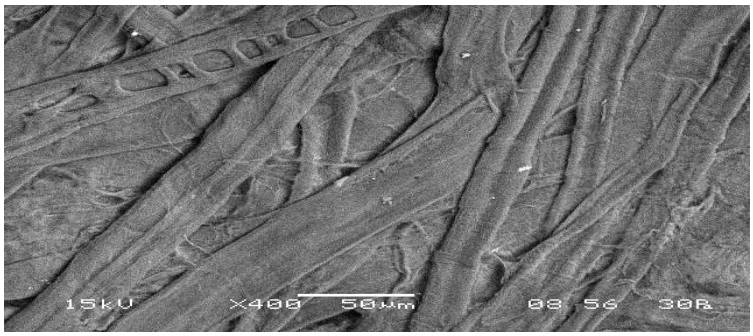

a)

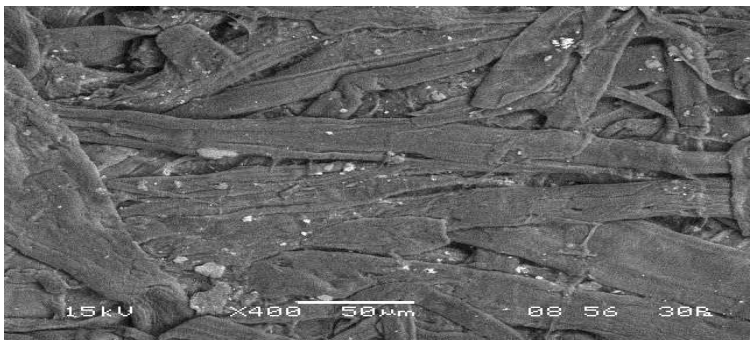

b)

c)

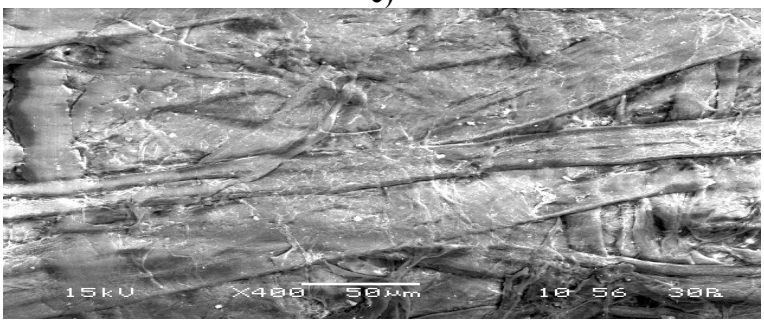

d)

Figure 2.14: SEM observations for Lather Minilex samples; (a) Virgin, and stressed at (b) 1.1 kV, (c) 1.6 kV and (d) 2.2 kV (Breakdown) AC Voltages (t = 0.245mm, t_1 = 0.025mm and d =3 mm).

2.5 Breakdown voltage variation under DC and AC test conditions

The experimental results under DC and AC conditions and the statistically analyzed breakdown voltage data are available in Table 2.1, Table 2.2, Table 2.4 and Table 2.5. These data can be utilized to study the variation of the breakdown voltage with each of the input parameters, namely the thickness of the insulating material, void depth and void diameter.

- **DC condition**

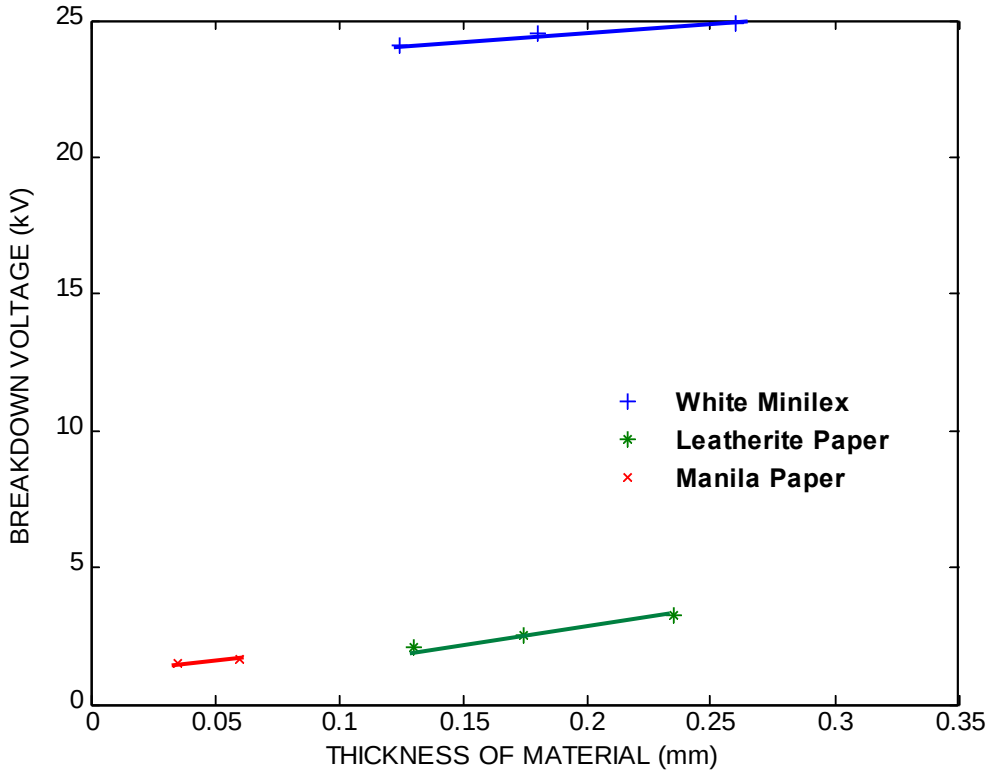

Figure 2.15: Variation of Breakdown voltage of White Minilex, Leatherite Paper and Manila Paper with sample thickness t under DC test condition (t_1=0.125 mm, d=1.5 mm)

Figure 2.15 shows the breakdown voltage of the three insulating materials, namely, White Minilex, Leatherite Paper and Manila Paper under DC test conditions, against their respective thicknesses keeping void diameter as 1.5 mm and void depth of 0.125mm. The figure clearly indicates that the breakdown voltage of the three insulating materials increases

with increase in thickness and the breakdown voltage of White Minilex is very high in comparison to the breakdown voltage of Leatherite Paper in almost the same range of thickness. Hence, White Minilex has superior insulating properties compared to Leatherite Paper under DC conditions.

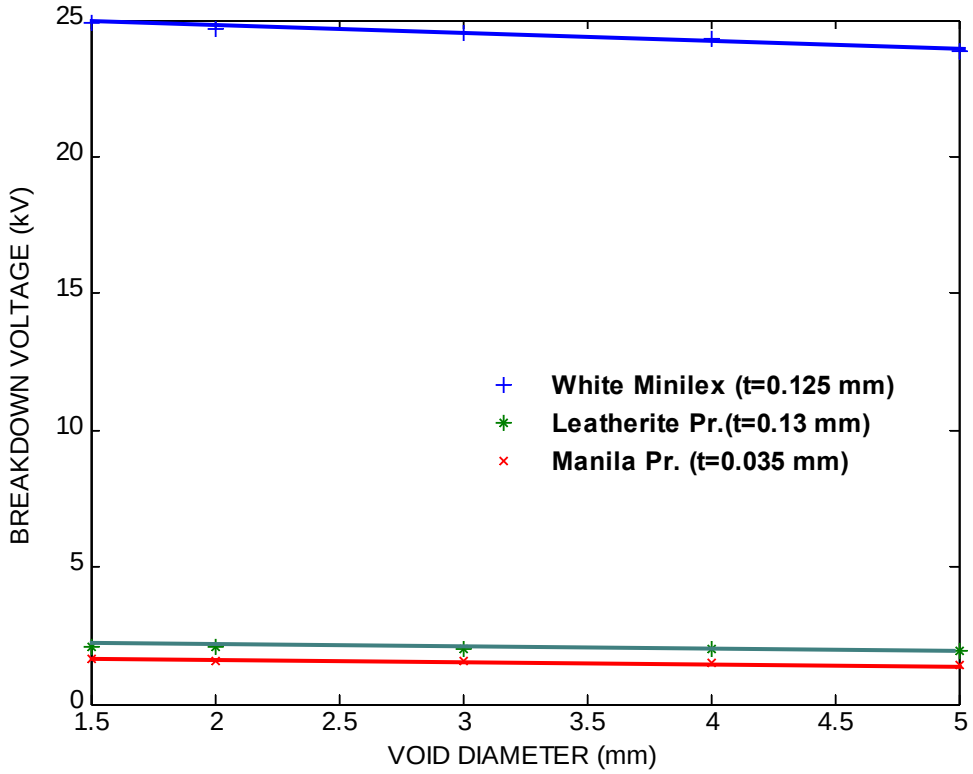

Figure 2.16: Variation of Breakdown voltage of White Minilex (t = 0.125mm), Leatherite Paper (t = 0.13mm), Manila Paper (t = 0.035mm) with the void diameter d under DC test condition (t_1=0.125 mm)

Figure 2.16 shows that the breakdown voltage of three solid insulating materials decreases with the increase in the void diameter keeping their respective thicknesses and void depth to be constant. This result is quiet expected, as the PD activity would be higher at larger void diameters. Moreover, the breakdown voltage values of White Minilex are very high in comparison to the breakdown voltage values of Leatherite Paper and Manila Paper. This clearly confirms that White Minilex has far superior insulating properties compared not only to Leatherite Paper but also Manila Paper .

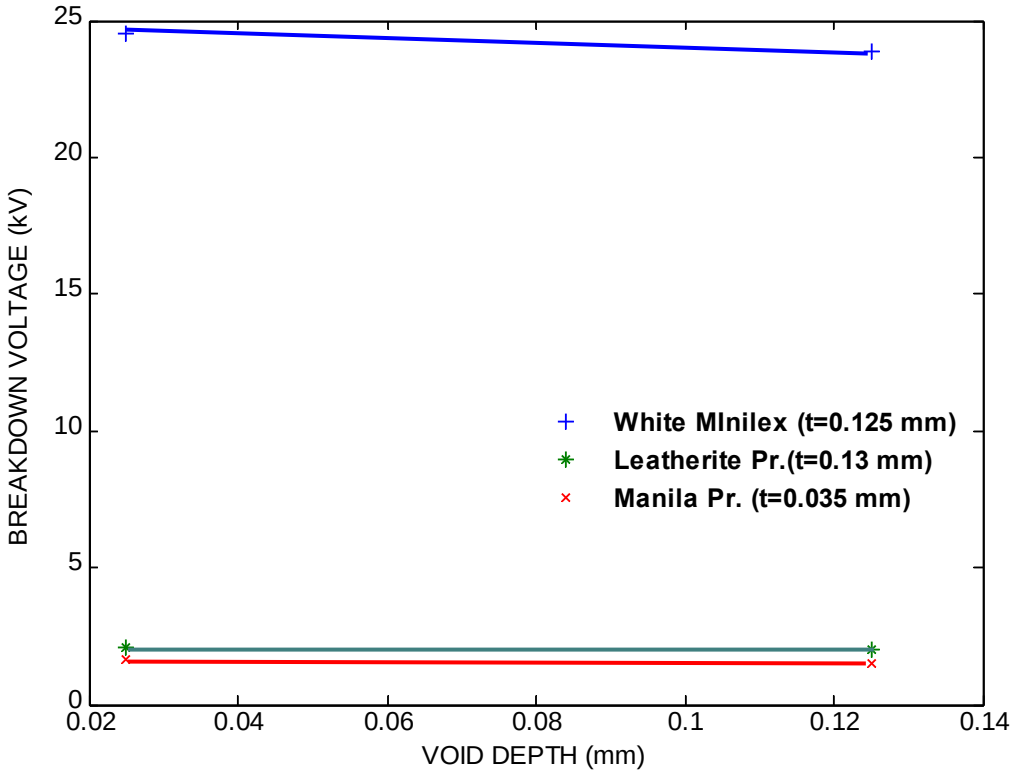

Figure 2.17: Variation of Breakdown voltage (kV) of White Minilex (t = 0.125mm), Leatherite Paper (t = 0.13mm), Manila Paper (t = 0.035mm) with the void depth t_1 under DC test condition (d=1.5 mm)

Figure 2.17 shows that the breakdown voltage of the three insulating materials decreases with the increase in the void depth keeping their respective thicknesses and void diameter to be constant. as at larger void depth PD activity would substantially increase.

- **AC condition**

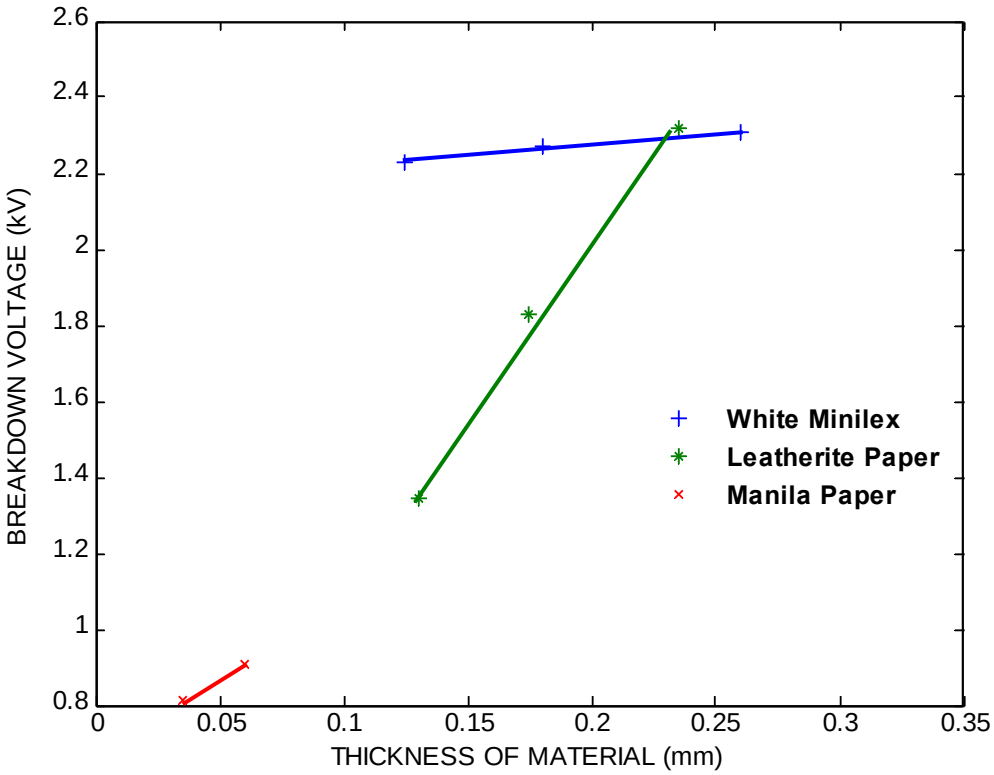

Figure 2.18: Variation of Breakdown voltage of White Minilex, Leatherite Paper and Manila Paper with sample thickness t under AC test condition (t_1=0.125 mm, d=1.5 mm)

Figure 2.18 shows the variation of the breakdown voltage of the three solid insulating materials with the variation of their thickness keeping void depth as 0.125 mm and void diameter as 1.5 mm under AC conditions. This Figure clearly indicates that the breakdown voltage increases with the increase in thickness for all the three insulating materials. Moreover from Figure 2.15 and Figure 2.18 it can be seen that White Minilex at DC condition has breakdown voltage values nearly 10 times that under AC conditions. Hence White Minilex is highly recommended for DC applications.

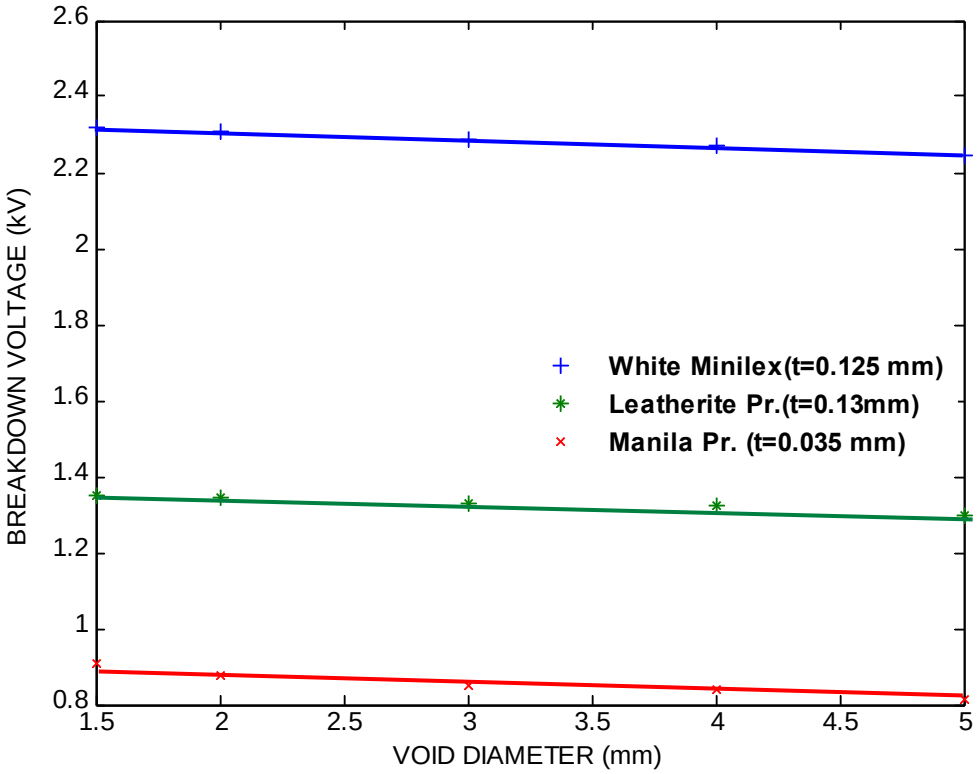

Figure 2.19: Variation of Breakdown voltage (kV) of White Minilex (t = 0.125mm), Leatherite Paper (t = 0.13mm), Manila Paper (t = 0.035mm) with the void diameter d under AC test condition (t_1 = 0.125 mm)

Figure 2.19 shows that the breakdown voltage of all the three solid insulating materials decreases with the increase in the void diameter keeping their respective thickness and void depth to be constant. This result is quiet obvious as the PD activity would definitely increase at larger values of the void diameter. Since the breakdown voltage values of White Minilex are greater than that of Leatherite Paper, the White Minilex is a better insulator compared to Leatherite Paper . The Leatherite Paper in turn is a better insulator compared to Manila Paper.

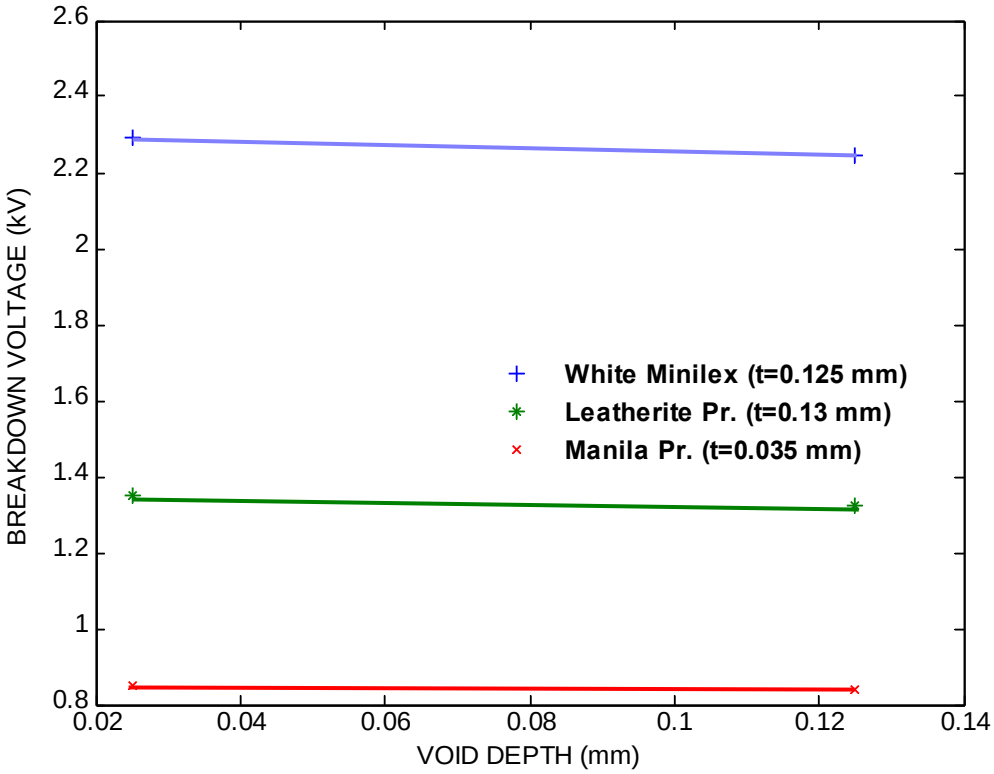

Figure 2.20: Variation of Breakdown voltage (kV) of White Minilex(t=0.125mm), Leatherite Paper(t=0.13mm), Manila Paper(t=0.035mm) with the void depth t_1 under AC test conditions (d=1.5 mm)

Figure 2.20 similarly shows that the breakdown voltage decreases with the increase in the void depth for all the three solid insulating materials keeping their thicknesses and the void diameter to be constant. The reason for this is the same as discussed for Figure 2.19.

2.6 Conclusion

This Chapter has provided the groundwork for prediction of the breakdown voltage due to PD in cavities by carrying out experimental data generation and statistical analysis of the same. The state of some of the solid insulating materials was exhibited at various voltages under both DC and AC test conditions in the form of SEM images. In addition, the variation of the breakdown voltage of three insulating materials was studied under both DC and AC conditions as a function of the thickness of the material, void diameter and void depth.

Chapter 3

BREAKDOWN VOLTAGE MODELING USING MULTILAYER FEEDFORWARD NEURAL NETWORK

3.1 Introduction

In Chapter 2, the breakdown voltage data of different sheet samples due to the void inclusions have been obtained using Cylinder-Plane electrode system under both DC and AC conditions. The statistical analysis of the experimental data has been then carried out to arrive at the 63.2% breakdown voltage ά. This Chapter details the attempt at modeling of the breakdown voltage using Multilayer Feedforward Neural Network (MFNN).

3.2 Multilayer Feedforward Network

- **MFNN Structure**

Artificial Neural Networks (ANNs) have become the subject of widespread interest, largely because of their wide range of applicability and the ease with which they handle complex and non-linear problems. They are massively parallel-interconnected networks of simple elements intended to interact with the real world in the same way as the biological nervous system. They offer an unusual scheme based programming standpoint and exhibit higher computing speeds compared to other conventional methods. ANNs are characterized by their topology, that is, the number of interconnections, the node characteristics that are classified by the type of nonlinear elements used and the kind of learning rules employed. The ANN is composed of an organized topology of Processing Elements (PEs) called neurons. In Multilayer Feedforward Neural Network (MFNN) the PEs are arranged in layers and only PEs in adjacent layers are connected. The MFNN structure used in this thesis consists of three layers, namely, the input layer, the hidden layer and the output layer as shown in Figure 3.1.

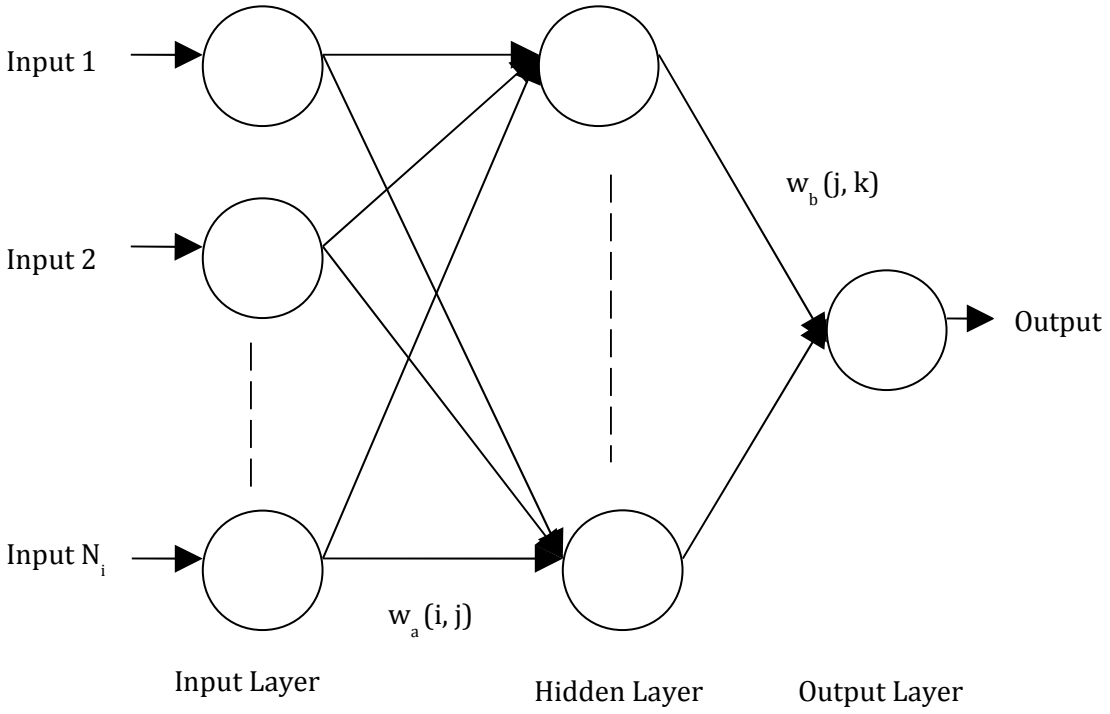

Figure 3.1 Multilayer Feedforward Neural Network

The input layer consists of N_i neurons corresponding to the N_i inputs. The number of output neurons is decided by the number of predicted parameters. The Back Propagation[108-110] Algorithm (BPA) is used to train the network. The sigmoidal function represented by equation (3.1) is used as the activation function for all the neurons except for those in the input layer.

$$S(x) = 1 / (1+e^{-x}) \qquad (3.1)$$

- **Choice of Hidden Neurons**

The choice of optimal number of hidden neurons, N_h is the most interesting and challenging aspect in designing the MFNN. There are various schools on thought in deciding the value of N_h. Simon Haykin [108] has specified that N_h should lie between 2 and ∞. Hecht-Nielsen [109] uses ANN interpretation of Kolmogorov's theorem to arrive at the upper bound on the N_h for a single hidden layer network as $2(N_i+1)$, where N_i is the number of input neurons. However, this value should be decided very judiciously depending on the requirement of a problem. A large value of N_h may reduce the training error associated with the MFNN, but at the cost of increasing the computational complexity and time. For example, if one gets a tolerably low value of training error with certain value of N_h, there is no point in further increasing the value of N_h to enhance the performance of the MFNN.

- **Normalization of Input-Output data**

The input and the output data are normalized before being processed in the network. In this scheme of normalization, the maximum values of the input and output vector components are determined as follows:

$$n_{i,\max} = \max(n_i(p)) \quad p = 1,\ldots\ldots, N_p,\ i = 1,\ldots\ldots, N_i \qquad (3.2)$$

Where N_p is the number of patterns in the training set

$$o_{k,\max} = \max(o_k(p)) \quad p = 1,\ldots\ldots N_p,\ i = 1,\ldots\ldots N_k \qquad (3.3)$$

Where N_k is the number of neurons in the output layer, that is, the number of predicted parameters.

Normalized by these maximum values, the input and output variables are obtained as follows:

$$n_{i,nor}(p) = \frac{n_i(p)}{n_{i,\max}} \quad p = 1,\ldots\ldots, N_p,\ i = 1,\ldots\ldots, N_i \qquad (3.4)$$

and

$$o_{k,nor}(p) = \frac{o_k(p)}{o_{k,\max}} \quad p = 1,\ldots\ldots N_p,\ i = 1,\ldots\ldots N_k \qquad (3.5)$$

After normalization, the input and output variables lie [77] in the range of 0 to 1.

- **Choice of ANN parameters**

The learning rate, η_1 and the momentum factor, α_1 have a very significant effect on the learning speed of the BPA. The BPA provides an approximation to the trajectory in the weight space computed by the method of steepest descent method [108]. If the value of η_1 is considered very small, this results in slow rate of learning, while if the value of η_1 is too large in order to speed up the rate of learning, the MFNN may become unstable (oscillatory). A simple method of increasing the rate of learning without making the MFNN unstable is by adding the momentum factor α_1 [110]. Preferably, the values of η_1 and α_1 should lie between 0 and 1 [108].

- **Weight Update Equations**

The weights between the hidden layer and the output layer are updated based on the equation (3.6) as follows:

$w_b(j, k, m+1) = w_b(j, k, m) + \eta_1 * \delta_k(m) * S_b(j) + \alpha_1 [w_b(j, k, m) - w_b(j, k, m-1)]$ (3.6)

Where m is the number of iterations, j varies from 1 to N_h and k varies from 1 to N_k. $\delta_k(m)$ is the error for the k^{th} output at the m^{th} iteration. $S_b(j)$ is the output from the hidden layer.

Similarly, the weights between the hidden layer and the input layer are updated as follows:

$w_a(i, j, m+1) = w_a(i, j, m) + \eta_1 * \delta_j(m) * S_a(i) + \alpha_1 [(w_a(i, j, m) - w_a(i, j, m-1)]$ (3.7)

Where i varies from 1 to N_i as there are N_i inputs to the network, $\delta_j(m)$ is the error for the j^{th} output after the m^{th} iteration and $S_a(i)$ is the output from the first layer. The $\delta_k(m)$ in equation (3.6) and $\delta_j(m)$ in equation (3.7) are related as

$$\delta_j(m) = \sum_{k=1}^{K} \delta_k(m) * w_b(j, k, m) \quad (3.8)$$

- **Evaluation Criterion**

The Mean Square Error E_{tr} for the training patterns after the m^{th} iteration is defined as

$$E_{tr}(m) = (1/N_p) * [\sum_{p=1}^{Np} \{V_{1p} - V_{2p}(m)\}^2] \quad (3.9)$$

Where V_{1p} is the experimental value of the breakdown voltage. $V_{2p}(m)$ is the estimated value of the breakdown voltage after m^{th} iteration. The training is stopped when the least value of E_{tr} has been obtained and this value does not change much with the number of iterations.

The Mean Absolute Error E_{ts} is a good performance measure for judging the accuracy of the MFNN System. The E_{tr} tells how well the network has adopted to fit the training data only, even if the data are contaminated. On the other hand, the E_{ts} indicates how well a trained network behaves on a new data set not included in the training set. The value of E_{ts} is calculated based on the least value of E_{tr}. The E_{ts} for the test data expressed in percentage is given by

$$E_{ts} = (1/N_S) * [\sum_{s=1}^{Ns} | (V_{4s} - V_{3s}) | / V_{3s}] * 100 \quad (3.10)$$

Where V_{3s} is the experimental value of the breakdown voltage taken for testing purpose, V_{4s} is the estimated value of the breakdown voltage after the test input data is passed through the trained network and N_s is the number of test patterns.

3.3 Modeling of Breakdown Voltage using MFNN

This section details the attempt at modeling of breakdown voltage due to PD in voids under DC / AC conditions using MFNN. These models predicts the breakdown voltages as a function of different void parameters, namely, void diameter and void depth and insulation sheet thickness both under DC and AC conditions. The network is provided with both input data and desired response; and is trained in a supervised fashion using the back propagation

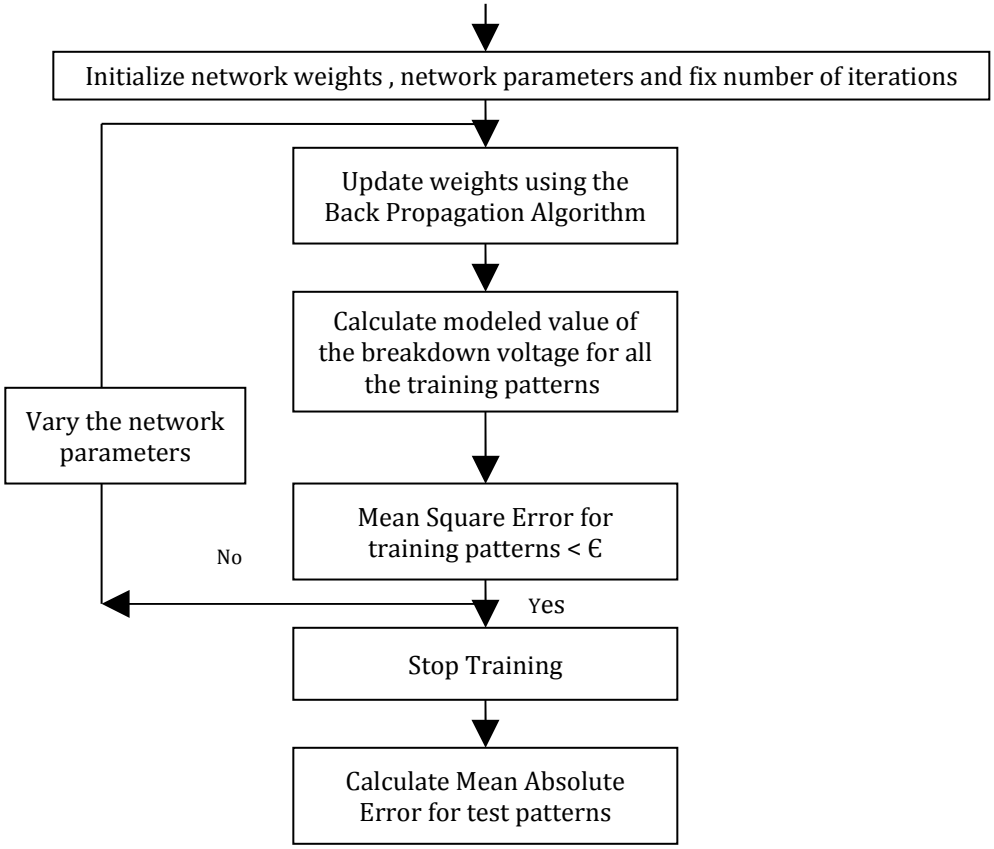

Figure 3.2 : Flow Chart for the MFNN

algorithm. The back propagation algorithm performs the input to output mapping by making weight connection adjustment following the discrepancy between the computed output value and the desired output response. The training phase is completed after a series of iterations. In each iteration, output is compared with the desired response and a match is obtained. Figure 3.2 shows the flowchart for the MFNN.

In order to predict the breakdown voltage under DC / AC conditions a software program has been developed in MATLAB 7.1 to solve equations (3.1) to (3.10). The program is suitably modified for different models based on input – output parameters.

3.3.1 Prediction of the breakdown voltage due to PD in voids under DC conditions

Two models are proposed as follows

- **Model 1**

In model 1, the number of input parameters is two, that is, the thickness of the insulation sheets t and the void diameter d; and the output parameter is the breakdown voltage to be predicted. The void depth t_1 is kept constant at 0.125mm. Since, the input parameters are two, the value of N_i is two for this model. In addition, since the output parameter is only one, the value of N_k is one.

The total number of insulating materials considered for the purpose of modeling is five. There are three values of thickness for each of White Minilex, Leatherite and Lather Minilex materials and five different values of void diameter. Therefore, the number of input-output data sets generated is 45. On the other hand, there are two values of thickness for each of Glass Cloth and Manila Paper and five different values of void diameter. Therefore, number of input-output data sets generated is 20. Thus, the total number of input-output data sets used for the proposed model is 45 +20 = 65. The 65 sets of input output patterns of five insulating materials are taken from Table 2.6. Out of the 65 sets of input-output patterns, 50 sets of input-output patterns are utilized to train the MFNN and the remaining 15 sets are used for the testing purpose.

Results and Discussions

In this study, the optimum values of network parameters are obtained based on Mean Square Error E_{tr} for the training patterns. The network is trained in a sequential mode. In applying the BPA for the proposed prediction work the following key issues are addressed

1. Network parameters

2. Number of hidden neurons
3. Number of iterations

For BPA with fixed values of learning rate η_1 and momentum factor α_1, the optimum values are obtained by simulation with different values of $\eta_1$and α_1. So, to start with a value of η_1 =0.3and α_1 = 0.1 are chosen and then varied to get an optimum value. It may be noted that the range of values of η_1 and α_1 should be between 0 and 1. Finally, a best combination is seem to yield with a value of η_1= 0.99 and α_1=0.86. For the above combination and with three hidden neurons the value E_{tr} is decreasing to a lowest value of $3.8976*10^{-7}$. The network structure is thus as shown in Figure 3.3. The variation of E_{tr} of the training data with the number of iterations with η_1= 0.99, α_1=0.86, N_h=3.0 is shown in Figure 3.4. Tables 3.1 - 3.3 shows the variation of E_{tr} as a function of η_1, α_1 and N_h respectively.

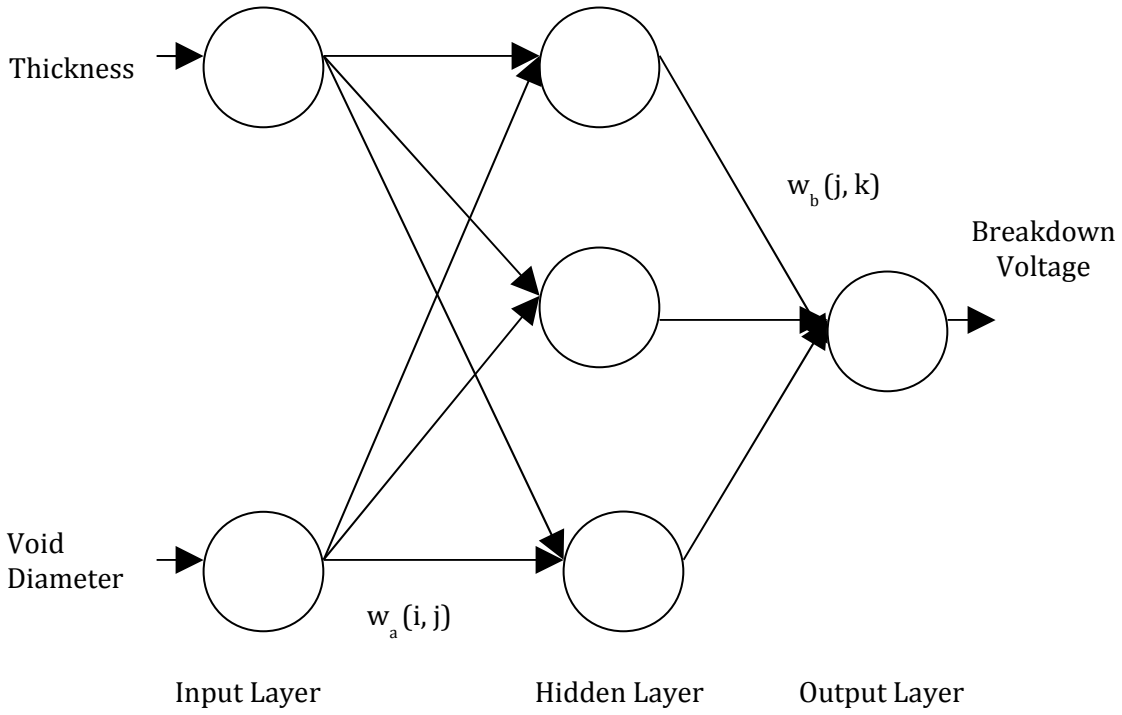

Figure 3.3 MFNN (Model 1)

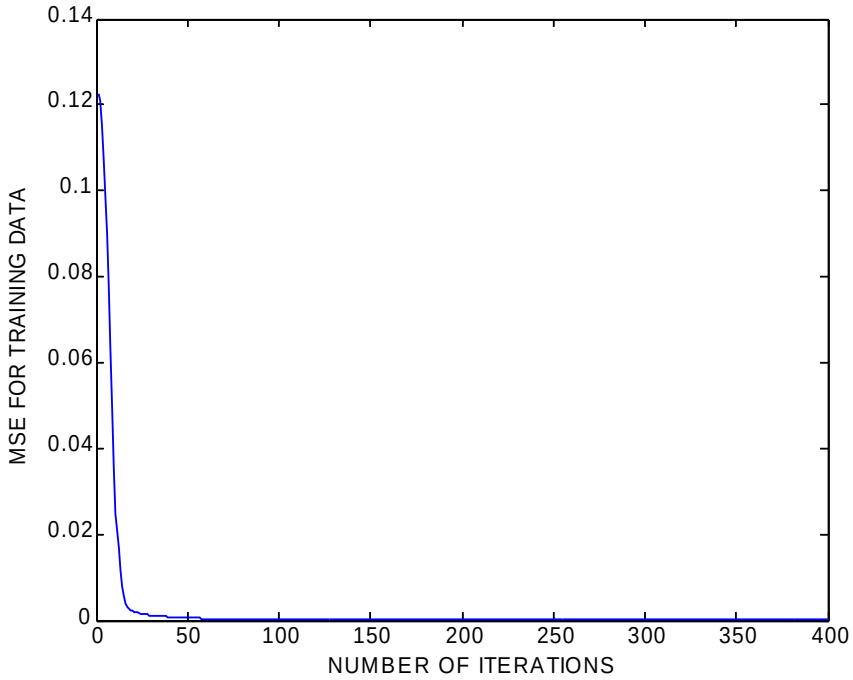

Figure 3.4 E_{tr} of the training data as a function of Number of iterations

Table 3.1: Variation of E_{tr} with η_1 (N_h = 2, α_1 = 0.1, Number of iterations = 400)

η_1	E_{tr}
0.3	0.0016
0.5	$5.2381*10^{-4}$
0.6	$3.4372*10^{-4}$
0.7	$2.3886*10^{-4}$
0.8	$1.7342*10^{-4}$
0.9	$1.3038*10^{-4}$
0.99	$\mathbf{1.0337*10^{-4}}$

Table 3.2: Variation of E_{tr} with α_1 ($N_h = 2$, $\eta_1 = 0.99$, Number of iterations = 400)

α_1	E_{tr}
0.1	$1.0337*10^{-4}$
0.3	$5.8654*10^{-5}$
0.5	$2.8738*10^{-5}$
0.6	$1.8622*10^{-5}$
0.65	$1.4500*10^{-5}$
0.7	$1.0806*10^{-5}$
0.75	$7.3352*10^{-6}$
0.8	$3.9604*10^{-6}$
0.85	$1.1018*10^{-6}$
0.86	$\mathbf{6.9462*10^{-7}}$
0.87	$8.1357*10^{-7}$

Table 3.3: Variation of E_{tr} with N_h ($\eta_1 = 0.99$, $\alpha_1 = 0.86$, Number of iterations = 400)

N_h	E_{tr}
2	$6.9462*10^{-7}$
3	$\mathbf{3.8976*10^{-7}}$
4	$4.5193*10^{-7}$

Finally, the breakdown voltage V = f (t, d) for the test data are calculated by simply passing the input data in the forward path of the network and using the updated weights of the network. Table 3.4 shows a comparison of the experimental and the modeled breakdown voltage using this model after 400 iterations.

Table 3.4: Comparison of the experimental and modeled breakdown voltage

Insulating Material	t (mm)	d (mm)	Breakdown Voltage (kV) (Experimental)	Breakdown Voltage (kV) (Modeled)	MAE of the Test data E_{ts} (%)
White Minilex	0.26	3	25.4903	25.4211	
	0.125	2	24.7000	24.6984	
	0.18	1.5	24.7000	24.7007	
Leatherite Paper	0.13	5	2.0127	2.0127	
	0.175	4	2.5152	2.5152	
	0.235	2	3.3105	3.3105	
Glass Cloth	0.195	5	17.9443	17.9443	
	0.155	3	13.9502	13.9502	0.0182
	0.155	1.5	13.8725	13.8725	
Manila Paper	0.035	3	1.5456	1.5456	
	0.06	2	1.4413	1.4412	
	0.06	4	1.5088	1.5088	
Lather Minilex	0.245	5	16.6824	16.6824	
	0.185	1.5	16.5625	16.5625	
	0.125	2	10.5760	10.5760	

- **Model 2**

In model 2, the number of input parameters is three, that is, the thickness of the insulation sheets t, void depth t_1 and the void diameter d; and the output parameter is the breakdown voltage to be predicted. Since, the input parameters are three, the value of N_i is three for this model. In addition, since the output parameter is only one, the value of N_k is one.

The total number of insulating materials considered for the purpose of modeling is five. There are three values of thickness for each of White Minilex, Leatherite and Lather Minilex

materials , two different values of void depth and five different values of void diameter. Therefore, the number of input-output data sets generated is 90. On the other hand, there are two values of thickness for each of Glass Cloth and Manila Paper, two different values of void depth and five different values of void diameter. Therefore, number of input-output data sets generated is 40. Thus, the total number of input-output data sets used for the proposed model is 90 +40 = 130. The 130 sets of input output patterns of five insulating materials are taken from Table 2.6. Out of the 130 sets of input-output patterns, 115 sets of input-output patterns are utilized to train the MFNN and the remaining 15 sets are used for the testing purpose.

Results and Discussions

In this model 2, η_1 =0.3 and α_1 =0.1 are chosen as the starting point and then they are varied to get an optimum value. A best combination is obtained with a value of η_1= 0.99 and α_1=0.6. For the above combination and with five hidden neurons, the value E_{tr} is decreasing to the lowest value of $7.4093*10^{-6}$. It may be noted that the number of hidden neurons are varied till five, as the value of E_{tr} corresponding to this value of hidden neuron is quiet low. There is no need to decrease the E_{tr} value further by making number of hidden neurons greater than five. The network structure is thus as shown in Figure 3.5. The variation of E_{tr} of the training data with the number of iterations with η_1= 0.99, α_1=0.6, N_h=5.0 is shown in Figure 3.6. Tables 3.5 - 3.7 shows the variation of E_{tr} as a function of η_1, α_1 and N_h respectively.

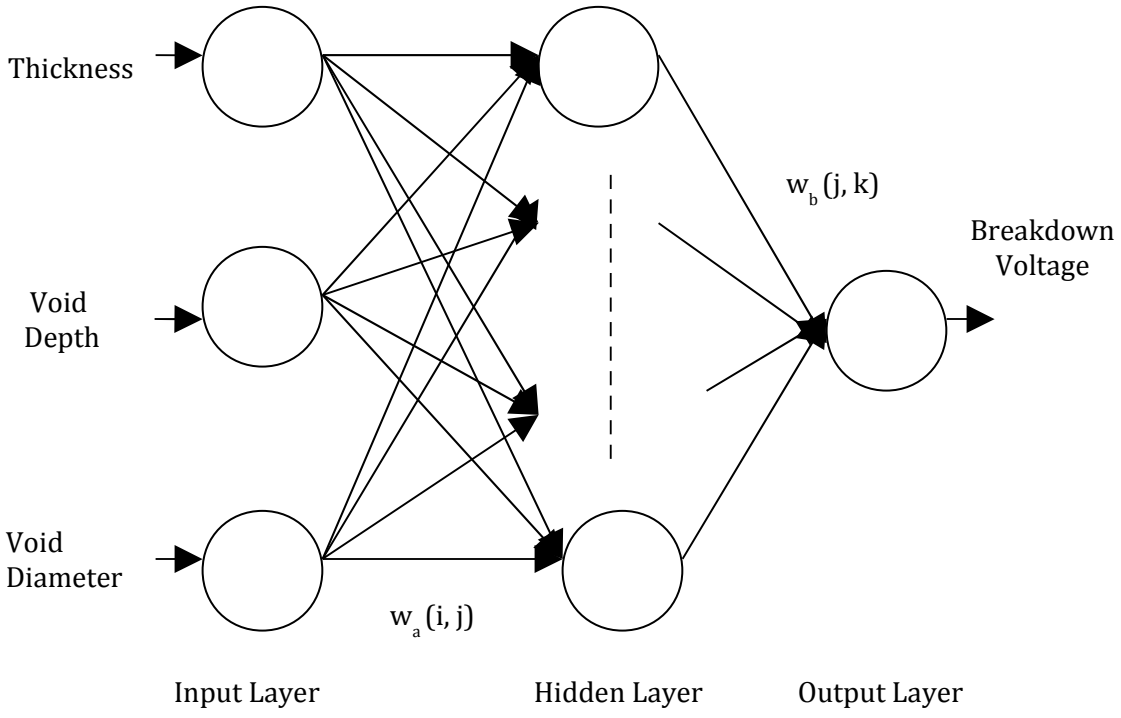

Figure 3.5 MFNN (Model 2)

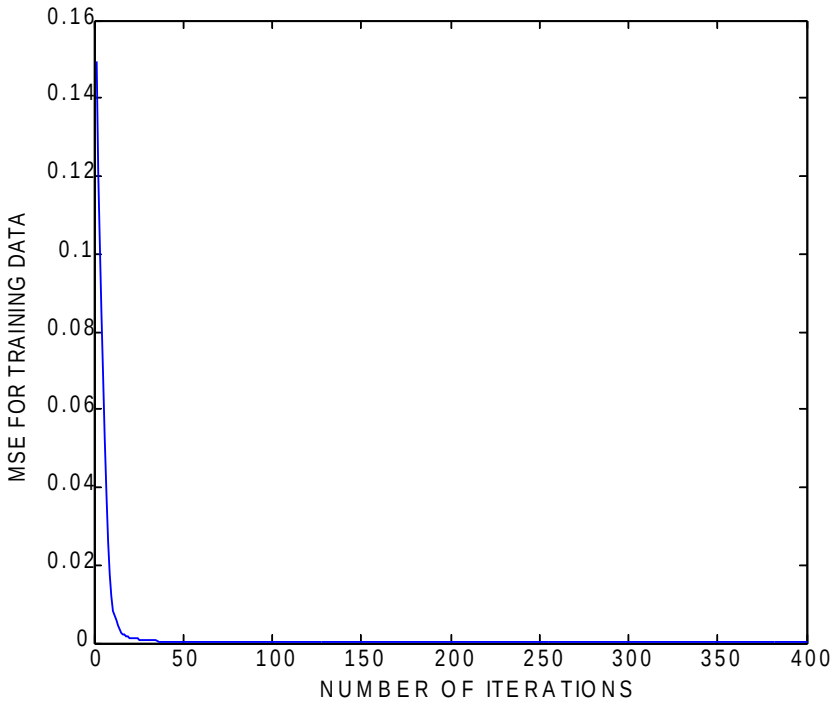

Figure 3.6: E_{tr} of the training data as a function of Number of iterations

Table 3.5: Variation of E_{tr} with η_1 (N_h = 2, α_1 = 0.1, Number of iterations = 400)

η_1	E_{tr}
0.3	$9.9670*10^{-4}$
0.5	$2.9965*10^{-4}$
0.6	$1.9273*10^{-4}$
0.7	$1.3229*10^{-4}$
0.8	$9.5462*10^{-5}$
0.9	$7.1701*10^{-5}$
0.99	$\mathbf{5.7020*10^{-5}}$

Table 3.6: Variation of E_{tr} with α_1 (N_h=2 , η_1 =0.99, Number of iterations =400)

α_1	E_{tr}
0.1	$5.7020*10^{-5}$
0.3	$3.4121*10^{-5}$
0.5	$2.3347*10^{-5}$
0.6	$\mathbf{2.1672*10^{-5}}$
0.65	$4.7290*10^{-5}$
0.7	$7.6003*10^{-4}$

Table 3.7: Variation of E_{tr} with N_h (η_1 = 0.99, α_1 = 0.6, Number of iterations = 400)

N_h	E_{tr}
2	$2.1672*10^{-5}$
3	$1.6594*10^{-5}$
4	$1.5217*10^{-5}$
5	$\mathbf{7.4093*10^{-6}}$

Finally, the V = f (t, t_1, d) for the test data are calculated by simply passing the input data in the forward path of the network and using the updated weights of the network. Table 3.8 shows a comparison of the experimental and modeled breakdown voltage after 400 iterations.

Table 3.8: Comparison of the experimental and modeled breakdown voltage

Insulating Material	t (mm)	t_1 (mm)	d (mm)	Breakdown Voltage (kV) (Experimental)	Breakdown Voltage (kV) (Modeled)	MAE of the Test data E_{ts} (%)
White Minilex	0.26	0.025	3	25.4903	24.9811	0.2260
	0.125	0.125	2	24.7000	24.5570	
	0.18	0.025	1.5	24.7000	24.5520	
Leatherite Paper	0.13	0.125	5	2.0127	2.0129	
	0.175	0.125	4	2.5152	2.5152	
	0.235	0.025	2	3.3105	3.3105	
Glass Cloth	0.195	0.025	5	17.9443	17.9443	
	0.155	0.025	3	13.9502	13.9502	
	0.155	0.125	1.5	13.8725	13.8725	
Manila Paper	0.035	0.125	3	1.5456	1.5558	
	0.06	0.025	2	1.4413	1.4624	
	0.06	0.125	4	1.5088	1.5156	
Lather Minilex	0.245	0.025	5	16.6824	16.6824	
	0.185	0.125	1.5	16.5625	16.5625	
	0.125	0.025	2	10.5760	10.5760	

3.3.2 Prediction of the breakdown voltage due to PD in voids under AC conditions

The four models are proposed as follows

- **Model 3**

In this particular model[111] , the number of input parameters is two, that is, the thickness of the insulation sheets t and the void diameter d; and the output parameter is the breakdown voltage to be predicted. Since, the input parameters are two, the value of N_i is two for this model. In addition, since the output parameter is only one, the value of N_k is one.

The total number of insulating materials considered for the purpose of modeling is one, namely Leatherite paper . There are three values of thickness for Leatherite paper and five different values of void diameter. Therefore, the number of input-output data sets generated is 15. The 15 sets of input output patterns of Leatherite paper are taken from Table 2.7. Out of the 15 sets of input-output patterns, 8 sets of input-output patterns are utilized to train the MFNN and the remaining 7 sets are used for the testing purpose.

Results and Discussions

The η_1 and α_1 are initialized to 0.3 and 0.1 respectively and then varied till an optimum value of these network parameters is reached. Finally, a best combination is seem to yield with a value of η_1= 0.99 and α_1=0.85. For the above combination and with three hidden neurons, the value E_{tr} is decreasing to a lowest value of $1.4329*10^{-6}$. The network structure is the same as shown in Figure 3.3. The variation of E_{tr} of the training data with the number of iterations with η_1= 0.99, α_1=0.85, N_h=3.0 is shown in Figure 3.7. Tables 3.9 - 3.11 shows the variation of E_{tr} as a function of η_1, α_1 and N_h respectively.

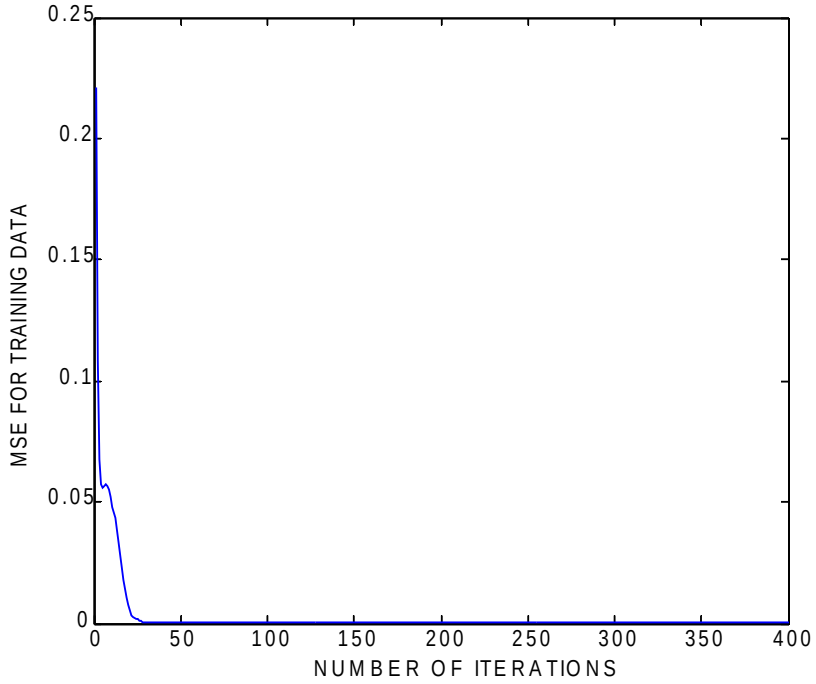

Figure 3.7: E_{tr} of the training data as a function of Number of iterations

Table 3.9: Variation of E_{tr} with η_1 (N_h = 2, α_1 = 0.1, Number of iterations = 400)

η_1	E_{tr}
0.3	0.0011
0.5	$4.5131*10^{-4}$
0.6	$3.3385*10^{-4}$
0.7	$2.5919*10^{-4}$
0.8	$2.0803*10^{-4}$
0.9	$1.7182*10^{-4}$
0.99	$\mathbf{1.4705*10^{-4}}$

Table 3.10: Variation of E_{tr} with α_1 (N_h=2 , η_1 =0.99, Number of iterations=400)

α_1	E_{tr}
0.1	$1.4705*10^{-4}$
0.3	$1.0096*10^{-4}$
0.5	$6.9818*10^{-5}$
0.6	$5.8833*10^{-5}$
0.65	$4.8820*10^{-5}$
0.7	$3.5452*10^{-5}$
0.8	$8.3101*10^{-6}$
0.85	**$1.2947*10^{-6}$**
0.9	$1.5796*10^{-4}$

Table 3.11: Variation of E_{tr} with N_h (η_1 = 0.99, α_1= 0.85, iter = 400)

N_h	E_{tr}
2	**$1.2947*10^{-6}$**
3	$1.4329*10^{-6}$
4	$1.5463*10^{-6}$

Finally, the V = f (t, d) for the test data are calculated by simply passing the input data in the forward path of the network and using the updated weights of the network. Table 3.12 shows a comparison of the experimental and the modeled breakdown voltage after 400 iterations.

Table 3.12: Comparison of the experimental and modeled breakdown voltage

Insulating Material	t (mm)	d (mm)	Breakdown Voltage (kV) (Experimental)	Breakdown Voltage (kV) (Modeled)	MAE of the Test data E_{ts} (%)
Leatherite Paper	0.13	1.5	1.3452	1.3458	0.08
	0.13	2	1.3306	1.3306	
	0.13	3	1.2972	1.2972	
	0.175	2	1.8313	1.8313	
	0.175	3	1.7981	1.7981	
	0.235	2	2.2697	2.2732	
	0.235	4	2.2909	2.2837	

- **Model 4**

In model 4 the number of input parameters, the number of output parameters and the number of insulating materials is the same as model 1. But the 65 sets of input output patterns of five insulating materials are now taken from Table 2.7.

Out of the 65 sets of input-output patterns, 50 sets of input-output patterns are utilized to train the MFNN and the remaining 15 sets are used for the testing purpose.

Results and Discussions

The η_1 =0.3 and α_1 = 0.1 are the initializing values in model 4 and then they are varied to get an optimum value. A best combination is seem to yield with a value of η_1= 0.99 and α_1=0.85. For the above combination and with three hidden neurons, the value E_{tr} reaches the lowest value of $2.3152*10^{-5}$. The network structure is the same as shown in Figure 3.3. The variation of E_{tr} of the training data with the number of iterations with η_1= 0.99, α_1=0.85, N_h=3.0 is shown in Figure 3.8. Tables 3.13 - 3.15 shows the variation of E_{tr} as a function of η_1, α_1 and N_h respectively.

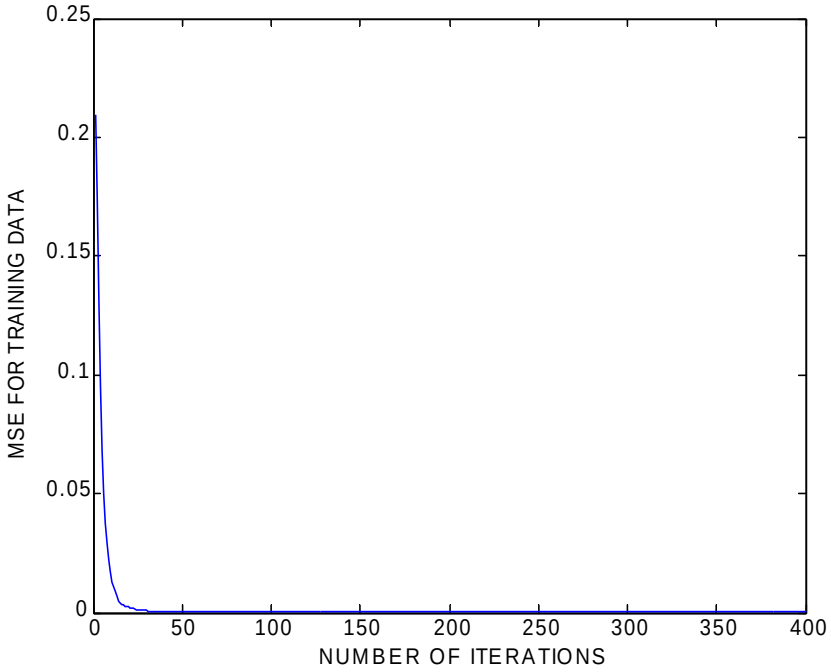

Figure 3.8: E_{tr} of the training data as a function of Number of iterations

Table 3.13: Variation of E_{tr} with η_1 (N_h = 2, α_1 = 0.1, Number of iterations = 400)

η_1	E_{tr}
0.3	0.0039
0.5	0.0018
0.6	0.0014
0.7	0.0011
0.8	$8.7714*10^{-4}$
0.9	$7.3386*10^{-4}$
0.99	$\mathbf{6.3510*10^{-4}}$

Table 3.14: Variation of E_{tr} with α_1 (N_h=2 , η_1 =0.99, Number of iterations=400)

α_1	E_{tr}
0.1	$6.3510*10^{-4}$
0.3	$4.4486*10^{-4}$
0.5	$2.8066*10^{-4}$
0.6	$2.0796*10^{-4}$
0.65	$1.7289*10^{-4}$
0.7	$1.3767*10^{-4}$
0.75	$1.0127*10^{-4}$
0.8	$6.3415*10^{-5}$
0.85	$\mathbf{2.8717*10^{-5}}$
0.9	$4.4498*10^{-5}$

Table 3.15:Variation of E_{tr} with N_h (η_1 = 0.99, α_1 = 0.85, Number of iterations= 400)

N_h	E_{tr}
2	$2.8717*10^{-5}$
3	$\mathbf{2.3152*10^{-5}}$
4	$2.9294*10^{-5}$
5	$3.3684*10^{-5}$

Finally, the V = f (t, d) for the test data are calculated by simply passing the input data in the forward path of the network and using the updated weights of the network. Table 3.16 shows a comparison of the experimental and the modeled breakdown voltage using this model after 400 iterations.

Table 3.16: Comparison of the experimental and modeled breakdown voltage

Insulating Material	t (mm)	d (mm)	Breakdown Voltage (kV) (Experimental)	Breakdown Voltage (kV) (Modeled)	MAE of the Test data E_{ts} (%)
White Minilex	0.26	3	2.2807	2.2914	0.2581
	0.125	2	2.2697	2.2667	
	0.18	1.5	2.2885	2.2836	
Leatherite Paper	0.13	5	1.3306	1.3306	
	0.175	4	1.8313	1.8313	
	0.235	2	2.2909	2.2917	
Glass Cloth	0.195	5	2.2294	2.2294	
	0.155	3	2.2447	2.2447	
	0.155	1.5	2.3088	2.2918	
Manila Paper	0.035	3	0.8154	0.8154	
	0.06	2	0.8388	0.8388	
	0.06	4	0.8758	0.8758	
Lather Minilex	0.245	5	2.2697	2.2841	
	0.185	1.5	2.3088	2.2948	
	0.125	2	2.3170	2.2948	

- **Model 5**

In model 5 the number of input parameters, the number of output parameters and the number of insulating materials is the same as model 2. But the 130 sets of input ouput patterns of five insulating materials are now taken from Table 2.7.

Out of the 130 sets of input-output patterns, 115 sets of input-output patterns are utilized to train the MFNN and the remaining 15 sets are used for the testing purpose.

Results and Discussions

Initially, η_1 and α_1 are fixed at 0.4 and 0.6 respectively in model 5. Then η_1 is varied keeping α_1 and N_h fixed. After this is done, α_1 is varied keeping η_1 and N_h fixed. A best combination is seem to be obtained with a value of η_1= 0.99 and α_1=0.65. For the above combination and with five hidden neurons, the value E_{tr} is decreasing to a lowest value of $5.1982*10^{-5}$. It may be noted that the number of hidden neurons is varied till five, as the value of E_{tr} corresponding to this value of hidden neuron is quiet low. There is no need to decrease the E_{tr} value further by making number of hidden neurons greater than five. The network structure is the same as shown in Figure 3.5. The variation of E_{tr} of the training data with the number of iterations with η_1= 0.99, α_1=0.65, N_h=5.0 is shown in Figure 3.9. Tables 3.17 - 3.19 shows the variation of E_{tr} as a function of η_1, α_1 and N_h respectively.

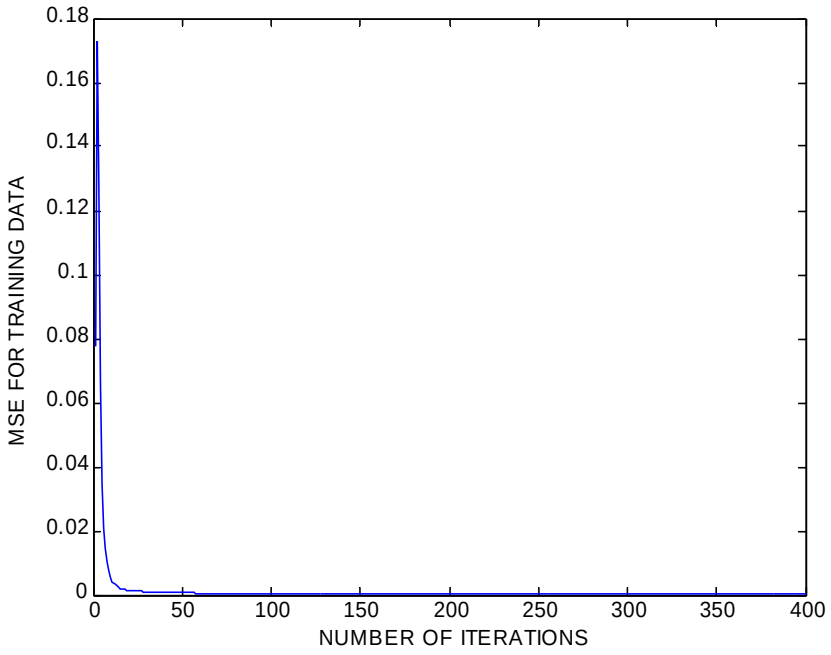

Figure 3.9: E_{tr} of the training data as a function of Number of iterations

Table 3.17: Variation of E_{tr} with η_1 (N_h = 2, α_1 = 0.6, Number of iterations = 400)

η_1	E_{tr}
0.4	0.0086
0.5	0.0016
0.7	$4.654*10^{-4}$
0.9	$3.3098*10^{-4}$
0.99	$\mathbf{1.8579*10^{-4}}$

Table 3.18: Variation of E_{tr} with α_1 (N_h=2 , η_1 =0.99, Number of iterations =400)

α_1	E_{tr}
0.6	$1.8579*10^{-4}$
0.65	$\mathbf{1.6864*10^{-4}}$
0.7	$2.8756*10^{-4}$

Table 3.19:Variation of E_{tr} with N_h (η_1 = 0.99, α_1 = 0.65, Number of iterations = 400)

N_h	E_{tr}
2	$1.6864*10^{-4}$
3	$1.4423*10^{-4}$
4	$\mathbf{1.1656*10^{-4}}$
5	$5.1982*10^{-5}$

Finally, the V = f (t, t_1, d) for the test data are calculated by simply passing the input data in the forward path of the network and using the updated weights of the network. Table 3.20 shows a comparison of the experimental and modeled breakdown voltage after 400 iterations.

Table 3.20: Comparison of the experimental and modeled breakdown voltage

Insulating Material	t (mm)	t_1 (mm)	d (mm)	Breakdown Voltage (kV) (Experimental)	Breakdown Voltage (kV) (Modeled)	MAE of the Test data E_{ts} (%)
White Minilex	0.26	0.025	3	2.2294	2.2224	
	0.125	0.125	2	2.2447	2.2317	
	0.18	0.025	1.5	2.2697	2.2458	
Leatherite Paper	0.13	0.125	5	1.2972	1.2972	
	0.175	0.125	4	1.8520	1.8520	
	0.235	0.025	2	2.2697	2.2465	
Glass Cloth	0.195	0.025	5	2.3088	2.2712	
	0.155	0.025	3	2.3088	2.2662	0.7401
	0.155	0.125	1.5	2.2294	2.2205	
Manila Paper	0.035	0.125	3	0.8388	0.8388	
	0.06	0.025	2	0.8154	0.8154	
	0.06	0.125	4	0.8479	0.8479	
Lather Minilex	0.245	0.025	5	2.2447	2.2369	
	0.185	0.125	1.5	2.2294	2.2205	
	0.125	0.025	2	2.2909	2.2565	

- **Model 6**

In model 6 [112] since the input parameters are assumed to be the thickness of the paper t , the void depth t_1 , the void diameter d and the relative permittivity ϵ_r, the value of N_i is four . Also, since the output parameter is the breakdown voltage to be predicted as a function of these four parameters, the value of N_k is one.

The total number of insulating materials considered for the purpose of modeling is five. There are three values of thickness for each of White Minilex, Leatherite and Lather Minilex materials, two different values of void depth, one value of the relative permittivity for each

material and five different values of void diameter. Therefore, the number of input-output data sets generated is 90. On the other hand, there are two values of thickness for each of Glass Cloth and Manila Paper, two different values of void depth, one value of the relative permittivity for each material and five different values of void diameter. Therefore, number of input-output data sets generated is 40. Thus, the total number of input-output data sets used for the proposed model is 90 +40 = 130. The 130 sets of input output patterns of five insulating materials are taken from Table 2.7. Out of the 130 sets of input-output patterns, 115 sets of input-output patterns are utilized to train the MFNN and the remaining 15 sets are used for the testing purpose.

Results and Discussions

The network structure for the model 6 is shown in Figure 3.9. The η_1 and α_1 are initialized with 0.3 and 0.1 respectively and then varied to get an optimum value. The best combination of η_1 and α_1 are 0.99 and 0.75 respectively, with a reasonably low value of E_{tr} . For the above combination and with five hidden neurons, the value E_{tr} is decreasing and reaches the lowest value of $1.2343*10^{-5}$. The variation of E_{tr} of the training data with the number of iterations with η_1= 0.99, α_1=0.75, N_h=5.0 is shown in Figure 3.11. Tables 3.21 - 3.23 shows the variation of E_{tr} as a function of η_1, α_1 and N_h respectively.

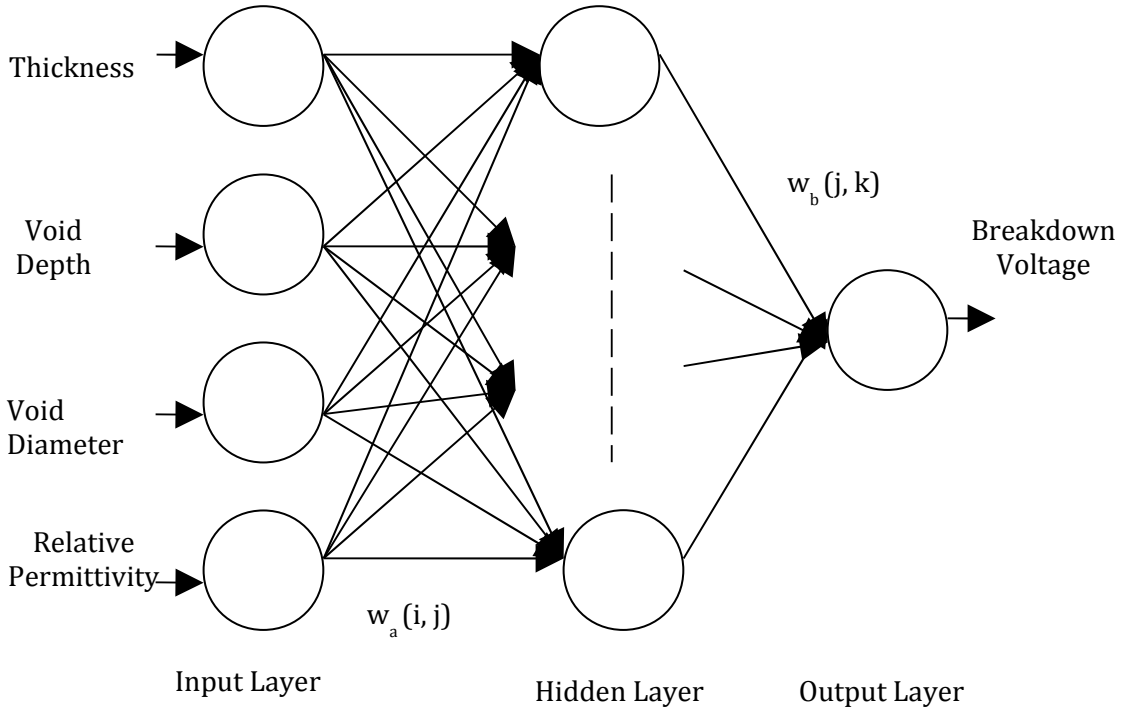

Figure 3.10 MFNN (Model 6)

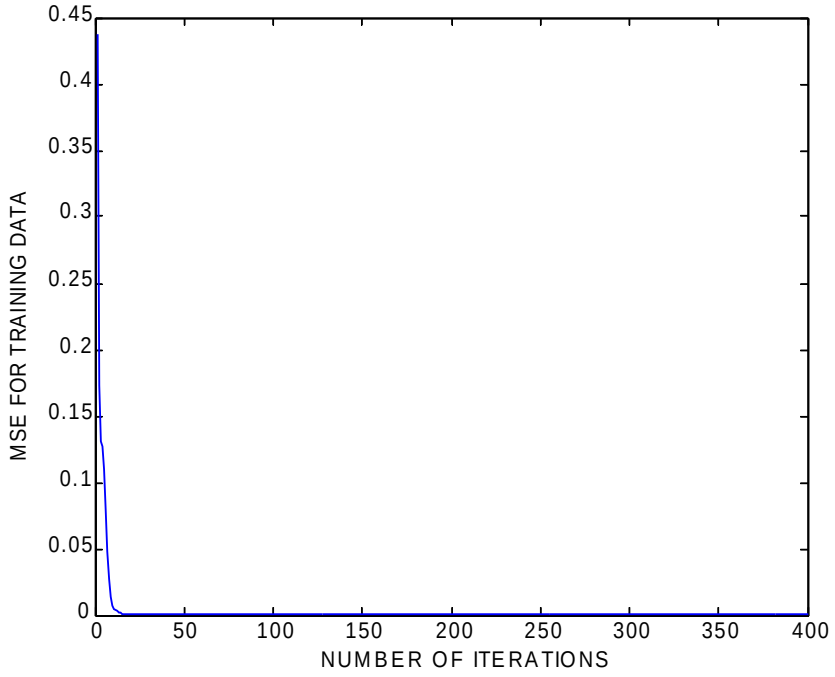

Figure 3.11: E_{tr} of the training data as a function of Number of iterations

Table 3.21: Variation of E_{tr} with η_1 (N_h = 2, α_1 = 0.7, Number of iterations = 400)

η_1	E_{tr}
0.3	$2.3187*10^{-4}$
0.5	$9.8411*10^{-5}$
0.7	$5.6561*10^{-5}$
0.8	$4.5409*10^{-5}$
0.9	$3.7348*10^{-5}$
0.99	$\mathbf{3.1949*10^{-5}}$

Table 3.22 :Variation of E_{tr} with α_1 (N_h=2 , η_1 =0.99, Number of iterations=400)

α_1	E_{tr}
0.7	$3.1949*10^{-5}$
0.75	$\mathbf{1.9529*10^{-5}}$
0.8	$2.5081*10^{-5}$
0.85	$2.9475*10^{-4}$

Table 3.23: Variation of E_{tr} with N_h (η_1 = 0.99, α_1 = 0.75, Number of iterations=400)

N_h	E_{tr}
2	$1.9520*10^{-4}$
3	$2.4571*10^{-5}$
4	$1.5125*10^{-5}$
5	$\mathbf{1.2343*10^{-5}}$
6	$1.2487*10^{-5}$

Finally, the $V = f(t, t_1, d, \epsilon_r)$ for the test data are calculated by simply passing the input data in the forward path of the network and using the updated weights of the network. Table 3.24 shows a comparison of the experimental and modeled breakdown voltage after 400 iterations..

Table 3.24: Comparison of the experimental and modeled breakdown voltage

Insulating Material	t (mm)	t_1 (mm)	d (mm)	ϵ_r	Breakdown Voltage (kV) (experimental)	Breakdown Voltage (kV) (Modeled)	MAE of the Test data E_{ts} (%)
White Minilex	0.26	0.025	3	4.40	2.2294	2.2294	0.1638
	0.125	0.125	2	4.40	2.2447	2.246	
	0.18	0.025	1.5	4.40	2.2697	2.2678	
Leatherite Paper	0.13	0.125	5	4.21	1.2972	1.2972	
	0.175	0.125	4	4.21	1.8520	1.8520	
	0.235	0.025	2	4.21	2.2697	2.2677	
Glass Cloth	0.195	0.025	5	4.97	2.3088	2.2904	
	0.155	0.025	3	4.97	2.3088	2.2904	
	0.155	0.125	1.5	4.97	2.2294	2.2294	
Manila Paper	0.035	0.125	3	4.68	0.8388	0.8388	
	0.06	0.025	2	4.68	0.8154	0.8154	
	0.06	0.125	4	4.68	0.8479	0.8479	
Lather Minilex	0.245	0.025	5	5.74	2.2447	2.2447	
	0.185	0.125	1.5	5.74	2.2294	2.2294	
	0.125	0.025	2	5.74	2.2909	2.2835	

From Table 3.24 it may be seen that the modeled values closely follows the experimental breakdown values and the E_{ts} is found to be 0.1638%, thus shows the effectiveness of the proposed Model 6.

3.3.3 Extrapolation capability of the Model 6

The proposed model 6 was trained with three values of thickness each for Leatherite paper and Lather Minilex , two different values of void depth and five different values of void diameter. Therefore, the number of input-output data training sets generated for these two materials is 60. On the other hand, there are two values of thickness for each of Glass Cloth and White Minilex, two different values of void depth and five different values of void diameter for the training. Therefore, number of input-output data training sets generated for these two materials is 40. Moreover, there is only one value of thickness for Manila paper, two different values of void depth and five different values of void diameter for the same training purpose. Therefore, number of input-output data training sets generated for this material is 10. Therefore, the number of input-output data training sets generated for these five materials is 110. After the training is over, the MFNN was tested for it's extrapolation capability with the help of input output patterns of Manila Paper (10 sets) and White Minilex (10 sets) making a total of 20 sets. This is because these 20 sets for the thickness of Manila Paper (0.035mm) and White Minilex (0.26 mm) lies outside the range of the other thicknesses for the five insulating materials and the extrapolation capability in the lower and the upper range are considered. A E_{ts} of 0.30% is obtained with model 6 . This clearly shows that the proposed model has very good extrapolation capability also.

Table 3.25 :Comparison of the experimental and modeled breakdown voltage (Extrapolation Capability)

Insulating Material	t (mm)	t_1 (mm)	d (mm)	ϵ_r	Breakdown Voltage (kV) (Experimental)	Breakdown Voltage (kV) (Modeled)	MAE of the Test data E_{ts} (%)
Manila Paper	0.035	0.025	3	4.68	0.8154	0.8146	0.30
	0.035	0.125	2	4.68	0.8758	0.8708	
	0.035	0.025	1.5	4.68	0.8758	0.8693	
	0.035	0.125	5	4.68	0.9089	0.8973	
	0.035	0.125	4	4.68	0.8479	0.8477	
	0.035	0.025	2	4.68	0.8479	0.8472	
	0.035	0.025	5	4.68	0.8683	0.8679	
	0.035	0.025	4	4.68	0.9089	0.9044	
	0.035	0.125	1.5	4.68	0.8154	0.8134	
	0.035	0.125	3	4.68	0.8388	0.8339	
White Minilex	0.26	0.025	2	4.4	2.3088	2.3002	
	0.26	0.125	4	4.4	2.2909	2.2899	
	0.26	0.025	5	4.4	2.3170	2.3031	
	0.26	0.125	1.5	4.4	2.2885	2.2880	
	0.26	0.125	3	4.4	2.2885	2.2798	
	0.26	0.025	1.5	4.4	2.2294	2.2294	
	0.26	0.125	2	4.4	2.2697	2.2701	
	0.26	0.025	3	4.4	2.2294	2.2294	
	0.26	0.025	4	4.4	2.2885	2.2880	
	0.26	0.125	5	4.4	2.2909	2.2879	

3.3.4 Prediction of the breakdown voltage due to PD in voids under AC conditions (CIGRE Method II Electrode System)

One model is proposed as follows

- **Model 7**

The models 1 to 6 proposed so far for the prediction of breakdown voltage had utilized the experimental generated data using Cylinder-Plane Electrode System, which is discussed in details in Chapter 2. In model 7, prediction of breakdown voltage is proposed with the help of experimentally generated data using CIGRE Method II Electrode System reported in [75]. The thickness of the Leatherite paper used is 0.18 mm, 0.23 mm and 0.3 mm. The void depth had three values, 0.0625mm, 0.125 mm and 0.25 mm, while the void diameter has three values, namely 1mm, 2 mm and 5 mm. Hence the proposed model [113] is carried out with the help of 27 sets of experimental input-output patterns generated for this paper insulation. Out of this 27 sets, the 21 sets of input-output patterns are utilized to train MFNN and the remaining 6 sets are used for the testing purpose. The equations 3.1) to 3.10) have been used in arriving at the results of this model discussed below.

Results and Discussions

The model 7 starts with a value of η_1 =0.2 and α_1 = 0.8 and then these network parameters are varied to get an optimum value. Finally, a best combination is seem to yield with a value of η_1= 0.3 and α_1=0.9. For the above combination of η_1 and α_1 and with three hidden neurons, the value E_{tr} is decreasing to a lowest value of $7.29*10^{-4}$. The network structure is the same as Figure 3.3. The variation of E_{tr} of the training data with the number of iterations with η_1= 0.3, α_1=0.9, N_h=3.0 is shown in Figure 3.12. Tables 3.26 - 3.28 shows the variation of E_{tr} as a function of N_h, η_1 and α_1 respectively.

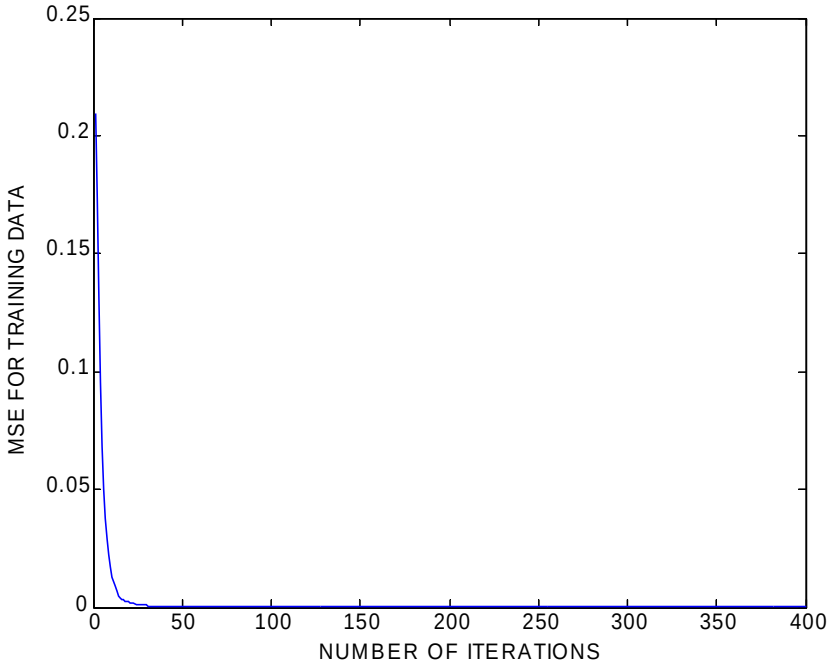

Figure 3.12: E_{tr} of the training data as a function of Number of iterations

Table 3.26: Variation of E_{tr} with the N_h (η_1 = 0.3, α_1 = 0.9, Number of iterations = 400)

N_h	E_{tr}
3	**$7.29*10^{-4}$**
4	$3.71*10^{-3}$
5	0.0111
6	0.0111
7	0.0111

Table 3.27: Variation of E_{tr} with η_1 (N_h = 3, α_1 = 0.9, Number of iterations = 400)

η_1	E_{tr}
0.2	$7.41*10^{-4}$
0.25	$7.29*10^{-4}$
0.3	**$7.29*10^{-4}$**
0.35	$7.35*10^{-4}$
0.4	$7.41*10^{-4}$

Table 3.28: Variation of E_{tr} with α_1 (N_h=3 , η_1 =0.3, Number of iterations=400)

α_1	E_{tr}
0.8	$7.59*10^{-4}$
0.85	$7.41*10^{-4}$
0.9	**$7.29*10^{-4}$**
0.95	$7.35*10^{-4}$

Finally, the V = f (t, t_1, d) for the test data are calculated by simply passing the input data in the forward path of the network and using the updated weights of the network. Table 3.29 shows a comparison of the experimental and modeled breakdown voltage after 400 iterations...

Table 3.29: Comparison of the experimental and modeled breakdown voltage

Insulating Material	t (mm)	t_1 (mm)	d (mm)	Breakdown Voltage (kV) (Experimental)	Breakdown Voltage (kV) (Modeled)	MAE of the Test data E_{ts} (%)
Leatherite Paper	0.3	0.0625	2	4.0	3.95	1.13
	0.3	0.25	1	3.9	3.87	
	0.23	0.125	5	3.6	3.6	
	0.23	0.25	2	3.8	3.71	
	0.18	0.0625	5	3.7	3.62	
	0.18	0.125	1	3.9	3.85	

3.4 Conclusion

In this Chapter the six proposed models based on the MFNN structure have predicted the breakdown voltage of solid insulating materials from the Cylinder Plane Electrode System set up and one model has predicted the breakdown voltage from the CIGRE Method II Electrode System set up. All the seven models clearly indicate their effectiveness in predicting the breakdown voltage as is evident from the seven Mean Absolute Error values. Also the extrapolation capability of the model No 6 has been explored . This too gives very satisfactory results.

Chapter 4

BREAKDOWN VOLTAGE MODELING USING RADIAL BASIS FUNCTION NETWORK

4.1 Introduction

In Chapter 3, the modeling of the breakdown voltage using Multilayer Feedforward Neural Network (MFNN) had been attempted. The proposed six models had used the experimental data obtained by using Cylinder-Plane Electrode system and one model proposed based on data available in literature which are essentially generated by using CIGRE Method II Electrode system. In this Chapter, the same experimental data have been used and modeling of breakdown voltage is proposed based on the Radial Basis Function Network (RBFN) structure. First, a brief introduction on the theory of the RBFN has been presented. Finally, detailed discussions on the proposed models are made.

4.2 Radial Basis Function Network

- **RBFN Structure**

The MFNN may be viewed as the application of a recursive technique known in statistics as stochastic approximation. The RBFN follows a different approach with respect to MFNN. The RBFN attempts to design a neural network as a curve fitting approximation problem in a high-dimension space. The learning is equivalent to finding a surface in a multidimensional space that provides a best fit to the training data. Corresponding, generalization is equivalent to the use of this multidimensional surface to interpolate the test data. The RBFN structure is shown in Figure 4.1. As shown, there are N_i input nodes of this network in the input layer corresponding to the N_i inputs that is quiet similar to MFNN shown in Figure 3.1. The second layer is the hidden layer composed of nonlinear units [100]. In the context of a neural network, the hidden units provide a set of functions that constitute an arbitrary basis for the input patterns when they are expanded into hidden space. The number of nonlinear units is m_1. The output layer comprises of a summer. The nonlinear units in the hidden layer and the output layer are connected by linear weights.

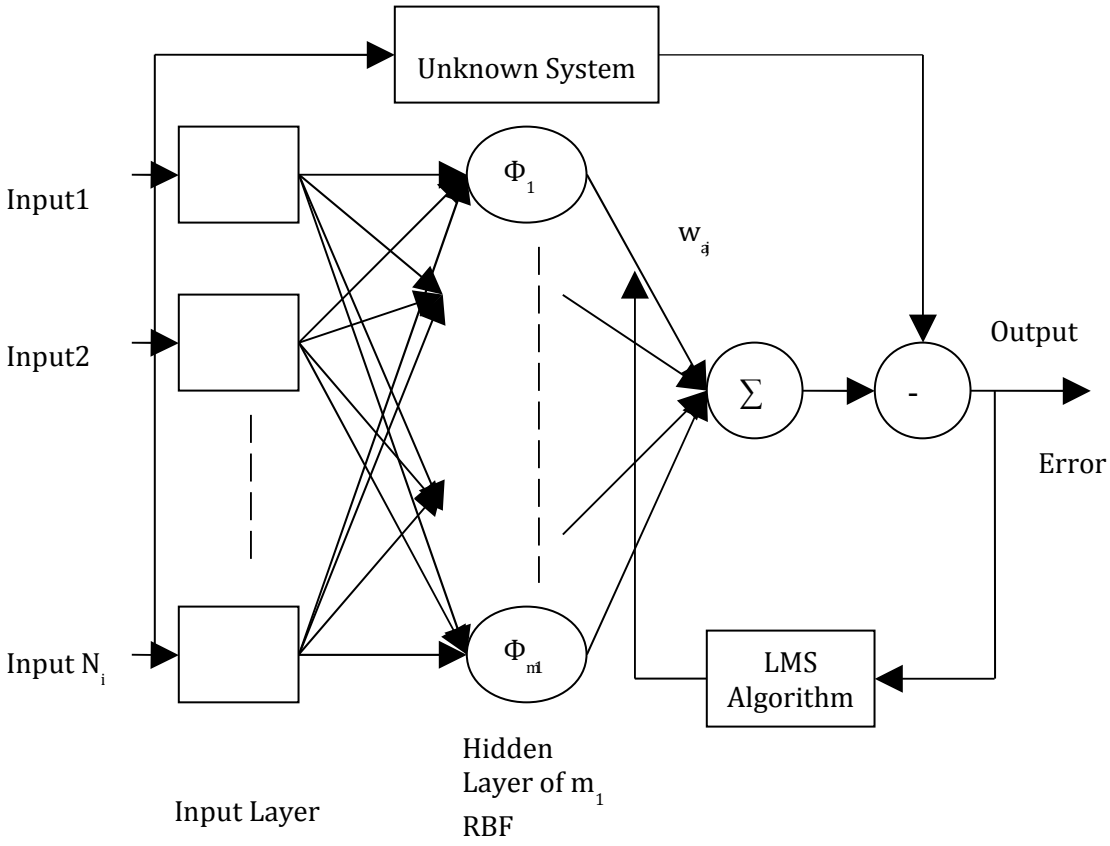

Figure 4.1: A typical Radial Basis Functions Network (RBFN)

The linear weights tend to evolve on a different time scale compared to the nonlinear activation functions of the hidden layer. The hidden layer's activation functions also known as Radial Basis Functions (RBF) evolve slowly in accordance with some nonlinear optimization strategy. The linear weights adjust themselves rapidly through a linear optimization strategy, such as, the LMS Algorithm and the RLS Algorithm.

There are different learning strategies that may be followed in the design of the RBFN, depending on how the centers of the RBF of the network are specified. In the present work the Fixed Centers Selected at Random (FCSR) strategy are adopted to specify the centers.

- **Fixed Centers Selected at Random (FCSR)**

According to this approach the location of the centers are chosen randomly from the input training patterns involving the thickness of insulation sample, void depth, diameter of void and relative permittivity of the insulating material. The RBF is assumed isotropic Gaussian function whose standard deviation is fixed according to the spread of the centers.

- **Fixed Radial Basis Functions**

The Fixed RBF are defined as follows:

$$G(||x_1-x_2||^2) = \exp(-(m_1/ d_{max}^2)*||x_1-x_2||^2) \quad (4.1)$$

Where x_1 is the input pattern, x_2 is the coordinates of the center, m_1 is the number of chosen centers or number of nonlinear radial basis functions, d_{max} is the maximum distance between the chosen centers. $||x_1-x_2||$ is the Euclidean distance between x_1 and x_2.

Suppose, $x_1 = [t_a , t_{1b} , d_c , \epsilon_{rd}]$ and $x_2 = [t_e , t_{1f} , d_g , \epsilon_{rf}]$

Then $||x_1-x_2||^2 = (t_a- t_e)^2 + (t_{1b}- t_{1f})^2 + (d_c- d_g)^2 + (\epsilon_{rd} - \epsilon_{rf})^2 \quad (4.2)$

The RBF are multiplied by the respective weights and are summed.

The modeled value of breakdown voltage at the m^{th} iteration is given as

$$V_{2p}(m) = \sum_{j=1}^{m1} G(||x_1-x_2||^2)* w_{aj}(m) \quad (4.3)$$

Where w_{aj} are the weights connected between the hidden layer and the output layer.

The error at the m^{th} iteration is given by

$$e_{1p}(m) = V_{1p} - V_{2p}(m) \quad (4.4)$$

- **Weight Update Equation**

The weights w_{aj} are updated through a linear optimization strategy. The linear optimization strategy employed in this work is the LMS algorithm.

The weight update equation as per the LMS algorithm is given by

$$w_{aj}(m+1) = w_{aj}(m) + \eta_2 * G(|| x_1-x_2|| ^2)* e_{1p}(m) \quad (4.5)$$

Where η_2 is learning rate.

- **Evaluation Criteria**

The stopping criteria adopted is these proposed models are same as the MFNN models. The training errors, E_{tr} from the RBFN are calculated using equation (3.9). The training phase is completed once the training error seems to reach a desired minimum.

Equation (3.10) is then used to calculate the Mean Absolute Error E_{ts} of the test data, just by passing the input data through the network and modeled values of the output data are obtained.

4.3 Modeling of Breakdown Voltage using RBFN

This section details the attempt at modeling of breakdown voltage due to PD in voids under DC and AC conditions separately using RBFN. These models predicts the breakdown voltages as a function of different void parameters, namely, void diameter and void depth, insulation sheet thickness and relative permittivity. The network is provided with both input data and desired response; and is trained in a supervised fashion, similar to that of MFNN. The weights are updated using the LMS algorithm. The training phase is completed after a series of iterations. Output is compared with the desired response in each iteration, and a match is obtained.

In order to predict the breakdown voltage a software program has been developed in MATLAB 7.1 to implement equations (4.1) to (4.5). The program also calculates the error values using equations (3.9) and (3.10). The program is suitably modified for different models based on input – output parameters. The flowchart for the RBFN is shown in Figure 4.2.

4.3.1 Prediction of the breakdown voltage due to PD in voids under DC condition

For prediction of breakdown voltage under DC condition two models are proposed with different input conditions as follows

- **Model 1**

This model has used the same number of input-output parameters as in the MFNN model 1 presented in Chapter 3, that is, number of input parameters are two corresponding to thickness of the insulation and void diameter, and output parameter is the breakdown voltage. Moreover, this model has also used the same set of input- output patterns as model 1. Hence, the total input-output data sets for this model are 65. The 65 sets of input output patterns of five insulating materials are thus taken from Table 2.6. Out of the 65 sets of input-output patterns, 50 sets of input-output patterns are utilized to train the RBFN and the remaining 15 sets are used for the testing purpose.

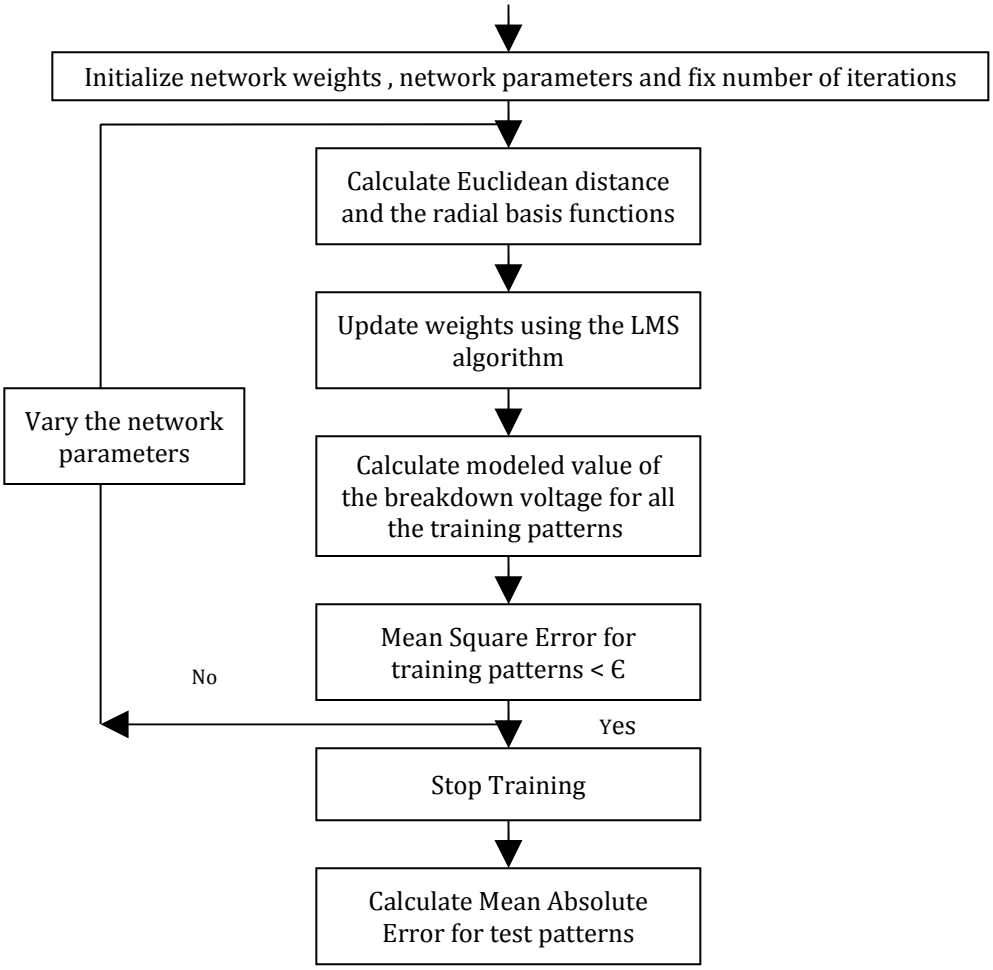

Figure 4.2 : Flow Chart for the RBFN

Results and Discussions

In this study, the optimum values of network parameters are obtained based on Mean Square Error E_{tr} for the training patterns. The network is trained in a sequential mode. In applying the RBF and LMS algorithm for the proposed prediction work the following key issues are addressed

1. Number of chosen centers m_1
2. Learning rate of the LMS algorithm η_2
3. Number of iterations

To decide upon the optimum values, m_1 and η_2 values are varied extensively. It is found that the values of E_{tr} are of the order 10^{-2} when $1 \leq m_1 \leq 5$ & $0 \leq \eta_2 \leq 1.89$ or when $1 \leq m_1 \leq 5$ & $\eta_2 > 2.0$. However, with the increase of m_1 values and η_2 in the range between 1.90 and 2.00, value of E_{tr} falls sharply. Thus, m_1 is increased in steps of 1 from 6 to 13. Corresponding to each value of m_1, the value of E_{tr} is calculated. Tables 4.1 and 4.2 show the variation of E_{tr} as a function of m_1 and η_2 respectively. Out of the eight values of E_{tr}, the least value occurs at $m_1 = 11$.

The value of η_2 is then varied in the range of 1.90 to 2.00, with m_1 fixed at 11. Out of the seven values of E_{tr}, the minimum value of E_{tr} occurs at $\eta_2 = 1.98$. Hence, after trying out 14 combinations of m_1 and η_2, the least value of E_{tr} is obtained as $9.621*10^{-6}$ when $\eta_2 = 1.98$ and $m_1 = 11$. The network structure is as shown in Figure 4.3. The variation of error E_{tr} of the training data with the number of iterations with $\eta_2 = 1.98$, $m_1 = 11$ is shown in Figure 4.4.

Table 4.1: Variation of Training error E_{tr} with number of centers m_1 (η_2 = 1.98, Number of iterations = 400)

m_1	E_{tr}
6	$2.167*10^{-4}$
7	$1.709*10^{-5}$
8	$1.606*10^{-5}$
9	$1.579*10^{-5}$
10	$1.570*10^{-5}$
11	$\mathbf{9.621*10^{-6}}$
12	$2.082*10^{-5}$
13	$1.094*10^{-4}$

Table 4.2: Variation of Training error E_{tr} with η_2 (m_1 = 11, Number of iterations = 400)

η_2	E_{tr}
1.90	$7.685*10^{-4}$
1.95	$9.727*10^{-6}$
1.96	$9.683*10^{-6}$
1.97	$9.638*10^{-6}$
1.98	$\mathbf{9.621*10^{-6}}$
1.99	$4.187*10^{-4}$
2.00	$3.523*10^{-3}$

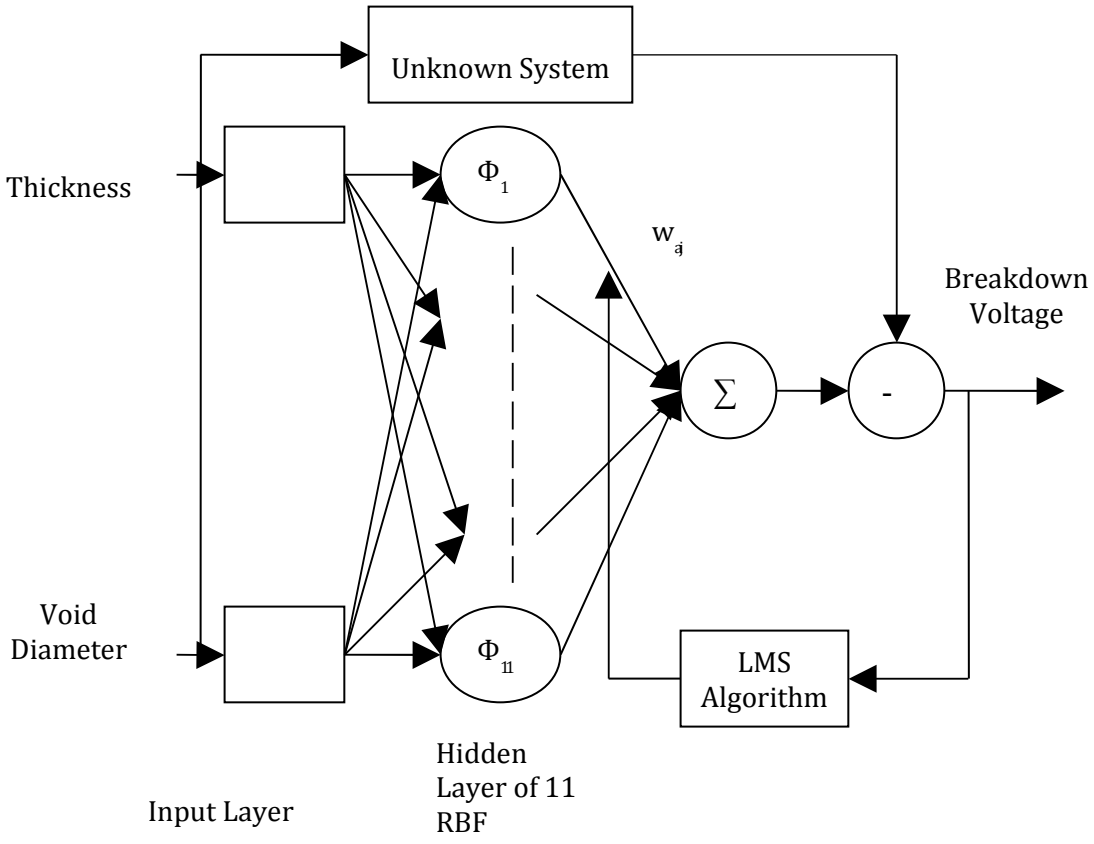

Figure 4.3: RBF Network employed in Model 1

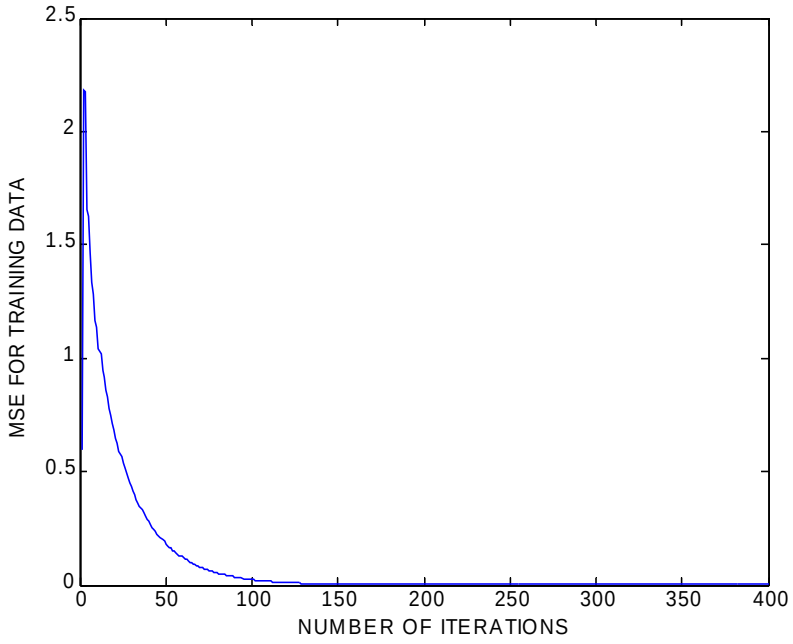

Figure 4.4: Variation of E_{tr} of the Training data as a function of Number of iterations

On completion of the training, the breakdown voltage, $V_b = f$ (t, d) for the 15 sets of test input data for all the five insulating materials are calculated using the trained network. Table 4.3 shows a comparison of the experimental and the modeled values of the breakdown voltage. As may be seen from this Table that the value of MAE of the test data E_{ts} is 1.5953 %.

Table 4.3: Comparison of the Experimental and the Modeled value of breakdown voltage

Insulating Material	t (mm)	d (mm)	Breakdown Voltage (kV) (Experimental)	Breakdown Voltage (kV) (Modeled)	MAE of the Test data E_{ts} (%)
White Minilex	0.26	3	25.4903	25.5901	1.5953
	0.125	2	24.7000	24.7001	
	0.18	1.5	24.7000	24.7000	
Leatherite Paper	0.13	5	2.0127	2.0113	
	0.175	4	2.5152	2.8346	
	0.235	2	3.3105	3.2788	
Glass Cloth	0.195	5	17.9443	17.9393	
	0.155	3	13.9502	13.9508	
	0.155	1.5	13.8725	13.8725	
Manila Paper	0.035	3	1.5456	1.5850	
	0.06	2	1.4413	1.4419	
	0.06	4	1.5088	1.6334	
Lather Minilex	0.245	5	16.6824	16.6826	
	0.185	1.5	16.5625	16.5625	
	0.12	2	10.5760	10.5760	

- **Model 2**

This model is proposed in line with model 2 in Chapter 3 with same number of input and output parameters, that is, number of input parameters are three corresponding to thickness of the insulation, depth of void and void diameter, and output parameter is the

breakdown voltage. Total input-output data sets used for this model are 130. As mentioned in Chapter 3, 130 sets of input output patterns of five insulating materials are taken from Table 2.6. Similarly, out of the 130 sets of input-output patterns, 115 sets of input-output patterns are utilized to train the RBFN and the remaining 15 sets are kept for the testing purpose.

Results and Discussions

The m_1 and η_2 values are varied in a similar manner as in the previous model It is revealed that the error values of the training data E_{tr} are of the order 10^{-2} when $1 \leq m_1 \leq 6$ & $0 \leq \eta_2 \leq 1.92$ or when $1 \leq m_1 \leq 6$ & $\eta_2 > 1.98$. However, with the increase of m_1 values and η_2 in the range between 1.93 and 1.98, value of E_{tr} falls sharply. Thus, m_1 is increased in steps of 1 from 7 to 11. Corresponding to each value of m_1, the value of E_{tr} is calculated. Tables 4.4 and 4.5 show the variation of E_{tr} as a function of m_1 and η_2 respectively. Out of the five values of E_{tr}, the least value occurs at $m_1 = 9$.

Then m_1 is fixed at 9, and η_2 is varied in the range of 1.93 to 1.98. Out of the six values of the training error, the minimum value of E_{tr} seems to occur at $\eta_2 = 1.96$. Hence, after trying out 10 combinations of m_1 and η_2, the least value of E_{tr} is obtained as $5.29*10^{-5}$ when $\eta_2 = 1.96$ and $m_1 = 9$. The network structure for this model is depicted in Figure 4.5. The variation of error E_{tr} of the training data with the number of iterations with $\eta_2 = 1.96$, $m_1 = 9$ is shown in Figure 4.6.

Table 4.4: Variation of Training error E_{tr} with m_1
($\eta_2 = 1.96$, Number of iterations = 400)

m_1	E_{tr}
7	$3.90*10^{-3}$
8	$1.21*10^{-4}$
9	$\mathbf{5.29*10^{-5}}$
10	$1.28*10^{-4}$
11	$2.95*10^{-4}$

Table 4.5: Variation of Training error E_{tr} with η_2
(m_1 = 9, Number of iterations = 400)

η_2	E_{tr}
1.93	$5.43*10^{-5}$
1.94	$5.38*10^{-5}$
1.95	$5.32*10^{-5}$
1.96	$\mathbf{5.29*10^{-5}}$
1.97	$6.26*10^{-5}$
1.98	$3.56*10^{-2}$

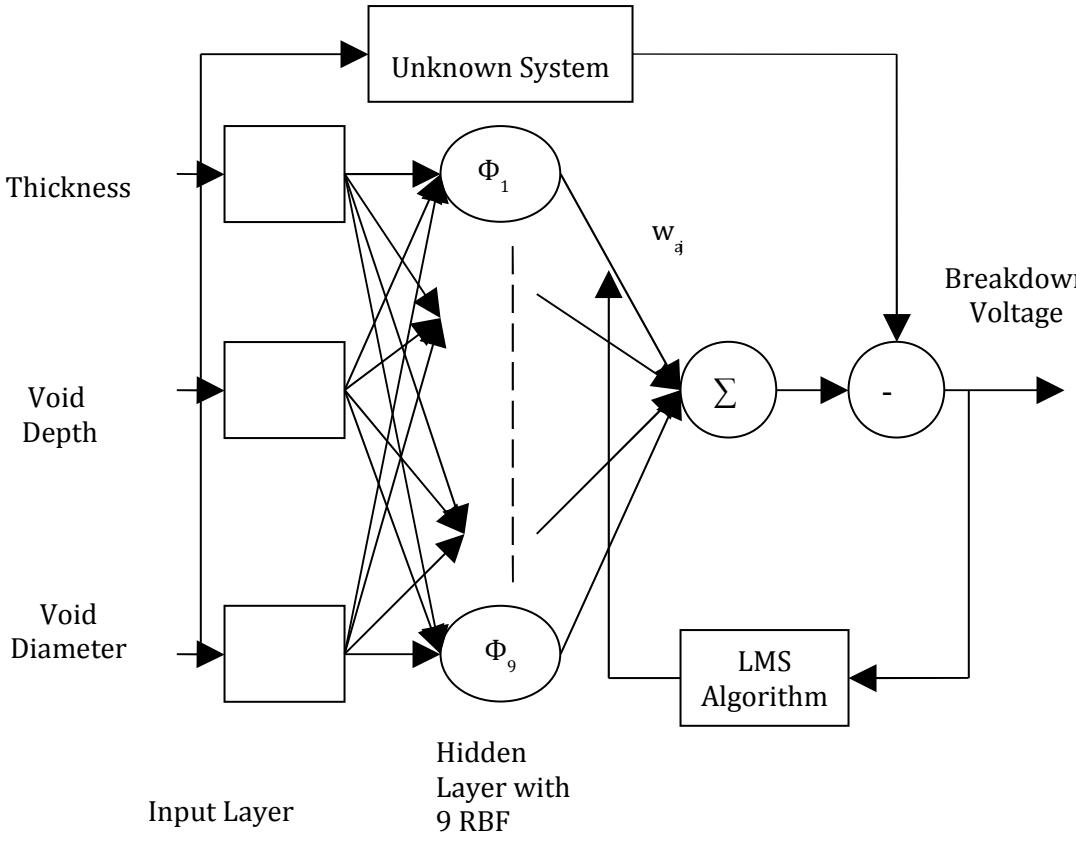

Figure 4.5: RBF Network used in Model 2

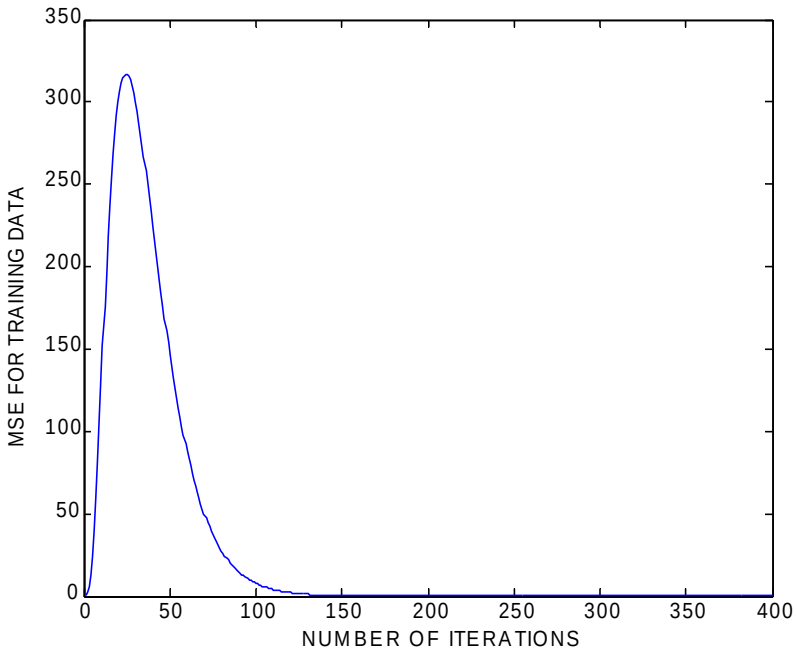

Figure 4.6: Variation of E_{tr} of the training data as a function of Number of iterations

On completion of the training, the breakdown voltage, $V_b = f$ (t, t_1, d) for the 15 sets of test input data for all the five insulating materials are calculated using the trained network. A comparison of the experimental and the modeled values of the breakdown voltage is presented in Table 4.6. As indicated in the Table, it may be seen that the value of MAE of the test data E_{ts} is 0.3868 %.

Table 4.6: Comparison of the experimental and modeled values of breakdown voltage

Insulating Material	t (mm)	t_1 (mm)	d (mm)	Breakdown Voltage (kV) (Experimental)	Breakdown Voltage (kV) (Modeled)	MAE of the Test data E_{ts} (%)
White Minilex	0.26	0.025	3	25.4903	25.5317	
	0.125	0.125	2	24.7000	24.7642	
	0.18	0.025	1.5	24.7000	24.7000	
Leatherite Paper	0.13	0.125	5	2.0127	2.0138	
	0.175	0.125	4	2.5152	2.5313	
	0.235	0.025	2	3.3105	3.3104	
Glass Cloth	0.195	0.025	5	17.9443	18.0374	
	0.155	0.025	3	13.9502	13.9502	0.3868
	0.155	0.125	1.5	13.8725	13.7376	
Manila Paper	0.035	0.125	3	1.5456	1.5364	
	0.06	0.025	2	1.4413	1.4413	
	0.06	0.125	4	1.5088	1.5035	
Lather Minilex	0.245	0.025	5	16.6824	16.8771	
	0.185	0.125	1.5	16.5625	16.7567	
	0.12	0.025	2	10.5760	10.5760	

4.3.2 Prediction of the breakdown voltage due to PD in voids under AC conditions

For prediction of breakdown voltages under AC conditions four models are proposed, details of which are as follows

- **Model 3**

This model has used the same input-output parameters to develop breakdown voltage model for Leatherite paper, similar to the model 3 presented in Chapter 3, using MFNN. Further, the model has also used the identical number of input-output data sets as model 3, which are 15. Thus, the input output data are taken from Table 2.7. Out of the 15 sets of input-output patterns, 8 sets of input-output patterns are utilized to train the RBFN and the remaining 7 sets are used for the testing purpose.

Results and Discussions

On varying the values of m_1 and η_2 in order to obtain the optimum values, it is found that the values of training error E_{tr} are of the order of 10^{-3} and above when $1 \leq m_1 \leq 6$ & $0 \leq \eta_2 \leq 1.89$ or when $1 \leq m_1 \leq 6$ & $\eta_2 > 1.98$. However, when m_1 is increased from 7 to 13 in steps of 1, the values of E_{tr} are in the order of 10^{-4} or 10^{-5} for a fixed value of η_2 between 1.90 and 1.98. Hence, out of the 7 values of E_{tr}, the least value of E_{tr} occurs for $m_1 = 12$.

Then m_1 is fixed at 12 and η_2 is varied in the range of 1.90 to 1.98 in steps of 0.01. It is found that the least value of $E_{tr} = 1.263*10^{-5}$ occurs, when $\eta_2 = 1.97$ and $m_1 = 12$. The variation of E_{tr} of the training data with the number of iterations with $\eta_2 = 1.97$, $m_1 = 12$ is shown in Figure 4.7. Hence the network structure for this model is similar to Figure 4.3. But there are 12 radial basis functions in the hidden layer. Tables 4.7 - 4.8 shows the variation of E_{tr} as a function of m_1 and η_2 respectively.

Table 4.7: Variation of Training error E_{tr} with m_1

(η_2 = 1.98, Number of iterations = 400)

m_1	E_{tr}
7	$8.246*10^{-4}$
8	$2.231*10^{-4}$
9	$1.044*10^{-4}$
10	$3.270*10^{-5}$
11	$2.333*10^{-5}$
12	$\mathbf{1.327*10^{-5}}$
13	$1.627*10^{-5}$

Table 4.8: Variation of Training error E_{tr} with η_2

(m_1 = 12, Number of iterations = 400)

η_2	E_{tr}
1.90	$1.521*10^{-4}$
1.91	$1.313*10^{-5}$
1.92	$1.305*10^{-5}$
1.93	$1.297*10^{-5}$
1.94	$1.289*10^{-5}$
1.95	$1.280*10^{-5}$
1.96	$1.273*10^{-5}$
1.97	$\mathbf{1.263*10^{-5}}$
1.98	$1.327*10^{-5}$

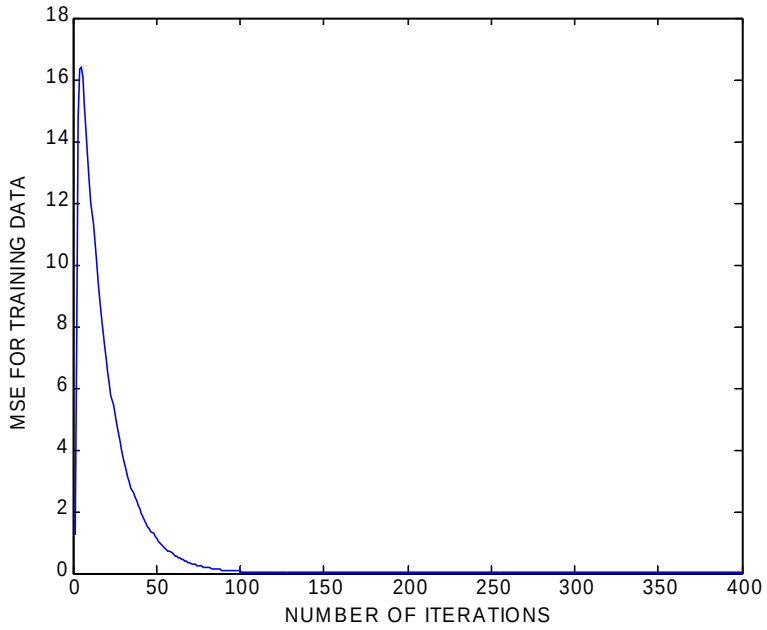

Figure 4.7: Variation of E_{tr} of the training data as a function of Number of iterations

On completion of the training, the breakdown voltage, $V_b = f$ (t, d) for the 7 sets of test input data for Leatherite paper are calculated using the trained network. Table 4.9 shows a comparison of the experimental and the modeled value of the breakdown voltage. The value of E_{ts} is 0.5611 % is also indicated in the Table.

Table 4.9: Comparison of the Experimental and Modeled values of Breakdown voltage

Insulating Material	t (mm)	d (mm)	Breakdown Voltage (kV) (Experimental)	Breakdown Voltage (kV) (Modeled)	MAE of the Test data E_{ts} (%)
Leatherite Paper	0.13	1.5	1.3452	1.3452	0.5611
	0.13	2	1.3306	1.3306	
	0.13	3	1.2972	1.2754	
	0.175	2	1.8313	1.8313	
	0.175	3	1.7981	1.7698	
	0.235	2	2.2697	2.2757	
	0.235	4	2.2909	2.3018	

- **Model 4**

The model 4 has used the same number of input parameters, the same number of output parameters, the same number of insulating materials and the identical input output patterns as model 4 in Chapter 3. This implies that the number of sets of input and output patterns of the five insulating materials is 65. Hence these input output patterns are taken from Table 2.7. Out of the 65 sets of input-output patterns, 50 sets of input-output patterns are utilized to train the RBFN and the remaining 15 sets are used for the testing purpose.

Results and Discussions

Since, the main objective is to obtain the least value of training error E_{tr} for a combination of m_1 and η_2, these two parameters are varied extensively. It is revealed that when $1 \leq m_1 \leq 5$ & $0 \leq \eta_2 \leq 1.89$ or when $1 \leq m_1 \leq 5$ & $\eta_2 > 1.99$ the values of E_{tr} are of the order of 10^{-3} and above. Hence, essentially two steps are carried out. In the first step, m_1 varies from 6 to 13 in steps of 1, while keeping η_2 constant at a value between 1.90 to 1.99. The least value of E_{tr} occurs at m_1=11.

In the second step, η_2 is varied from 1.90 to 1.99 keeping m_1 fixed at 11, and at η_2 = 1.98, the least value of E_{tr} is obtained. Hence, from both the steps, it is found that the least value of E_{tr} is $1.010*10^{-5}$ for the combination of η_2 = 1.98 and m_1 = 11. Tables 4.10 - 4.11 show the variation of E_{tr} as a function of m_1 and η_2 respectively. The network structure for this model is the same as Figure 4.3 The variation of E_{tr} of the training data with the number of iterations with η_2 = 1.98, m_1 = 11 is represented in Figure 4.8.

Table 4.10: Variation of Training error E_{tr} with m_1

(η_2 = 1.96, Number of iterations = 400)

m_1	E_{tr}
6	$1.82*10^{-4}$
7	$1.73*10^{-5}$
8	$1.64*10^{-5}$
9	$1.55*10^{-5}$
10	$1.47*10^{-5}$
11	$\mathbf{1.02*10^{-5}}$
12	$2.30*10^{-5}$
13	$2.86*10^{-5}$

Table 4.11: Variation of Training error E_{tr} with η_2

(m_1 = 11, Number of iterations = 400)

η_2	E_{tr}
1.90	$3.060*10^{-4}$
1.95	$1.023*10^{-5}$
1.96	$1.020*10^{-5}$
1.97	$1.013*10^{-5}$
1.98	$\mathbf{1.010*10^{-5}}$
1.99	$4.410*10^{-4}$

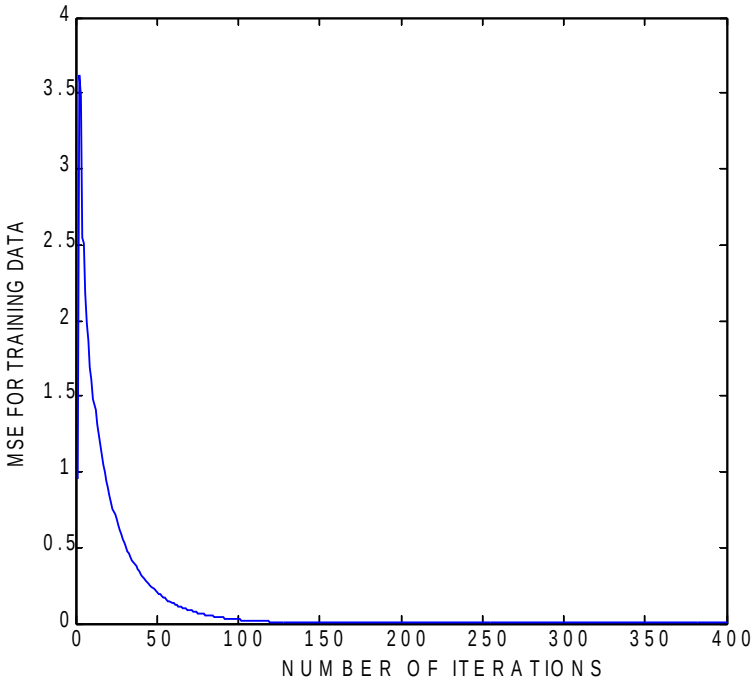

Figure 4.8: Variation of E_{tr} of the Training data as a function of Number of iterations

Finally, the modeled value of the breakdown voltage $V_b = f$ (t, d) is obtained for the test data by passing through the trained network. Table 4.12 shows a comparison of the experimental and the modeled value of the breakdown voltage for the 15 sets of the test data. The value of MAE of the test data E_{ts} is obtained as 0.2334%, as may be seen from Table.

Table 4.12: Comparison of the Experimental and modeled values of Breakdown voltage

Insulating Material	t (mm)	d (mm)	Breakdown Voltage (kV) (Experimental)	Breakdown Voltage (kV) (Modeled)	MAE of the Test data E_{ts} (%)
White Minilex	0.26	3	2.2807	2.2898	0.2334
	0.125	2	2.2697	2.2697	
	0.18	1.5	2.2885	2.2885	
Leatherite Paper	0.13	5	1.3306	1.3305	
	0.175	4	1.8313	1.8603	
	0.235	2	2.2909	2.2880	
Glass Cloth	0.195	5	2.2294	2.2289	
	0.155	3	2.2447	2.2448	
	0.155	1.5	2.3088	2.3088	
Manila Paper	0.035	3	0.8154	0.8158	
	0.06	2	0.8388	0.8387	
	0.06	4	0.8758	0.8871	
Lather Minilex	0.245	5	2.2697	2.2697	
	0.185	1.5	2.3088	2.3088	
	0.12	2	2.3170	2.3170	

- **Model 5**

The model 5 is proposed based on an additional input parameter, namely the void depth $t_{1,}$ with respect to the model 4. Hence, the total number of input-output patterns in this model has increased by a factor of two and becomes 130. The 130 sets of input output patterns have been taken from Table 2.7. The training of the model is carried out with 115 sets of input output patterns and the rest 15 sets are utilized for testing purpose.

Results and Discussions

The reasons for fixing the range of values of m_1 and η_2 in order to obtain the least value of training error E_{tr} have been discussed exhaustively in the previous four models and the same process is also adopted in this model. On following these guidelines it can be confirmed from Tables 4.13, 4.14 and Figure 4.9 that the least value of E_{tr} is seem to obtain as $5.61*10^{-5}$ for m_1 = 9 , η_2 = 1.96 after 400 iterations. The network structure for this model is the same as Figure 4.5.

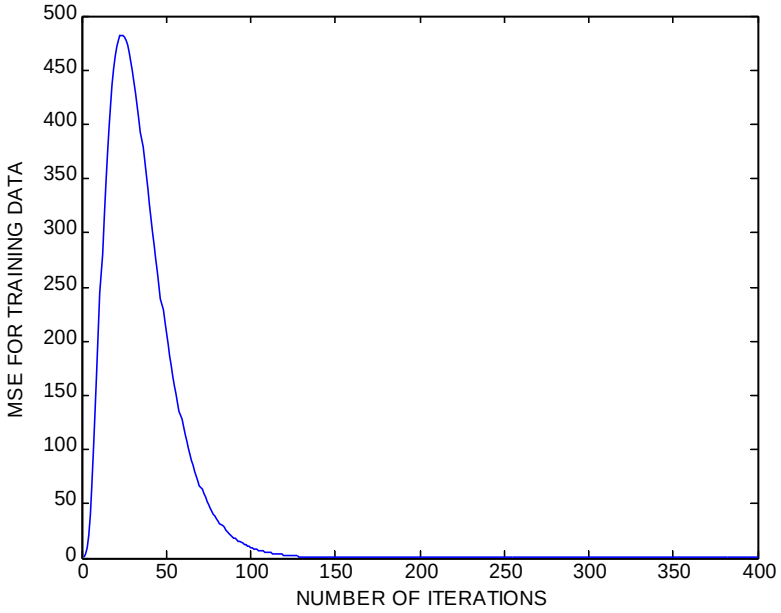

Figure 4.9: Variation of E_{tr} of the Training data as a function of Number of iterations

Table 4.13: Variation of Training error E_{tr} with m_1

(η_2 = 1.96, Number of iterations = 400)

m_1	E_{tr}
6	$2.10*10^{-2}$
7	$4.50*10^{-3}$
8	$1.57*10^{-4}$
9	$\mathbf{5.61*10^{-5}}$
10	$1.46*10^{-4}$

Table 4.14: Variation of Training error E_{tr} with η_2
(m_1 = 9, Number of iterations = 400)

η_2	E_{tr}
1.90	$4.82*10^{-3}$
1.95	$5.64*10^{-5}$
1.96	$\mathbf{5.61*10^{-5}}$
1.97	$6.72*10^{-5}$
1.98	$4.08*10^{-2}$

On completion of the training, the breakdown voltage, $V_b = f(t, t_1, d)$ for the 15 sets of test input data for all the five insulating materials are calculated using the trained network. The value of the Mean Absolute Error E_{ts} is 0.2586% for this model and this may be confirmed from Table 4.15. In addition, the experimental and the modeled value of the breakdown voltage have been compared in this Table.

Table 4.15: Comparison of the experimental and modeled values of the breakdown voltage

Insulating Material	t (mm)	t_1 (mm)	d (mm)	Breakdown Voltage (kV) (Experimental)	Breakdown Voltage (kV) (Modeled)	MAE of the Test data E_{ts} (%)
White Minilex	0.26	0.025	3	2.2294	2.2330	
	0.125	0.125	2	2.2447	2.2505	
	0.18	0.025	1.5	2.2697	2.2697	
Leatherite Paper	0.13	0.125	5	1.2972	1.2973	
	0.175	0.125	4	1.8520	1.8535	
	0.235	0.025	2	2.2697	2.2697	
Glass Cloth	0.195	0.025	5	2.3088	2.3171	
	0.155	0.025	3	2.3088	2.3088	0.2586
	0.155	0.125	1.5	2.2294	2.2172	
Manila Paper	0.035	0.125	3	0.8388	0.8380	
	0.06	0.025	2	0.8154	0.8154	
	0.06	0.125	4	0.8479	0.8474	
Lather Minilex	0.245	0.025	5	2.2447	2.2792	
	0.185	0.125	1.5	2.2294	2.2470	
	0.12	0.025	2	2.2909	2.2909	

- **Model 6**

In all the previous models proposed in this Chapter, the breakdown voltage due to PD in voids was predicted as a function of the thickness of the material t and the void parameter(s). However, it is reported that the PD activities and thus breakdown of insulation are dependent on the value of relative permittivity ϵ_r of a material [50, 51]. Hence, in this model, the relative permittivity ϵ_r of the sheet samples are considered as an additional input parameter with

respect to model 5. The value of N_i is thus four. The number of training and the testing patterns is the same as model 5.

Results and Discussions

To obtain the least value of the training error, network parameters are varied extensively as before to obtain the optimum values. It is found that the least value of E_{tr} is seemed to obtain as $8.79*10^{-5}$ for the combination of $\eta_2 = 1.96$ and $m_1 = 9$. Tables 4.16 - 4.17 shows the variation of E_{tr} as a function of m_1 and η_2 respectively. The network structure for this model is depicted in Figure 4.10. The variation of E_{tr} of the training data with the number of iterations with $\eta_2 = 1.96$, $m_1 = 9$ is shown in Figure 4.11.

Table 4.16: Variation of Training error with m_1
($\eta_2 = 1.96$, Number of iterations = 400)

m_1	E_{tr}
6	$2.52*10^{-2}$
7	$7.20*10^{-3}$
8	$1.94*10^{-4}$
9	$\mathbf{8.79*10^{-5}}$
10	$2.10*10^{-4}$

Table 4.17: Variation of Training error E_{tr} with η_2
($m_1 = 9$, Number of iterations = 400)

η_2	E_{tr}
1.90	$9.15*10^{-4}$
1.95	$8.84*10^{-5}$
1.96	$\mathbf{8.79*10^{-5}}$
1.97	$9.88*10^{-5}$
1.98	$4.08*10^{-2}$

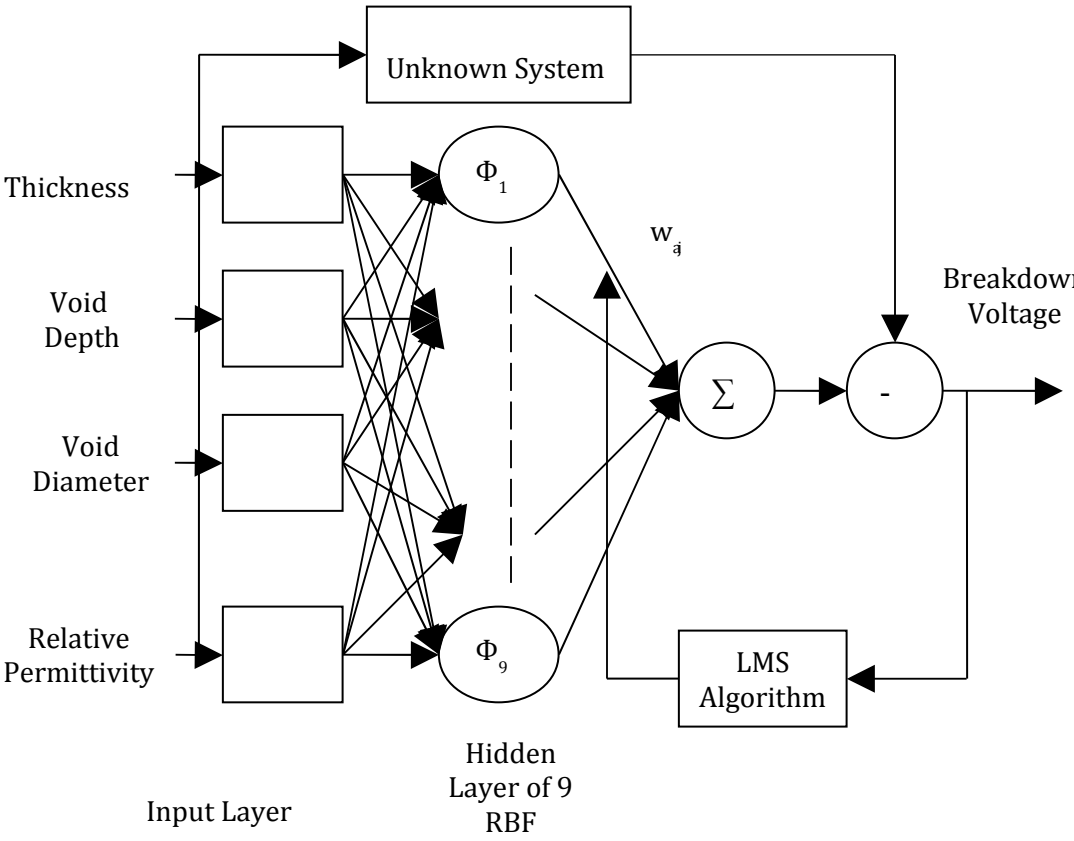

Figure 4.10: RBF Network used in Model 6

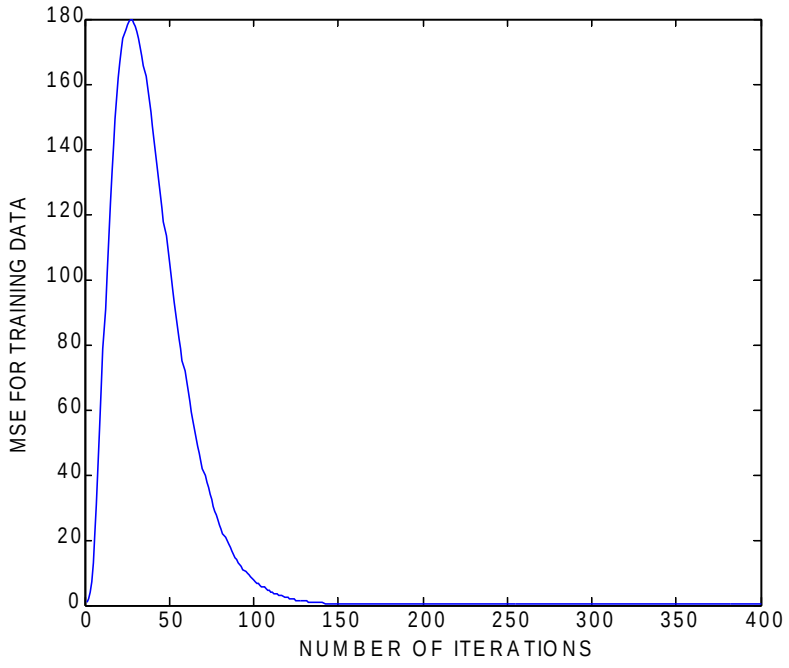

Figure 4.11: E_{tr} of the training data as a function of Number of iterations

Finally, the breakdown voltage, $V_b = f(t, t_1, d, \epsilon_r)$ for the 15 sets of test input data for all the five insulating materials are calculated using the trained network. A comparison of the experimental and the modeled value of the breakdown voltage is presented in Table 4.18. The MAE value of test data E_{ts} is obtained as 0.5735 %.

Table 4.18: Comparison of the Experimental and Modeled values of the Breakdown voltage

Insulating Material	t (mm)	t_1 (mm)	d (mm)	ϵ_r	Breakdown Voltage (kV) (Experimental)	Breakdown Voltage (kV) (Modeled)	MAE of the Test data E_{ts} (%)
White Minilex	0.26	0.025	3	4.4	2.2294	2.2330	0.5735
	0.125	0.125	2	4.4	2.2447	2.2505	
	0.18	0.025	1.5	4.4	2.2697	2.2697	
Leatherite Paper	0.13	0.125	5	4.21	1.2972	1.2973	
	0.175	0.125	4	4.21	1.8520	1.8534	
	0.235	0.025	2	4.21	2.2697	2.2607	
Glass Cloth	0.195	0.025	5	4.97	2.3088	2.3164	
	0.155	0.025	3	4.97	2.3088	2.3088	
	0.155	0.125	1.5	4.97	2.2294	2.2179	
Manila Paper	0.035	0.125	3	4.68	0.8388	0.8380	
	0.06	0.025	2	4.68	0.8154	0.8154	
	0.06	0.125	4	4.68	0.8479	0.8474	
Lather Minilex	0.245	0.025	5	5.74	2.2447	2.3918	
	0.185	0.125	1.5	5.74	2.2294	2.2419	
	0.12	0.025	2	5.74	2.2909	2.2909	

4.3.3 Extrapolation capability of RBFN

Model 6 just presented before is based on RBFN that was trained with 110 input-output data sets of five insulating sheet materials of thickness in the range of 0.06 to 0.245 mm. The depth of the artificial voids is 0.025 and 0.125 mm and the void diameter ranges between 1.5 and 5 mm. After the training is over as in Model 6, the RBFN was tested for it's extrapolation capability with the help of 20 sets of new test input data sets of Manila Paper and White Minilex with insulation thickness 0.035mm and 0.26 mm, void depth of 0.025 and 0.125 mm and void diameter of 1.5 to 5 mm. Thus, the insulation thickness of 0.035mm and 0.26 mm lies outside the range of the other thicknesses used for the training purpose for the five insulating materials. With the new test data sets, the MAE, E_{ts} of the test data is found slightly increased to 0.9896% than is obtained with model 6. The comparison of experimental and modeled values of the test data sets are presented in Table 4.19. This clearly indicates the adaptability of the network for a data, which is beyond the ranges of training set.

Table 4.19: Comparison of the Experimental and modeled breakdown voltage (Extrapolation capability)

Insulating Material	t (mm)	t_1 (mm)	d (mm)	ϵ_r	Breakdown Voltage (kV) (Experimental)	Breakdown Voltage (kV) (Modeled)	MAE of the Test data E_{ts} (%)
Manila Paper	0.035	0.025	3	4.68	0.8154	0.8154	0.9896
	0.035	0.125	2	4.68	0.8758	0.8527	
	0.035	0.025	1.5	4.68	0.8758	0.8757	
	0.035	0.125	5	4.68	0.9089	0.9096	
	0.035	0.125	4	4.68	0.8479	0.8573	
	0.035	0.025	2	4.68	0.8479	0.8430	
	0.035	0.025	5	4.68	0.8683	0.8683	
	0.035	0.025	4	4.68	0.9089	0.9036	
	0.035	0.125	1.5	4.68	0.8154	0.8246	
	0.035	0.125	3	4.68	0.8388	0.8379	
White Minilex	0.26	0.025	2	4.4	2.3088	2.3112	
	0.26	0.125	4	4.4	2.2909	2.2959	
	0.26	0.025	5	4.4	2.3170	2.3165	
	0.26	0.125	1.5	4.4	2.2885	2.2640	
	0.26	0.125	3	4.4	2.2885	2.4432	
	0.26	0.025	1.5	4.4	2.2294	2.2958	
	0.26	0.125	2	4.4	2.2697	2.2799	
	0.26	0.025	3	4.4	2.2294	2.2208	
	0.26	0.025	4	4.4	2.2885	2.2678	
	0.26	0.125	5	4.4	2.2909	2.2883	

4.4 Conclusion

In this Chapter, six models are proposed based on the RBFN structure to predict the breakdown voltage of solid insulating materials. The combinations of network parameters for best result in each model are identified. All the six models clearly indicate their effectiveness in predicting the breakdown voltage as is evident from the low Mean Absolute Error values of the test data. Further, the extrapolation capability of the RBFN has been explored. This too gives very satisfactory results.

Chapter 5

BREAKDOWN VOLTAGE MODELING USING MAMDANI FUZZY LOGIC TECHNIQUE

5.1 Introduction

In Chapters 3 and 4, the modeling of the breakdown voltage of solid insulating materials was attempted with the help of several ANN models utilizing MFNN and RBFN structures with the help of experimental data, generated in the laboratory and those are available in the literature. In this Chapter, the same data sets have been utilized and the modeling of the breakdown voltage is proposed based on the Fuzzy Logic (FL) technique with Mamdani inferencing. First, a general outline of the Mamdani Fuzzy Logic (MFL) has been presented in brief. Then, detailed discussions on the proposed models are made.

5.2 Mamdani Fuzzy Logic (MFL)

The ANN models discussed in the last two Chapters such as the MFNN and the RBFN model can recognize input-output data patterns and are able to update their weights. The weight updating is possible in the MFNN and the RBFN model by using the BPA and the LMS algorithm respectively. Hence, these ANN models are able to adapt themselves to cope with changing environments. The Fuzzy Logic (FL) models on the other hand incorporate human knowledge and perform inferencing and decision-making. It is essentially knowledge representation via fuzzy if then rules.

In this section, first of all the general theory of the MFL inferencing for the purpose of prediction is discussed before applying it to certain models in the next section.

- **General Theory of the inferencing**

The MFL Rule Based inferencing [82-83] is computationally very efficient. For applying this inferencing to the various models, the relationship between the linguistic values and the actual values of the input and the output parameters is required. The relationship between the linguistic values and the actual values of the input parameters is created with the help of Table

5.1, while Table 5.2 shows the relationship between the linguistic and actual values for the output parameter, namely the breakdown voltage.

Table 5.1: Relationship between the Linguistic and the Actual values from Input 1 to Input N_i

Linguistic Values	Input 1	Input 2	Input N_i
Low	i_{1L1}-i_{1L2}	i_{2L1}-i_{2L2}	i_{NiL1}-i_{NiL2}
Medium Low	i_{1ML1}-i_{1ML2}	i_{2ML1}-i_{2ML2}	i_{NiML1}-i_{NiML2}
Medium	i_{1M1}-i_{1M2}	i_{2M1}-i_{2M2}	i_{NiM1}-i_{NiM2}
Medium High	i_{1MH1}-i_{1MH2}	i_{2MH1}-i_{2MH2}	i_{NiMH1}-i_{NiMH2}
High	i_{1H1}-i_{1H2}	i_{2H1}-i_{2H2}	i_{NiH1}-i_{NiH2}

Table 5.2: Relationship between the Linguistic and the Actual values for V

Linguistic Values	V (kV)
Low	V_{L1}-V_{L2}
Medium Low	V_{ML1}-V_{ML2}
Medium	V_{M1}-V_{M2}
Medium High	V_{MH1}-V_{MH2}
High	V_{H1}-V_{H2}

The set of linguistic values assigned to input 1, input 2, ……., input N_i and the breakdown voltage V is given by equation (5.1).

Ł= {Low (L), Medium Low (ML), Medium (M), Medium High (MH), High (H)} (5.1)

While the Membership Functions (MFs) for input 1, input 2 and input N_i are μ_{i1}, μ_{i2} and μ_{iNi} respectively.

μ_{i1}, μ_{i2} and μ_{iNi} would be having components corresponding to each linguistic value defined as follows

$\mu_{i1} = \{\mu_{ilL}, \mu_{ilML}, \mu_{ilM}, \mu_{ilMH}\ \mu_{i1H}\}$ (5.2)

$\mu_{i2} = \{\mu_{i2L}, \mu_{i2ML}, \mu_{i2M}, \mu_{i2MH}\ \mu_{i2H}\}$ (5.3)

$\mu_{iNi} = \{\mu_{iNiL}, \mu_{iNiML}, \mu_{iNiM}, \mu_{iNiMH}\ \mu_{iNiH}\}$ (5.4)

The Membership Functions (MFs) for V is μ_V.

μ_V would be having five components corresponding to each linguistic value as

$\mu_V = \{\mu_{VL}, \mu_{VML}, \mu_{VM}, \mu_{VMH}, \mu_{VH}\}$ (5.5)

The procedure for finding the number of rules is model specific. Let the total number of rules be R_1.

Out of the total number of input output sets, N_p of them is used for creating R_1 rules in the rule base and N_s is used for testing purpose.

A typical clipped fuzzified MFs obtained by firing the first rule is as follows:

$\mu_1 = \text{minimum}_{Ni+1}(\mu_{iN1}^* , \mu_{iN2}^*, \ldots\ldots \mu_{iNi}^*, \mu_{VMH})$ (5.6)

Where μ_{N1}^*.... μ_{Ni}^* are the MFs corresponding to the crisp inputs for the input 1 up to input N_i respectively.

Similarly, the other fuzzified MFs obtained by firing the rest R_1-1 rules are

$\mu_2, \mu_3, \mu_4, \ldots\ldots\ldots\ldots\ldots\ldots, \mu_{R1-1}, \mu_{R1.}$ All the R_1 clipped fuzzified MFs are aggregated to form the aggregated fuzzified MFs. A typical rule base appears as follows in Table 5.3.

Table 5.3: Typical Mamdani Rule Base

IF Input parameters				THEN Output parameters
SL No.	Input 1	Input 2	Input N_i	Breakdown Voltage V
1.	L	M	L	MH
2.	ML	L	MH	M
3.	H	L	L	H
¦				¦
¦				¦
¦				¦
R_1-1	MH	ML	L	ML
R_1	M	L	H	L

The aggregated fuzzified MFs is given by

$$\mu_{A1}(V) = \text{maximum}_{R1} (\mu_1, \mu_2, \mu_3 \ldots\ldots\ldots\ldots\ldots, \mu_{R1-1}, \mu_{R1}) \quad (5.7)$$

- **Membership Function (MF) used in the proposed models**

For computational efficiency, efficient use of memory, and performance analysis needs, a uniform representation of the MFs for the input and the output parameters are required. This may be achieved by employing MFs with uniform shapes. The most popular choices for the shapes of the MFs include triangular, trapezoidal, gaussian, generalized Bell and pi shaped. The shape of the MFs considered for the input and the output parameters are assumed to be triangular and trapezoidal for all the discussed models in this Chapter which are defined as follows. Figure 5.1 and 5.2 shows the sketches of the triangular and trapezoidal MF .

The triangular MF is defined as

$$\mu_x = 0 \qquad x < a$$

$$= (x-a) / (b-a) \qquad a \le x \le b \quad (5.8)$$

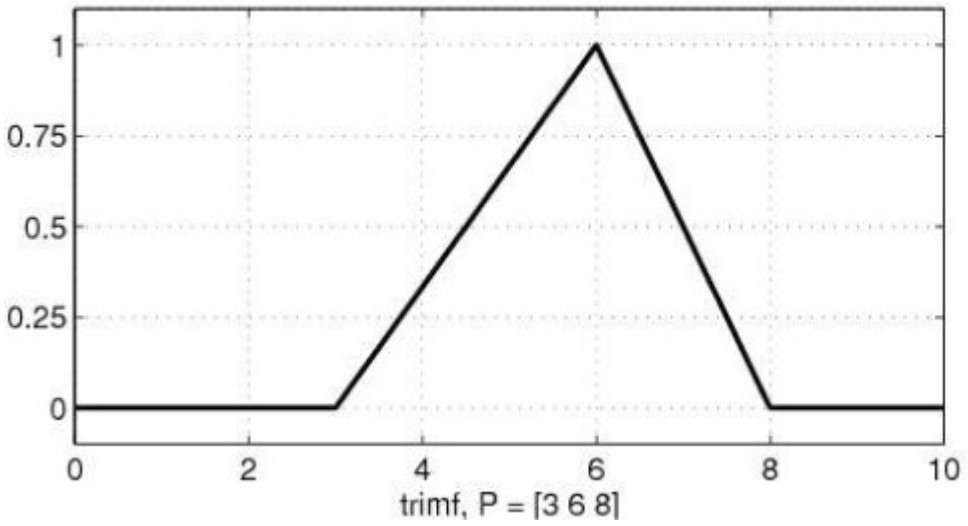

The parameters *a* and *c* locate the "feet" of the triangle and the parameter *b* locates the peak.

Figure 5.1: Triangular MF

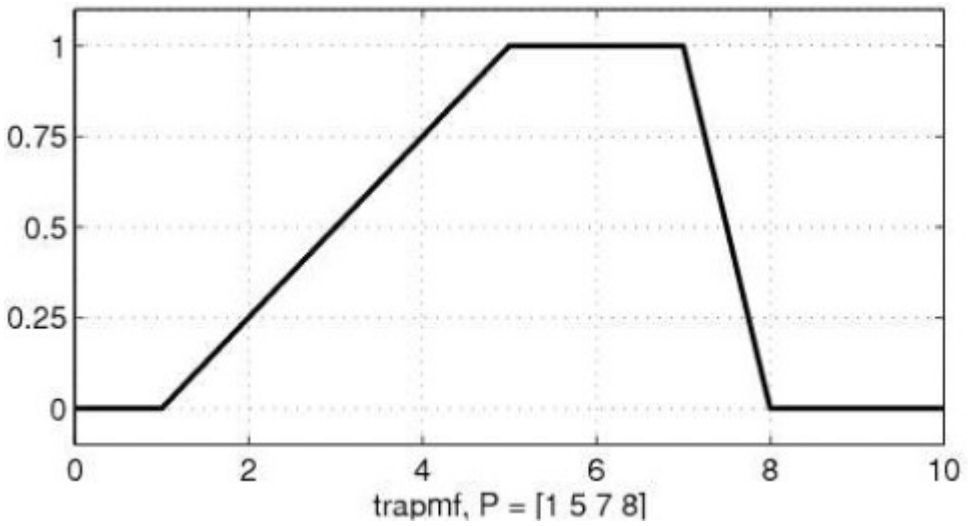

The parameters *a* and *d* locate the "feet" of the trapezoid and the parameters *b* and *c* locate the "shoulders.

Figure 5.2: Trapezoidal MF

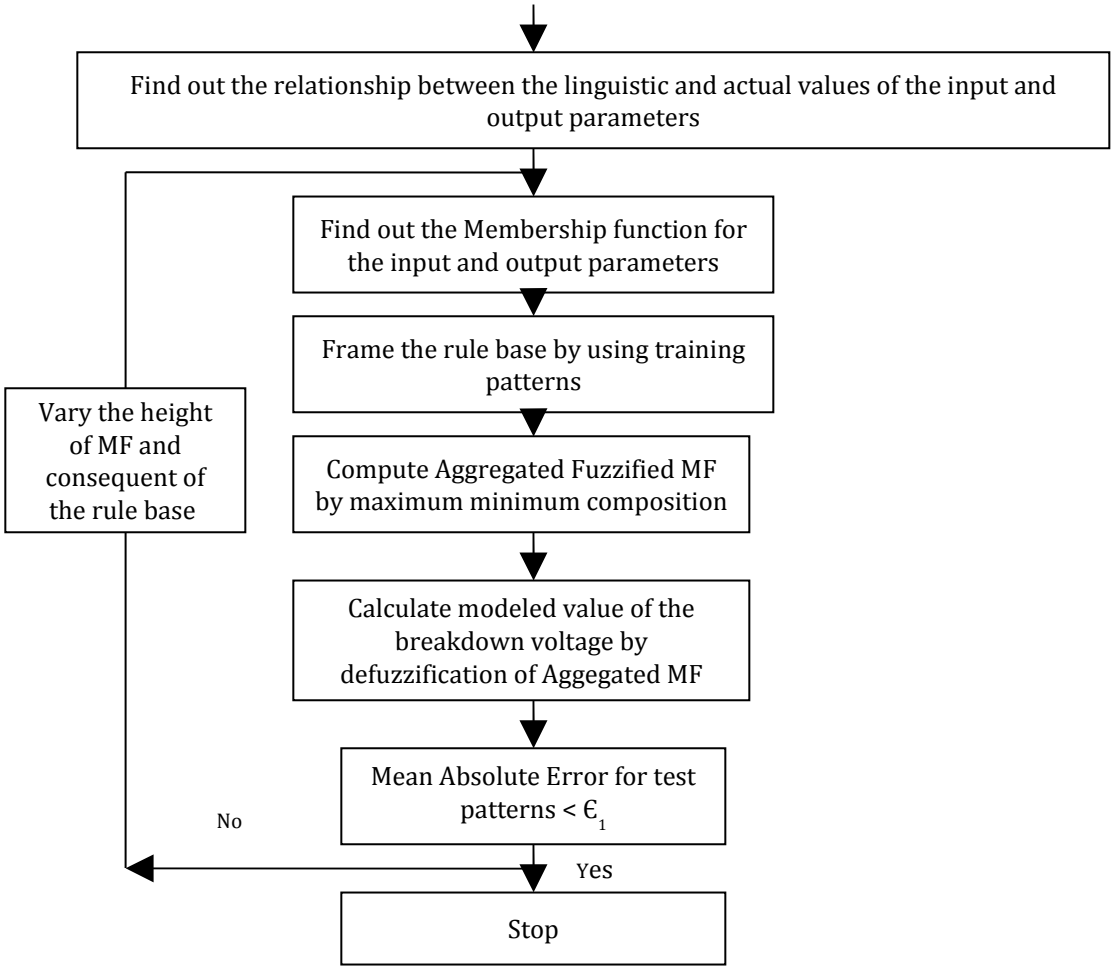

Figure 5.3 : Flow Chart for the MFL

$= (c-x) / (c-b)$ $b \le x \le c$

$= 0$ $x > c$

The trapezoidal MF is defined as

$$\mu_x = \begin{cases} 0 & x < a \\ (x-a)/(b-a) & a \le x \le b \\ 1 & b \le x \le c \\ (d_1-x)/(d_1-c) & c \le x \le d_1 \\ 0 & x > d_1 \end{cases} \quad (5.9)$$

The fuzzy toolbox was used for equations (5.8) and (5.9).

5.3 Modeling of Breakdown Voltage using MFL

In this section, the breakdown voltage is predicted as a function of different void parameters, namely, void diameter and void depth and insulation sheet thickness both at DC and AC conditions using the MFL. Figure 5.3 shows the flowchart for the MFL.

In order to predict the breakdown voltage under DC / AC conditions a software program has been developed in MATLAB 7.1 which solves equations (5.1) to (5.7). However, the defuzz function in the fuzzy toolbox was used to compute the defuzzified or the modeled value of the breakdown voltage from $\mu_{A1}(V)$. In addition, the program calculates the Mean Absolute Error (MAE) of the test patterns E_{ts} using equation (3.10). The program is suitably modified for different models based on the input – output parameters.

5.3.1 Prediction of the breakdown voltage due to PD in voids under DC conditions

The two proposed models have predicted the breakdown voltage of a single insulating material as a function of two and three input parameters using triangular and trapezoidal shapes for MFs.

- **Model 1**

In this model [114], the number of input parameters is assumed to be two i.e. the thickness of the paper t and the void diameter d and the output parameter is the breakdown voltage to be predicted as a function of these input parameters. The void depth t_1 is kept constant at 0.125 mm. The model data sets used the experimental data generated using White Minilex paper. Since, the input parameters are two, the value of N_i is two for this model. In addition, since the output parameter is only one, the value of N_k is one.

Further, there are three values of thickness t of White Minilex paper and five values of void diameter d, thus, the number of input-output data sets is 15. These 15 sets of input-output patterns are taken from Table 2.6. Table 5.4 represents the relationship between the linguistic and the actual values of t and d and Table 5.5 showing the relationship between the linguistic and the actual values of V, which are obtained from these input-output patterns. Out of the 15 sets of input-output patterns, N_p = 8 sets of input-output patterns, Tables 5.4 and 5.5 are utilized for creating the rule base. The remaining N_s = 7 sets are used for the testing the rule base.

The general form of this Table has been highlighted in Table 5.1.

Table 5.4: Relationship between the Linguistic and the Actual values for t and d

Linguistic Values	t (mm)	d (mm)
Low	0-0.15	1.0-3.8
Medium	0.09-0.24	2.0-4.8
High	0.18- 0.33	3.0-5.8

Table 5.5: Relationship between the Linguistic and the Actual values for V_{dc}

Linguistic Values	V_{dc} (kV)
Low	23.3-24.8
Medium	24.1-25.6
High	24.9-26.4

The set of linguistic values assigned to t and d are given by

$Ł_1$= {Low (L), Medium (M), High (H)} (5.10)

on using equation (5.1).

The Membership Functions (MFs) for t and d are μ_t and μ_d respectively.

μ_t and μ_d would be having components corresponding to each linguistic value as

$\mu_t = \{\mu_{tL}, \mu_{tM}, \mu_{tH}\}$ (5.11)

$\mu_d = \{\mu_{dL}, \mu_{dM}, \mu_{dH}\}$ (5.12)

on following equations (5.2) to (5.4).

Results and Discussions

A. Triangular MF

The rule base is as shown in Table 5.6. Since the linguistic values associated with t and d are both 3, there are 9 rules in the rule base. Hence, in this model the value of R_1 is 9. This rule base Table is similar to the general rule base Table 5.3.

Table 5.6: Mamdani Rule Base

IF Input parameters		THEN Output parameters
Thickness, t	Diameter of the void, d	Breakdown Voltage, V
L	L	L
L	M	M
L	H	L
M	L	M
M	M	M
M	H	M
H	L	H
H	M	M
H	H	M

The variation of the height b of the triangular MF defined in equation (5.8) plays a very critical role in reducing the MAE of the test data E_{ts}. After trying out 15 combinations of the heights b_{tL} (corresponding to μ_{tL} in equation (5.11)), b_{dL} (corresponding to μ_{dL} in equation (5.12)) and b_{VL} (corresponding to μ_{VL} in equation (5.5)), it was found that when b_{tL}=0.08, b_{dL}=2.4 and b_{VL}=23.8, the E_{ts} turns out to be the least .

The modeled value of the breakdown voltage is obtained by defuzzification of equation (5.7). Table 5.7 shows a comparison of the experimental and the modeled values of the breakdown voltage when 7 sets of input-output patterns are presented to the MFL model as test data with triangular MF for the input and the output parameters. The least value of MAE of the test data E_{ts} is found to be 0.7789 %.

Figure 5.4 shows the aggregated MFs plot for the test inputs using equation (5.7).

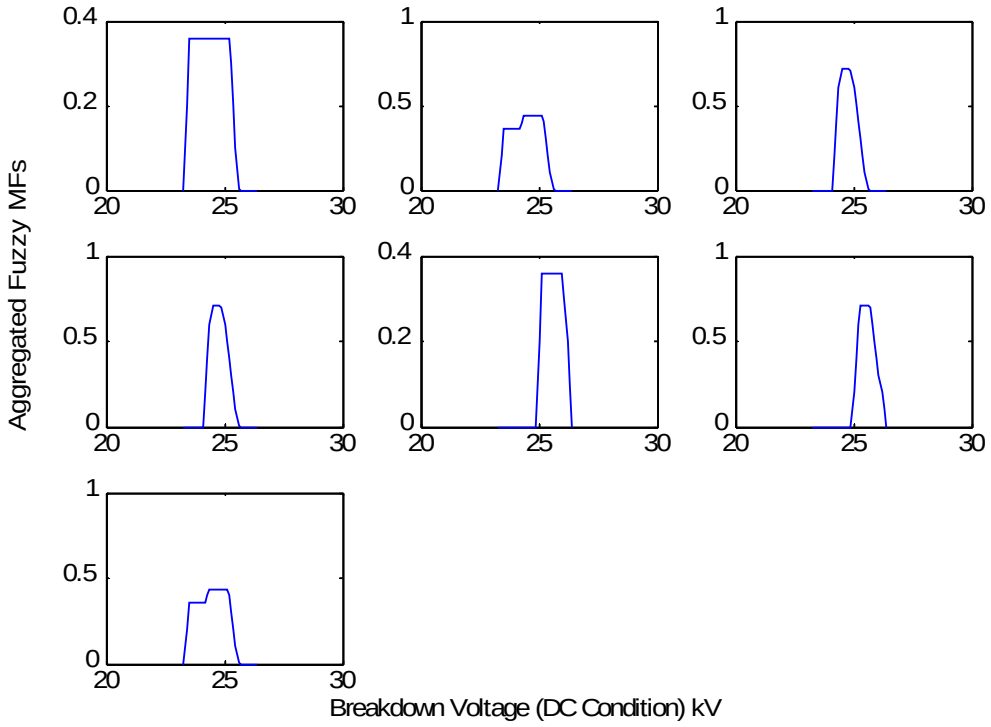

Figure 5.4: Aggregated Fuzzy MFs for the Test inputs with Triangular MF

Table 5.7: Comparison of the Experimental and Modeled values of the Breakdown voltage

t (mm)	d (mm)	Breakdown Voltage (Experimental) (kV)	Breakdown Voltage (Modeled) (kV)	MAE of the Test data E_{ts} (%)
0.125	1.5	23.85	24.4081	0.7789
0.125	2	24.32	24.4394	
0.18	1.5	24.70	24.7783	
0.18	3	24.77	24.7783	
0.26	5	25.66	25.6095	
0.26	1.5	25.42	25.5783	
0.125	4	24.09	24.4394	

B. Trapezoidal MF

This Case is very similar to Case A except that the triangular MF is now replaced by the trapezoidal MF. Hence, Tables 5.4 - 5.6 are also used here. The heights b and c of the trapezoidal MF defined in equation (5.9) solely decides the value of MAE of the test data E_{ts}.

After trying out 25 combinations of the heights b_{tL} and c_{tL} (corresponding to μ_{tL} in equation (5.11)); b_{dL} and c_{dL} (corresponding to μ_{dL} in equation (5.12)), b_{VL} and c_{VL} (corresponding to μ_{VL} in equation (5.5)), it is found that when these heights of μ_{tL}, μ_{dL} and μ_{VL} are b_{tL}= 0.07, c_{tL}= 0.13, b_{dL}=1.5, c_{dL}= 3.1 , b_{VL}= 23.6 & c_{VL}= 24.3 respectively, the E_{ts} seems to be the minimum.

Table 5.8 shows a comparison of the experimental and the modeled values of the breakdown voltage when 7 sets of input data are presented to the MFL model as test data with trapezoidal MF for the input and the output parameters. The procedure for obtaining the modeled value of the breakdown voltage is identical to that of Case A. The least value of MAE of the test data E_{ts} is found to be 0.6477 %.

Figure 5.5 shows the aggregated MFs plot for the same test inputs as Case A.

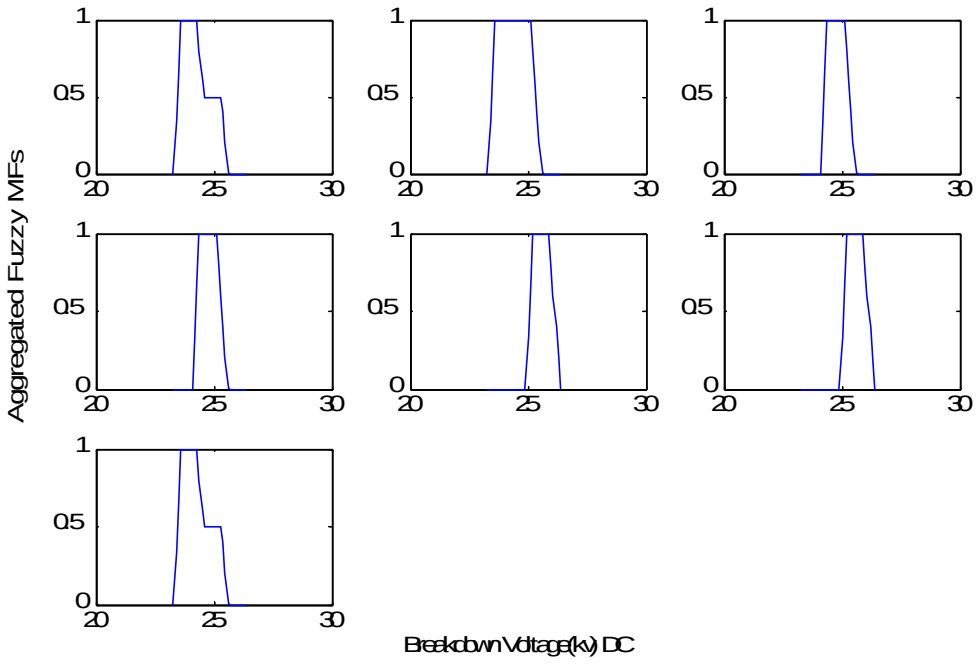

Figure 5.5: Aggregated Fuzzy MFs for the Test inputs with Trapezoidal MF

Table 5.8: Comparison of the Experimental and Modeled values of the breakdown Voltage

t (mm)	d (mm)	Breakdown Voltage (Experimental) (kV)	Breakdown Voltage (Modeled) (kV)	MAE of the Test data E_{ts} (%)
0.125	1.5	23.85	24.2898	0.6477
0.125	2	24.32	24.4035	
0.18	1.5	24.70	24.8061	
0.18	3	24.77	24.8061	
0.26	5	25.66	25.6061	
0.26	1.5	25.42	25.6061	
0.125	4	24.09	24.2898	

- **Model 2**

In this model, the experimental data are obtained using Manila paper but the number of input parameters is assumed to be three, that is, the thickness of the paper t, void depth t_1 and the void diameter d and the output parameter is the breakdown voltage to be predicted as a function of these input parameters. Hence, the value of N_i is three and the value of N_k is one for this model.

Now, there are two values of thickness t of Manila paper considered here, two values of void depth t_1 and five values of void diameter d. Thus, the number of input-output sets is 20. The 20 sets of input output patterns of Manila paper are taken from Table 2.6. Table 5.9 and Table 5.10 represents the relationship between the linguistic and actual values of 20 sets of input-output patterns. Out of the 20 sets of input-output patterns, 13 sets of input-output patterns are utilized for formulating the rule base and the remaining 7 sets are used for testing the rule base.

Table 5.9: Relationship between the Linguistic and the Actual values for t, t_1 and d

Linguistic Values	t (mm)	t_1(mm)	d (mm)
Low	0.015-0.04	0-0.07	1.0-3.8
Medium	0.03-0.055		2.0-4.8
High	0.045- 0.07	0.08-0.15	3.0-5.8

Table 5.10: Relationship between the Linguistic and the Actual values for V_{dc}

Linguistic Values	V_{dc} (kV)
Low	1.60-1.66
Medium	1.63-1.69
High	1.66-1.72

In this case μ_{tL}, μ_{dL} (defined by equation (5.11) , (5.12)) and μ_{VL} (defined in equation (5.5)) have been used.

The set of linguistic values assigned to t_1 are given by

$Ł_2$= {Low (L), High (H)} (5.13)

using equation (5.1).

Whereas the set of linguistic values to t and d are given in equation (5.10).

The Membership Functions (MFs) for t_1 is μ_{t1}.

$\mu_{t1} = \{\mu_{t1L}, \mu_{t1H}\}$ (5.14)

Results and Discussions

A. Triangular MF

The rule base is as shown in Table 5.11. Since the linguistic values associated with t, t_1 and d are 3, 2 and 3 respectively; there are 18 rules in the rule base. Hence, in this model the value of R_1 is 18. This rule base as represented by Table 5.11 is similar to Table 5.3.

19 combinations of the heights b_{tL} (corresponding to μ_{tL} in equation (5.11)), b_{t1L} (corresponding to μ_{t1L} in equation (5.14)) b_{dL} (corresponding to μ_{dL} in equation (5.12)) and b_{VL} (corresponding to μ_{VL} in equation (5.5)) have been tried. On carrying out this exercise, it is found that when the heights are b_{tL}= 0.03, b_{t1L}= 0.04, b_{dL}= 2.6 and b_{VL}= 1.63 , the E_{ts} turns out to be the least value at 1.2705 %.

Table 5.11: Mamdani Rule Base

IF Input parameters			THEN Output parameters
Thickness, t of the material	Thickness, t_1 of void	Diameter of the void, d	Breakdown Voltage, V
L	L	L	L
M	L	L	L
H	L	L	H
L	L	M	H
M	L	M	M
H	L	M	L
L	L	H	H
M	L	H	H
H	L	H	M
L	H	L	M
M	H	L	H
H	H	L	L
L	H	M	H
M	H	M	L
H	H	M	M
L	H	H	H
M	H	H	H
H	H	H	L

Table 5.12 shows the comparison of the experimental and modeled values of the breakdown voltage along with the least value of E_{ts}. Figure 5.6 shows the aggregated MFs plot for the test inputs.

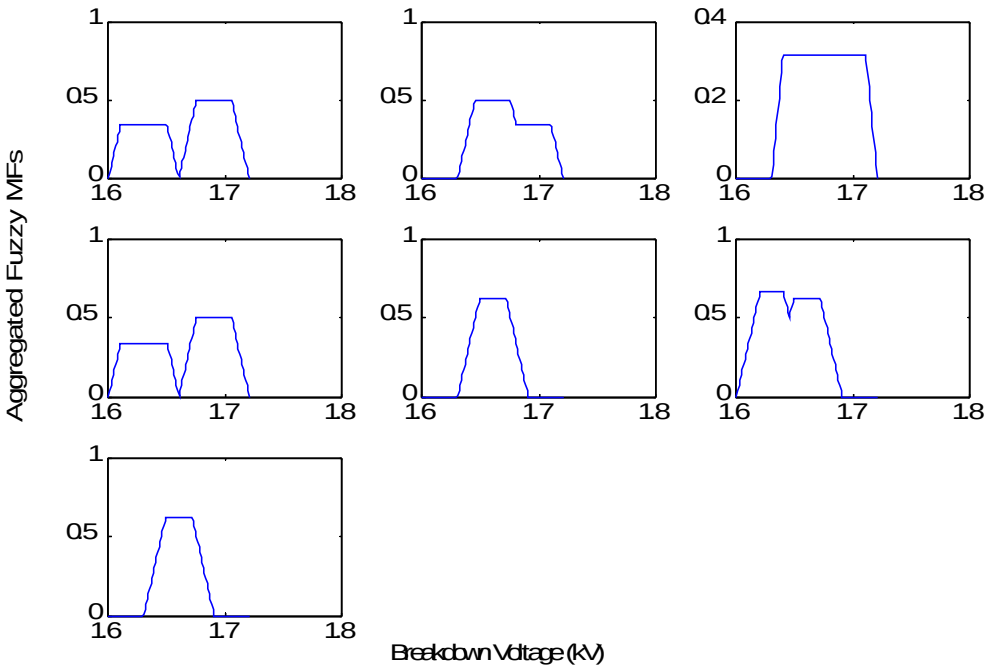

Figure 5.6: Aggregated Fuzzy MFs for the Test inputs with Triangular MF

Table 5.12: Comparison of the Experimental and Modeled values of the Breakdown voltage

t (mm)	t_1 (mm)	d (mm)	Breakdown Voltage (Experimental) (kV)	Breakdown Voltage (Modeled) (kV)	MAE of the Test data E_{ts} (%)
0.035	0.025	1.5	1.6389	1.6645	1.2705
0.035	0.125	2	1.6821	1.6723	
0.06	0.025	1.5	1.6682	1.6750	
0.06	0.125	3	1.6454	1.6645	
0.035	0.025	5	1.6323	1.6600	
0.06	0.125	1.5	1.7002	1.6447	
0.035	0.025	4	1.6563	1.6600	

A. Trapezoidal MF

This Case is similar to Case A, except the fact the triangular Membership function for the input parameters is replaced by trapezoidal Membership function. The number of rules is obviously 18. It is revealed here that when the heights b and c defined in equation (5.9) for $\mu_{tL,}$ μ_{t1L}, μ_{dL}, μ_{VL} are b_{tL}= 0.023, c_{tL}= 0.032, b_{t1L}= 0.03, c_{t1L}= 0.05, b_{dL}= 1.7, c_{dL}= 3.1, b_{VL}= 1.615 & c_{VL}= 1.645 , the E_{ts} turns out to be the least at 1.1674 %. It may be noted this particular combination of b's and c's is obtained after 32 trials. The Tables 5.9 to 5.11 may also be used in this Case.

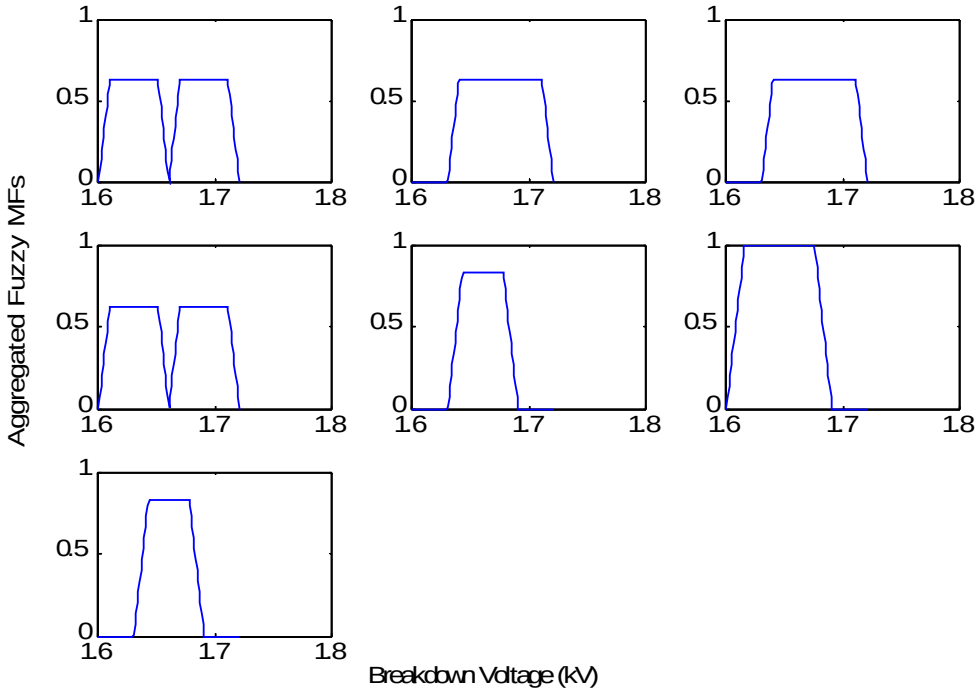

Figure 5.7: Aggregated Fuzzy MFs for the Test inputs with Trapezoidal MF

When the same test inputs as in Case A is presented to the MFL, a comparison between the experimental and the modeled value of the breakdown voltage is presented in Table 5.13. The MAE of the test data E_{ts} also indicated in the same Table is 1.1674 %. Figure 5.7 shows the aggregated MFs plot for the same test inputs as Case A.

Table 5.13: Comparison of the Experimental and Modeled values of the Breakdown voltage

t (mm)	t_1 (mm)	d (mm)	Breakdown Voltage (Experimental) (kV)	Breakdown Voltage (Modeled) (kV)	MAE of the Test data E_{ts} (%)
0.035	0.025	1.5	1.6389	1.6645	1.1674
0.035	0.125	2	1.6821	1.6723	
0.06	0.025	1.5	1.6682	1.6750	
0.06	0.125	3	1.6454	1.6645	
0.035	0.025	5	1.6323	1.6600	
0.06	0.125	1.5	1.7002	1.6447	
0.035	0.025	4	1.6563	1.6600	

5.3.2 Prediction of the breakdown voltage due to PD in voids under AC conditions

The number of proposed models under AC conditions is three. Out of these models, two of them have predicted the breakdown voltage of a single insulating material as a function of two and three input parameters and one of them has predicted the breakdown voltage of five insulating materials as a function of four input parameters

- **Model 3**

This model has predicted the breakdown voltage of White Minilex quiet similar to model 8, but under AC conditions. The number of input parameters and the number of input-output data sets are the same as model 1. But since AC conditions are being discussed, the input output data sets are taken from Table 2.7. The Tables 5.4 and 5.14 showing the relationship between the linguistic values and the actual values of the input output parameters is prepared from the input output data sets. Since the input parameters are the same as model 1, the rule base can be created with 9 rules. In addition, the equations (5.10) to (5.12) are used in this model.

Table 5.14: Relationship between the Linguistic and the Actual values for V_{ac}

Linguistic Values	V_{ac} (kV)
Low	2.15-2.25
Medium	2.20-2.30
High	2.25-2.35

Results and Discussions

A. Triangular MF

The rule base as shown in Table 5.15 has been created using 8 input-output patterns and referring to Table 5.4 and Table 5.14. When the rule base is fired with the 7 input test patterns and when b_{tL}= 0.09, b_{dL}= 2.0 and b_{VL}= 2.2, the E_{ts} turns out to be the least. This particular combination of the heights of $\mu_{tL,}$ $\mu_{dL,}$ μ_{VL} is obtained after 13 trials.

The least value of the MAE of the test data E_{ts} is 0.5188% as may be seen from Table 5.16. In addition, the comparison between the modeled and the experimental values of the breakdown voltage is provided in the same Table. Figure 5.8 shows the aggregated MFs plot for the test inputs.

Table 5.15: Mamdani Rule Base

IF Input parameters		THEN Output parameters
Thickness, t	Diameter of the void, d	Breakdown Voltage, V
L	L	H
L	M	H
L	H	H
M	L	M
M	M	H
M	H	M
H	L	H
H	M	L
H	H	L

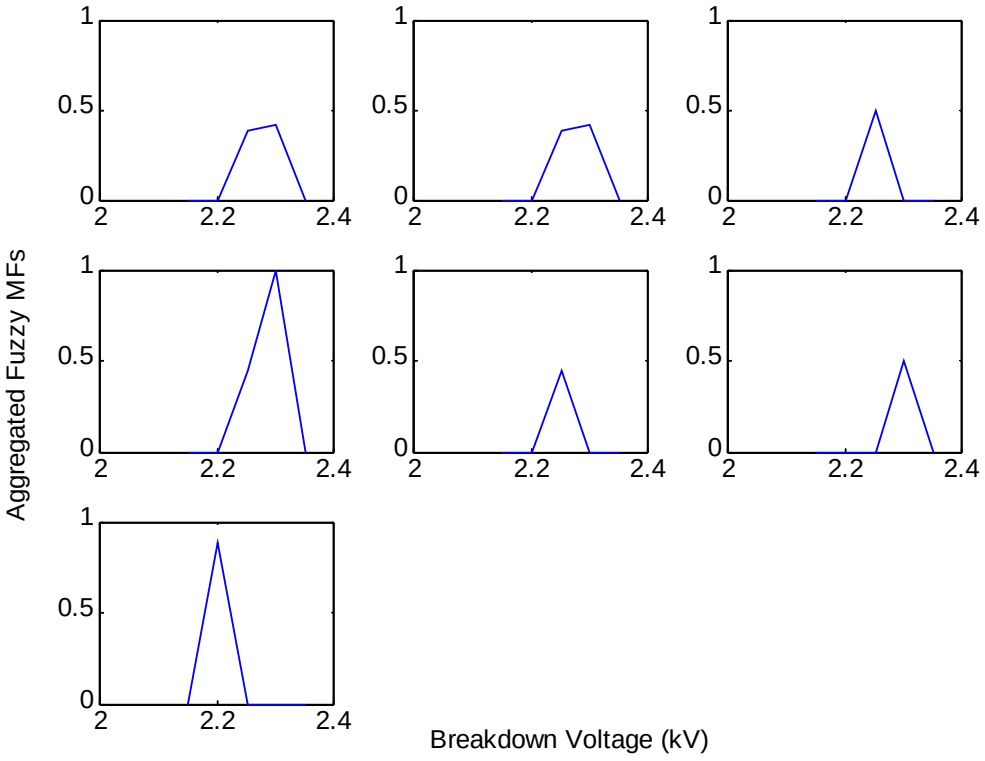

Figure 5.8: Aggregated Fuzzy MFs for the Test inputs with Triangular MF

Table 5.16: Comparison of the Experimental and Modeled values of the Breakdown voltage

t (mm)	d (mm)	Breakdown Voltage (Experimental) (kV)	Breakdown Voltage (Modeled) (kV)	MAE of the Test data E_{ts} (%)
0.125	1.5	2.2697	2.2759	0.5188
0.125	2	2.2807	2.2759	
0.18	1.5	2.2447	2.2500	
0.18	3	2.2909	2.2846	
0.18	5	2.2407	2.2500	
0.26	1.5	2.3170	2.3000	
0.26	4	2.2294	2.2000	

B. Trapezoidal MF

The procedure for this Case is identical to Case A. Hence, Table 5.4, Table5.14 and Table 5.15 are also used here. When the combinations of heights b and c of trapezoidal MF (as defined in equation (5.9)) for $\mu_{tL,}$ μ_{dL} & μ_{VL}) are varied 24 times, the least value of E_{ts} is obtained. The combination of b_{tL}= 0.06, c_{tL}= 0.11, b_{dL}=1.5, c_{dL}= 3.1, b_{VL}= 2.175, c_{VL}= 2.225 has given the least value of E_{ts} .

Along with these combination of the heights, the same test inputs as Case A is used for firing the rule base Table 5.15. As may be seen from Table 5.17, the least value of the MAE of the test data E_{ts} is 0.5788%. The seven modeled and the experimental values of the breakdown voltage validate the accuracy of the model for the prediction purpose.

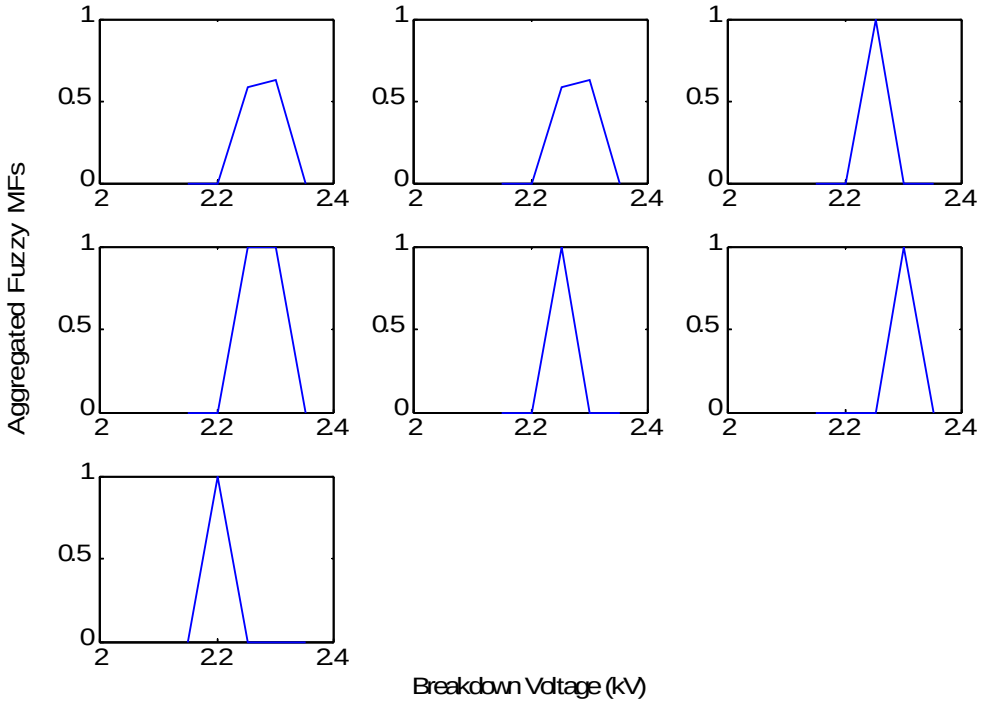

Figure 5.9: Aggregated Fuzzy MFs for the test inputs with Trapezoidal MF

Table 5.17: Comparison of the Experimental and Modeled values of the Breakdown voltage

t (mm)	d (mm)	Breakdown Voltage (Experimental) (kV)	Breakdown Voltage (Modeled) (kV)	MAE of the Test data E_{ts} (%)
0.125	1.5	2.2697	2.2759	0.5788
0.125	2	2.2807	2.2759	
0.18	1.5	2.2447	2.2500	
0.18	3	2.2909	2.2750	
0.18	5	2.2407	2.2500	
0.26	1.5	2.3170	2.3000	
0.26	4	2.2294	2.2000	

- **Model 4**

The model 4 has the same number of input parameters as model 2. Hence, Table 5.9 can also be used in this model. The relationship between the linguistic and the actual values of V is given in Table 5.18. Table 2.7 has been used to extract 20 input-output data patterns.

Table 5.18: Relationship between the Linguistic and the Actual values for V_{ac}

Linguistic Values	V_{ac} (kV)
Low	0.76-0.83
Medium	0.81-0.88
High	0.86-0.93

Results and Discussions

A. Triangular MF

The Table 5.19 for the rule base is formulated by referring to Table 5.9, Table 5.18 and using 13 out of the 20 input-output patterns. The number of rules R_1 is 18, which is the same as model 2.

The heights b_{tL}, b_{t1L}, b_{dL}, b_{VL} for μ_{tL}, μ_{t1L}, μ_{dL} & μ_{VL} have been varied. 21 combinations of these heights were explored and when b_{tL}= 0.03, b_{t1L}= 0.04, b_{dL}= 2.6 and b_{VL}= 0.8 , the E_{ts} turns out to be the least.

Table 5.19: Mamdani Rule Base

IF Input parameters			THEN Output parameters
Thickness of the material, t	Depth of void, t_1	Diameter of the void, d	Breakdown Voltage , V
L	L	L	L
M	L	L	L
H	L	L	H
L	L	M	H
M	L	M	M
H	L	M	L
L	L	H	H
M	L	H	H
H	L	H	M
L	H	L	M
M	H	L	H
H	H	L	L
L	H	M	H
M	H	M	L
H	H	M	M
L	H	H	H
M	H	H	H
H	H	H	L

When the rule base get fired by the test inputs, aggregated MF as per equation (5.7) results. The aggregated Fuzzy MFs on defuzzification results in the modeled value of the breakdown voltage. Table 5.20 shows the comparison of the experimental and modeled values

of the breakdown voltage. Figure 5.10 shows the aggregated MFs plot for the test inputs. The least value of the MAE of the test data E_{ts} is 2.3702%.

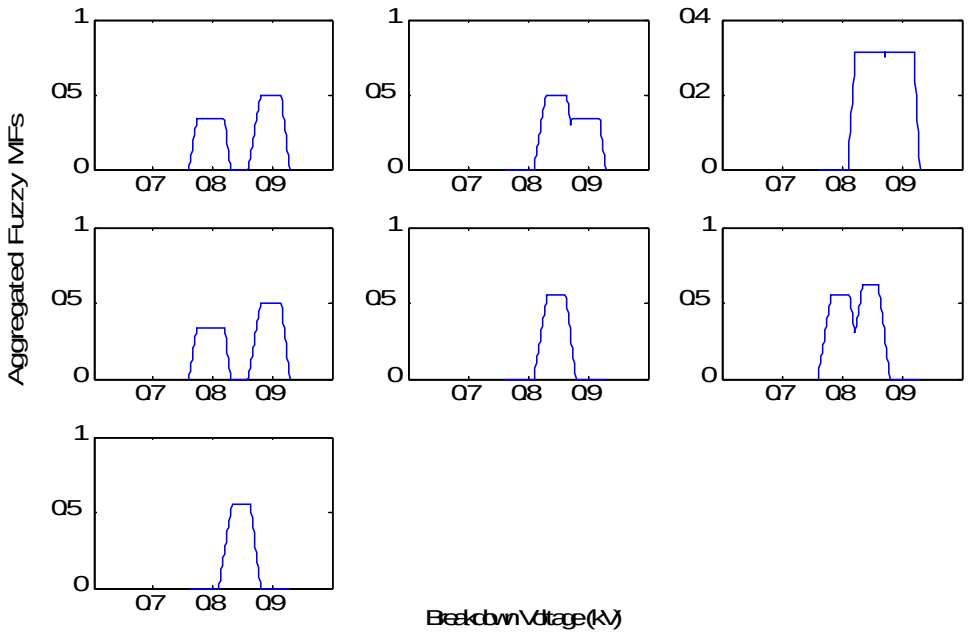

Figure 5.10: Aggregated Fuzzy MFs for the Test inputs with Triangular MF

Table 5.20: Comparison of the Experimental and Modeled values of the Breakdown voltage

t (mm)	t_1 (mm)	d (mm)	Breakdown Voltage (Experimental) (kV)	Breakdown Voltage (Modeled) (kV)	MAE of the Test data E_{ts} (%)
0.035	0.025	1.5	0.8758	0.8534	2.3712
0.035	0.125	2	0.8683	0.8670	
0.06	0.025	1.5	0.8479	0.8708	
0.06	0.125	3	0.9089	0.8534	
0.035	0.025	5	0.8388	0.8462	
0.06	0.125	1.5	0.8154	0.8222	
0.035	0.025	4	0.8758	0.8462	

A. Trapezoidal MF

The trapezoidal Case for model 4 also uses Table 5.9, Table 5.18 and Table 5.19. In order to obtain the least value of MAE of the test data E_{ts}, the heights b and c of the trapezoidal MF defined in equation (5.9) for the material thickness, void depth, void diameter and breakdown voltage are varied. 31 combinations of b_{tL}, b_{t1L}, b_{dL}, b_{VL}, c_{tL}, c_{t1L}, c_{dL}, c_{VL} have been tried. It is found that when b_{tL}= 0.025, b_{t1L}= 0.03, b_{dL}= 1.6, b_{VL}= 0.775, c_{tL}= 0.034, c_{t1L}= 0.05, c_{dL}= 3.1, c_{VL}= 0.815, the E_{ts} turns out to be the least at 2.2002%.

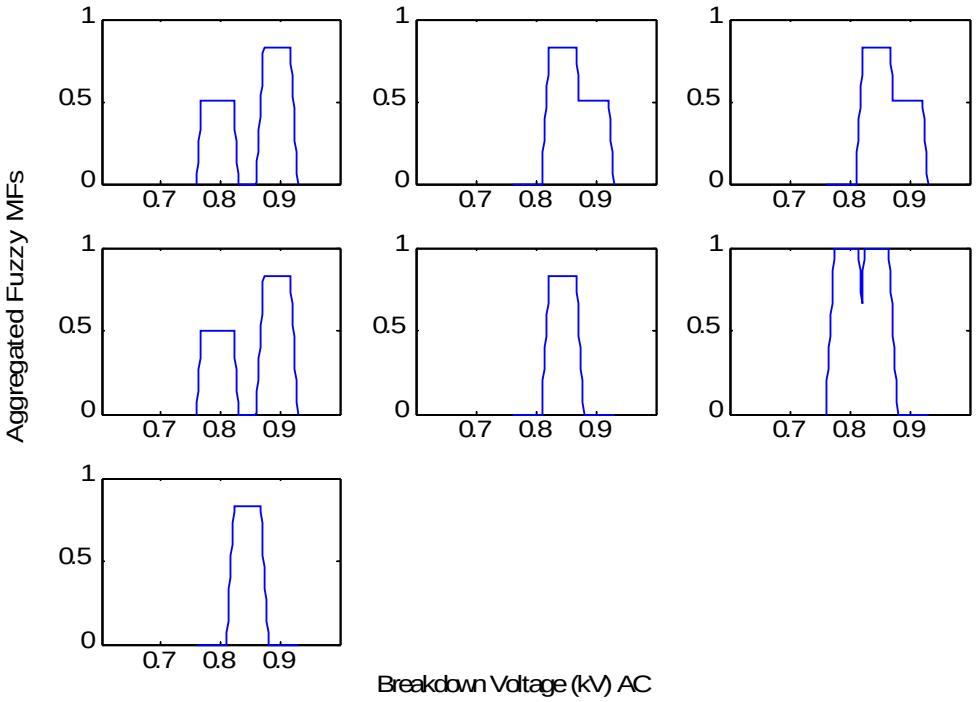

Figure 5.11: Aggregated Fuzzy MFs for the test inputs with Trapezoidal MF

When test inputs are provided to rule base Table 5.19, a comparison between the experimental and the modeled value of the breakdown voltage is obtained in Table 5.21. Figure 5.11 shows the aggregated MFs plot for the same test inputs as Case A.

Table 5.21: Comparison of the Experimental and Modeled values of the Breakdown voltage

t (mm)	t_1 (mm)	d (mm)	Breakdown Voltage (Expeimental) (kV)	Breakdown Voltage (Modeled) (kV)	MAE of the Test data E_{ts} (%)
0.035	0.025	1.5	0.8758	0.8555	2.2002
0.035	0.125	2	0.8683	0.8643	
0.06	0.025	1.5	0.8479	0.8643	
0.06	0.125	3	0.9089	0.8555	
0.035	0.025	5	0.8388	0.8450	
0.06	0.125	1.5	0.8154	0.8200	
0.035	0.025	4	0.8758	0.8450	

- **Model 5**

The model 5 based on the MFL scheme has used the same training and testing sets of input output patterns as that used for the model 6 based on the MFNN structure in Chapter 3 and model 6 based on the RBFN structure in Chapter 4.

Moreover, in this model, it was found that while framing two rules associated with two different insulating materials, the two rules had identical linguistic values for t, t_1, d and ϵ_r (antecedent part of the rule). As a result, it was extremely difficult to identify an insulating material based on the rules. This problem was solved by assigning a different identification number I to a particular material. Hence, in addition to the fuzzification of the thickness t, void depth t_1, void diameter d and relative permittivity ϵ_r , the identification number I was also fuzzified and incorporated in the antecedent part of the rules.

The relative permittivity is the additional input parameter with respect to model 3 and model 4. The 130 sets of input output patterns are taken from Table 2.7.

The relationship between the linguistic values and the actual values for t, t_1, d and ϵ_r are presented in Table 5.22 and the relationship between the linguistic and actual values of

identification number I are presented in Table 5.23. The Table 5.24 shows the relationship between the linguistic and actual values of the breakdown voltage V. The Table 5.22, Table 5.23 and Table 5.24 have been prepared from the input output patterns. Out of 130 input output patterns, 115 patterns and Tables 5.22, 5.23, 5.24 are used for creating 72 rules in the rule base Table 5.25.

Table 5.22: Relationship between the Linguistic and the Actual values for t, t_1, d and ϵ_r

Linguistic Values	t (mm)	t_1 (mm)	d (mm)	ϵ_r
Low	0.02-0.16	0-0.07	1.0-3.5	4.0-5.2
Medium	0.08-0.22	-	2.0-4.5	4.8-6.0
High	0.14-0.28	0.08-0.15	3.0-5.5	-

Table 5.23: Relationship between the Linguistic and the Actual values for Identification numbers for the materials

Linguistic Values	I
Low (White Minilex)	0.5-1.5
Medium Low (Leatherite Paper)	1.0-2.0
Medium (Glass Cloth)	1.5-2.5
Medium High (Manila Paper)	2.0-3.0
High (Lather Minilex)	2.5-3.5

The set of linguistic values assigned to t, t_1 and d are defined in equation (5.10) and (5.13) and the components of μ_t, μ_{t1} and μ_d are defined in equations (5.11), (5.12) and (5.14).

The Membership Functions (MFs) for ϵ_r and I are μ_e and μ_i respectively.

The set of linguistic values assigned to ϵ_r is given by

$Ł_3$= {Low (L),Medium (M)} (5.15)

The set of linguistic values assigned to I is given by

$Ł_4$= {Low (L), Medium Low (ML), Medium (M), Medium High (MH), High(H)}(5.16)

Also, μ_e and μ_i would be having components corresponding to each linguistic value as

$$\mu_e = \{\mu_{eL}, \mu_{eM}\} \quad (5.17)$$

$$\mu_i = \{\mu_{iL}, \mu_{iML}, \mu_{iM}, \mu_{iMH}, \mu_{iH}\} \quad (5.18)$$

Table 5.24: Relationship between the Linguistic and the Actual values for V_{ac}

Linguistic Values	V_{ac} (kV)
Low	0.5-1.2
Medium Low	0.9-1.6
Medium	1.3-2.0
Medium High	1.7-2.4
High	2.1-2.8

Results and Discussions

A. Triangular MF

Table 5.25 shows the rule base under AC condition for the five insulating materials. The value of number of rules in the rule base R_1 is 72 in this model and the procedure for arriving at this value is explained below:

The number of rules for White Minilex is calculated as follows.

Since the linguistic values associated with the thickness of the material, void depth, diameter of the void, relative permittivity and the identification number are 3, 2, 3, 1 and 1 respectively the number of rules is 3*2*3*1*1 =18. Similarly, for other materials such as Leatherite Paper, Glass Cloth, Manila Paper and Lather Minilex the number of rules can be calculated following the procedure of White Minilex. They are 18, 12, 6 and 18 respectively. Hence, the total number of rules is 18+18+12+6+18 = 72.

Table 5.25: Mamdani Rule Base

A. White Minilex

IF Input parameters						THEN Output parameters
SL No.	Identification number, I	Thickness of material, t	Thickness of void, t_1	Diameter of the void, d	Relative Permittivity ϵ_r	Breakdown Voltage, V
1.	L	L	L	L	L	MH
2.	L	L	L	M	L	H
3.	L	L	L	H	L	MH
4.	L	L	H	L	L	MH
5.	L	L	H	M	L	H
6.	L	L	H	H	L	MH
7.	L	M	L	M	L	MH
8.	L	L	H	L	L	H
9.	L	M	L	H	L	H
10.	L	M	H	L	L	H
11.	L	M	H	M	L	MH
12.	L	M	H	H	L	MH
13.	L	H	L	L	L	H
14.	L	H	L	M	L	MH
15.	L	H	L	H	L	H
16.	L	H	H	L	L	MH
17.	L	H	H	M	L	H
18.	L	H	H	H	L	MH

B. Leatherite Paper

IF Input parameters						THEN Output parameters
SL No.	Identification number, I	Thickness of material, t	Thickness of void, t_1	Diameter of the void, d	Relative Permittivity ϵ_r	Breakdown Voltage, V
19.	ML	L	L	L	L	M
20.	ML	L	L	M	L	M
21.	ML	L	L	H	L	ML
22.	ML	L	H	L	L	M
23.	ML	L	H	M	L	Ml
24.	ML	L	H	H	L	ML
25.	ML	M	L	M	L	MH
26.	ML	L	H	L	L	MH
27.	ML	M	L	H	L	M
28.	ML	M	H	L	L	MH
29.	ML	M	H	M	L	MH
30.	ML	M	H	H	L	M
31.	ML	H	L	L	L	H
32.	ML	H	L	M	L	H
33.	ML	H	L	H	L	H
34.	ML	H	H	L	L	MH
35.	ML	H	H	M	L	MH
36.	ML	H	H	H	L	MH

C. Glass Cloth

IF Input parameters						THEN Output parameters
SL No.	Identification number, I	Thickness of material, t	Thickness of void, t_1	Diameter of the void, d	Relative Permittivity ϵ_r	Breakdown Voltage, V
37.	M	M	L	L	L	H
38.	M	M	L	M	L	H
39.	M	M	L	H	L	H
40.	M	M	H	L	L	H
41.	M	M	H	M	L	H
42.	M	M	H	H	L	MH
43.	M	H	L	L	L	MH
44.	M	H	L	M	L	MH
45.	M	H	L	H	L	H
46.	M	H	H	L	L	H
47.	M	H	H	M	L	MH
48.	M	H	H	H	L	MH

D. Manila Paper

IF Input parameters						THEN Output parameters
SL No.	Identification number, I	Thickness of material, t	Thickness of void, t_1	Diameter of the void, d	Relative Permittivity ϵ_r	Breakdown Voltage, V
49.	MH	L	L	L	L	L
50.	MH	L	H	M	L	L
51.	MH	L	L	H	L	L
52.	MH	L	H	L	L	L
53.	MH	L	L	M	L	L
54.	MH	L	H	H	L	L

E. Lather Minilex

IF Input parameters						THEN Output parameters
SL No.	Identification number, I	Thickness of material, t	Thickness of void, t_1	Diameter of the void, d	Relative Permittivity ϵ_r	Breakdown Voltage, V
55.	H	L	L	L	M	MH
56.	H	L	L	M	M	MH
57.	H	L	L	H	M	H
58.	H	L	H	L	M	MH
59.	H	L	H	M	M	H
60.	H	L	H	H	M	MH
61.	H	M	L	M	M	H
62.	H	L	H	L	M	MH
63.	H	M	L	H	M	H
64.	H	M	H	L	M	H
65.	H	M	H	M	M	H
66.	H	M	H	H	M	MH
67.	H	H	L	L	M	MH
68.	H	H	L	M	M	MH
69.	H	H	L	H	M	H
70.	H	H	H	L	M	MH
71.	H	H	H	M	M	H
72.	H	H	H	H	M	MH

The rule base presented in Table 5.25 gets fired by the 15 test inputs. Moreover the combination of the six heights $b_{tL,}$ $b_{t1L,}$ $b_{dL,}$ $b_{eL,}$ $b_{IL,}$ b_{VL} have been varied 39 times in order to

obtain the minimum value of E_{ts}. The minimum value of E_{ts} occurs when b_{tL}=0.07, b_{t1L}=0.05, b_{dL}=2.0, b_{eL}=4.5 , b_{IL}=0.8 and b_{VL}=0.8 and this value is 2.8444%.

Table 5.26 shows the comparison of the experimental and modeled values of the breakdown voltage for all the five materials under AC conditions. Figure 5.12 shows the aggregated MFs plot for all the 15 test inputs with this value of E_{ts}.

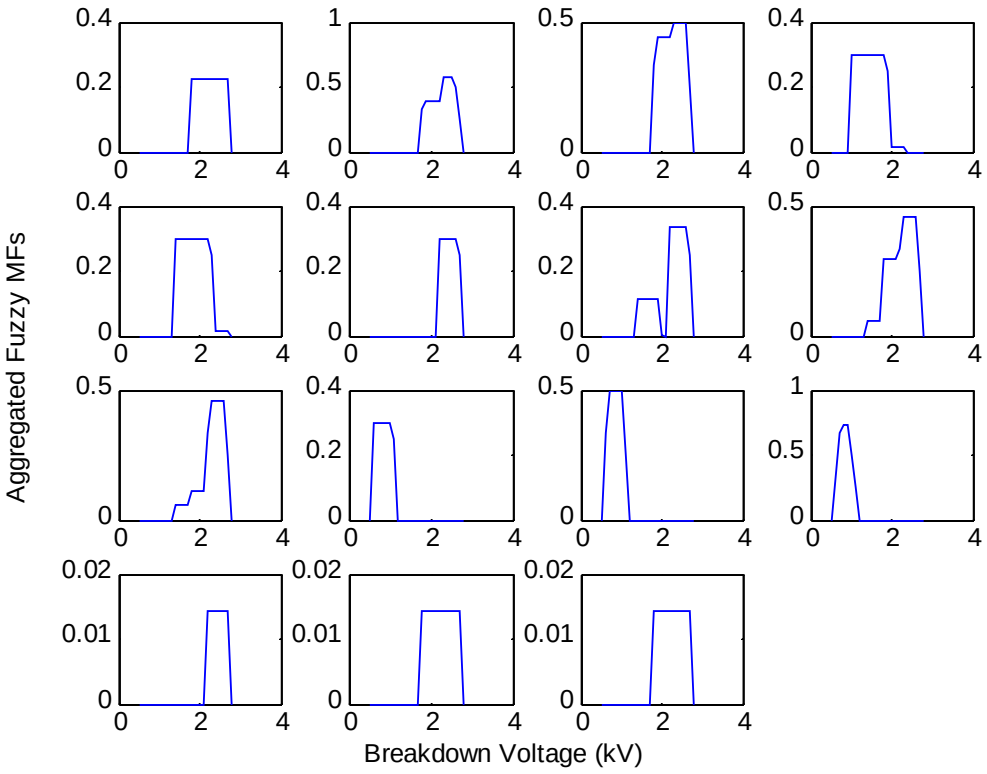

Figure 5.12: Aggregated Fuzzy MFs for the Test Inputs with Triangular MF

Table 5.26: Comparison of the Experimental and Modeled values of the Breakdown voltage

Insulating Material	t (mm)	t_1 (mm)	d (mm)	ϵ_r	Breakdown Voltage (Experimental) (kV)	Breakdown Voltage (Modeled) (kV)	MAE of the Test data E_{ts} (%)
White Minilex	0.26	0.025	3	4.40	2.2807	2.2500	2.8444
	0.125	0.125	2	4.40	2.2697	2.2692	
	0.18	0.025	1.5	4.40	2.2885	2.2516	
Leatherite Paper	0.13	0.125	5	4.21	1.3306	1.4558	
	0.175	0.125	4	4.21	1.8313	1.8558	
	0.235	0.025	2	4.21	2.2909	2.4429	
Glass Cloth	0.195	0.025	5	4.97	2.2294	2.2312	
	0.155	0.025	3	4.97	2.2447	2.2366	
	0.155	0.125	1.5	4.97	2.3088	2.3052	
Manila Paper	0.035	0.125	3	4.68	0.8154	0.8429	
	0.06	0.025	2	4.68	0.8388	0.8419	
	0.06	0.125	4	4.68	0.8758	0.8357	
Lather Minilex	0.245	0.025	5	5.74	2.2697	2.4500	
	0.185	0.125	1.5	5.74	2.3088	2.2500	
	0.125	0.025	2	5.74	2.3170	2.4500	

B. Trapezoidal MF

In this Case also, the Table 5.25 is fired by the same test inputs as Case A. 45 combinations of the 12 heights b_{tL}, c_{tL}, b_{t1L}, c_{t1L}, b_{dL}, c_{dL}, b_{eL}, c_{eL}, b_{IL}, c_{IL}, b_{VL} and c_{VL} have been tried. The E_{ts} turns out to be the least at 2.9741% when b_{tL}= 0.06, c_{tL}= 0.115, b_{t1L}= 0.03, c_{t1L}= 0.05, b_{dL}= 1.6, c_{dL}= 3.0, b_{eL}= 4.3, c_{eL}= 5.0, b_{IL}= 0.75, c_{IL}=1.2, b_{VL}= 0.65 and c_{VL}= 1.0. It may be recalled that b's and c's are the notations used in equation (5.9).

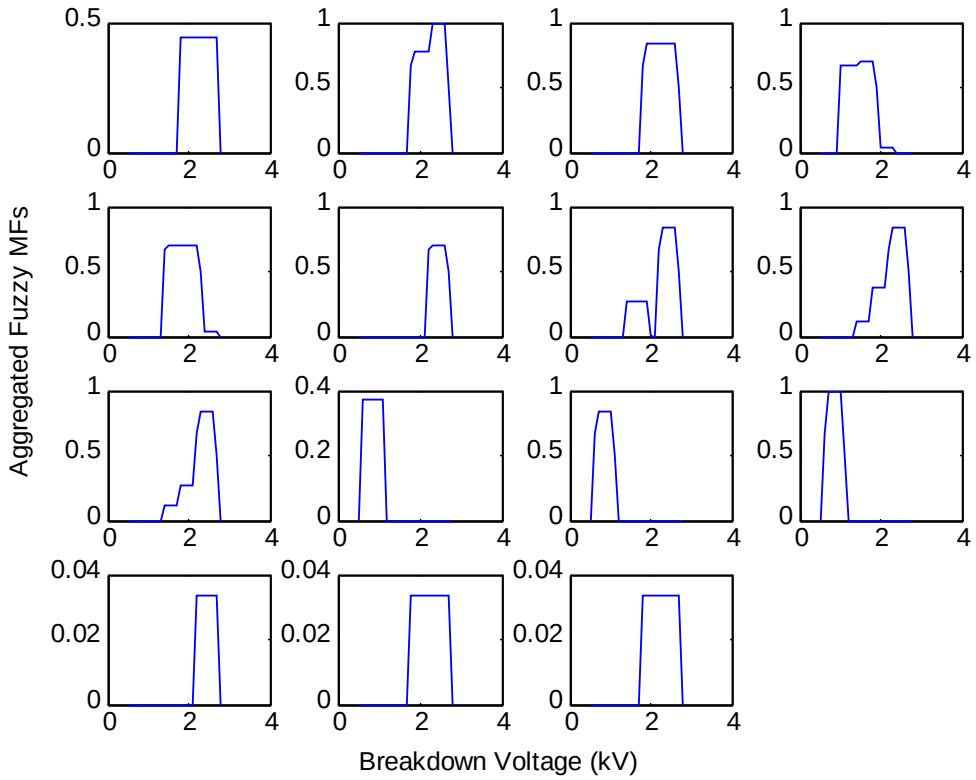

Figure 5.13: Aggregated Fuzzy MFs for the Test Inputs with Trapezoidal MF

Table 5.27 shows the comparison of the experimental and modeled values of the breakdown voltage. Figure 5.13 shows the aggregated MFs plot for the same 15 test inputs.

Table 5.27: Comparison of the Experimental and Modeled values of the Breakdown voltage

Insulating Material	t (mm)	t_1 (mm)	d (mm)	ϵ_r	Breakdown Voltage (Experimental) (kV)	Breakdown Voltage (Modeled) (kV)	MAE of the Test data E_{ts} (%)
White Minilex	0.26	0.025	3	4.40	2.2807	2.2500	
	0.125	0.125	2	4.40	2.2697	2.2624	
	0.18	0.025	1.5	4.40	2.2885	2.2404	
Leatherite Paper	0.13	0.125	5	4.21	1.3306	1.4567	
	0.175	0.125	4	4.21	1.8313	1.8527	
	0.235	0.025	2	4.21	2.2909	2.4395	
Glass Cloth	0.195	0.025	5	4.97	2.2294	2.2333	2.9741
	0.155	0.025	3	4.97	2.2447	2.2651	
	0.155	0.125	1.5	4.97	2.3088	2.2878	
Manila Paper	0.035	0.125	3	4.68	0.8154	0.8500	
	0.06	0.025	2	4.68	0.8388	0.8407	
	0.06	0.125	4	4.68	0.8758	0.8419	
Lather Minilex	0.245	0.025	5	5.74	2.2697	2.4500	
	0.185	0.125	1.5	5.74	2.3088	2.2500	
	0.125	0.025	2	5.74	2.3170	2.2500	

5.3.3 Prediction of the breakdown voltage due to PD in voids using CIGRE Method II Electrode System under AC conditions

- **Model 6**

The models 1, 2 ,3, 4, 5 proposed so far for the prediction of breakdown voltage had utilized the experimental generated data using Cylinder-Plane Electrode System, which is discussed in details in Chapter 2. In this model, prediction of breakdown voltage is proposed with the help of experimentally generated data using CIGRE Method II Electrode System reported in [75]. The thickness of the Leatherite paper used is 0.18 mm, 0.23 mm and 0.3 mm. The void depth had three values, 0.0625mm, 0.125 mm and 0.25 mm, while the void diameter has three values, namely 1mm, 2 mm and 5 mm. Hence, the proposed model [115] is carried out with the help of 27 sets of experimental input-output patterns generated for the Leatherite Paper insulation. The equations (5.5) to (5.9) have been used in arriving at the results of this model discussed below.

The procedure used for finding the relationship between the actual and the linguistic values of t, t_1, d and V and formation of Tables 5.28 and 5.29 has been discussed for all the five models in Section 5.3.1 and 5.3.2.

Table 5.28: Relationship between the Linguistic and the Actual values for t, t_1 and d

Linguistic Values	t (mm)	t_1 (mm)	d (mm)
Low	0.13-0.23	0.00-0.125	0.0-3.0
Medium	0.20-0.30	0.05-0.212	1.5-4.5
High	0.28-0.35	0.173-0.298	3.0-6.0

Table 5.29: Relationship between the Linguistic and the Actual values for V_{ac}

Linguistic Values	V_{ac} (kV)
Low(L)	3.25-3.50
Medium Low(ML)	3.35-3.65
Medium(M)	3.55-3.80
Medium High(MH)	3.70-3.95
High(H)	3.85-4.30

Results and Discussions

A. Triangular MF

Out of the 27 sets of input output patterns, the rule base Table 5.30 is created using 21 sets of input output patterns, Table 5.28 and Table 5.29. Since the linguistic values of t, t_1 and d are 3 each, the rule base Table has 27 rules.

Table 5.30: Mamdani Rule Base

IF Input parameters				THEN Output parameters
SL No.	Thickness of the material, t	Depth of the void, t_1	Diameter of the void, d	Breakdown Voltage , V
1.	L	L	L	H
2.	L	L	M	M
3.	L	L	H	M
4.	L	M	L	MH
5.	L	M	M	M
6.	L	M	H	ML
7.	L	H	L	MH
8.	L	H	M	ML
9.	L	H	H	L
10.	M	L	L	H
11.	M	L	M	H
12.	M	L	H	MH
13.	M	M	L	H
14.	M	M	M	MH
15.	M	M	H	M
16.	M	H	L	MH
17.	M	H	M	MH
18.	M	H	H	M
19.	H	L	L	H
20.	H	L	M	H
21.	H	L	H	MH
22.	H	M	L	H
23.	H	M	M	MH
24.	H	M	H	M
25.	H	H	L	MH
26.	H	H	M	M
27.	H	H	H	H

The rule base has been tested with 6 sets of input output patterns for the triangular MF for t, t_1, d and V defined in equation (5.8) . We find that when b_{tL}= 0.18, b_{t1L}= 0.063, b_{dL}= 1.5 and b_{VL}= 3.37, the E_{ts} value is 1.4%.

Table 5.31 shows the comparison of the experimental and modeled values of the breakdown voltage for Leatherite Paper under AC conditions.

Table 5.31: Comparison of the Experimental and Modeled values of the Breakdown voltage

Insulating Material	t (mm)	t_1 (mm)	d (mm)	Breakdown Voltage (Experimental) (kV)	Breakdown Voltage (Modeled) (kV)	MAE of the test data E_{ts} (%)
Leatherite Paper	0.3	0.0625	2	4.0	4.0458	1.4
	0.3	0.25	1	3.9	3.8236	
	0.23	0.125	5	3.6	3.6736	
	0.23	0.25	2	3.8	3.8237	
	0.18	0.0625	5	3.7	3.6737	
	0.18	0.125	1	3.9	3.8237	

B. Trapezoidal MF

This Case has all things in common with Case A, except that the triangular MF is replaced by trapezoidal MF. This implies that Table 5.28, 5.29 and 5.30 can be utilized here for calculation of E_{ts}.

It is revealed that when b_{tL}= 0.16, c_{tL}= 0.20, b_{t1L}= 0.04, c_{t1L}= 0.08, b_{dL}= 0.8, c_{dL}= 1.8, b_{VL}= 3.30 and c_{VL}= 3.44, the value of E_{ts} is 1.324%.

Table 5.32 shows the comparison of the experimental and modeled values of the breakdown voltage for Leatherite Paper under AC conditions.

Table 5.32: Comparison of the Experimental and Modeled values of the Breakdown voltage

Insulating Material	t (mm)	t_1 (mm)	d (mm)	Breakdown Voltage (Experimental) (kV)	Breakdown Voltage (Modeled) (kV)	MAE of the test data E_{ts} (%)
Leatherite Paper	0.3	0.0625	2	4.0	4.0465	1.324
	0.3	0.25	1	3.9	3.8435	
	0.23	0.125	5	3.6	3.6638	
	0.23	0.25	2	3.8	3.8444	
	0.18	0.0625	5	3.7	3.6642	
	0.18	0.125	1	3.9	3.8410	

5.4 Conclusion

In this Chapter, five models have been proposed to predict the breakdown voltage due to PD in voids by use of the experimental data generated with Cylinder-Plane Electrode System under DC and AC conditions using FL and Mamdani inferencing. A model using the data obtained from the literature, which are essentially generated by CIGRE Method II Electrode System, has also been proposed to predict the breakdown voltage. The shape of the MFs for the input and output parameters are assumed to be triangular and trapezoidal in all cases. The MAE of the test data obtained in all the models clearly indicates that the MFL inferencing is reasonably effective in predicting the breakdown voltage of solid insulating materials.

Chapter 6

BREAKDOWN VOLTAGE MODELING USING ADAPTIVE SUGENO FUZZY LOGIC TECHNIQUE

6.1 Introduction

In Chapter 5, the modeling of the breakdown voltage of solid insulating materials was attempted with the help of Mamdani Fuzzy Logic (MFL) using the experimental data. The Fuzzy Logic (FL) model based on the Sugeno-inferencing and with adaptive features may also be used for the same modeling purpose. In this Chapter, the same experimental data as Chapter 5 has been utilized and the modeling of the breakdown voltage is proposed based on the Adaptive Sugeno Fuzzy Logic (ASFL) inferencing. First, an outline of the ASFL inferencing has been presented. Then, a detailed discussion on the proposed models are made.

6.2 Adaptive Sugeno Fuzzy Logic (ASFL) Inferencing

As discussed in Chapter 5, the Fuzzy Logic (FL) models such as the Mamdani Fuzzy Logic (MFL) and the Sugeno Fuzzy Logic (SFL) incorporate human knowledge and perform inferencing and decision making.

Although the MFL and the SFL have a structured knowledge representation in the form of fuzzy if then rules, it lacks the adaptability to deal with changing environments. But in recent times the researchers primarily working in the control systems faced certain interesting issues such as designing a controller for a nonlinear system [116] or designing a controller for a static compensator[117] in a multi machine power system. These issues were expertly handled by designing a robust adaptive Sugeno controller. These controllers had the essential attributes of an intelligent controller having the learning capability and could reduce computation via reducing the size of the rule base. Since these controllers are intelligent in nature they can be termed as Adaptive Sugeno Fuzzy Logic (ASFL) controllers. Hence there is a scope for creating a ASFL scheme depending on a specific application. In this section first of all the general theory of the ASFL scheme for the purpose of prediction is discussed before applying it to certain models in the next section.

- **General Theory of the Inferencing**

In this inferencing, first of all the relationship between the linguistic values and the actual values of the input parameters is created with the help of Table 5.1 shown in Chapter 5. The set of linguistic values assigned to input 1, input 2 and up to input N_i is given by equation (5.1).

The Membership Functions (MFs) for input 1, input 2 and input N_i are μ_{i1}, μ_{i2} and μ_{iNi} respectively. In addition, μ_{i1}, μ_{i2} and μ_{iNi} would be having components corresponding to each linguistic value as given by equations (5.2) to (5.4).

The procedure for finding the number of rules is model specific. Let the total number of rules be R_1 .

A typical fuzzy rule in a Sugeno fuzzy model has the form

If input1 is L and input 2 is M ……..and input N_i is L

then Output = *f* (input1, input2,……..input N_i) (6.1)

Where L, M and L are the linguistic values of the input 1, input 2 and input N_i respectively and the output is a crisp function in the consequent. Usually *f* (input1, input2,……..input N_i) is a polynomial in the input variables input 1, input 2 ,…. input N_i . When *f* (input1, input2,….input N_i) is a 1^{st} order polynomial, the resulting fuzzy inference system is called a 1^{st} order Sugeno Fuzzy model (SFL) [81]. Since each rule has a crisp output, the output is obtained by a weighted average, thus avoiding the time-consuming process of defuzzification required in a Mamdani Fuzzy Logic (MFL). The SFL model can be made adaptive by updating the coefficients of the polynomial in the consequent part of the rules. The updating is possible by using the LMS algorithm. Hence, the SFL model would be now termed as Adaptive Sugeno Fuzzy Logic (ASFL) model. A typical 1^{st} Order Sugeno Rule base is illustrated in Table 6.1 using equation (6.1). Out of the total number of input-output data sets, the N_p sets are used for training or updating the coefficients of R_1 1^{st} order polynomials in the rule base and the N_s sets are used for testing the trained rule base. The details of the updating with ASFL model are explained with the help of equations below the Table 6.1.

Table 6.1 : 1st Order Sugeno Rule Base

IF Input parameters				THEN Output parameters
SL No.	Input 1	Input 2	Input N_i	Output Function V_{r1m}
1.	L	M	L	$a_{1m}*i_1+b_{1m}*i_2$ ..+$s_{1m}*i_{Ni}$
2.	ML	L	MH	$a_{2m}*i_1+b_{2m}*i_2$ ..+$s_{2m}*i_{Ni}$
3.	H	L	L	$a_{3m}*i_1+b_{3m}*i_2$ ..+$s_{3m}*i_{Ni}$
⋮				⋮
⋮				⋮
⋮				⋮
R_1-1	MH	ML	L	$a_{(R1-1)m}*i_1+b_{(R1-1)m}*i_2$ ..+$s_{(R1-1)m}*i_{Ni}$
R_1	M	L	H	$a_{R1m}*i_1+b_{R1m}*i_2$ ..+$s_{R1m}*i_{Ni}$

A typical firing strength of a rule is as follows:

w_{r1z} = minimum $_{Ni}(\mu_{i1z}$, μ_{i2z} ,..... $\mu_{iNiz})$ (6.2)

Where z = 1 to N_p for training patterns

and z= 1 to N_s for testing patterns

r_1 varies from 1 to R_1.

The sum of the firing strengths of rules is given by

$$w_z = \sum_{r1=1}^{R1} w_{r1z} \quad (6.3)$$

Similarly, a typical 1st order polynomial for the r_1^{th} rule at the m^{th} iteration is given by

$V_{r1m} = a_{r1m}*i_{1z} + b_{r1m}*i_{2z}$ ..... $s_{r1m}*i_{Niz}$ (6.4)

Where i_{1z}, i_{2z} and i_{Niz} are the inputs corresponding to the z^{th} pattern and a_{r1m}, b_{r1m} and s_{r1m} are the coefficients at the m^{th} iteration for the r_1^{th} rule . These are updated using the LMS algorithm.

The modeled value of the breakdown voltage for the z^{th} pattern at the m^{th} iteration is given by

$V_{2z}(m)= V_{1zm} / w_z$ (6.5)

Where $$V_{1zm} = \sum_{r1=1}^{R1} w_{r1z} * V_{r1m} \quad (6.6)$$

The error for the z^{th} pattern at the m^{th} iteration is given by

$e_{1zm} = V_{1z} - V_{2z}(m)$ (6.7)

Where V_{1z} is the experimental value of the breakdown voltage for the z^{th} pattern .

The Mean Square Error for the training pattern at the m^{th} iteration is calculated using equation (3.9) and (6.7).

The coefficient a_{r1m} in equation (6.4) is updated as follows

$$a_{r1m+1} = a_{r1m} + (\eta_3) * e_{1zm} * i_{1z} \quad (6.8)$$

η_3 is the learning rate for the LMS algorithm. All the other coefficients in equation (6.4) are similarly updated till a reasonably low value of Mean Square Error for the training patterns is obtained. After the training is over , the N_s sets of input output patterns are used for testing purpose. The Mean Absolute Error (MAE) for the test data E_{ts} is calculated in equation (3.10) based on the least value of Mean Square Error in equation (3.9).

6.3 Modeling of Breakdown Voltage using ASFL

In this section, the breakdown voltage is predicted as a function of different void parameters, namely, void diameter and void depth and insulation sheet thickness both at DC and AC conditions using the ASFL. The rule base is provided with both input data and desired response; and the first order polynomials are updated using the LMS algorithm. The training phase is completed when polynomials are updated after a series of iterations. In each iteration, the output is compared with the desired response and a match is obtained.

In order to predict the breakdown voltage under DC / AC conditions a software program has been developed in MATLAB 7.1 for the equations (6.1) to (6.8). Also the program has calculated the Mean Square Error E_{tr} of the training patterns and the Mean Absolute Error E_{ts} of the test patterns. The program is suitably modified for different models based on the input – output parameters. The flowchart for the ASFL inferencing is shown in Figure 6.1.

The shape of the MFs considered for the input parameters are assumed to be triangular and trapezoidal for all the discussed models in the Chapter. The reason for selecting an uniform shape of the MF has been discussed in Chapter 5. The triangular and the trapezoidal MF are defined by equations (5.8) and (5.9) respectively.

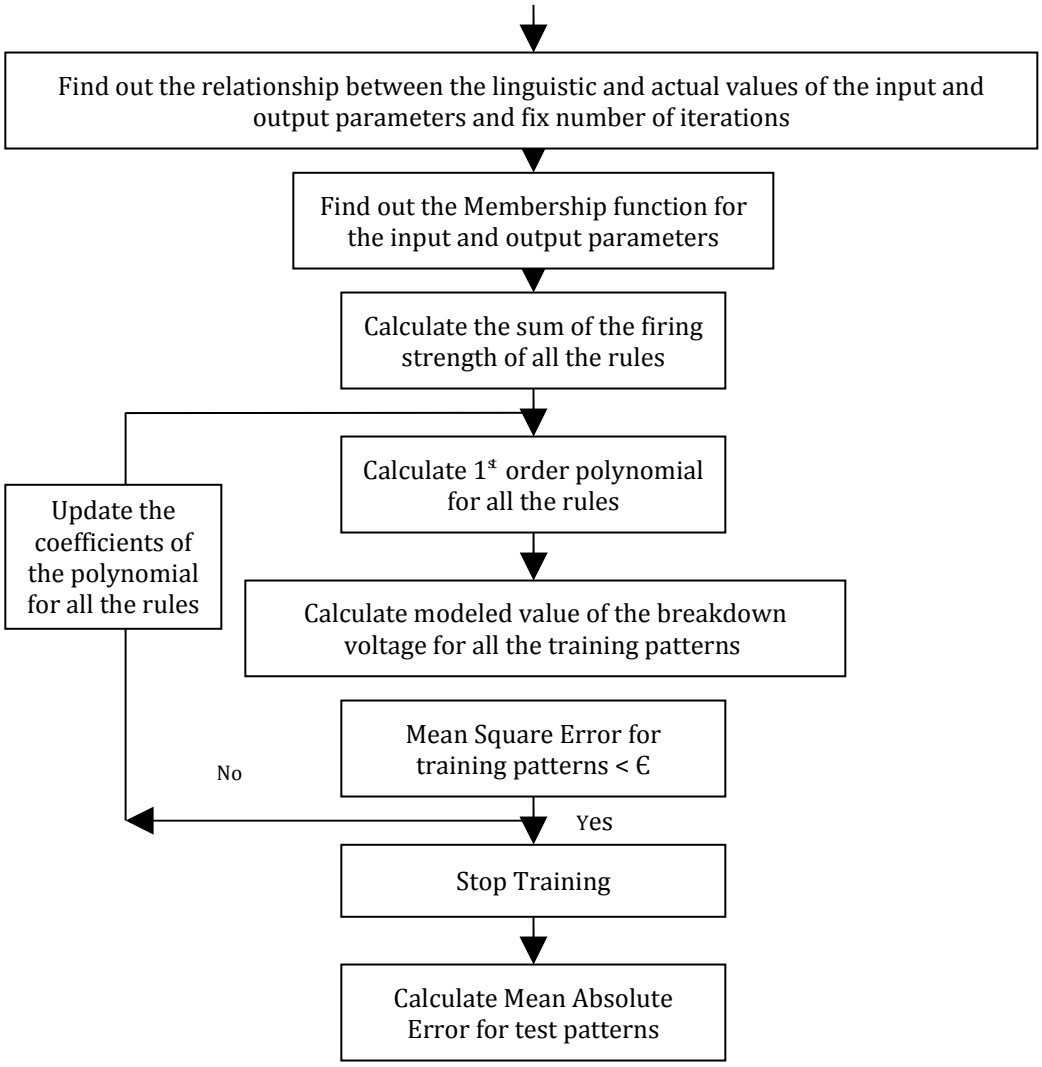

Figure 6.1 : Flow Chart for the ASFL

6.3.1 Prediction of the breakdown voltage due to PD in voids under DC conditions

The two proposed models discussed in this subsection is the same as discussed in subsection 5.3.1.

- **Model 1**

The model 1 based on the ASFL inferencing has the same number of input and output parameters as model 1 based on the MFL inferencing. Hence the number of input output patterns is 15. These 15 sets of input output patterns of White Minilex paper are taken from Table 2.6.

Out of the 15 sets of input-output patterns, $N_p = 8$ sets of input-output patterns are utilized to update the 1^{st} order polynomials in the rule base and the remaining $N_s = 7$ sets are used for the testing the rule base.

Table 5.3 showing the relationship between the linguistic and the actual values of t and d can also be used in this model.

The set of linguistic values assigned to t and d are given by equation (5.10).

The Membership Functions (MFs) for t and d are μ_t and μ_d respectively.

μ_t and μ_d would be having components corresponding to each linguistic value given by equations (5.11) and (5.12)

Results and Discussions

A Triangular MF

The value of η_3 defined in equation (6.8) plays a very important role in order to obtain the least value of Mean Square Error E_{tr} for the training patterns. Initially η_3 value is chosen to be 1.80 as the values of E_{tr} corresponding to η_3 less than 1.80 are in the order of 10^{-4} and above. Then it is varied till the value becomes 1.92. It is found that the least value of E_{tr} is $1.1703*10^{-6}$ when $\eta_3 = 1.90$ after 100 iterations. The Table 6.2 shows the rule base for model 8 and this is very similar to Table 6.1. Since the linguistic values associated with t and d are both 3, there are 9 rules in the rule base. Hence, in this model the value of R_1 is 9. The $\mu_{tL,}$ and μ_{dL} defined in equations (5.11) and (5.12) have assumed the triangular shape defined in equation (5.8). It may be noted that b_{tL} (corresponding to μ_{tL}) is 0.08 and b_{dL}(corresponding to μ_{dL}) is 2.3 and these represent the heights of μ_{tL} and μ_{dL} respectively. The variation of E_{tr} of the training data with the number of iterations with η_3= 1.90 is shown in Figure 6.2. Table 6.3 shows the variation of E_{tr} as a function of η_3.

Table 6.2: 1st Order Sugeno Rule Base

IF Input parameters			THEN Output parameters
SL No	Thickness of material, t	Diameter of the void, d	Breakdown voltage function Vr_1
1.	L	L	180.9367*t +179.4988*d
2.	L	M	180.2502*t +180.0084*d
3.	L	H	180.8191*t +180.5607*d
4.	M	L	179.9494*t +179.0735*d
5.	M	M	180.6793*t +179.9259*d
6.	M	H	180.2673*t +180.6204*d
7.	H	L	180.8801*t +180.5129*d
8.	H	M	179.3890*t +179.8479*d
9.	H	H	0.9571*t -0.9561*d

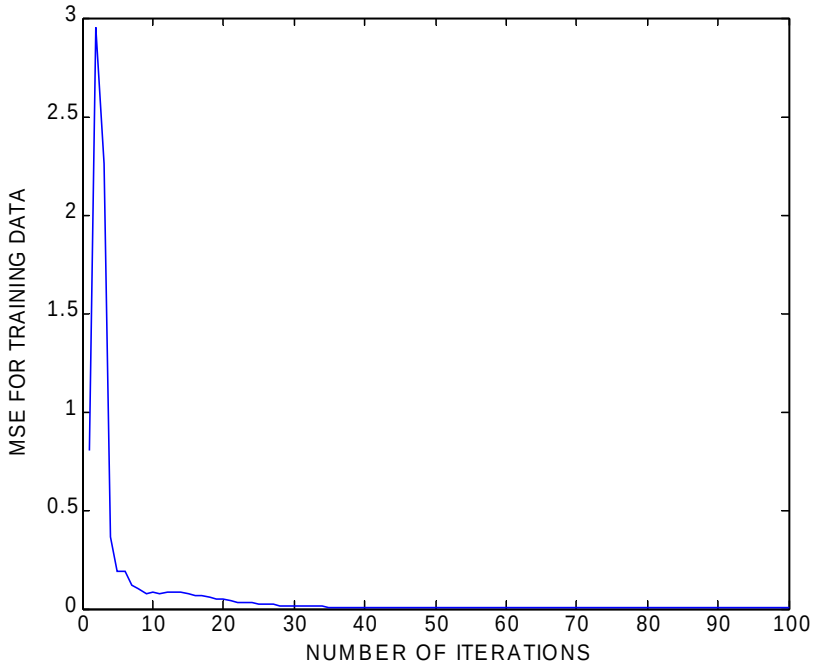

Figure 6.2: Variation of E_{tr} of the training data as a function of Number of iterations

Table 6.3: Variation of E_{tr} with η_3
(Number of iterations = 100)

η_3	E_{tr}
1.80	$2.8382*10^{-6}$
1.85	$1.7862*10^{-6}$
1.89	$1.2223*10^{-6}$
1.90	$\mathbf{1.1703*10^{-6}}$
1.91	$1.6053*10^{-6}$
1.92	$6.1249*10^{-6}$

The modeled value of the breakdown voltage is obtained from equations (6.4) and equations (6.6) by substituting R_1 as 9. Table 6.4 shows a comparison of the experimental and the modeled values of the breakdown voltage when 7 sets of input-output patterns are presented to the trained ASFL model as test data with triangular MF for the input parameters. The value of MAE of the test data E_{ts} is found to be 0.0583% .

Table 6.4 : Comparison of the experimental and modeled breakdown voltage

t (mm)	d (mm)	Breakdown Voltage (Experimental) (kV)	Breakdown Voltage (Modeled) (kV)	MAE of the Test data E_{ts} (%)
0.125	1.5	23.85	23.9453	0.0583
0.125	2	24.32	24.3207	
0.18	1.5	24.70	24.7000	
0.18	3	24.77	24.7700	
0.26	5	25.66	25.6612	
0.26	1.5	25.42	25.4202	
0.125	4	24.09	24.0900	

B Trapezoidal MF

The procedure for varying η_3 is the same as discussed for the triangular MF. Initially η_3 is kept at 1.80 and then it is varied till the value becomes 1.91. It is found that the least value of E_{tr} is $1.4991*10^{-6}$ when η_3 =1.90 and the number of iterations is 100. The rule base Table 6.2 used for Case A can be used here. The $\mu_{tL,}$ and μ_{dL} defined in equations (5.11) and (5.12) have assumed the trapezoidal shape defined in equation (5.9). It may be noted that b_{tL}& c_{tL}(corresponding to μ_{tL})= 0.08& 0.12 and b_{dL}& c_{dL} (corresponding to μ_{dL})=2.4 & 2.8 and these represent the heights 1 and 2 of μ_{tL} and μ_{dL} respectively. The variation of E_{tr} of the training data with the number of iterations with η_3= 1.90 is shown in Figure 6.3. Table 6.5 shows the variation of E_{tr} as a function of η_3.

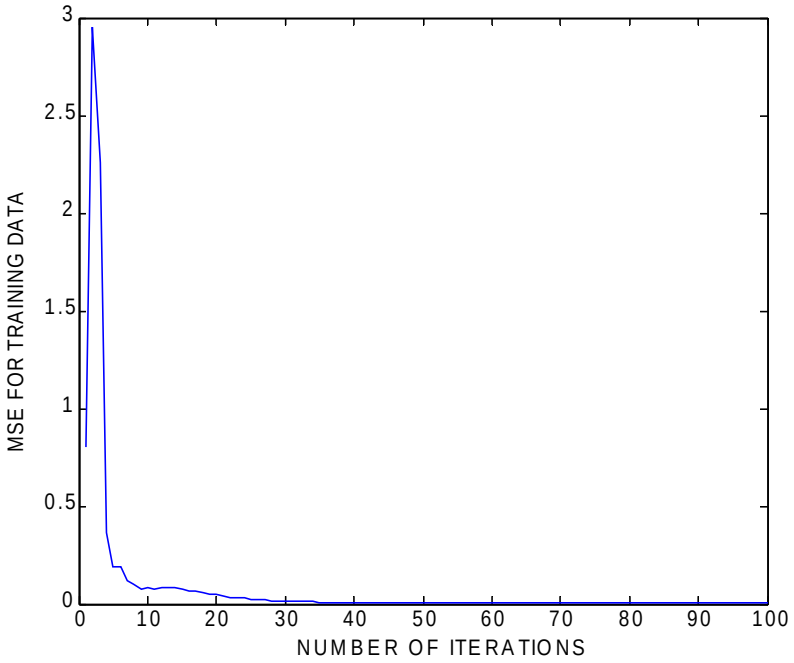

Figure 6.3: Variation of E_{tr} of the training data as a function of Number of iterations

Table 6.6 shows a comparison of the experimental and the modeled values of the breakdown voltage when 7 sets of input output patterns are presented to the trained ASFL model as test inputs with trapezoidal MF for the input parameters. The procedure for obtaining the modeled value of the breakdown voltage is identical to that for the triangular MF. The value of MAE of the test data E_{ts} is found to be 0.0591% with trapezoidal MF.

Table 6.5: Variation of E_{tr} with η_3
(Number of iterations=100)

η_3	E_{tr}
1.80	$3.3218*10^{-6}$
1.85	$2.2121*10^{-6}$
1.90	$\mathbf{1.4991*10^{-6}}$
1.91	$1.9129*10^{-6}$

Table 6.6 : Comparison of the experimental and modeled breakdown voltage

t (mm)	d (mm)	Breakdown Voltage (Experimental) (kV)	Breakdown Voltage (Modeled) (kV)	MAE of the Test data E_{ts} (%)
0.125	1.5	23.85	23.9453	0.0591
0.125	2	24.32	24.3221	
0.18	1.5	24.70	24.7000	
0.18	3	24.77	24.7700	
0.26	5	25.66	25.6612	
0.26	1.5	25.42	25.4202	
0.125	4	24.09	24.0900	

- **Model 2**

This model[118] has used the same 20 input output patterns of Manila paper as that used for model 2 based on the MFL inferencing. These 20 sets of input output patterns are taken from Table 2.6. Out of the 20 sets of input-output patterns, 13 sets of input-output patterns are utilized to update the 1st Order polynomials in the rule base and the remaining 7 sets are used for testing the rule base.

Table 5.9 showing the relationship between the linguistic and the actual values of t, t_1 and d can also be used here.

The set of linguistic values assigned to t_1 are given by equations (5.13) and (5.14).

Whereas the set of linguistic values to t and d are given in equation (5.10).

While the Membership Functions (MFs) for t and d are μ_t and μ_d defined in equation (5.11) and (5.12).

Results and Discussions

A Triangular MF

The b_{tL}(corresponding to μ_{tL}) is 0.03, b_{t1L}(corresponding to μ_{t1L}) is 0.04 and b_{dL}(corresponding to μ_{dL}) is 2.4. These represent the heights of μ_{tL}, μ_{t1L} and μ_{dL}. Table 6.7 represents the rule base of model 9 with 18 rules. This Table is very similar to Table 6.1. The starting value of η_3 is 1.7 as the values of E_{tr} for η_3 less than 1.7 are in the order of 10^{-3} and above. After carrying out the training for 100 iterations, it is revealed that the least value of E_{tr} is $3.3683*10^{-4}$ at η_3 =1.86. Figure 6.4 shows the variation of E_{tr} with the number of iterations. Table 6.8 shows the variation of E_{tr} with η_3. Table 6.9 has compared the modeled and the experimental value of the breakdown voltage. The modeled value of the breakdown voltage is obtained from equation (6.4) to (6.6) by substituting R_1=18. The value of MAE of the test data E_{ts} is found to be 0.0165 %.

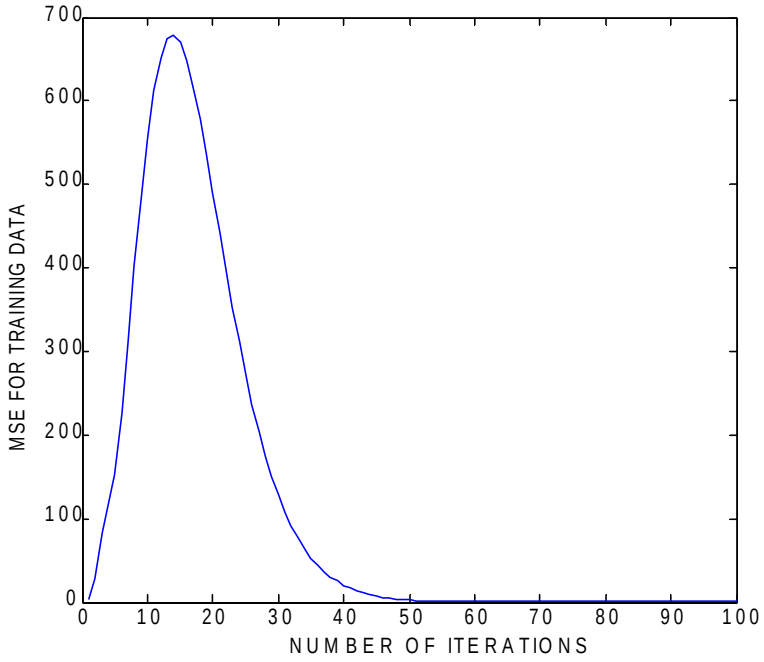

Figure 6.4: Variation of E_{tr} of the training data as a function of Number of iterations

Table 6.7: 1st Order Sugeno Rule Base

IF Input parameters				THEN Output parameters
SL No.	Thickness of material, t	Thickness of void, t_1	Diameter of the void, d	Breakdown voltage function Vr_1
1.	L	L	L	$104.0255*t+176.2484*t_1+141.6426*d$
2.	M	L	L	$103.0972*t+177.5687*t_1+141.9531*d$
3.	H	L	L	$103.0382*t+175.8231*t_1+142.0717*d$
4.	L	L	M	$103.0146*t+177.0170*t_1+142.0128*d$
5.	M	L	M	$103.9688*t+177.2625*t_1+140.7814*d$
6.	H	L	M	$102.9366*t+177.6570*t_1+142.2627*d$
7.	L	L	H	$102.9458*t+177.5734*t_1+140.5447*d$
8.	M	L	H	$102.8310*t+177.4124*t_1+140.4486*d$
9.	H	L	H	$102.4030*t+176.1916*t_1+140.8263*d$
10.	L	H	L	$102.3328*t+176.3305*t_1+140.8265*d$
11.	M	H	L	$102.1558*t+177.2797*t_1+141.3191*d$
12.	H	H	L	$103.9889*t+176.7181*t_1+141.2662*d$
13.	L	H	M	$6.4461*t-3.7602*t_1-0.0000*d$
14.	M	H	M	$0.0000*t-0.0001*t_1+0.0002*d$
15.	H	H	M	$1.0632*t+0.9601*t_1+1.6245*d$
16.	L	H	H	$-0.0002*t+0.0003*t_1-0.0004*d$
17.	M	H	H	$0.0007*t-0.0008*t_1+0.0005*d$
18.	H	H	H	$0.8119*t+0.3726*t_1+0.6970*d$

Table 6.8: Variation of E_{tr} with η_3

(Number of iterations=100)

η_3	E_{tr}
1.70	0.0010
1.75	$7.5766*10^{-4}$
1.80	$5.2978*10^{-4}$
1.85	$3.5560*10^{-4}$
1.86	$\mathbf{3.3683*10^{-4}}$
1.87	$4.0870*10^{-4}$

Table 6.9: Comparison of the experimental and modeled values of the breakdown voltage

t (mm)	t_1(mm)	d (mm)	Breakdown Voltage (Experimental) (kV)	Breakdown Voltage (Modeled)(kV)	MAE of the Test data E_{ts} (%)
0.035	0.025	1.5	1.6389	1.6389	0.0165
0.035	0.125	2	1.6821	1.6821	
0.06	0.025	1.5	1.6682	1.6689	
0.06	0.125	3	1.6454	1.6454	
0.035	0.025	5	1.6323	1.6329	
0.06	0.125	1.5	1.7002	1.7002	
0.035	0.025	4	1.6563	1.6569	

B Trapezoidal MF

In this Case Table 5.9 and Table 6.7 are also used. The learning rate η_3 varies between 1.75 and 1.87 and the values of E_{tr} for these values of η_3 are $6.7849*10^{-4}$ and $3.5766*10^{-4}$ respectively. The number of iterations is the same as Case A that is 100. The E_{tr} touches it's nadir at η_3 =1.86 and this value is $2.8267*10^{-4}$. The Table 6.10 depicts the variation of E_{tr} with η_3. The heights b_{tL} and height c_{tL} of μ_{tL} are 0.023 and 0.032. Similarly for μ_{t1L} they are 0.03 and 0.05 and for μ_{dL} they are 1.7 and 3.1. Figure 6.5 shows the variation of E_{tr} with the number of iterations.

Table 6.10 :Variation of E_{tr} with η_3
(Number of iterations=100)

η_3	E_{tr}
1.75	$6.7849*10^{-4}$
1.80	$4.5847*10^{-4}$
1.85	$2.9834*10^{-4}$
1.86	**$2.8267*10^{-4}$**
1.87	$3.5766*10^{-4}$

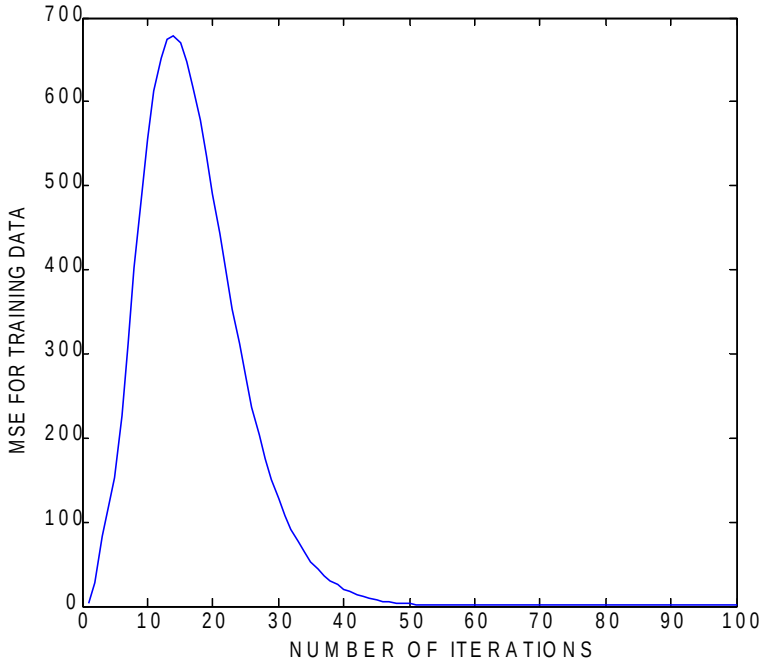

Figure 6.5: Variation of E_{tr} of the training data as a function of Number of iterations

When the same test data as in Case A is presented to the trained ASFL, a comparison between the experimental and the modeled value of the breakdown voltage is presented in Table 6.11. The MAE of the test data E_{ts} also indicated in the same Table is 0.0161%.

Table 6.11 : Comparison of the experimental and modeled values of the breakdown voltage

t (mm)	t_1(mm)	d (mm)	Breakdown Voltage (Experimental) (kV)	Breakdown Voltage (Modeled)(kV)	MAE of the Test data E_{ts} (%)
0.035	0.025	1.5	1.6389	1.6389	0.0161
0.035	0.125	2	1.6821	1.6821	
0.06	0.025	1.5	1.6682	1.6689	
0.06	0.125	3	1.6454	1.6454	
0.035	0.025	5	1.6323	1.6329	
0.06	0.125	1.5	1.7002	1.7002	
0.035	0.025	4	1.6563	1.6569	

6.3.2 Prediction of the breakdown voltage due to PD in voids under AC conditions

The three proposed models in this subsection are identical to the models discussed in subsection 5.3.2.

- **Model 3**

This model has predicted the breakdown voltage of White Minilex quiet similar to model 1, but under AC conditions. The number of input parameters, the number of input output data sets are the same as model 1. But since AC conditions is being discussed, the input output patterns are taken from the Table 2.7. The Table 5.3 can be used for here and the rule base can be created with 9 rules. Also the equations (5.10) to (5.12) are used in this model.

Results and Discussions

A Triangular MF

The Table 6.12 shows the rule base for model 3 with 9 rules. In order to obtain the lowest value of E_{tr}, the η_3 is varied between 1.75 and 1.92. The η_3 =1.75 has been decided to be the initial value in this case as the values of E_{tr} are greater than $4.7654*10^{-6}$ for η_3 less than 1.75. The E_{tr} decreases with the increase in η_3 till η_3= 1.90. Then it again increases from there onwards. Hence the lowest value of E_{tr} is $1.3334*10^{-6}$ occurring for η_3= 1.90. The Table 6.13 shows the variation of E_{tr} with η_3. Figure 6.6 shows the variation of E_{tr} with the number of iterations. It may be noted that b_{tL}(corresponding to μ_{tL}) is 0.09 and b_{dL}(corresponding to μ_{dL})=2.0.

Table 6.12 : 1st Order Sugeno Rule Base

IF Input parameters			THEN Output parameters
SL No	Thickness of material, t	Diameter of the void, d	Breakdown voltage function Vr_1
1.	L	L	186.6866*t +185.2486*d
2.	L	M	186.0*t +185.7583*d
3.	L	H	186.5689*t +186.3105*d
4.	M	L	185.6992*t +184.8283*d
5.	M	M	186.4291*t +185.6757*d
6.	M	H	186.0172*t +186.3702*d
7.	H	L	186.6299*t +186.2677*d
8.	H	M	185.1388*t +185.5977*d
9.	H	H	0.9877*t -0.9863*d

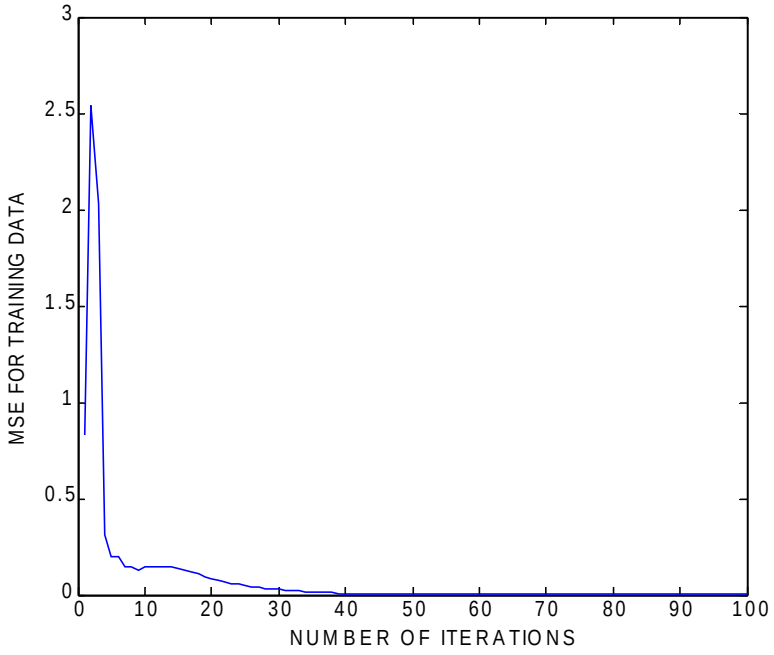

Figure 6.6: Variation of E_{tr} of the training data as a function of Number of iterations

Table 6.13 :Variation of E_{tr} vs. η_3

(Number of iterations=100)

η_3	E_{tr}
1.75	$4.7654*10^{-6}$
1.80	$3.0757*10^{-6}$
1.85	$1.9389*10^{-6}$
1.86	$1.7642*10^{-6}$
1.87	$1.6044*10^{-6}$
1.89	$1.3401*10^{-6}$
1.90	$\mathbf{1.3334*10^{-6}}$
1.91	$2.2355*10^{-6}$
1.92	$1.0818*10^{-5}$

The MAE of the test data E_{ts} is 0.0590% and it is based on the least value of E_{tr} after 100 iterations. This can be seen from Table 6.14. Also the comparison between the modeled and the experimental values of the breakdown voltage is provided in the same Table.

Table 6.14 : Comparison of the experimental and modeled values of the breakdown voltage

t (mm)	d (mm)	Breakdown Voltage (Experimental) (kV)	Breakdown Voltage (Modeled)(kV)	MAE of the Test data E_{ts} (%)
0.125	1.5	2.2697	2.2789	0.0590
0.125	2	2.2807	2.2808	
0.18	1.5	2.2447	2.2447	
0.18	3	2.2909	2.2909	
0.18	5	2.2447	2.2448	
0.26	1.5	2.3170	2.3170	
0.26	4	2.2294	2.2294	

B Trapezoidal MF

In this Case Table 5.4 and the Table 6.12 are also used. The Table 6.15 provides the values of E_{tr} for different values of η_3 at 100 iterations. The values of η_3 from 0 to less than 1.85 are not considered as the values of E_{tr} in this range are greater than $2.4360*10^{-6}$. Hence η_3 is varied from 1.85 till the lowest value of E_{tr} is reached. From the same Table it can be seen that lowest value of E_{tr} occurs at η_3=1.90. The heights of the trapezoidal shape of μ_{tL} are 0.08 and 0.12 and the heights of μ_{dL} are 2.4 and 2.8 . Figure 6.7 shows the variation of E_{tr} with the number of iterations.

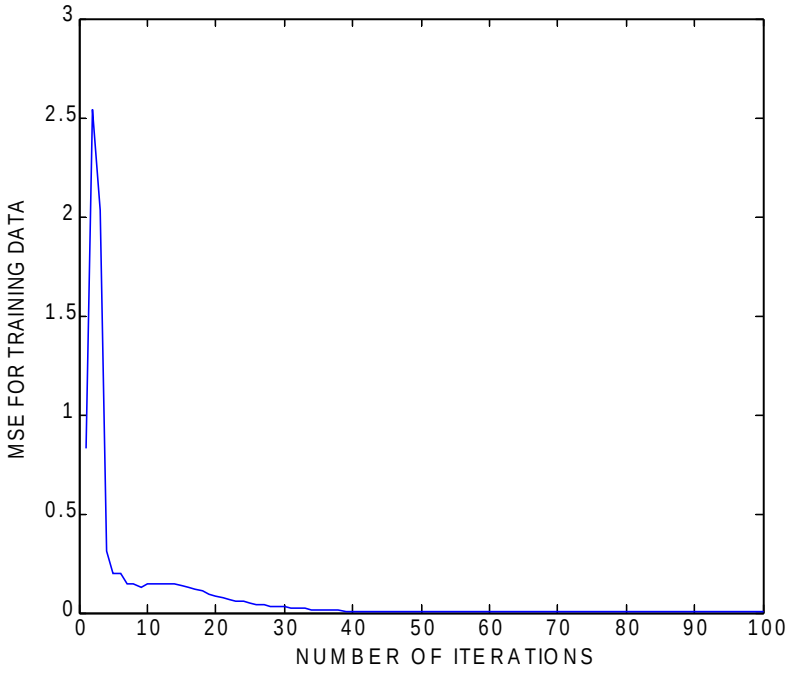

Figure 6.7: Variation of E_{tr} of the training data as a function of Number of iterations

Table 6.15 : Variation of E_{tr} with η_3

(Number of iterations=100)

η_3	E_{tr}
1.85	$2.4360*10^{-6}$
1.88	$1.8848*10^{-6}$
1.90	$\mathbf{1.7070*10^{-6}}$
1.91	$2.5831*10^{-6}$
1.92	$3.0083*10^{-5}$

When the same test data as Case A is provided to the trained ASFL , the MAE of the test data E_{ts} is 0.0597% as can be seen from Table 6.16. The seven modeled and the experimental values of the breakdown voltage validates the accuracy of the model for prediction purpose.

Table 6.16 : Comparison of the experimental and modeled values of the breakdown voltage

t (mm)	d (mm)	Breakdown Voltage (Experimental) (kV)	Breakdown Voltage (Modeled)(kV)	MAE of the Test data E_{ts} (%)
0.125	1.5	2.2697	2.2789	0.0597
0.125	2	2.2807	2.2809	
0.18	1.5	2.2447	2.2447	
0.18	3	2.2909	2.2909	
0.18	5	2.2447	2.2448	
0.26	1.5	2.3170	2.3170	
0.26	4	2.2294	2.2294	

- **Model 4**

The breakdown voltage of Manila paper has been predicted under AC conditions with the same number of input parameters and the same number of input output sets as model 2. But the input output parameters are now taken from Table 2.7.

Results and Discussions

A Triangular MF

With triangular MF for the input parameters the heights of μ_{tL}, μ_{t1L} and μ_{dL} are 0.03, 0.04 and 2.4 respectively. The Table 5.9 can be used here as the number of input parameters is the same as model 2. The Table 6.17 shows the rule base with 18 rules for this model. The training of the rule base has been carried with 13 input output patterns and the E_{tr} has been studied as a function of η_3 in Table 6.18 and as a function of number of iterations in Figure 6.8. The

equations (5.10) to (5.14) are used for this model. The η_3 is varied between 1.70 and 1.87 and at 1.86 the lowest value of E_{tr} is obtained. For η_3 less than 1.70, the values of E_{tr} are greater than 0.0010.

Table 6.17 : 1st Order Sugeno Rule Base

IF Input parameters				THEN Output parameters
SL No.	Thickness of material, t	Thickness of void, t_1	Diameter of the void, d	Breakdown voltage function Vr_1
1.	L	L	L	$104.4035*t+176.8963*t_1+142.1609*d$
2.	M	L	L	$103.4752*t+178.2167*t_1+142.4714*d$
3.	H	L	L	$103.4161*t+176.4711*t_1+142.5901*d$
4.	L	L	M	$103.3926*t+177.6649*t_1+142.5311*d$
5.	M	L	M	$104.3468*t+177.9105*t_1+141.2998*d$
6.	H	L	M	$103.3146*t+178.3050*t_1+142.7811*d$
7.	L	L	H	$103.3237*t+178.2214*t_1+141.0630*d$
8.	M	L	H	$103.2089*t+178.0604*t_1+140.9670*d$
9.	H	L	H	$102.7810*t+176.8396*t_1+141.3447*d$
10.	L	H	L	$103.7108*t+176.9784*t_1+141.3449*d$
11.	M	H	L	$102.5337*t+177.9276*t_1+141.8374*d$
12.	H	H	L	$104.3668*t+177.3660*t_1+141.7845*d$
13.	L	H	M	$6.4696*t-3.7740*t_1-0.0000*d$
14.	M	H	M	$0.0000*t-0.0001*t_1+0.0002*d$
15.	H	H	M	$1.0632*t+0.9601*t_1+1.6245*d$
16.	L	H	H	$-0.0002*t+0.0003*t_1-0.0004*d$
17.	M	H	H	$0.0007*t-0.0008*t_1+0.0005*d$
18.	H	H	H	$0.8119*t+0.3726*t_1+0.6970*d$

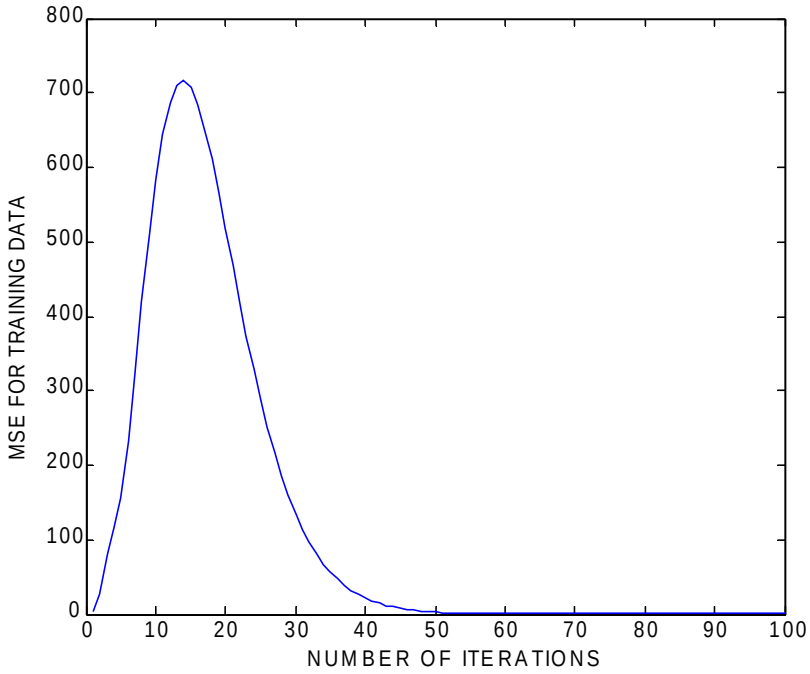

Figure 6.8: Variation of E_{tr} of the training data as a function of Number of iterations

Table 6.18 :Variation of E_{tr} with η_3

(Number of iterations=100)

η_3	E_{tr}
1.70	0.0010
1.75	$7.4161*10^{-4}$
1.80	$5.2016*10^{-4}$
1.85	$3.5090*10^{-4}$
1.86	**$3.3353*10^{-4}$**
1.87	$4.1223*10^{-4}$

After the training is over, the test data is provided to the trained ASFL. A very good comparison is drawn between the modeled and the experimental value of the breakdown voltage in Table 6.19. The MAE of the test data E_{ts} is 0.0166%.

Table 6.19: Comparison of the experimental and modeled values of the breakdown voltage

t (mm)	t_1(mm)	d (mm)	Breakdown Voltage (Experimental) (kV)	Breakdown Voltage (Modeled) (kV)	MAE of the Test data E_{ts} (%)
0.035	0.025	1.5	0.8758	0.8758	0.0166
0.035	0.125	2	0.8683	0.8683	
0.06	0.025	1.5	0.8479	0.8482	
0.06	0.125	3	0.9089	0.9089	
0.035	0.025	5	0.8388	0.8391	
0.06	0.125	1.5	0.8154	0.8154	
0.035	0.025	4	0.8758	0.8761	

B Trapezoidal MF

The η_3 is varied between 1.75 and 1.87 in this Case with the number of iterations fixed at 100. It is revealed that when η_3 is 1.86, the value of E_{tr} is the lowest. This value is $2.8258*10^{-4}$. The Tables 5.9 and 6.17 used in Case A are also used here. The heights of μ_{tL} are 0.023& 0.032 , the heights of μ_{dL} are 1.7 & 3.1, the heights of μ_{dL} are 0.03 & 0.05. The variation of E_{tr} of the training data with the number of iterations with η_3= 1.86 is shown in Figure 6.9. Table 6.20 shows the variation of E_{tr} as a function of η_3.

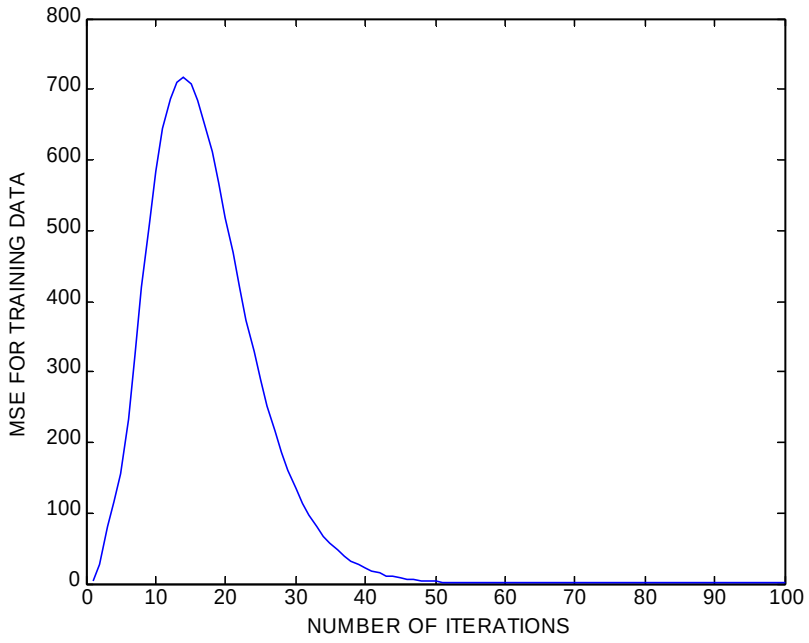

Figure 6.9: Variation of E_{tr} of the training data as a function of Number of iterations

Table 6.20 : Variation of E_{tr} with η_3

(Number of iterations=100)

η_3	E_{tr}
1.75	$6.6702*10^{-4}$
1.80	$4.5312*10^{-4}$
1.85	$2.9705*10^{-4}$
1.86	$\mathbf{2.8258*10^{-4}}$
1.87	$3.6419*10^{-4}$

The MAE of the test data Ets is 0.0163% and it occurs when the same 7 sets of input output data as A are provided to the trained ASFL. The performance with the triangular and trapezoidal MFs are very similar for model 11. Table 6.21 has shown the comparison between the breakdown voltage values along with the value of E_{ts}.

Table 6.21: Comparison of the experimental and modeled values of the breakdown voltage

t (mm)	t_1(mm)	d (mm)	Breakdown Voltage (Experimental) (kV)	Breakdown Voltage (Modeled) (kV)	MAE of the Test data E_{ts} (%)
0.035	0.025	1.5	0.8758	0.8758	0.0163
0.035	0.125	2	0.8683	0.8683	
0.06	0.025	1.5	0.8479	0.8483	
0.06	0.125	3	0.9089	0.9089	
0.035	0.025	5	0.8388	0.8391	
0.06	0.125	1.5	0.8154	0.8154	
0.035	0.025	4	0.8758	0.8761	

- **Model 5**

The model 5 based on the ASFL inferencing has used the same training and testing sets of input output patterns as that used for the model 5 in Chapter 5.

Proceeding in a similar way as model 5 in Chapter 5, the fuzzification of the thickness t, void depth t_1, void diameter d and relative permittivity ϵ_r took place. Also the identification number was also fuzzified and incorporated in the antecedent part of the rules. The reason for assigning a different identification number to a particular material has been explained in Chapter 5.

As with model 5 based on the MFL inferencing, the 130 sets of input output patterns are taken from Table 2.3 in addition to Table 2.7. Out of these 130 sets , N_p=115sets are utilized to update the 1^{st} Order polynomials in the rule base and the remaining N_s=15 sets are used for the testing the rule base.

The relationship between the linguistic values and the actual values for t, t_1 ,d and ϵ_r are presented in Table 5.22 and the relationship between the linguistic and actual values of identification number I are presented in Table 5.23.

The set of linguistic values assigned to t,t_1 and d are defined in equation (5.10) and (5.13) and the components of μ_t, μ_{t1} and μ_d are defined in equations (5.11), (5.12) and (5.14).

The Membership Functions (MFs) for ϵ_r and I are μ_e and μ_i respectively.

The set of linguistic values assigned to ϵ_r is given by equation (5.15).

The set of linguistic values assigned to I is given by equation (5.16).

Also, μ_e and μ_i would be having components corresponding to each linguistic value by equations (5.17) and (5.18) respectively.

Results and Discussions

A Triangular MF

The η_3 is varied between 1.80 and 1.91 in steps of 0.01. The values of η_3 less than 1.80 and greater than 1.91 are not considered, as the corresponding E_{tr} values are greater than 0.2181 and 0.1296 respectively. It is found that the least value of E_{tr} is 0.0021 when η_3 =1.85 and the number of iterations is 400. The value of R_1 is 72 in this model and the procedure for arriving at this value is explained in Chapter 5.

Table 6.22 shows the rule base for the model 6. Table 6.23 shows the variation of E_{tr} with η_3 . The variation of E_{tr} of the training data with the number of iterations with η_3= 1.85 is shown in Figure 6.10 . The heights of μ_{tL}, μ_{t1L}, μ_{dL}, μ_{eL} and μ_{iL} are 0.07, 0.05 ,2.0, 4.5 and 0.8 .

Table 6.22: 1st Order Sugeno Rule Base

A. White Minilex

IF Input parameters						THEN Output parameters
SL No.	Identification number , I	Thickness of material, t	Thickness of void, t_1	Diameter of the void, d	Relative Permittivity ϵ_r	Breakdown voltage function V_{r1}
1.	L	L	L	L	L	674.7*t +714.5*t_1 +715.3*d+715.1*ϵ_r+715.9*I
2.	L	L	L	M	L	674.4*t +715.1*t_1 +714.1*d+715.7*ϵ_r+715.0*I
3.	L	L	L	H	L	674.1*t +715.7*t_1 +715.9*d+715.6*ϵ_r+714.4*I
4.	L	L	H	L	L	673.6*t +715.9*t_1 +715.9*d+715.9*ϵ_r+715.9*I
5.	L	L	H	M	L	674.9*t +714.8*t_1 +715.7*d+715.1*ϵ_r+715.3*I
6.	L	L	H	H	L	674.2*t +715.5*t_1 +714.3*d+715.6*ϵ_r+715.5*I
7.	L	M	L	L	L	674.9*t +715.6*t_1 +715.0*d+715.9*ϵ_r+714.0*I
8.	L	M	L	M	L	673.7*t +715.8*t_1 +715.1*d+715.5*ϵ_r+715.5*I
9.	L	M	L	H	L	674.5*t +715.1*t_1 +715.5*d+715.9*ϵ_r+714.8*I
10.	L	M	H	L	L	673.9*t +715.5*t_1 +715.9*d+715.7*ϵ_r+715.5*I
11.	L	M	H	M	L	674.2*t +715.5*t_1 +715.7*d+715.2*ϵ_r+714.4*I
12.	L	M	H	H	L	673.2*t +715.8*t_1 +715.8*d+715.8*ϵ_r+715.3*I

.

IF Input parameters						THEN Output parameters
SL No.	Identification number , I	Thickness of material, t	Thickness of void, t_1	Diameter of the void, d	Relative Permittivity ϵ_r	Breakdown voltage function V_{r1}
13.	L	H	L	L	L	674.8*t +714.9*t_1 +715.7*d+715.4*ϵ_r+715.7*I
14.	L	H	L	M	L	674.2*t +715.8*t_1 +714.7*d+715.8*ϵ_r+715.2*I
15.	L	H	L	H	L	674.3*t +715.7*t_1 +715.8*d+715.2 *ϵ_r+714.8*I
16.	L	H	H	L	L	673.3*t +715.2*t_1 +715.0*d+715.5*ϵ_r+715.4*I
17.	L	H	H	M	L	674.5*t +714.0*t_1 +715.1*d+715.9*ϵ_r+715.5*I
18.	L	H	H	H	L	674.8*t +715.6*t_1 +714.6*d+715.8*ϵ_r+715.6*I

.

B. Leatherite Paper

IF Input parameters						THEN Output parameters
SL No.	Identification number , I	Thickness of material, t	Thickness of void, t_1	Diameter of the void, d	Relative Permittivity ϵ_r	Breakdown voltage function V_{r1}
19.	ML	L	L	L	L	674.1*t +714.1*t_1 +715.9*d+715.5*ϵ_r+7 15.7*I
20.	ML	L	L	M	L	674.2*t +715.7*t_1 +714.0*d+715.3*ϵ_r+7 15.1*I
21.	ML	L	L	H	L	674.1*t +715.7*t_1 +715.9*d+715.6*ϵ_r+7 14.4*I
22.	ML	L	H	L	L	673.6*t +715.9*t_1 +715.9*d+715.9*ϵ_r+7 15.9*I
23.	ML	L	H	M	L	674.9*t +714.8*t_1 +715.7*d+715.1*ϵ_r+7 15.3*I
24.	ML	L	H	H	L	674.2*t +715.5*t_1 +714.3*d+715.6*ϵ_r+7 15.5*I
25.	ML	M	L	L	L	674.9*t +715.6*t_1 +715.0*d+715.9*ϵ_r+7 14.0*I
26.	ML	M	L	M	L	673.7*t +715.8*t_1 +715.1*d+715.5*ϵ_r+7 15.5*I
27.	ML	M	L	H	L	674.5*t +715.1*t_1 +715.5*d+715.9*ϵ_r+7 14.8*I
28.	ML	M	H	L	L	673.9*t +715.5*t_1 +715.9*d+715.7*ϵ_r+7 15.5*I
29.	ML	M	H	M	L	674.3*t +715.6*t_1 +715.8*d+715.4*ϵ_r+7 14.4*I
30.	ML	M	H	H	L	673.3*t +715.3*t_1 +715.4*d+715.9*ϵ_r+7 15.3*I

.

IF Input parameters						THEN Output parameters
SL No.	Identification number , I	Thickness of material, t	Thickness of void, t_1	Diameter of the void, d	Relative Permittivity ϵ_r	Breakdown voltage function V_{r1}
31.	ML	H	L	L	L	674.8*t +714.9*t_1 +715.7*d+715.4*ϵ_r+715.7*I
32.	ML	H	L	M	L	674.2*t +715.8*t_1 +714.7*d+715.8*ϵ_r+715.2*I
33.	ML	H	L	H	L	674.3*t +715.7*t_1 +715.8*d+715.2 *ϵ_r+714.8*I
34.	ML	H	H	L	L	673.3*t +715.2*t_1 +715.0*d+715.5*ϵ_r+715.4*I
35.	ML	H	H	M	L	674.5*t +714.0*t_1 +715.1*d+715.9*ϵ_r+715.5*I
36.	ML	H	H	H	L	674.8*t +715.6*t_1 +714.6*d+715.8*ϵ_r+715.6*I

.

C. Glass Cloth

IF Input parameters						THEN Output parameters
SL No.	Identification number , I	Thickness of material, t	Thickness of void, t_1	Diameter of the void, d	Relative Permittivity ϵ_r	Breakdown voltage function V_{r1}
37.	M	M	L	L	L	674.1*t +714.1*t_1 +715.5*d+715.9*ϵ_r+715.6*I
38.	M	M	L	M	L	674.4*t +715.9*t_1 +714.6*d+715.7*ϵ_r+715.9*I
39.	M	M	L	H	L	674.3*t +715.6*t_1 +715.2*d+715.3*ϵ_r+714.4*I
40.	M	M	H	L	L	673.6*t +715.9*t_1 +715.9*d+715.9*ϵ_r+715.9*I
41.	M	M	H	M	L	674.9*t +714.8*t_1 +715.7*d+715.1*ϵ_r+715.3*I
42.	M	M	H	H	L	674.2*t +715.5*t_1 +714.3*d+715.6*ϵ_r+715.5*I
43.	M	H	L	L	L	674.9*t +715.6*t_1 +715.0*d+715.9*ϵ_r+714.0*I
44.	M	H	L	M	L	673.7*t +715.8*t_1 +715.1*d+715.5*ϵ_r+715.5*I
45.	M	H	L	H	L	674.5*t +715.1*t_1 +715.5*d+715.9*ϵ_r+714.8*I
46.	M	H	H	L	L	673.2*t +715.8*t_1 +715.5*d+715.4*ϵ_r+715.5*I
47.	M	H	H	M	L	674.7*t +715.8*t_1 +715.1*d+715.7*ϵ_r+714.0*I
48.	M	H	H	H	L	673.8*t +715.0*t_1 +715.9*d+715.9*ϵ_r+715.1*I

.

D. Manila Paper

IF Input parameters						THEN Output parameters
SL No.	Identification number , I	Thickness of material, t	Thickness of void, t_1	Diameter of the void, d	Relative Permittivity ϵ_r	Breakdown voltage function V_{r1}
49.	MH	L	L	L	L	674.5*t +714.2*t_1 +715.5*d+715.4*ϵ_r+715.0*I
50.	MH	L	H	M	L	674.9*t +715.9*t_1 +714.5*d+715.3*ϵ_r+715.6*I
51.	MH	L	L	H	L	674.3*t +715.7*t_1 +715.8*d+715.2 *ϵ_r+714.8*I
52.	MH	L	H	L	L	673.3*t +715.2*t_1 +715.0*d+715.5*ϵ_r+715.4*I
53.	MH	L	L	M	L	674.3*t +714.9*t_1 +715.2*d+715.4*ϵ_r+715.6*I
54.	MH	L	H	H	L	674.9*t +715.9*t_1 +714.7*d+715.4*ϵ_r+715.9*I

.

E. Lather Minilex

IF Input parameters						THEN Output parameters
SL No.	Identification number , I	Thickness of material, t	Thickness of void, t_1	Diameter of the void, d	Relative Permittivity ϵ_r	Breakdown voltage function V_{r1}
55.	H	L	L	L	M	674.1*t +714.5*t_1 +715.9*d+715.9*ϵ_r+715.4*I
56.	H	L	L	M	M	674.5*t +715.9*t_1 +714.9*d+715.3*ϵ_r+715.2*I
57.	H	L	L	H	M	674.3*t +715.1*t_1 +715.7*d+715.1*ϵ_r+714.5*I
58.	H	L	H	L	M	673.6*t +715.9*t_1 +715.9*d+715.9*ϵ_r+715.9*I
59.	H	L	H	M	M	674.9*t +714.8*t_1 +715.7*d+715.1*ϵ_r+715.3*I
60.	H	L	H	H	M	674.2*t +715.5*t_1 +714.3*d+715.6*ϵ_r+715.5*I
61.	H	M	L	L	M	674.9*t +715.6*t_1 +715.0*d+715.9*ϵ_r+714.0*I
62.	H	M	L	M	M	673.7*t +715.8*t_1 +715.1*d+715.5*ϵ_r+715.5*I
63.	H	M	L	H	M	674.5*t +715.1*t_1 +715.5*d+715.9*ϵ_r+714.8*I
64.	H	M	H	L	M	673.7*t +715.3*t_1 +715.6*d+715.9*ϵ_r+715.1*I
65.	H	M	H	M	M	674.3*t +715.9*t_1 +715.0*d+715.2*ϵ_r+714.4*I
66.	H	M	H	H	M	673.5*t +715.8*t_1 +715.7*d+715.5*ϵ_r+715.3*I

.

IF Input parameters						THEN Output parameters
SL No.	Identification number , I	Thickness of material, t	Thickness of void, t_1	Diameter of the void, d	Relative Permittivity ϵ_r	Breakdown voltage function V_{r1}
67.	H	H	L	L	M	$674.6*t +714.1*t_1 +715.9*d+715.2*\epsilon_r+715.3*I$
68.	H	H	L	M	M	$674.0*t +715.9*t_1 +714.6*d+715.7*\epsilon_r+715.7*I$
69.	H	H	L	H	M	$674.2*t +715.5*t_1 +715.6*d+715.3 *\epsilon_r+714.2*I$
70.	H	H	H	L	M	$673.3*t +715.2*t_1 +715.0*d+715.5*\epsilon_r+715.4*I$
71.	H	H	H	M	M	$674.5*t +714.0*t_1 +715.1*d+715.9*\epsilon_r+715.5*I$
72.	H	H	H	H	M	$674.0*t +715.9*t_1 +714.6*d+715.8*\epsilon_r+715.6*I$

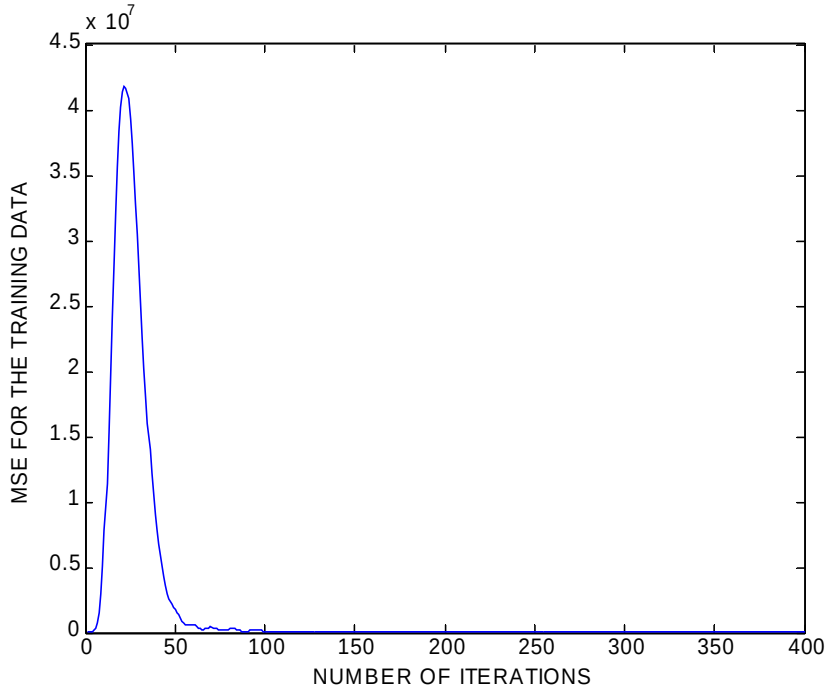

Figure 6.10: Variation of E_{tr} of the training data as a function of Number of iterations

Table 6.23: Variation of E_{tr} with η_3
(Number of iterations=400)

η_3	E_{tr}
1.80	0.2181
1.81	0.1399
1.82	0.0786
1.83	0.0356
1.84	0.0106
1.85	**0.0021**
1.86	0.0075
1.87	0.0238
1.88	0.0474
1.89	0.0750
1.90	0.1033
1.91	0.1296

The modeled value of the breakdown voltage as per the equations (6.5) to (6.7) with R_1= 72 and the experimental values of the breakdown voltage have been compared with the triangular shape of MF in Table 6.24. The MAE of the test data E_{ts} with 15 input output data patterns is 1.5650%.

Table 6.24 : Comparison of the experimental and modeled values of the breakdown voltage

Insulating Material	t (mm)	t_1 (mm)	d (mm)	ϵ_r	Breakdown Voltage (kV (Experimental)	Breakdown Voltage(kV) (Modeled)	MAE of the Test data E_{ts} (%)
White Minilex	0.26	0.025	3	4.40	2.2294	2.1853	
	0.125	0.125	2	4.40	2.2447	2.2412	
	0.18	0.025	1.5	4.40	2.2697	2.2653	
Leatherite Paper	0.13	0.125	5	4.21	1.2972	1.2912	
	0.175	0.125	4	4.21	1.8520	1.8470	
	0.235	0.025	2	4.21	2.2697	2.2595	
Glass Cloth	0.195	0.025	5	4.97	2.3088	2.2833	1.5650
	0.155	0.025	3	4.97	2.3088	2.2845	
	0.155	0.125	1.5	4.97	2.2294	2.1744	
Manila Paper	0.035	0.125	3	4.68	0.8388	0.8162	
	0.06	0.025	2	4.68	0.8154	0.8075	
	0.06	0.125	4	4.68	0.8479	0.8322	
Lather Minilex	0.245	0.025	5	5.74	2.2447	2.2036	
	0.185	0.125	1.5	5.74	2.2294	2.2278	
	0.125	0.025	2	5.74	2.2909	2.2479	

B Trapezoidal MF

In this Case the Table 5.22, 5.23 and 6.22 can also be used. The heights b and c of μ_{tL}, μ_{t1L}, μ_{dL}, μ_{eL} and μ_{iL} are (0.055, 0.125), (0.03, 0.05) , (1.7,3.1), (4.3,4.9) and (0.75,1.25) respectively .The η_3 is varied between 1.85 and 1.89 . The values of η_3 less than 1.85 and greater than 1.89 are not considered as the E_{tr} values corresponding to this range of η_3 are greater than 0.6651

and 0.1351 respectively. The lowest value of E_{tr} is 0.0989 occuring at η_3=1.88 and after 400 iterations. Table 6.25 shows the variation of E_{tr} with η_3. Figure 6.11 shows the variation of E_{tr} with the number of iterations.

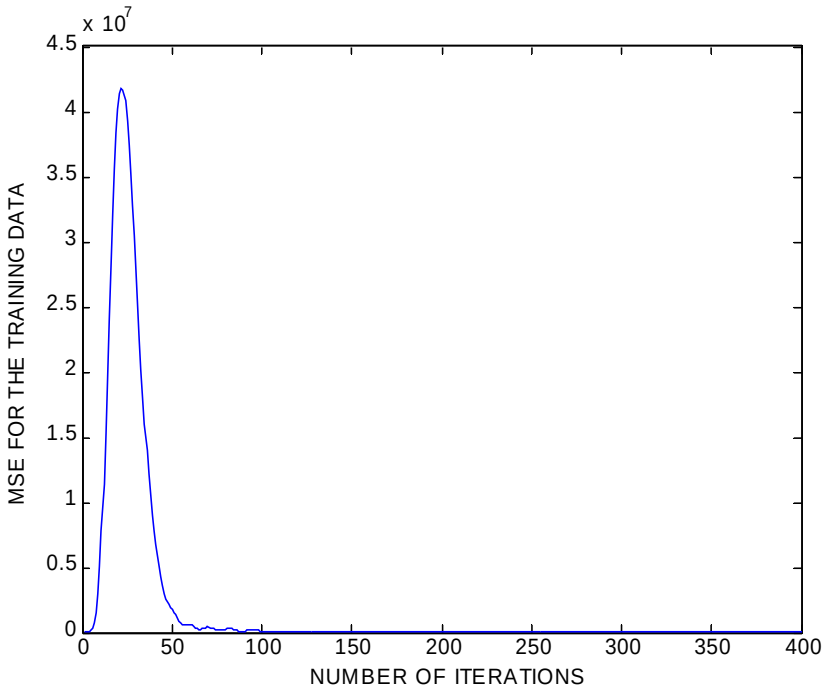

Figure 6.11: Variation of E_{tr} of the training data as a function of Number of iterations

Table 6.25: Variation of E_{tr} with η_3

(Number of iterations=400)

η_3	E_{tr}
1.85	0.6651
1.86	0.3492
1.87	0.1640
1.88	**0.0989**
1.89	0.1351

Table 6.26 shows that the MAE of the test data E_{ts} with trapezoidal MF for the input parameters and 15 input output data patterns is 2.9538%. The comparison between the breakdown voltage values is similar to Case A.

Table 6.26: Comparison of the experimental and modeled values of the breakdown voltage

Insulating Material	t (mm)	t_1 (mm)	d (mm)	ϵ_r	Breakdown Voltage (kV) (Experimental)	Breakdown Voltage(kV) (Modeled)	MAE of the Test data E_{ts} (%)
White Minilex	0.26	0.025	3	4.40	2.2294	2.1752	2.9538
	0.125	0.125	2	4.40	2.2447	2.2312	
	0.18	0.025	1.5	4.40	2.2697	2.2453	
Leatherite Paper	0.13	0.125	5	4.21	1.2972	1.2712	
	0.175	0.125	4	4.21	1.8520	1.8270	
	0.235	0.025	2	4.21	2.2697	2.2247	
Glass Cloth	0.195	0.025	5	4.97	2.3088	2.2433	
	0.155	0.025	3	4.97	2.3088	2.2345	
	0.155	0.125	1.5	4.97	2.2294	2.1244	
Manila Paper	0.035	0.125	3	4.68	0.8388	0.8062	
	0.06	0.025	2	4.68	0.8154	0.8034	
	0.06	0.125	4	4.68	0.8479	0.8308	
Lather Minilex	0.245	0.025	5	5.74	2.2447	2.1986	
	0.185	0.125	1.5	5.74	2.2294	2.1178	
	0.125	0.025	2	5.74	2.2909	2.2079	

6.4 Conclusion

In this Chapter the five ASFL based models with triangular and trapezoidal shape of MFs for the input parameters have predicted the breakdown voltage of solid insulating materials from the Cylinder Plane Electrode System set up. For a single insulating material

under DC and AC condition, the prediction of the voltage is extremely good as is evident from the E_{ts} values. Even for five solid insulating materials under AC condition, reasonably good values of E_{ts} results.

Chapter 7

MAJOR CONCLUSIONS AND FUTURE WORK

7.1 Introduction

This thesis work deals with some studies on breakdown of solid dielectrics and it's modeling using soft computing techniques. Detailed discussions have been presented in different chapters and conclusions have been made at the end of each chapter. Therefore, this concluding chapter is devoted to the summarization of the main contributions of the work and arriving at general conclusions.

7.2 Summary

The major studies reported in this thesis pertain to:

1. The experimental procedure adopted in the laboratory in order to generate breakdown voltage data under DC and AC conditions has described in Chapter 2. The experimental data are obtained with artificially created voids of various dimensions and with different insulation thicknesses of three common insulating materials, namely, White Minilex Paper, Leatheroid Paper, Glass Cloth, Manila Paper and Lather Minilex using Cylinder-Plane Electrode System. The purpose and the procedure for carrying out the statistical analysis of the breakdown voltage have been explained. An attempt has been made to monitor the state of an insulating material at various percentages of the applied voltage ultimately leading to breakdown with the help of SEM. The SEM images for White Minilex, Leatherite paper, Lather Minilex and Manila paper under DC and AC conditions has been illustrated and explained. Finally, the Chapter ends with few plots showing the variations of the breakdown voltage of some of the insulating materials as a function of insulation thickness, void depth and void diameter.
2. In Chapter 3, seven models are proposed for prediction of the breakdown voltage of solid insulating materials due to PD in cavities as a function of two, three and four input parameters using MFNN. Out of these seven models, six models, that is, model No. 1 to 6 have used the input -output data patterns generated in the laboratory using Cylinder-Plane Electrode System and one model (model No. 7) has utilized the data from the literature, which are essentially obtained experimentally using CIGRE Method II Electrode

System. The Mean Square Error for the training patterns and the Mean Absolute Error for the testing patterns has been calculated for all the seven models.

3. In Chapter **4** attempt has been made to use another ANN structure for the purpose of breakdown voltage prediction. The number of chosen centers of the radial basis functions and the learning rate of the LMS algorithm are varied in order to obtain a low value of the Mean Square Error for the training patterns E_{tr}. Based on the lowest value of the E_{tr}, Mean Absolute Error E_{ts} for the test data is calculated. Six models developed, have used the same data patterns as used by the corresponding model No. based on the MFNN structure.
4. In Chapter 5, the capability of fuzzy logic technique as a function estimator has been exploited to predict the breakdown voltage of solid insulating materials as a function of two, three and four input parameters with the help of six models and MFL inferencing. The maximum minimum composition is adopted in order to obtain the modeled value of the breakdown voltage. The rule base for any model has been framed using the training input-output data patterns. The number of rules is model specific. The shape of the MFs for the input and output parameters are assumed to be triangular and trapezoidal in all the cases. The Mean Absolute Error for the testing patterns E_{ts} is the main evaluation criteria used in this type of inferencing and the heights of the MF play a major role in reducing this value.
5. An attempt has been made to use Adaptive Sugeno FL inferencing scheme for the purpose of breakdown voltage modeling in Chapter 6. This type of inferencing has an adaptability feature incorporated in it. The coefficients of the polynomial in the consequent part of the rules are updated using the LMS algorithm and the training input output patterns. The training is complete when the value of E_{tr} reaches a tolerably low value and then the rule base is tested with the testing patterns. The shape of the MFs for the input and output parameters are assumed to be triangular and trapezoidal in all the cases.

7.3 Conclusions

Before the thesis draws to a close, the general conclusions that emerge out from this work are highlighted. These conclusions are mainly arrived at based on the performance and the capabilities of the soft computing techniques presented here for breakdown voltage modeling. Based on such a critical appraisal, the current state of technology, its promises and pitfalls are charted. This finally leads to an outline of the future directions for research and development efforts in this subject area.

The main conclusions drawn are:

1. The combination of parameters for the best results in each of the models has been identified. A comparison of modeled and experimental results indicates that SC techniques can be very well employed for estimation of breakdown voltage as a function of insulation and void dimensions.
2. Tables 7.1 – 7.2 depicts the comparison between the MAE values obtained for different models using different techniques. As may be seen from Table 7.1 that for most of the models, the MFNN structure is better at predicting the breakdown voltage compared to the RBFN structure.

Table 7.1: Comparison of the MAE of the test data for the ANN techniques (in %age)

	MFNN	RBFN
Model No. 1	0.0182	1.5953
Model No. 2	0.2260	0.3868
Model No. 3	0.0801	0.5611
Model No. 4	0.2581	0.2334
Model No. 5	0.7401	0.2586
Model No. 6	0.1638	0.5735

Again, Table 7.2 indicates that as far as the FL inferencing is concerned, ASFL predictor performs much better than MFL.

Table 7.2: Comparison of the MAE of the test data for the FL techniques (in %age)

	MFL (Triangular)	MFL (Trapezoidal)	ASFL (Triangular)	ASFL (Trapezoidal)
Model No. 1	0.7789	0.6477	0.0583	0.0591
Model No. 2	1.2705	1.1674	0.0165	0.0161
Model No. 3	0.5188	0.5788	0.0590	0.0597
Model No. 4	2.3702	2.2002	0.0166	0.0163
Model No. 5	2.8444	2.9741	1.5650	2.9538

3. The study indicates that ASFL models predict the breakdown value more accurately in most of the cases while the MFL models perform inferior amongst all. Moreover, in all cases the model values closely follow the experimental values and the MAE between the two values lie within 3%.
4. Tables 7.3 – 7.4 depicts the comparison between the execution time/ computational overheads obtained for different models using different techniques. As may be seen from Table 7.3- 7.4 that for most of the models, the execution time is quiet low.

Table 7.3: Comparison of the Computational Overheads for the ANN techniques (in s)

	MFNN	RBFN
Model No. 1	3 s	3 s
Model No. 2	6 s	4 s
Model No. 3	2 s	2 s
Model No. 4	3 s	3 s
Model No. 5	6 s	4 s
Model No. 6	10 s	7 s

Table 7.4: Comparison of the Computational Overheads for the FL techniques (in s)

	MFL (Triangular)	MFL (Trapezoidal)	ASFL (Triangular)	ASFL (Trapezoidal)
Model No. 1	3 s	2 s	1 s	1 s
Model No. 2	2 s	2 s	1 s	1 s
Model No. 3	2 s	2 s	1 s	1 s
Model No. 4	2 s	2 s	1 s	1 s
Model No. 5	3 s	3 s	16 s	16 s

5. The execution time for model No. 6 in Table 7.3 based on the MFNN and RBFN structure and model No. 5 based on the ASFL inferencing in Table 7.4 exceeds 7 s. The result is quiet expected as these models process the highest data out of all the proposed models.
6. The processor used is Intel Pentium 4 CPU with 2.40 GHz being the clock frequency.

Thus, this work is successful in applying SC techniques for prediction of breakdown voltages under both DC and AC conditions as a function of insulation and void parameters.

For a more generalization of the models developed, it would be interesting to include more parameters responsible for breakdown of insulating materials. Moreover, the entire process is data specific. Thus, more insulating materials may be tested, so that there is likelihood that this opens up areas for future research.

Further, in this thesis work, the shapes of the MF considered for FL techniques are triangular and trapezoidal in nature. More shapes of MF can be included in the FL inferencing scheme and the corresponding analysis carried out in calculating the values of E_{tr} and E_{ts}. Again, more SC techniques can be explored in order to carry out the prediction with more accuracy.

Biography

Sri Sanjeeb Mohanty was born on January 12th 1971. He did his B.E. and M.E. in the Department of Electrical Engineering, National Institute of Technology, Rourkela, India in 1992 and 1995 respectively. He was appointed in the same Department as Lecturer in 1996. Subsequently, he was promoted to Assistant Professor in 2009. He has taught various theory courses at the UG and the PG level, such as, Basic Electrical Engineering, Electrical Machines, Circuit Theory, Analog and Digital Communication System. Moreover, he has also handled various Laboratory courses, such as, Circuit Theory Laboratory, Electrical Machines Laboratory, Communication System Laboratory, and Analog Electronics Laboratory. He has guided six M tech students. His research interest includes soft computing techniques and modeling of solid insulation systems.

Reference

[1]J. C. Fothergill, "Ageing, Space Charge and Nanodielectrics: Ten things we don't know about dielectrics", IEEE *9th International Conference on Solid Dielectrics*, U.K., Winchester, July 2007, pp. 1-10.

[2]C.G. Carton, "Intrinsic and related forms of breakdown in solids", in: Alston LL, editor. High Voltage Technology, United Kingdom: Oxford University press; 1968, pp. 144-183.

[3]J. R. Laghari, P. Cygan and W. Khechen, "A Short method of estimating lifetime of Polypropylene film using step-stress Tests", IEEE Transactions on Electrical Insulation, Vol. 25, No. 6, Dec. 1990, pp. 1180-1182.

[4]T. Hashizume, C. Shinoda, K. Nakamura, M. Hotta and T. Tani, "The residual ac Breakdown voltage of 6.6 kV Dry – Cured XLPE Power Cable under wet-accelerated aging tests", IEEE Transactions on Dielectrics and Electrical Insulation, Vol. 5, No.2, April 98, pp. 169-173.

[5]U. Riechert, M. Eberhardt, J. Kindersberger and J. Speek, "Breakdown behaviour of Polyethylene at dc voltage Stress", IEEE *International Conference on Conduction and Breakdown in Solid Dielectrics*, 2008, pp. 510-513.

[6]P. Basappa, S. Jang and J. Kim, "Electrical Breakdown Studies on Electro-Active Paper", IEEE Transactions on Dielectrics and Electrical Insulation, Vol. 14, No. 5, Oct. 2007, pp. 1125-1132.

[7]S. Grzybowski, E. A. Feilat, P. Knight and L. Doriott, "Breakdown voltage behaviour of PET thermoplastics at dc and ac voltages", Proceedings of *IEEE, Southeastcon,* U.S.A., Kentucky, 1999, pp. 284-287.

[8]N. Nedjar and A. Beroual, "Aging under ac voltage of Polyurethane by using Weibull Statistics", IEEE, *9th International Conference on Solid Dielectrics*, U.K., Winchester, July 2007, pp. 654-657.

[9]Y. Yin, X. Dong, Z. Li and X. Li, "The effect of electrically prestressing on dc breakdown strength in the nanocomposite of low density Polyethylene/ Nano SiO_x", IEEE, *9th International Conference on Solid Dielectrics*, U.K., Winchester, July 2007, pp. 372-376.

[10]T. Mori, T. Matsaoka and T. Mizutani, "The breakdown mechanism of Poly-p-xylene film", IEEE Transactions on Dielectrics and Electrical Insulation, Vol. No. 1, Feb. 1994, pp. 71-76.

[11]T. Niwa, M. Hatada, H. Miyata and T. Takahashi, " Studies on the improvement of breakdown strength of Polyolefins", IEEE Transactions on Electrical Insulation, Vol. 28, No.1, Feb. 1993, pp. 30-34.

[12]K. Elanseralathan, J. Thomas and G.R. Nagabhusana, "Breakdown of solid insulating materials under high frequency high voltage Stress", Proceedings of the *6th International*

Conference on Properties and Applications Of Dielectric Materials, China, June 2000, pp. 999-1001.

[13]W. Khachen and J. R. Laghari, "Determination of aging-model constants under high frequency and high electric fields", IEEE Transactions on Dielectrics and Electrical Insulation, Vol. 1, No. 6, Dec. 1994, pp. 1034-1038.

[14]J. H. Mason, "Effect of thickness and area on the electric strength of polymers", IEEE Transactions on Electrical Insulation, Vol. 26, No. 2, April 1991, pp. 318-322.

[15]S. Ghosh and N. K. Kishore, "Breakdown voltage behaviour of Leatherite paper with or without a void," Proceedings of *IEEE Conference*, ICIT, India, Mumbai, 2006, pp. 2990-2992.

[16]T. Tanaka, "Interfacial improvement of XLPE cable insulation at reduced thickness", IEEE Transactions on Dielectrics and Electrical Insulation, Vol. 3, No.3, June 1996, pp. 345-350.

[17]I. L. Hosier, A. S. Vaughan and S. G. Swingler, "The effects of measuring technique and sample preparation on breakdown strength of Polyethylene", IEEE Transactions on Dielectrics and Electrical Insulation, Vol. 9, No. 3, June 2002 pp. 353-361.

[18]M. G. Danikas, "On the breakdown strength of Silicon Rubber", IEEE Transactions on Dielectrics and Electrical Insulation, Vol. 1, No. 6, Dec. 1994, pp. 1196-1200.

[19]O. S. Gefle, S. M. Lebedev, S. N. Tkachenko and Y. P. Pokholkov, "Relationship between the breakdown strength and low frequency dispersion of complex permittivity of polymeric dielectrics", IEEE, *9th International Conference on Solid Dielectrics*, U.K., Winchester, July 2007, pp. 651-653.

[20]Y. Zhu, H. G. Yoon and K. S. Suh, "Electrical properties of Silane Cross-linked Polyethylene in comparison with DCP Cross-linked Polyethylene", IEEE Transactions on Dielectrics and Electrical Insulation, Vol. 6, No.2, April 1999,pp. 164-168.

[21]P. Bjellheim and B. Helgee, "AC breakdown strength of aromatic polymers under partial discharge reducing conditions", IEEE Transactions on Dielectrics and Electrical Insulation, Vol. 1, No.1, Feb. 1994,pp. 89-96.

[22]K. S. Suh, C. R. Lee, Y. Zhu and J. Lim, "Electrical properties of chemically modified polyethylenes", IEEE Transactions on Dielectrics and Electrical Insulation, Vol.4, No. 6, Dec. 1997, pp. 681-687.

[23]Y. Yamano and H. Endoh, "Increase in breakdown strength of PE film by additives of Azo Compounds", IEEE Transactions on Dielectrics and Electrical Insulation, Vol. 5, No. 2, April 98, pp. 270-275.

[24]S. Fujita, M. Ruike and M. Baba, "Treeing breakdown voltage and TSC of alumina filled Epoxy Resin", IEEE *Annual Report- Conference on Electrical Insulation and Dielectric Phenomenon,* U.S.A, San Fransisco, Oct. 1996, pp. 738-741.

[25]T. Takahashi, T. Okamoto, Y. Ohki and K. Shibata, "Breakdown strength at the interface between Epoxy Resin and Silicon Rubber- A basic study for the development of all solid insulation", IEEE Transactions on Dielectrics and Electrical Insulation, Vol. 12, No. 4, Aug. 2005, pp. 719-725.

[26]Y. Shiji, Y. Muramoto and N. Shimizu, "AC breakdown properties of Bamboo Pulp-ice composite system at cryogenic temperature", IEEE Transactions on Dielectrics and Electrical Insulation, Vol. 14, No. 2, April 2007, pp. 296-301.

[27]D. P. Agoris, V. I. Chichikin, O. S. Gefle, S. M. Lebedev and I. Vitellas, "The breakdown study of 3 layer solid dielectrics", IEEE 7th *International Conference on Solid Dielectrics,* Netherlands, June 2001, pp. 434-437.

[28]I. L. Hosier, A. S. Vaughan and W. Tseng, "Effect of Polyethylene on morphology and dielectric breakdown in EVA blends", IEEE *9th International Conference on Solid Dielectrics,* U.K. Winchester, July 2007, pp. 184-187.

[29]A. Schnewwly, P. Groning and L. Schlapbach, "Breakdown behaviour of oil- impregnated Propylene as a dielectric in film capacitors", IEEE Transactions on Dielectric and Electrical Insulation, Vol. 5, No. 6, Dec. 1998, pp. 862-868.

[30]H. Z. Ding, Z. D. Wang and P. Jarman, "Ageing and moisture effects on ac electric strength of transformer board", IEEE *9th International Conference on Solid Dielectrics,* U.K. Winchester, July 2007, pp. 106-109.

[31]D. Martin, Z. D. Wang, P. Dyer, A. W. Darwin and I. R. James, "A comparative study of the dielectric strength of Ester impregnated cellulose for use in larger power transformers", IEEE *9th International Conference on Solid Dielectrics,* U.K. Winchester, July 2007, pp. 294-297.

[32]Y. Kamiya, Y. Muramoto and N. Shimizu, "Influence of absorbed gas in Silicon Rubber on electrical tree initiation", IEEE *9th International Conference on Solid Dielectrics,* U.K. Winchester, July 2007, pp. 134-137.

[33]T. M. Matheson, A. S. Vaughan and S. J. Sutton, "Electrical characteristics of Epoxy/ Nanoclay nano dielectric systems", IEEE *9th International Conference on Solid Dielectrics,* U.K. Winchester, July 2007, pp. 326-329.

[34]C. D. Green and A. S. Vaughan., "Polyethylene / Montmorillonite nanocomposites: effect of masterbatch composition and Maleic Anhydride on ac breakdown performance", IEEE *9th International Conference on Solid Dielectrics,* U.K. Winchester, July 2007, pp. 364-367.

[35]Q. Tan, Y. Cao and P. Irwin, "DC breakdown in Polyetherimide composites for implication for structural engineering", IEEE *9th International Conference on Solid Dielectrics,* U.K. Winchester, July 2007, pp. 411-414.

[36]C.A. Bailey, “A study of internal discharges in cable insulation”, IEEE Transactions on Electrical Insulation ,Vol. EI-2, No. 3, 1967, pp.155-159.
[37]F. J. Pohnan, “Voids and wax in solid high-voltage cables”, AIEE Transactions on Electrical Insulation, Vol. 70, Issue 2, 1951, pp. 1372-1376.
[38]C. Laurent, C. Mayoux and A. Sergent, “Electrical breakdown due to discharges in different types of insulation”, IEEE Transactions on Electrical Insulation ,Vol. EI-16, No. 1, 1981, pp.52-58.
[39]A.W.W. Cameron, “Diagnoses of ac generator insulation condition by nondestructive tests”, Power Apparatus and Systems, Part III, Transactions of A.I.E.E., Vol. 71, 1952, pp. 263-274.
[40]G.J. Crowdes, “A 35 kV Polyethylene-insulated cable insulation”, Power Apparatus and Systems, Part III, Transactions of A.I.E.E., Vol. 78, 1959, pp. 1086-1090.
[41]G.L. Atkinson and W.R. Thomas, “An Epoxy-paper insulation system for high-voltage applications”, IEEE Transactions on Electrical Insulation, Vol. EI-2, No. 1, 1967, pp. 18-24.
[42]D.A. Nattrass, “Partial discharge XVIII: The early history of partial discharge research”, IEEE Electrical Insulation Magazine , Vol. 9, No. 4, 1993,pp. 27-31.
[43]F.H. Kreuger, M.G. Wezelenburg, A.G. Wiemer and W.A. Sonneveld, “Partial discharge part XVIII: errors in the location of partial discharges in high voltage cables”, IEEE Electrical Insulation Magazine ,Vol. 9, No. 6, 1993, pp. 15-25.
[44]T. Tanaka, Y. Ohki, M. Ochi , M. Harada and T. Imai, “Enhanced partial discharge resistance of Epoxy/ Clay nanocomposite prepared by newly developed organic modification and solubilization methods” ,IEEE Transactions on Dielectrics and Electrical Insulation ,Vol. 15, No. 1, 2008, pp. 81-89.
[45]Y. Kikuchi, T. Murata, Y.Uozumi, N. Fukumoto, M. Nagata, “Effects of ambient humidity and temperature on partial discharge characteristics of conventional and nanocompsite enameled magnet wires” ,IEEE Transactions on Dielectrics and Electrical Insulation , Vol. 15, No. 6, 2008, pp. 1617-1625.
[46]P. H.F. Morshuis , “Degradation of solid dielectrics due to internal partial discharge: some thoughts on progress made and where to go now”, IEEE Transactions on Dielectrics and Electrical Insulation , Vol.12, No. 5, 2005, pp. 905-913.
[47]S. A. Boggs, “Partial discharge- Part III: Cavity-induced PD in solid dielectrics”, IEEE Electrical Insulation Magazine, Vol. 6, No. 6, 1990, pp. 11-18.
[48]J.C. Devins, “The physics of partial discharges in solid dielectrics”, IEEE Transactions on Electrical Insulation ,Vol. EI-19, 1984, pp.475-495.

[49]S. Cygan and J.R. Laghari, “Dependence of the electric strength on the thickness, area and volume of polypropylene”, IEEE Transactions on Electrical Insulation , Vol.22, No. 6, 1987, pp. 835-837.

[50]K.S. Naidu, S.K. Jain, V.N. Maller and P. Satyanarayana, “Partial discharge studies in non-uniform fields with insulating barriers”, IEEE Transaction on Electrical Insulation ,Vol. EI-14, No. 5, 1979, pp. 285-287.

[51]J.H. Mason, “Discharges”, IEEE Transactions on Electrical Insulation ,Vol. EI-13, No.4, 1978, pp. 211-238.

[52]T.W. Dakin, H.M. Philofsky and W.C. Divens , “Effect of electric discharges on breakdown of solid insulation”, Transactions A.I.E.E. Electrical Insulation ,73, pt.1, 1954, pp. 155-162.

[53]Abdel-Razak Nossier, “Calculation of discharge inception voltage due to the presence of voids in power cables”, IEEE Transaction on Electrical Insulation ,Vol. EI-14, No. 2, 1979, pp. 117-120.

[54]D. Kind and D. Konig, “AC breakdown of Epoxy Resins by partial discharges in voids”, IEEE Transaction on Electrical Insulation ,Vol. EI-3, No. 2, 1968, pp. 40-46.

[55]G.C. Crichton, P.W. Karlsson and A. Pedersen, “Partial discharges in ellipsoidal and spheroidal voids”, IEEE Transaction on Electrical Insulation ,Vol. 24, No. 2, 1989, pp. 335-342.

[56]S.I. Reynolds, “On the behaviour of natural and artificial voids in insulation under internal discharge”, Power Apparatus and Systems, Part III, Transactions of A.I.E.E., Vol. 77, Issue 3, 1959, pp. 1604-1608.

[57]H.T. Ward, W.O. Puro and D.M. Bowie, “Artificial dielectrics utilizing cylindrical and spherical voids”, Proceedings of the IRE, Vol. 44, Issue 2, 1956, pp. 171-174.

[58]E. Takahashi, Y. Tsutsumi, K. Okuyama and F. Ogata, “Partial discharge characteristics of oil- immersed insulation systems under dc, combined ac-dc and dc reversed polarity voltage”, IEEE Transactions on Power Apparatus and Systems, Vol. PAS-95, No. 1, 1976, pp. 411-420.

[59]F. S. Ahmed and A.S. Ahmed, “Breakdown of solid insulating films by partial discharge using sinusoidal and pulse voltages”, IEEE Transactions on Electrical Insulation, Vol. EI-13, No. 5, 1978, pp. 337-342.

[60]R.J. Densley, “Partial discharges in gaseous cavities in solid dielectrics under impulse voltage conditions”, IEEE Transactions on Electrical Insulation, Vol. EI-6, No. 2, 1971, pp. 54-62.

[61]T. Kurihara, S. Tsuru, K. Imasaka, J. Suehiro and M. Hara , “PD characterstics in an air-filled void at room temperature under superimposed sinusoidal voltages”, IEEE Transactions on Dielectrics and Electrical Insulations, Vol. 8, No. 2, 2001, pp. 269-275.

[62]S. W. Schwenterly, M.M. Menon, R.H. Kernohan and H.M. Long , "AC dielectric performance of Helium impregnated multi-layer plastic film insulation", IEEE Transactions on Electrical Insulation, Vol. EI-12, No. 1, 1977, pp. 46-50.

[63]R.J. Densley, A.T. Bulinski and T.S. Sudarshan, "Short-term electrical insulating characteristics of some polymeric materials immersed in LN_2", IEEE Transactions on Electrical Insulation, Vol. EI-14, No. 4, 1979, pp. 211-221.

[64]H. Okubo, M. Hazeyama, N. Hayakawa, S. Honjo and T. Masuda , "V-t characteristics of partial discharge inception in Liquid Nitrogen/ PPLP composite insulation system for HTS cable", IEEE Transactions on Dielectrics and Electrical Insulations, Vol. 9, No. 6, 2002, pp. 945-951.

[65]A. Masood, M.U. Zuberi and E. Hussain , "Breakdown strength of solid dielectrics in Liquid Nitrogen", IEEE Transactions on Dielectrics and Electrical Insulation, Vol. 15, No.4, 2008, pp. 1051-1055.

[66]N.B. Timpe and S.V. Heyer, "Laboratory and field partial-discharge studies by a utility", IEEE Transactions on Electrical Insulation, Vol. EI-12, No. 2, 1977, pp. 159-164.

[67]H. Borsi, O. Cachay, "Partial discharge behaviour of epoxy-resin impregnated transformer coils", IEEE Transactions on Electrical Insulation, Vol. 27, No. 6, 1992, pp. 1118-1126.

[68]R. Schifani, R. Candela and P. Romano, "On PD mechanisms at high temperature in voids included in an epoxy resin", IEEE Transactions on Dielectrics and Electrical Insulations, Vol. 8, No. 4, 2001, pp. 589-597.

[69]I. W. Mc Allister, "Partial discharges in spheroidal voids: void orientation", IEEE Transactions on Dielectrics and Electrical Insulations, Vol. 4, No. 4, 1997, pp. 456-461.

[70]H. Feibus, "Corona in Solid-insulation systems", IEEE Transactions on Electrical Insulation, Vol. EI-5, No. 3, 1970, pp. 72-78.

[71]E. J. McMahon, "The chemistry of corona degradation of organic insulating materials in high-voltage fields and under mechanical strain", IEEE Transactions on Electrical Insulation, Vol. EI-3, No. 1, 1968, pp. 3-10.

[72]Y. Toriyama, H. Okamoto, M. Kamazashi and K. Horii, "Degradation of polyethylene by partial discharge", IEEE Transactions on Electrical Insulation, Vol. EI-2, No. 2, 1967, pp. 83-92.

[73]J. H. Mason, "Breakdown of solid dielectrics in divergent fields", Proceedings IEE, Vol. 100 , Part C., 1955, pp.254-263.

[74]N.P. Kolev and N. M. Chalashkanov, "Modeling of partial discharge inception and extinction voltages using adaptive neuro-fuzzy inference system (ANFIS)", IEEE *9th International Conference on Solid Dielectrics*, U.K. Winchester, July 2007, pp. 605-608.

[75]S. Ghosh, " Study of some aspects of artificial neural network modeling of partial discharge phenomenon", Ph. D. Dissertation, IIT, Kharagpur, 1999.

[76]S. Ghosh and N.K. Kishore, "Modeling of partial discharge inception and extinction voltages of sheet samples of solid insulating materials using an artificial neural network", IEE Proc- Sci. Meas. Technol, Vol. 149, No. 2 , 2002, pp. 73-78 .

[77]S. Ghosh and N. K Kishore, " Modeling PD inception voltage of Epoxy Resin post insulators using an adaptive neural network", IEEE Trans. Dielectrics and Electrical Insulation, Vol. 6, No. 1, 1999, pp. 131-134.

[78]S.B. Stechkin and Y.N. Subbotin, " Splines in numerical mathematics", Moscow (1976) (In Russian).

[79]O.L. Mangasarian, J.W. Shavlik and E.W. Wild, " Knowledge-based Kernel approximation", Journal of Machine Learning and Research, Vol. 5, 2004, pp. 1127-1141.

[80]J.R. Rice, " The approximation of functions", Linear theory,(Addison-Wesley, 1964).

[81]L. Ruihua, G. Meng, N. Gao and H. Xie, " Combined use of partial least-squares regression and neural network for residual estimation of larger generator stator insulation", IET Proc- Sci. Meas. Technol, Vol. 18 , 2007, pp. 2074-2082 .

[82]J.S.R. Jang, C.T. Sun and E. Mizutani, "Neuro-Fuzzy and soft computing: A computational approach to learning and machine intelligence", (Prentice Hall International, Inc., (2^{nd} Edition 1997), pp. 24-79.

[83]D.Driankov, H. Hellendoorn and M. Reinfrank, "An introduction to fuzzy control", (Narosa Publishing House, Springer International Student Union, (1993), pp. 100-101.

[84]L A Zadeh. Fuzzy logic, neural networks and soft computing. One-page course announcement of CS 294-4, 1993, the University of California at Berkeley, November 1992.

[85]W. Khachen and J.R. Laghari, "Estimating lifetime of PP,PI and PVDF under artificial void conditions using step-stress tests", IEEE Transactions on Electrical Insulation , Vol. 27, No. 5, 1992, pp.1022-1025.

[86]M. Hammer ,T. Kozlovsky and J. Svoboda, "The use of neural networks for life prediction of insulating materials for electrical machines windings", IEEE *8^{th} International Conference on Solid Dielectrics*, France, June 2004, pp. 546-549.

[87]M. Hammer, T. Kozlovsky and J. Svoboda, "Fuzzy systems for simulation and prediction of the residual life of insulating materials for electrical machines windings", IEEE *8^{th} International Conference on Solid Dielectrics*, France, June 2004, pp. 542-545.

[88]P. Bonissone and K. Goebel, "Soft computing for diagnostics in equipment service" ,Journal of Artificial Intelligence for Engineering Design, Analysis and Manufacturing, Vol. 15 , No. 4, 2001,pp.267-279.

[89]A. Samee ,Z.H. Li, C.H. Zhang and Z. P. Huang, "Fractal cluster based aging model of electrical treeing in polymeric insulation", Information Technology Journal, Vol. 8, No. 6, 2009, pp.855-862.

[90]M.D. Noskov, A.S. Malinovski, M. Sack and A.J. Schwab, "Modeling of partial discharge development in electrical trees channels" ,IEEE Transactions on Dielectrics and Electrical Insulation, Vol. 10, 2003, pp. 425-434.

[91]K. Wu, Y. Suzoki, T. Mizutani and H. Xie, "Model for partial discharges associated to tree breakdown, I. PDs in tree channels", Journal Physics. D: Applied Physics, Vol. 33, 2000, pp.1197-1201.

[92]A. Cavallini, G.C. Montanari and F. Puletti, "A fuzzy logic algorithm to detect electrical trees in polymeric insulation systems", IEEE Transactions on Dielectrics and Electrical Insulation , Vol. 12, No.6, 2005, pp. 1134-1144.

[93]H. G. Kranz and R. Krump, "PD diagnosis using statistical parameter optimization on a PC based system", IEEE Transactions on Electrical Insulation , Vol. 27, No.1, 1992, pp. 93-98.

[94]N. C. Sahoo , M.M.A. Salama and R. Bartnikas, "Trends in partial discharge pattern classification – A survey", IEEE Transactions on Dielectrics and Electrical Insulation, Vol. 12, No. 2, 2005, pp. 248-264.

[95]T.K. Abdel-Galil, R.M. Sharkawy, M.M.A. Salama and R. Bartnikas, "Partial discharge pattern classification using the fuzzy decision tree approach", IEEE Transactions on Instrumentation and Measurement, Vol. 54, No.6, 2005, pp.2258-2263.

[96]S. Gopal ,B. Karthikeyan and D. Kavitha , "Partial discharge pattern classification using fuzzy expert system", IEEE *8th International Conference on Solid Dielectrics*, France, June 2004, pp. 500-503.

[97] D. Dey, B. Chatterjee, S. Chakravorti and S. Munshi, " Cross-wavelet transform as a new paradigm for feature extraction from noisy partial discharge pulses", IEEE Transactions on Dielectrics and Electrical Insulation, Vol. 17, Issue 1, 2010, pp. 157-166.

[98]E.M. Lalitha and L. Satish, " Fractal image compression for classification of PD sources", IEEE Transactions on Dielectrics and Electrical Insulation, Vol. 5, Issue 4, 1998, pp. 550-557.

[99]L. Satish and W.S. Zaengl, " Artificial Neural Network for recognition of 3-D partial discharge patterns", IEEE Trans. on Dielectrics and Electrical Insulation, Vol. 1, Issue 2, 1994, pp. 265-275.

[100]M.G. Danikas, N. Gao and M. Aro, " Partial discharge recognition using neural networks: A review", Electrical Engg (Archiv Γ. Elektro technik), Vol. 85, No. 2, 2003, pp. 87-93.

[101]M.G. Danikas, N. Gao and M. Aro, " Neural networks and their role in partial discharge recognition in gas insulated switchgear and transformers: A short review", Journal of Electrical Engg., Vol. 54, No. 3-4, 2003, pp. 107-112.

[102]T. Okamoto and T. Tanaka, "Partial discharge pattern recognition for three kinds of model electrodes with a neural network," IET on SMT, Vol. 142, Issue 1, 1995, pp. 75-84.

[103]P.S. Ghosh, S. Chakravorti and N. Chatterjee, "Estimation of time to flashover characteristics of contaminated electrolytic surfaces using a neural network", IEEE Trans. on Dielectrics and Electrical Insulation, Vol. 2, Issue 6, 1995,pp. 1064-1074.

[104]Standard test methods for sampling and testing untreated paper used for electrical insulation, ASTM Designation: D202 -97 ,2002.

[105]J. C. Fothergill, " Estimating the cumulative probability of failure data points to be plotted on Weibull and other probability paper", IEEE Transactions on Electrical Insulation, Vol. 25, No. 3, 1990,pp. 489-492.

[106]G.C. Stone and R.G. Van Heeswijk, "Parameter estimation for Weibull distribution", IEEE Transactions on Electrical Insulation, Vol. EI-12, No. 4, 1977,pp. 253-261.

[107]A. Clifford Cohen , " Maximum likelihood estimation in the Weibull distribution based on complete and on censored samples", Technometrics, Vol. 7, No. 4, 1965, pp. 579-588.

[108]Simon Haykin , *Neural Networks A Comprehensive Foundation*, New Jersey, U.S.A.: Prentice Hall International Inc., 1999, pp. 161-175, 270-300.

[109]Robert Hecht-Nielsen, *Neurocomputing*, Addison-Wesley Publishing Company, Inc. USA, 1990, I-XIII, pp. 1-433.

[110]D.E. Rumelhart and J. L. McClelland Eds., *Parallel distributed processing: Explorations in the microstructure of cognition*, Vol. 1, MIT Press, 1986.

[111]S. Mohanty and S. Ghosh, " Modeling of the breakdown voltage of Leatherite paper in the presence of void under ac conditions using artificial neural network", Available in CD, *32nd National System Conference*, Session D2 on Modern Systems Techniques and Applications –I, India, I.I.T. Roorkee, December 2008, pp. 1-6.

[112]S. Mohanty and S. Ghosh, " ANN modeling of breakdown voltage of solid insulating materials in the presence of void", IET Proc- Sci. Meas. Technol, Volume 4, Issue 5 , 2010, pp. 278-288.

[113]S. Ghosh and S. Mohanty, "Modeling of breakdown voltage behaviour of Leatherite paper in the presence of voids using artificial neural networks", IEEE *9th International Conference on Solid Dielectrics*, U.K. Winchester, July 2007, pp. 94-97.

[114]S. Mohanty and S. Ghosh , " Modeling of breakdown voltage of White Minilex Paper in the presence of voids under ac and dc conditions using fuzzy logic techniques", Elsevier,

International Journal on Electric Power and Energy Systems, Volume 32, Issue 5, 2010, pp. 518-523.

[115]S. Mohanty, S. Ghosh and S. K. Mohapatra, “Breakdown voltage modeling of Leatherite paper using fuzzy logic technique”, (Available in CD) *International Conference on Polymeric Materials in Power Engineering*, India, CPRI, Bangalore, Oct. 2007, pp. 1-10.

[116]Ibrahim, B. Kucukdemiral and G. Cansever, “ Sugeno based robust adaptive fuzzy sliding mode controller for SISO nonlinear systems”, Journal of Intelligent and Fuzzy Systems, Vol. 17, No. 2, 2006, pp. 113-124.

[117]S. Mohagheghi, G. K. Venayagamoorthy, and R. G. Harley, "Adaptive Critic Design Based Neuro-Fuzzy Controller for a Static Compensator in a Multimachine Power System", IEEE Transactions on Power Systems, Vol. 21, No. 4, 2006, pp. 1744-1754.

[118]S. Mohanty and S. Ghosh, “Modeling of the breakdown voltage of Manila Paper in the presence of voids using adaptive fuzzy logic techniques”, Digital Object Identifier: 10.1109/ICPWS.2009.5442738, *IEEE 3rd International Conference on Power Systems* , India, I.I.T. Kharagpur, Dec. 2009, pp. 1-6.

Dissemination of the Work

Published

[1]S. Ghosh and S. Mohanty, "Modeling of breakdown voltage behaviour of leatherite paper in the presence of voids using artificial neural networks", Proceedings of *IEEE 9th International Conference on Solid Dielectrics (ICSD)*, U.K., Winchester, July 2007, pp. 94-97.

[2]S. Mohanty, S. Ghosh and S. K. Mohapatra, "Breakdown voltage modeling of leatherite paper using fuzzy logic technique", (Available in CD) *International Conference on Polymeric Materials in Power Engineering*, India, CPRI, Bangalore, Oct. 2007, pp. 1-10.

[3]S. Mohanty and S. Ghosh, " Recent trends in breakdown voltage studies of different types of solid dielectrics", (Available in CD) *1st National Conference on Emerging trends and recent advances in Electrical Engineering and Renewable energy*, India, Sikkim, Dec. 2008, pp. 1-6.

[4]S. Mohanty and S. Ghosh, " Modeling of the breakdown voltage of Leatherite Paper in the presence of void under ac conditions using Artificial Neural Networks", (Available in CD) *32nd National System Conference (NSC)*, India, I.I.T. Roorkee, Dec. 2008. pp. 1-6.

[5]S. Mohanty and S. Ghosh , " Modeling of breakdown voltage of White Minilex Paper in the presence of voids under ac and dc conditions using fuzzy logic techniques", International Journal of Electric Power and Energy Systems (Elsevier), Volume 32, Issue 5, 2010, pp. 518-523.

[6] S. Mohanty and S. Ghosh, "Modeling of the breakdown voltage of Manila Paper in the presence of voids using adaptive fuzzy logic techniques", Digital Object Identifier: 10.1109/ICPWS.2009.5442738, *IEEE 3rd International Conference on Power Systems* , India, I.I.T. Kharagpur, Dec. 2009, pp. 1-6.

[7]S. Mohanty and S. Ghosh, " ANN modeling of breakdown voltage of solid insulating materials in the presence of void", IET Proc. Science, Measurement & Technology, Volume 4, Issue 5 , 2010, pp. 278-288.

Accepted for publication

[1] S. Mohanty and S. Ghosh , " Modeling of breakdown voltage of solid insulating materials in the presence of voids under ac conditions using fuzzy logic techniques", Accepted for publication, *IEEE International Conference on Electrical Insulation and Dielectric Polarization*, Mexico, Oct. 2011.